Systems analysis of the dynamic macrophage response to productive and non-productive murine cytomegalovirus infection

Paul Andrew Lacaze

s0561593

A thesis submitted in fulfilment of requirements for the degree of

Doctor of Philosophy

Division of Pathway Medicine, School of Biomedical Sciences

The University of Edinburgh

April 2011

Declaration

I hereby declare that this thesis is of my own composition, and that it contains no material previously submitted for the award of any other degree. The work reported in this thesis has been executed by myself, except where due acknowledgement is made in the text.

Paul Lacaze

Abstract

The mammalian immune system is capable of detecting and responding to different infectious conditions with specificity at the adaptive level, however whether this ability extends to individual cells of the innate immune system is unclear. The hypothesis of this thesis is that macrophages, as individual cells, can distinguish between productive and non-productive virus infections and respond differently at the gene expression and secreted protein level. To test the hypothesis, mouse bone marrow derived macrophages (BMDMs) were infected in parallel with either a productive (live) and non-productive (attenuated) strain of murine cytomegalovirus (MCMV) and profiled temporally using a range of techniques. Both productive and non-productive MCMV infection resulted in strong type I IFN induction in BMDMs, however induction was significantly more rapid in response to productive infection. In addition, chemoattractant and pro-inflammatory cytokines TNFα, IL-6, RANTES, MIG and MIP-2 were secreted to significantly higher levels in response to productive MCMV infection, and curtailed in response to non-productive MCMV infection. Furthermore, genome-wide microarray profiling revealed a number of co-expressed gene networks regulated differentially in response to the two conditions. This consisted of macrophage gene networks targeted for modulation by de novo MCMV proteins, and late macrophage response genes regulated specifically in response to productive MCMV infection. To further explore the mechanisms of transcriptional regulation during macrophage antiviral response, BMDMs from mice lacking either the type I IFN receptor (*Ifnar1*) or the IFNβ (*Ifnb1*) gene were profiled using a similar approach. The resulting genome-wide transcriptional data provided a unique insight into the relationship between type I IFN regulation and the macrophage transcriptome in response to MCMV infection. Overall, the study utilizes a combination of genetic mutants from both host and pathogen to investigate mechanisms of virus detection and host transcriptional regulation during the innate immune response to MCMV infection in macrophages.

Acknowledgements

Firstly, thank you to Prof Peter Ghazal for providing intellectual, scientific and financial support for this thesis. It was a privilege to work in your group in such a free environment. Thank you to Paul Dickinson, Tom Freeman, Kevin Robertson, Thorsten Forster, and Marilyn Horne for providing support and supervision in many different forms. Thank you also to Marie Craigon, Alan Ross Garwin Sing and Donal Wall for their lab support.

To all members of the Division of Pathway Medicine, University of Edinburgh, thank you contributing to the unique and interesting working environment that is DPM. Particular thanks to good friends and colleagues Mathieu Blanc, Diwakar S Kuma, Mike Chisholm, Kai Kropp, Michael Ochsenkuehn, and Jai Tree.

Thank you also to Lorraine Kerr and Eliane Salvo-Chirnside for their kind help at the Centre for Systems Biology Edinburgh, and to collaborators Birgit Strobl and Mathias Müller from the Institute of Animal Breeding and Genetics, University of Vienna, Austria. The BBSRC, Wellcome Trust and the University of Edinburgh must also be thanked for their generous financial support of the research.

To my family, you have always been in my mind and will always continue to be. Thank you for providing the strength.

Finally, I dedicate this thesis to my love, Tess, to whom I owe so much.

Table of Contents

List of figures

Chapter 1 - Introduction

Chapter 2 - Materials and Methods

Chapter 3 - Functional characterization of a non-productive virus

Chapter 4 - Systems analysis of the host response to productive and non-productive MCMV infection in macrophages

Chapter 5 - Modulation of transcriptional networks during macrophage infection by MCMV

Chapter 6 - Interferon control of the macrophage transcriptome

6.11 Genes induced specifically in response to productive MCMV infection are IFN-independent (n827).

6.12 Genes induced specifically by productive MCMV infection at 8hpi are IFN-independent (n62).

6.13 Pro-inflammatory genes induced in an equivalent manner by MCMV, MCMVdie3 and polyIC are IFN-independent (n48).

6.14 A sub-set of early response genes is induced rapidly by all stimuli but shut-off in the absence of IFN signalling (n25).

6.15 Expression of *Ccl4, Irf1* and *Socs3* is sustained in wild-type BMDMs but shut-off rapidly in *Ifnb1-/-* and *Ifnar1-/-* BMDMs.

6.16 Transcriptional induction of *Csf1* is partially dependent on the type I IFN receptor.

6.17 IFN-independent down-regulation of genes in response to MCMV, MCMVdie3 and polyIC (n141).

6.18 IFN-independent down-regulation of cell cycle genes in response to MCMV, MCMVdie3 and polyIC (n428).

6.19 Interferon-stimulated genes induced in response to MCMV, MCMVdei3 and polyIC with partial dependency on *Ifnb1* and complete dependency on *Ifnar1* (n776).

6.20 The induction of some macrophage ISGs is strictly dependent on *Ifnb1*.

6.21 Induction of *Stat1*, and *Mx1* is partially dependent on *Ifnb1* expression

6.22 Genes induced with late kinetics expressed higher in response to polyIC than to MCMV (n86).

6.23 Genes down-regulated in an IFN-dependent manner by MCMV, MCMVdie3 and polyIC (n66).

6.24 IFN-dependent down-regulation inhibited during productive MCMV infection (n263).

6.25 IFN-dependent down-regulation of cholesterol biosynthesis genes (n28).

6.26 Secretion of RANTES and MIG is dependent on the type I IFN receptor, but secretion of MIP-2 occurs in an IFN-independent manner

6.27 Secretion of TNF is partially dependent on *Ifnar1* and secretion of IL-6 in completely dependent on *Ifnar1* in BMDMs infected with MCMV.

6.28 Secretion of IL-10 is dependent on *Ifnar1* in BMDMs infected with MCMV.

List of Tables

Abbreviations

APC	Antigen presenting cell
BAC	Bacterial artificial chromosome
BCA	Bicinchoninic acid
BMDM	Bone marrow-derived macrophage
°C	Degrees Celsius
C57BL/6	C57 black 6 laboratory mouse strain
CHX	Cyclohexmide
CS	Calf serum
CSF	Collony-stimulating factor
Ct	Crossing point (PCR)
DAVID	Database for Annotation, Visualization, Integrated Discovery
DC	Dendritic cell
DMEM	Dulbecco's Modified Eagle Medium
DMSO	Dimethyl sulfoxide
DNA	Deoxyribonucleic acid
ds	Double stranded
EDGE	Extraction and analysis of differential gene expression
EDTA	Ethylenediaminetetraacetic acid
ELISA	Enzyme-linked immunosorbent assay
FACS	Fluorescence-activated cell sorting
FCS	Fetal calf serum
GCV	Ganciclovir
HCMV	Human cytomegalovirus
HCV	Hepatitis C virus
HIV	Human immunodeficiency virus
HSV	Herpes simplex virus
IE	Immediate early
IFN	Interferon
IFNAR	Interferon alpha receptor
IFNα	Interferon alpha
IFNβ	Interferon beta
IFNγ	Interferon gamma
IPA	Interferon regulatory factor

ISG	Interferon-simulated gene
Kb	Kilobase
kDa	Kilodalton
LPS	Lipopolysaccharide
MCL	Markov Clustering
MCMV	Murine cytomegalovirus
MEF	Mouse embryonic fibroblasts
MHC	Major histocompatibility complex
MIEP	Major immediate-early promoter
ml	Milliliter
MOI	Multiplicity of infection
MW	Molecular weight
NF-kB	Nuclear Factor-KappaB
NIH	National Institutes of Health
ORF	Open reading frame
PAMP	Pathogen associated molecular pattern
PBS	Phosphate buffered saline
PCA	Principle components analysis
PCR	Polymerase chain reaction
PFU	Plaque forming unit
polyIC	Polyinosinic:polycytidylic acid
PRR	Pattern recognition receptor
RNA	Ribonucleic acid
ROC	Receiver operating characteristic
Rpm	Revolutions per minute
RT	Reverse transcriptase
RT-PCR	Reverse transcriptase polymerase chain reaction
ss	single stranded
TLR	Toll-like receptor
TNF	Tumor necrosis factor
UK	United Kingdom
UPL	Universal Probe Library
USA	United States of America
UV	Ultraviolet
WT	Wild-type
µl	Microlitre

Introduction

1.1 Overview of the thesis

In this thesis, the concept of host discrimination between productive (live) and non-productive (attenuated) viral infection will be examined during the innate immune response in macrophages. The central hypothesis of the thesis is that macrophages respond differentially to productive and non-productive murine cytomegalovirus (MCMV) infection at the gene expression and secreted protein level. To test the hypothesis, a controlled *in vitro* experimental system of mouse bone marrow-derived macrophages (BMDMs) is implemented. To represent productive and non-productive viral infections respectively, wild-type MCMV is used alongside a replication-deficient and transcriptionally inert recombinant MCMV deletion mutant strain (MCMVdie3). The mutant strain acts as a genetic tool and control reagent to represent non-productive viral infection, as an alternative to UV-inactivated virions. BMDMs are infected in parallel with the two MCMV strains and the innate immune response profiled using a systems-level approach. One of the main focuses of the thesis is the dynamic genome-wide expression profiling of macrophages using microarray technology.

Following the Introduction and Materials and Methods sections, four results chapters will be presented. The first results chapter describes the characterization work required for the non-productive mutant MCMVdie3 strain. The second results chapter is a systems-level investigation of the macrophage host-response to productive and non-productive MCMV infection. The third results chapter focuses on macrophage gene expression networks targeted for modulation by MCMV during productive viral infection. The fourth results chapter focuses on the role of type I interferon (IFN) in the detection and response to MCMV infection in macrophages, and will involve the use of BMDMs derived from mice lacking either the type I IFN receptor (*Ifnar1*) or the IFNβ (*Ifnb1*) gene. Finally, a conclusion and discussion section will be provided at the end of the thesis to summarize the body of work.

In the following Introduction section, the model pathogen (MCMV) and the cell type (BMDMs) will be introduced. Subsequently, an overview of pathogen detection systems will be given, followed by an overview of the innate immune response to virus infection, with a particular focus on type I IFN signalling. This will include a literature review of studies using IFN-deficient mice in the context of virus infection. The concept of virus evasion of the host innate immune response will then be introduced, with particular focus on the ability of CMV to subvert the innate immune response. Following this, a literature review of all comparable studies measuring the host response to live (productive) versus attenuated (non-productive) viral infection will be given. A brief rationale section will also be included as part of the Introduction.

1.2 Cytomegalovirus (CMV)

1.2.1 CMV overview and pathogenesis

Cytomegalovirus (CMV) is a large double-stranded DNA virus and member of the beta-herpesvirus family. CMV is a ubiquitous and opportunistic pathogen capable of achieving life-long infection (latency) in a highly species-specific manner. Human CMV (HCMV) has a high incidence in human populations with positive seroprevalence ranging from 40-100%, with rates of infection varying with age, race, geographic distribution and socio-economic status(52). High seropositivity rates have been reported especially in blood transfusion patients, intravenous drug users, organ transplant recipients, and haemodialysis patients(375). HCMV is shed in most bodily fluids and, therefore, can be transmitted sexually or through saliva. HCMV infection is usually sub-clinical and non-threatening in healthy individuals, however can be serious in immunocompromised patients including organ transplant recipients, patients undergoing haemodialysis, patients with cancer, patients receiving immunosuppressive drugs and HIV-positive individuals. HCMV infection in immune-compromised cases can lead to liver failure, retinitis, colitis, and pneumonia. Congenital HCMV infection is a major problem, and reactivation in seronegative pregnant mothers can lead to *in utero* transmission to the developing

foetus, potentially resulting in permanent hearing loss, vision loss and neurological defects for the foetus in extreme cases. Long-term HCMV infection has also been linked to the development of atherosclerosis(4) and immunosenescence(54) later in life.

1.2.2 CMV diagnosis and treatment

Several methods are currently used for the diagnosis of HCMV such as ELISA-based serological tests for HCMV-specific antibodies, and PCR to monitor viral DNA levels in the bloodstream. A number of antiviral drugs have also been developed to combat HCMV infection, the most common of which are Ganciclovir and Foscarnet, both targeting CMV DNA polymerase to inhibit viral replication. These drugs, however, are limited by toxicity issues and the emergence of drug resistance(219). A vaccine against HCMV is also under investigation but has yet to be approved for clinical use(324).

1.2.3 MCMV as a model for cytomegalovirus infection

CMVs are highly host-adapted viruses and therefore exhibit species-specificity in regards to infectivity and tropism. As a result, HCMV cannot be used to infect animal models and experimental studies on HCMV are restricted to *in vitro*. Murine CMV (MCMV) has, therefore, become an established model for the study of CMV pathogenesis. There are similarities between MCMV and HCMV infection with respect to events during acute infection, establishment of latency and reactivation, and organ tropism (5). Similar to HCMV infection, the pathological outcomes of MCMV infection are defined by the immune status of the host(198). MCMV also shares biological similarity with HCMV regarding virion structure, genome structure, patterns of gene expression, and dynamics of the infectious cycle(361). The mouse model of CMV infection has been useful for the *in vivo* study of host–pathogen interactions, responses to antiviral drugs, host susceptibility to infection, and identification of host resistance genes(323).

Murine CMV can be used to infect its natural host, meaning host/pathogen interactions can be studied in a physiologically relevant context. A range of deletion mutants are available for MCMV(34, 42) adding to its utility as a model. The MCMV genome (Smith strain) has been sequenced and consists of 230,278 bp with an overall GC content of 58.7%(299). The distribution of G/C content is similar to that seen in the HCMV genome. Sequence similarity also exists for 78 open reading frames encoded within the core herpesvirus region(299). Homologs of the HCMV gene families UL25, UL82, and US22 and GCR can also be found in the MCMV genome (299).

Despite the similarities between MCMV and HCMV, there are important differences between the viruses that must be considered. MCMV and HCMV have co-evolved with their respective hosts over long periods in a highly species-specific manner. This is particularly the case with regards to evasion of the innate and adaptive immune response (237, 323) and sites of latency/reactivation (198, 258, 302). The function of homologous MCMV and HCMV proteins can also vary considerably, and many genes exist only in one species of the virus(299). There are also important differences in protein function at immediate early stages of infection, and with regards to host cell interactions (243). For example, the HCMV IE1 protein has been shown to bind chromatin, but this is not the case for the MCMV IE1 homolog (243). Table 1.1 summarizes some of the key differences between HCMV and MCMV proteins.

Table 1.1 Key differences between HCMV and MCMV proteins. Adapted from Maul *et al.* (243) and Rawlinson *et al* (299).

Property	**HCMV**	**MCMV**
Binding of chromatin	Achieved by IE1 (UL123)	Not achieved by IE1 (M123)
Blocking of the cell cycle	Achieved by IE2 (UL122)	Not achieved by IE3 (the MCMV equivalent of HCMV IE2) (M122)
Binding of the repressor Daxx	Achieved by pp71	Achieved by IE1
RL11, US1, US2, US6 and US12 gene families	Present in HCMV	No amino acid homologs in MCMV
Protein kinase UL97/M97	HCMV pUL97 accumulates in the nucleus	pM97 is predominantly located in the cytoplasm
Alkaline exonuclease (DNase)	No short inverted repeat in the HCMV DNase gene (UL98)	Short (22-base) inverted repeat close to the start of MCMV DNase gene (M98)
Viral DNA replication	UL101 is required for DNA replication in HCMV	MCMV does not possess a sequence or positional homolog of UL101
Origin of replication	HCMV does not contain homologs for MCMV genes m58 and m59	Contains ORFs m58 and m59 within the origin of replication

1.2.4 MCMV structure and life cycle

The MCMV virion structure is similar to that of all herpesviruses with an outer lipid envelope containing glycoproteins capable of interacting with the host cell membrane to facilitate viral entry. The envelope encapsulates an icosahedral capsid structure, within which the dsDNA genome of MCMV is located (Figure 1.1). Between the outer envelope and the capsid structure is a layer of virion-associated proteins known as the tegument. Tegument proteins are released into the host cell during viral entry as the viral envelope fuses with the host cell membrane. Up to 38 different MCMV proteins have been detected in the MCMV virion by mass spectrometry (184). Although the function of many of these proteins remains unknown, many are predicted to have roles in immune-modulation, inhibition of

apoptosis, and modulation the host cell environment (181, 182). HCMV tegument proteins have been suggested to contribute to the delivery of viral genomes to the nucleus and initiation of viral gene expression(182). Viral DNA polymerase and viral RNAs are also packaged within the MCMV and HCMV tegument.

Figure 1.1 Structure of the CMV virion. The lipid envelope of the CMV virion encloses tegument proteins and the viral capsid. The capsid encloses the dsDNA genome.

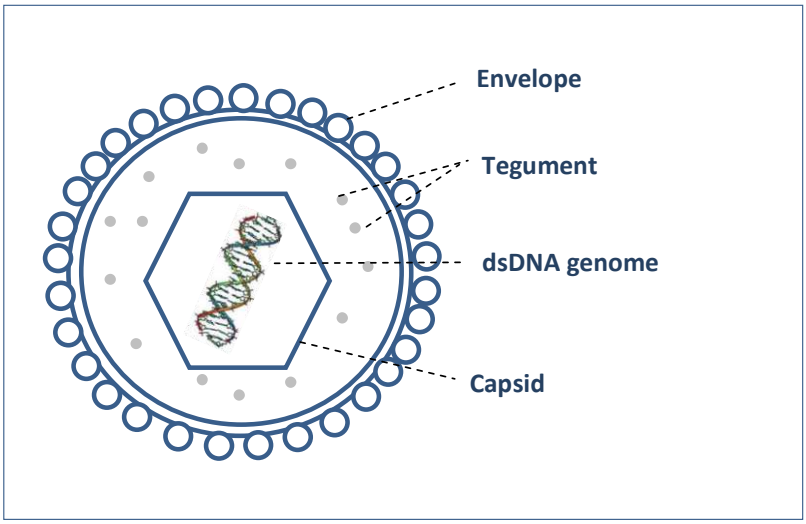

All herpesviruses share a common virion structure, and other characteristics including a) the use of genome-encoded enzymes for nucleotide metabolism and DNA replication, b) viral replication occurring within the nucleus, c) destruction of host cells after lytic infection, and d) establishment of latency within the infected host.

The viral entry process for HCMV and MCMV is complex and remains to be fully understood. Considerably more work, however, has been done on HCMV entry compared to MCMV. In both cases, viral envelope glycoproteins interact with host-cell receptors to cause membrane fusion. For HCMV, fusion has been shown to occur in a pH-independent manner(66). After fusion, the viral capsid and tegument proteins are introduced into the host cell cytoplasm.

HCMV has been shown to utilize multiple receptors to facilitate viral entry, possibly reflecting the broad tropism of the virus. More than 10 HCMV envelope proteins have been identified (369), the most well-characterized of which are glycoproteins gB, gM, gL and gN. These glycoproteins form homodimeric (i.e. gB/gB) or heterodimeric complexes (i.e. gM/N, and gH/gL). The gB complex is required for virus entry and cell-to-cell spread(163). The gM/gN complex is thought to play a role in viral attachment to heparan sulfate proteoglycans (HSPGs) found on the surface of many cells(64). gH/gL complexes play a role in fusion together with gB complexes, possibly through integrin receptors(94). In addition, HCMV has been shown to interact with the epidermal growth factor receptor (EGFR)(64) and the DC-SIGN receptor (dendritic cell-specific ICAM3-grabbing non-integrin)(253).

For MCMV, the host cell receptors required for viral entry have not been characterized. MCMV gB and gH have been expressed as recombinant proteins(297), however their direct role in MCMV entry has not been shown. The MCMV m74 protein (a functional homolog of HCMV gO) has also recently been shown to contribute to the viral entry and cell-to-cell spread of MCMV in fibroblasts by forming complexes with gH (m75)(326).

The interaction of HCMV glycoproteins with host-cell membrane receptors has been shown to induce robust and rapid intracellular signalling (34, 35, 65, 180, 330). The same may also be the case for MCMV proteins, however experimental evidence is lacking. The interaction of HCMV glycoproteins with the host cell membrane has been reported to induce the interferon response in a number of cell types (34, 35, 65, 180, 330), suggesting viral particles are detected on the host cell surface as part of a rapid antiviral mechanism. This point will have important implications in the interpretation of data presented later in the thesis.

After viral entry, CMV capsids migrate along microtubules to the nuclear pore complex where viral genomic DNA enters the nucleus. This has been shown for HCMV(181). Upon entry of viral DNA to the nucleus, transcription of viral mRNAs occurs in a manner that is dependent on host cell transcriptional machinery, although

some viral tegument proteins have also been proposed to contribute (182). After transcription, MCMV proteins are expressed resulting in the establishment of productive infection.

Figure 1.2 - CMV viral entry. Viral glycoproteins bind to the host cell membrane to cause membrane fusion. Viral capsids enter the cytoplasm and tegument proteins are released. Capsids then migrate along microtubules to the nuclear pore where they are uncoated and viral DNA is introduced into the host cell nucleus.

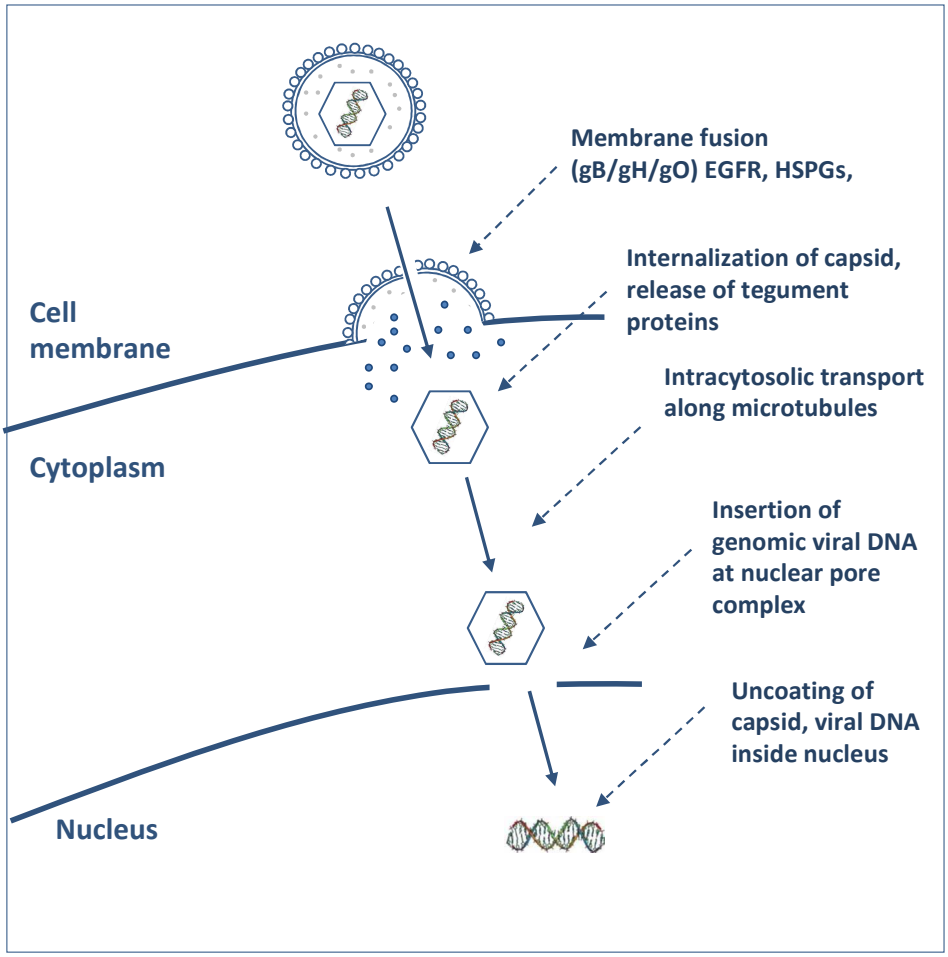

MCMV viral DNA replication occurs during the late stage of lytic infection and leads to the propogation of progeny virions. At the end of the lytic cycle, *de novo* MCMV particles are filled with nascent viral DNA (progeny genomes) and exported from the host cell, either via budding(252), or as a result of cell lysis. This process, however, is not entirely efficient as large numbers of non-infectious enveloped

particles and dense bodies (containing no viral DNA) are propagated during lytic infection. In the case of HCMV, dense bodies are composed of primarily the pp65 tegument protein(182). Abortive infection by MCMV and HCMV can also occur, whereby some or all components of the virus are synthesized, but no infective viral particles are produced. This can occur as result of infection with defective viruses, or as a result of nonpermissive cells inhibiting viral replication. In comparison to some other herpesviruses, CMV has a relatively slow replication cycle and can be characterized by enlargement of infected host cells (cytomegalia).

1.2.5 MCMV gene expression and genetics

During lytic infection, the MCMV genome is transcribed in a classical cascade fashion(188). *Immediate early* (IE) viral gene products are the first to be transcribed, independently of viral protein synthesis. The expression of MCMV IE genes is under the control of the *major immediate early promoter* (MIEP), a complex regulatory region that exhibits a high degree of functional similarity among the different members of the CMV family(340). The MCMV MIEP controls the expression of two bi-directional open reading frames (ORFs) encoding three spliced mRNA transcripts expressed abundantly at immediate early times (*ie1*, *ie2*, and *ie3*) (see Figure 1.3). The *ie1* and *ie3* transcripts share the same first three exons which are spliced either with a fourth exon into the mature *ie1* mRNA(188, 189) or with a fifth exon into the 2.75-kb *ie3* mRNA(249). The *ie2* mRNA of 1.75-kb is transcribed in the opposite direction and spliced from three separate exons(251).

The MIE region of MCMV is roughly colinear with that of HCMV, and splicing of IE mRNAs occurs in a similar manner (188-190, 249). In both viruses, transcription of the MIE genes is controlled by a strong enhancer region containing immune-stimulated transcription factor binding sites. Predicted or known sites for AP1, NFkB, CREB/ATF, SP1, RAR/RXR and NF1 have been located within the MCMV and HCMV MIEP regions(111, 112, 164, 166, 167, 212). It is hypothesized that these sites reflect the ability of the virus to utilize innate immune signalling pathways to drive viral gene expression, particularly as a result of NF-kB and IFN signalling.

The 88-kDa MCMV IE3 protein is essential for viral growth in cell culture and has an indispensable regulatory function during the lytic replication cycle of MCMV(12). On the basis of transient transfection assays IE3 also exerts a strong transcriptional trans-activator function on MCMV early promoters, and has auto-regulatory function through repression of the *iel/ie3* promoter(249, 350). The expression of downstream *early* (E) MCMV genes is dependent on *immediate early* gene products. *Early* genes are generally associated with functions related to viral DNA replication. After the expression of *early* genes, *late* MCMV genes are transcribed, dependently of the *early* gene products. Proteins encoded by *late* genes are generally associated with structural components of the MCMV virion required for egress(252).

Figure 1.3 - Schematic representation of MCMV genome and recombinant MCMV IE deletion mutants The MCMV genome is shown at the top and the immediate early (IE) region is expanded to show the MCMV enhancer (grey box) and structure of the *ie1, ie2* and *ie3* transcripts (line 1). Coding exons are shown in black with arrows indicating the direction of transcription and noncoding exons shown as white rectangles. Starting with the parental MCMV strain (line 1), the other strains MCMVdie3 (line 2), MCMVdie3rev (line 3), and MCMVdie1 (line 4), were generated by rounds of homologous recombination in E. coli. The deletion of the fourth exon of the *ie1* gene and the fifth exon of the *ie3* gene are marked by delta (Δ). The MCMVdie3rev strain (line 3) contains an inserted HCMV MIEP-GFP. Diagram adapted from Angulo *et al.* (12) and Ghazal *et al.* (86).

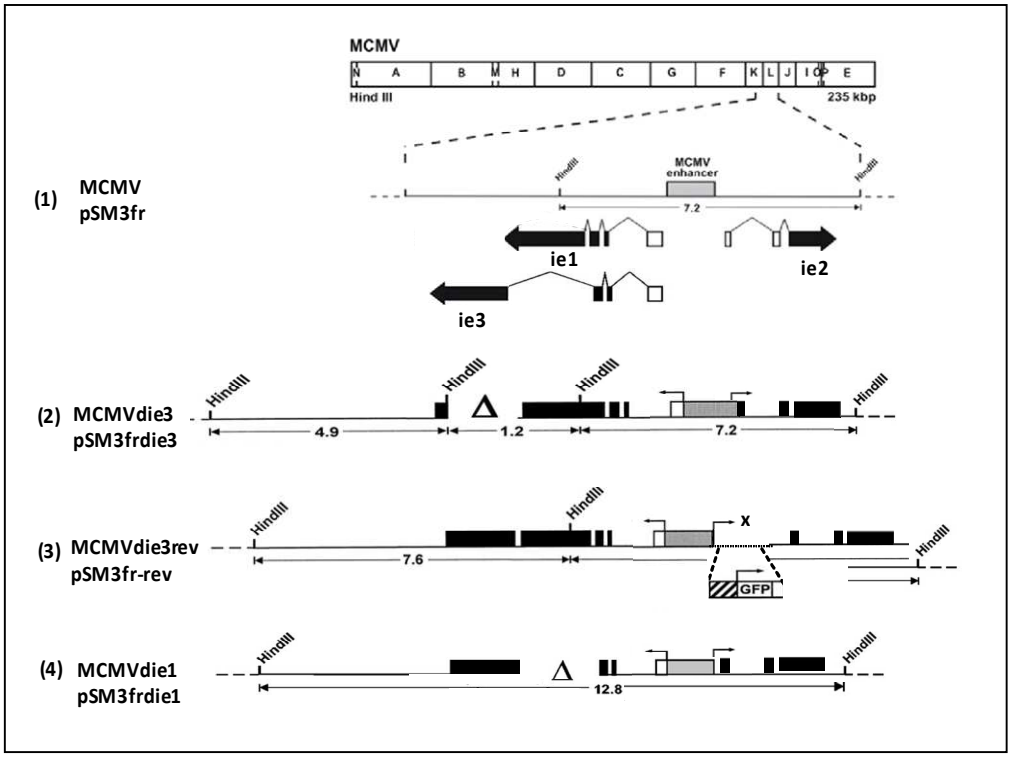

Recombinant deletion mutants have been generated for MCMV, including the removal of individual genes(29, 106) and the removal of large blocks of the MCMV genome(60). Deletion mutants for the *ie1* (MCMVdie1) and *ie3* genes (MCMVdie3) have been generated and characterized previously (reviewed in(49)). In the context of this thesis, it is notable that deletion of *ie1* attenuates MCMV virulence but does not alter replication in cell culture, and disruption of *ie2* causes no reported phenotype. Significantly, however, deletion of *ie3* however renders the virus incapable of replicating on fibroblasts even at high multiplicities of infection, and therefore the MCMVdie3 virus must be propagated on a complementing cell line.

1.2.6 CMV latency

MCMV and HCMV have the ability to establish latent (life-long and asymptomatic) infection in their respective hosts. Reactivation from latency represents a serious clinical threat in the case of immune- compromised patients, particularly organ transplant recipients. Although no precise molecular definition of CMV latency exists, latency is generally considered to be the presence of viral DNA in cells not producing infectious virus particles. Latent HCMV DNA has been detected in humans in cells of the monocyte lineage including macrophages, but not in mature B or T cells(332, 333, 338). Latent MCMV DNA has been detected in endothelial cells, bone marrow, and macrophages in latently infected mice(193). Reactivation from latency is generally thought to occur as a result of immunosuppression. Detection of IE1 transcription is generally used as marker of reactivation(158). Mechanisms of HCMV and MCMV latency have been reviewed in detail in recent years(158, 302).

1.3 Macrophages as a model cell for innate immunity

Both mouse and human CMV have a unique relationship with macrophages as part of their viral life cycle. MCMV(271, 334, 335) and HCMV(271, 334, 335) can both establish productive infection in macrophages and have been reported to use macrophages as a source for dissemination during acute infection. Macrophages have also been reported as a reservoir site for latency in mouse (172, 256, 286) and human(172, 256, 286) . MCMV replication is more favourable in differentiated macrophages than in immature monocytes(132) and HCMV has been reported to reprogram monocyte differentiation toward an activated M1 phenotype to favour viral replication(56). At least three MCMV genes (m139, 140, 141) have also been shown to play a key role in viral replication in monocyte/macrophages, but little or no role in replication in fibroblasts (131, 248, 312, 313) These genes are part of the US22 gene family(131, 248, 312, 313) including a MCMV CC chemokine homolog MCK-2 (m131-129) which promotes monocyte-assocaited viremia in mice (131, 248, 312, 313). These observations suggest MCMV and HCMV replication is favoured towards monocyte-derived macrophages in comparison to other cell types.

Macrophages are mononuclear phagocytes found ubiquitously in different tissues and represent a heterogeneous population of cells with varying function(154). Macrophages have the ability to phagocytose (engulf and digest) pathogens and other cells, and are involved in a range of physiological processes including immune surveillance, tissue repair, maintenance of homeostasis, and tumorigenesis(156).

The abundance and widespread tissue distribution of macrophages makes them well-suited to their role as a sentinel cell of the innate immune system. Macrophages are often therefore considered the first line of defence against invading bacteria and viruses in the mammalian immune system. Macrophages are capable of detecting foreign material and respond to infection rapidly through the up-regulation of antimicrobial defence mechanisms and secretion of cytokines. Macrophages also play an important role in antigen presentation and immune cell recruitment, particularly at sites of infection and inflammation(116).

1.3.1 Macrophage differentiation

Macrophages are leukocytes of the myeloid lineage and derive from haematopoietic progenitor cells produced in the bone marrow(109, 154). Progenitor cells leave the bone marrow as immature monocytes and circulate the bloodstream, undergoing partial differentiation. Circulating monocytes represent a mobile source of immune cells capable of differentiating into a wide range of macrophage sub-populations with varying function depending on the environmental signals they receive(154). Monocytes in the bloodstream come into contact with stimuli to induce entry into tissue sites, where further differentiation into mature macrophages occurs(109). The final differentiation phenotype of macrophages is defined by the combination of growth factors and cytokines present in the final tissue site (reviewed in (63, 86, 87)). The macrophage differentiation process, however, is driven primarily by two growth factors; the granulocyte-macrophage colony-stimulating factor (GM-CSF) and the macrophage colony-stimulating factor (M-CSF or CSF-1). Differentiated macrophages exhibit heterogeneity in phenotype and function based on their tissue location, and can have considerable plasticity upon migration to different sites in the body(108).

CSF-1 regulates the survival, proliferation and differentiation of monocytes into macrophages(55), and the survival and function of mature macrophages(123). CSF-1 binds to the colony stimulating factor-1 receptor (CSF-1R) to induce receptor phosphoylation, dimerization and downstream kinase signalling (40, 285, 343). CSF-1R expression is restricted to myeloid cells(123) and signalling through the CSF-1 receptor leads to changes in gene expression associated with macrophage cell survival and growth(130). Removal of CSF-1 from mouse macrophage cultures leads to apoptosis(144), suggesting CSF-1 is essential for macrophage survival.

1.3.2 Macrophage polarization

Macrophages are often classified into two distinct sub-groups based on their activation status. These are described as the "*classical*" (M1) and "*alternative*" (M2) activation phenotypes(240). *Classically* (M1) activated macrophages, are stimulated

by either IFNγ or microbial stimuli (e.g. LPS) and mount pro-inflammatory responses. Alternatively, (M2) activated macrophages are more associated with the resolution of inflammation and are thought to inhibit classical macrophage activation. M2 polarization is generally induced by IL-4 and IL-13, rather than by pro-inflammatory cytokines or microbial stimuli(121). M2 macrophages have also been further sub-divided into M2a, M2b and M2c sub-classes based on different combinations of cytokines used for differentiation. In general, M1 macrophages produce more antimicrobial effector molecules such as reactive oxygen species, nitrogen intermediates and pro-inflammatory cytokines(240), whereas M2 macrophages play more of an anti-inflammatory role with variable capacity to produce pro-inflammatory cytokines(121). M1 and M2 macrophages have also been shown to have distinct transcriptional profiles during differentiation and immune stimulation(239).

Although the classification of macrophages into M1 and M2 phenotypes may be considered by some to be useful in describing macrophage plasticity(233), the categorization is also considered to be an over-simplification of the potential spectrum of macrophage phenotypes *in vivo*. This issue has been discussed in depth recently(108), along with the ongoing debate regarding the distinct classification of macrophages and dendritic cells (DCs) into different cell types(155). In relation to CMV infection, the polarization state macrophages may contribute to tropism and permissiveness to infection(207), and define sites of latency for both MCMV(256) and HCMV(194).

1.3.3 Cytokine secretion

Activated macrophages contribute to inflammation by secreting pro-inflammatory cytokines including TNF, IL-1β, IL-6 and IL-18 which are regulated by NF-kB(71, 367). This results in a localized anti-microbial response and can also lead to TNF-mediated apoptosis(223). Macrophages can also be de-activated or given anti-inflammatory signals by other cytokines such as IL-10 and IL-4(121). IL-10 can

suppress the ability of macrophages to secrete pro-inflammatory cytokines including TNF(36, 37) and can inhibit antigen presentation(309).

Activated macrophages secrete a range of chemokines to recruit leukocytes to sites of infection and inflammation (206, 387). Some of the chemokines involved in this process include CCL3 (macrophage inflammatory protein-1α; MIP-1α), CCL4 (MIP-1β), CCL5 (RANTES), CXCL10 (Interferon gamma-induced protein 10, IP-10) and CXCL9 (Monokine induced by gamma interferon , MIG). These chemokines are up-regulated by NF-kB and IFN (315, 317). The coordination of cytokine and chemokine responses also controls natural killer (NK) cell recruitment which is of central importance to the clearance of viral infection. Chemokine networks have also been shown to play a key role in the NK-mediated clearance of MCMV(86, 316).

Plasmacytoid dendritic cells (pDCs) are another important cytokine-secreting cell and are closely involved in the response to MCMV infection. pDCs are a $CD4^{+}/CD11c^{-}$ sub-set of dendritic cells produced in the bone marrow(329) and are found in peripheral lymphoid organs. pDCs are the major source of type I IFN in response to virus infection *in vivo* and account for the majority of type I IFN production in response to MCMV(15, 68, 394, 395). pDCs also have the ability to activate T lymphocytes and express intracellular toll-like receptors to sense viral nucleic acids in early endosomes(168, 349). In humans, pDCs selectively express TLR7 and TLR9, but not other TLRs(115), suggesting they have a specified role in the detection of viruses and discrimination of self/non-self DNA.

1.3.4 Mouse bone marrow-derived macrophages (BMDMs)

For many years an *ex-vivo* experimental model system for mouse macrophage differentiation has been used to replicate the macrophage differentiation process. This model system consists of removing haematopoietic progenitor cells from mouse bone marrow cavities and differentiating the cells in culture in the presence of CSF-1 to produce 'mature' macrophages. This can be done either by using growth medium supplemented with recombinant CSF-1, or by using conditioned medium from a cell-line producing CSF-1(89). After a period of differentiation in the presence of CSF-1

(generally 5-7 days), monocyte cells can be assessed for the expression of macrophage-specific surface markers (such as CD11b and F4/80) to indicate the proportion of cells with macrophage-like phenotypes. At this point BMDMs will still be actively proliferating until receiving an immune-stimulus.

Although the BMDM model system for macrophage differentiation is not ideal (primarily because it relies on the activity of one growth factor rather than a combination of many as is the case *in vivo*), BMDMs have nonetheless provided a useful and tractable model for the study of macrophage function for several decades(157). During this time, BMDMs have been used for focused immunological and host/pathogen studies, and are now being used increasingly as a cell type for systems-level and functional genomics studies due to their transcriptional responsiveness, flexibility and plasticity. BMDMs have been used in system-level studies to investigate macrophage transcriptional networks dynamics in response to LPS(270, 294), and to show ATF3 is a key negative regulator of the TLR4-mediated LPS response(114). These studies combine global expression profiling analysis with *in silico* transcription factor binding site prediction. The global response to different TLR ligands has also been measured and computationally modelled in bone marrow-derived dendritic cells(7) and BMDMs have also been used as part of a broader review of the global transcriptional response to 77 different host-pathogen interactions(174).

1.4 Pattern recognition receptors and viral detection

The ability of host cells to detect pathogens is a central aspect of innate immunity and is achieved primarily through pattern recognition receptors (PRRs). PRRs are genome-encoded receptor proteins evolved specifically to bind pathogen-derived molecules. The concept of PRRs was first proposed at the molecular level by Charles Janeway over 20 years ago(171). Since then, PRRs have been studied extensively and shown to be expressed in most cells types, particularly in antigen-presenting cells (APCs) such as macrophages. Pathogen derived *non-self* structures, also known as pathogen-associated molecular patterns (PAMPs), range from components of the bacterial cell wall (lipopolysaccharide, muramyl dipeptide), to flagellin, to viral derived nucleic acids (dsRNA, uncapped ssRNA, cytosolic DNA) (see Table 1.2). PRRs capable of binding and detecting these foreign structures are expressed in different cellular locations based on criteria such as their target ligand, and life cycle of their target pathogen(s)(23).

1.4.1 The toll-like receptor family

The most well-studied PRR family is the toll-like receptor (TLR) family, first identified in Drosophila(107), and conserved throughout insect and mammalian species (reviewed in (30, 186)). TLRs are transmembrane proteins capable of detecting PAMPs derived from fungi, bacteria, parasites, or viruses via leucine-rich repeat (LRR) sequence motifs. TLRs can be found in various different intracellular and extracellular locations based on the ligand they are capable of binding. TLRs play a crucial role in the initiation of innate immunity and inflammation in a range of cell types. In mouse, the TLR family consists of 13 members, each of which are capable of binding a different ligand and signalling through down-stream adapter proteins (Table 1.2). The main TLRs capable of binding virus-derived PAMPs are *Tlr3, Tlr7, Tlr8* and *Tlr9* (viral nucleic acids in endosomes), and *Tlr2* and *Tlr4* which function as homo- or hetero-dimers with other proteins at the cell surface (reviewed in (362)).

Table 1.2 Mouse Toll-Like Receptors (TLRs), target ligands, and adaptors(30).

TLR	Associate Proteins	Ligands	Adaptors
TLR1/2	CD14, CD36, Dectin1	Ac3LP, Glycolipids	Myd88, Tirap
TLR2/6	CD14, Dectin	Ac2LP. LTA, Zymosan	Myd88, Tirap
TLR3		polyIC, dsRNA	TRIF
TLR4	CD14, MD-2	LPS, taxol, heparin, others	Myd88, Tirap, TRIF, TRAM
TLR5		Flagellin	Myd88
TLR7		ssRNA, imiquimod, others	Myd88
TLR9		CpG, DNA	Myd88
TLR11		Profilin	Myd88
TLR12		?	?
TLR13		?	?

1.4.2 RIG-I-like receptors (RLRs)

RLRs are a small family of PRRs characterized by a conserved DEAD protein motif (Asp-Glu-Ala-Asp). RLRs are putative RNA helicases involved in binding RNA within the cytoplasm and have, therefore, been implicated in the detection of RNA viruses. The primary RLR is the *retinoic acid-inducible gene-I* (RIG-I) which is an RNA-helicase protein capable of detecting virus-derived double-stranded RNA within the cytoplasm(385). Along with RIG-I, the MDA-5 (*melanoma differentiation associated gene 5*) and LGP2 genes make up the RLR family. All RLR members, in addition to binding RNA, have a conserved CARD-domain which is involved in the downstream activation of type I interferon (IFN) transcription. Engagement of RIG-I activates type I IFN transcription via signalling through downstream adapter proteins IPS-1, TRAF3, TANK, FADD, and RIP1, leading to activation of IRF3 and NF-κB (385).

1.4.3 Nod-like receptors (NLRs) and the inflammasome

Nod-like receptors (NLRs) are a large family of proteins with a conserved NOD motif for nucleotide binding and self-oligomerization(162). NLRs also have a conserved CARD-like caspase-recruitment domain(135) and a series of leucine-rich repeats (LRRs) at their carboxy-terminal, thought to be involved in the detection of microbial patterns. NOD signalling is generally linked to the regulation of apoptosis in response to pathogens, and 34 NLR genes have been predicted by bioinformatics studies to exist in the mouse genome(135, 162). The NOD genes (*Nod1* and *Nod2*) are involved in the induction of autophagy(356), and *Nod2* has also been shown to

signal through the mitochondrial antiviral signalling protein (MAVS; also known as VISA, CARDIF or IPS1) to induce the type I IFN response to viral infection(310).

Other NLR family members such as NLRP1, NLRP3 and NLRC4, along with other proteins such as IPAF and AIM2, can also assemble into large protein complexes known as inflammasomes. The AIM2 inflammasome has been linked to the detection of double-stranded bacterial and viral DNA in the cytoplasm(298). Activated inflammasomes regulate caspase-1 and the downstream production of pro-inflammatory cytokines interleukin-1β (IL-1β) and IL-18(241). Inflammasomes are linked to a range of different downstream processes, but play an important role in the cellular response to cytoplasmic DNA during viral infection (298, 380). More recently, RNA polymerase III was also identified as a PRR capable of detecting cytosolic DNA and inducing type I interferons through the RIG-I pathway(58). ZBP-1 and IFI16 have also recently been identified as innate immune sensors for intracellular DNA (191)(151).

1.4.4 PRRs and the detection of cytomegalovirus

The innate detection of CMV has been shown to occur through multiple PRRs. Structural HCMV envelope glycoproteins (gB) were first shown to the IFN response in fibroblasts in 2001 (330). Compton *et al*. later reported HCMV activates inflammatory cytokine responses via CD14 and TLR-2(65), and Boehme *et al.* showed soluble CMV gB proteins were capable of inducing IFN in an IRF3-dependent manner(35). Although HCMV envelope glycoproteins B and H were again later reported to be necessary for TLR2 activation in fibroblasts(34), alternative TLR2-independent pathways of activation were also reported during HCMV infection(180).

The first intracellular PRRs shown to have a role CMV detection were *Tlr3* and *Tlr9*, first identified by Bruce Beutler and colleagues in 2004 via mouse mutagenesis experiments(344). Mutation of the *Tlr3* or *Tlr9* genes resulted in highly increased susceptibility to MCMV infection in mice, particularly for mutation of *Tlr9*. MCMV

was further shown to activate the type I IFN response via either *Tlr9* or *Tlr3* pathways, however, neither pathway gave full protection against MCMV infection in the absence of the other(344). Further studies investigated the role of *Tlr9* in response to MCMV infection and found *Tlr9*-dependent recognition of MCMV occurs in interferon-producing APCs, leading to coordinated cytokine induction and activation of antiviral NK cells(200). CpG DNA was also found to play a pivotal role in *Tlr9*-mediated IFN-induction(169).

The expression of *Tlr9* varies between mouse and human, being expressed on all myeloid cells including macrophages in mice, but only on plasmacytoid dendritic cells (pDCs) in human(228, 357). In mouse macrophages, *Tlr9* expression is regulated by the PU.1 and ICSBP transcription factors and is strongly inducible upon IFNγ and LPS stimulation (325, 342). *Tlr9* expression is also strongly inducible in BMDMs in response to MCMV infection (see Results sections).

More recently, there have been numerous reports of additional pathways used for the detection of MCMV and HCMV. These include two studies from the group of Klaus Fruh claiming activation of the IFN-response by HCMV occurs via cytoplasmic double-stranded DNA, and not by glycoprotein B(75), and also that HCMV induces the IFN-response via the DNA sensor ZBP1(76). In addition, Kate Fitzgerald and colleagues showed the *Aim2* inflammasome is essential for host defence against MCMV infection *in vivo* using *Aim2*-deficient mice(298). In other studies, MCMV has also been shown to produce dsRNA during replication, and interact with protein kinase R during the antiviral response(48, 57, 365). The precise contribution of *Tlr3* in the detection and response to MCMV infection remains to be characterized.

The body of literature discussed above shows multiple PRRs can be used by the cell to detect CMV during infection. Consistent with this notion, the use of multiple PRRs has also been reported for a number of other viruses, including HSV1*(145, 231)*, vaccinia virus Ankara (MVA)(77), and sin nombre virus (SNV)*(290)*.

1.5 The innate antiviral immune response

1.5.1 Type I interferon (IFN)

Interferons (IFNs) are secreted cytokines capable of exerting potent autocrine and paracrine effects through the activation of signal transduction pathways and downstream transcriptional networks. IFNs exert their multiple cellular effects through the induction of *interferon-stimulated genes* (ISGs) with antiviral, anti-proliferative and immunomodulatory properties. Type I IFNs are induced as a result of PRR activation, and the type I IFN response is the primary mechanism of innate antiviral defence in most cells. The production of type I IFNs (IFN-α, IFN-β, IFN-ω, IFN-ε, or IFN-κ) is induced both *in vitro* and *in vivo* through engagement with viruses, microbial products or other pro-inflammatory stimuli(38). Type I IFNs act through a common cell-surface receptor composed of two ubiquitously expressed transmembrane proteins, IFNAR1 and IFNAR2 (Figure 1.4). IFNγ, the only type II IFN, shares little sequence homology with the type I IFNs and binds to a separate receptor complex(16). Both type I and type II IFNs are capable of inducing direct anti-microbial and anti-tumor mechanisms, up-regulating antigen presentation and arresting the cell cycle in macrophages and other cell types(38). Type III IFNs (also known as IFN-lambda or IL-28/29) are less characterized than type I and II, but are biologically similar to type I IFNs in exerting immune protection on epithelial surfaces(13).

Production of IFNs, whether it be *in vitro* or *in vivo*, occurs in a transient manner as inactive IFN genes are induced upon stimulation from pathogens, microbial products or synthetic ligands. The transcriptional induction of IFNβ is a particularly important event in response to viral infection, and the downstream consequences of IFNβ induction are widespread. For the induction of IFNβ to occur, a combination of transcription factors, (together known as the IFNβ enhanceosome) must converge on the IFNβ promoter(278) to induce the rapid expression of the IFNβ gene. Some of the key transcription factors involved in this regulatory event are interferon regulatory factors (IRF3 and IRF7), and members of the NFkB family. The secreted IFNβ cytokine can then bind to the high-affinity IFNAR receptor and induce further

signalling through the JAK-STAT (Janus kinase/Signal Transducers and Activators of Transcription) pathway (Figure 1.4). JAK-STAT signalling induces phosphorylation, dimerization and translocation of transcription factor complexes from the cytoplasm to the nucleus, primarily comprised of STAT1, STAT2 and IRF9 (known collectively as ISGF3)(149). The IFN-induced transcription factor complex then bind to consensus DNA sequences in the nucleus known as the *interferon-stimulated response elements* (ISREs). These sequences are located within promoter regions of downstream ISGs which become transcriptionally activated to exert the type I IFN response. The subsequent regulation of a diverse group of downstream interferon-regulated genes then mediates the biological effects of IFN.

Figure 1.4 Type I interferon signalling. During viral infection, PRRs bind viral-derived structures in different locations throughout the cell. PRR activation results in the formation of transcription factor complexes that bind the IFNα/β promoter and induce the production of type I IFNs. The action of type I IFNs is then mediated in an autocrine and/or paracrine manner through binding to dimeric IFNAR receptors, which signal through TYK2 and JAK1 proteins. This is followed by recruitment and phosphorylation of STAT proteins and IRF transcription factors to form the ISGF3 complex which translocates to the nucleus to induce IFN-stimulated gene expression via ISREs elements.

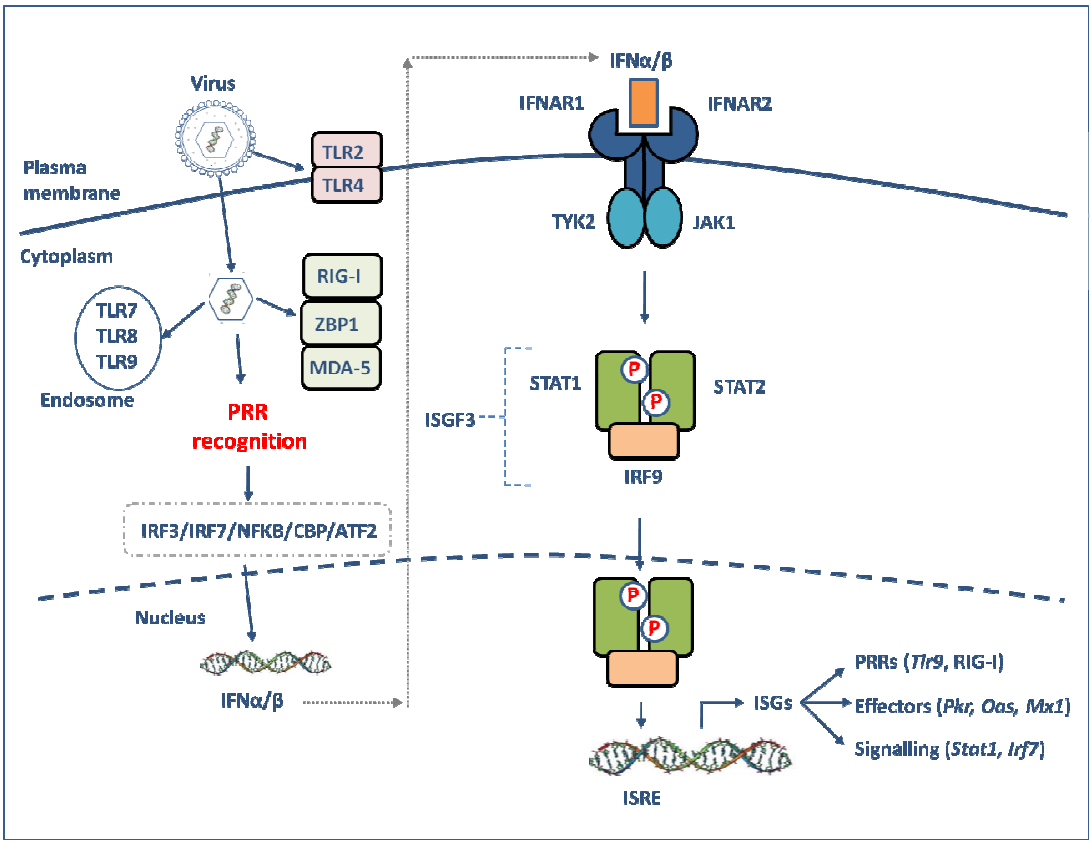

1.5.2 Interferon-stimulated genes (ISGs)

Although ISGs cover a broad spectrum of biological processes, gene targeting studies have distinguished four main antimicrobial effector pathways of the IFN-mediated antiviral response(311). These are the Mx GTPase pathway(129), the 2',5'-oligoadenylate-synthetase/RNase L pathway(32), the protein kinase R pathway(32) and the ISG15 ubiquitin-like pathway(136). Genes within each of these pathways encode proteins with direct antiviral capabilities involving inhibition of viral transcription, degradation of viral RNAs, inhibition of viral protein translation and modification of processes controlling viral replication(311). Many ISGs are also signalling proteins involved in regulation of the IFN-pathway, including IRF1, IRF7, STAT1, and STAT2. Genes involved directly in the detection of pathogens (i.e. TLR9, RIG-I, MDA-5, AIM-2) are also up-regulated as ISGs during the antiviral response.

Previous studies have attempted to characterize the global IFN response at the transcriptional level by measuring the sum of all gene expression changes occurring in response to IFNα, IFNβ or IFNγ cytokine treatment in different cell types (17, 62, 140, 152, 175, 176, 191, 209, 220, 234, 283, 300, 305, 352, 355, 377). As a result, databases have emerged summarizing the transcriptional data from many studies in an attempt to categorize ISGs into different classes (8, 72, 318). Although these databases have been useful to some degree, they have been limited in only describing IFN-responsiveness, rather than IFN-dependency at the gene expression level. They have only documented downstream gene expression after exogenous IFN treatment, but have not differentiated genes directly regulated by the type I IFN receptor from those regulated by secondary or tertiary factors. The only true way to mechanistically determine which genes are directly regulated through the type I IFN receptor is to to perform experiments using cells from animals lacking the Ifnar1 gene, then compare the response to that seen in cells from wild type animals. A systematic and genome-wide effort to do this has been lacking, especially for the study of viruses.

1.5.3 Literature review of studies using IFN-deficient mice

Mice lacking the type I IFN receptor (*Ifnar1*) and/or the IFNβ (*Ifnb1*) gene have been used to investigate virus susceptibility (28, 51, 80, 81, 120, 293) and other aspects of biology such as the functional crosstalk between type I and II interferons (122, 268), toll-like receptor (TLR) signalling(87, 341, 358), the response to dsDNA(328), the regulation of IFNα(90), IFN-feedback in B-cells(125), Il-6/TNFα signalling(160), and IFNβ pharmacokinetics(3). Despite these efforts however, gene expression profiling of IFN-deficient virus-infected macrophages from *Ifnar1-/-* or *Ifnb1-/-* mice has not been done.

The response to LPS in *Ifnb1-/-* macrophages has been characterized in some detail at the genome-wide level(355). In this study, distinct patterns of macrophage gene expression regulated by IFNβ were identified. Genes containing IFN-responsible elements in their promoter regions were also shown to have dependency on IFNβ. The study also found LPS-induced activation of signalling molecules such as AKT and STAT1 were significantly diminished in *Ifnb1-/-* macrophages. The diminished signalling in *Ifnb1-/-* cells, however, was not seen for p38, JNK, and ERK proteins. *In vivo* experiments conducted as part of the study showed *Ifnb1-/-* mice have an increased survival in response to LPS challenge, suggesting IFNβ contributes to LPS-induced lethality in mice.

In terms of virus infection, a comparable study has not been conducted a the genome-wide level. Perhaps the closest effort has been the profiling of infected mouse brain tissue from Balb/c (WT) and 129SvEv (WT and IFNAR-/-) mice infected with mouse hepatitis coronavirus (MHV)(293). In this study, gene expression data was generated at day 2 and day 5 from *in vivo* infected mouse brains and the results identified type I IFN-dependent and -independent transcriptional responses occurring. The study, however, was not conducted on the same genetic background for both mutant and WT mice, resulting in substantial variation in viral load between the mouse strains, eventually leading to complications in interpretation of the data. Other more recent studies have profiled antiviral gene expression in *Myd88-/-* and

Tlr9-/- cells in response to HSV (59), and transcriptional responses in tissues from *Stat1-/-* mice in response to coronavirus infection(393). These studies, however, have still not provided a temporal analysis of IFN-dependent gene expression.

Another study using murine embryonic fibroblasts (MEFs) from wild type and IFNα/β receptor deficient mice infected with influenza measured cellular gene expression at the single time point of 24hpi (120). This study found that antiviral gene expression was lower in the *Ifnar1-/-* cells compared to wild type, but inflammatory and apoptotic gene expression was equivalent. This study also reported higher levels of viral gene expression and increased levels of viral replication from *Ifnar1-/-* cells, which was consistent with some other studies (28, 51, 120, 293). Despite these observations however, the authors themselves conceded that "... *one may be able to better understand immunity during virus infection by infecting macrophages, dendritic cells, or lung epithelial cells isolated from mice lacking interferon receptors"* (Goodman *et al.* 2010). A transcriptional profiling analysis of *Ifnar1-/-* and *Ifnb1-/-* macrophages infected with productive and non-productive MCMV strains is presented in Chapter 6 of this thesis.

1.5.4 The nuclear factor-kappaB (NF-kB) response

Nuclear factor-kappaB (NF-kB) is a family of transcription factors forming homo- or hetero-dimers to regulate the expression of downstream genes involved in innate and adaptive immunity, inflammation, apoptosis, proliferation and the stress response(138). Upon detection of pathogens, the formation and activation of NF-kB transcription factor complexes occurs via the phosphorylation and degradation of inhibitory kB (IkB) signalling proteins in the cytoplasm. Rapid phosphorylation of IkB proteins then results in formation of the IKK complex and translocation of active NF-kB dimers into the nucleus. NF-kB activation then leads to the downstream induction of pro-inflammatory cytokines such as tumour necrosis factor-α (TNF-α) and IL-6(187). In mammalian cells, there are five members of the NF-kB transcription factor family including RelA (p65), RelB, C-Rel, p105 (NF-kB1; a precursor of p50) and p100 (NF-kB2; a precursor of p52)(187). The most abundant

NF-kB dimer in the innate immune response is a heterodimer composed of RelA and p50(138). NF-kB activation occurs either through IRAK and NEMO signalling, or via the TRIF pathway. Myd88-NEMO signalling (i.e. the canonical NF-kB pathway) generally leads to the induction of inflammatory cytokine genes, whereas TRIF-dependent signalling is more associated with the formation of IRF-3 homo-dimers and the activation of type I IFN(187).

1.6 Viral evasion of the innate immune response

Viruses have evolved an efficient ability to subvert and modulate the mammalian immune response at both the innate and adaptive level (6, 41, 105). This ability is a result of long periods of host/pathogen evolution during which viruses infect their hosts, multiply in large numbers, frequently undergo mutation and recombination events, and are then constantly subject to the strong selective pressures of the host immune system. Consequently, viral genomes evolve to become rich with immune-evasion genes. Cytomegalovirus and the other herpesviruses are prime examples, especially given their large genome sizes and long periods of species-specific co-evolution(69).

1.6.1 Viral subversion of PRR signalling

The ability of viruses to subvert cell-intrinsic innate immunity is particularly important for the establishment of infection and viral replication(308). One of the first aspects of the innate immune response the virus encounters, and therefore must subvert, is the pattern recognition receptors (PRRs). As a result, viruses have developed a range of strategies to avoid detection by PRRs during infection (reviewed in (41, 265). In particular, toll-like receptor signalling has been shown to be modulated by VACV and HCV proteins at key signalling hubs Myd88, IRAK2, and TRIF(41). Signalling through the RIG-I-like receptors is also modulated at various levels by RNA viruses such as influenza(254), paramyxoviruses(11) and poliovirus(22). Intracellular DNA detection pathways are also targeted by vaccinia virus, including inhibition of ZBP-1 (DAI) signalling (374) and inhibition of the

RNA polymerase III-mediated dsDNA-sensing pathway by the VACV protein E3(366).

1.6.2 Viral subversion of the IFN response

The ability of viruses to subvert the type I IFN response is common given the central role of IFN in host defence against virus infection (295). The subversion of type I IFN signalling has been shown for a range of different viruses(185, 280, 282, 306, 307, 376), including members of the herpesvirus family(141, 170, 262). The subversion of IFN by viruses can occur at various levels, including inhibition of IRF3 and IRF7 via the IKKs, modulation of NF-kB activity, and direct targeting of the IRFs (all reviewed in (41)). Several viruses also express viral IRF mimics that inhibit IRF3 and IRF7 signalling(178, 218, 227). The influenza NS1 protein, in particular, has been shown to have a complex and multifunctional ability to inhibit IFN-signalling at different levels. This occurs either through direct inhibition of type I IFN production, or through modulation of downstream IFN-stimulated genes (i.e. PKR, OAS/RNase)(128).

1.6.3 Innate immune evasion by CMV

The multifaceted ability of cytomegalovirus to modulate almost all levels of the immune response has been well studied and reviewed extensively in recently years (74, 225, 237, 288). The large ~230kb genome of MCMV encodes over 170 predicted viral ORFs(299), many of which have known or predicted roles in immune-evasion. Although much of the literature on MCMV immune-evasion is related to NK-cell function, the ability of MCMV to evade the type I IFN system has also been described. Of particular note is the reported ability of MCMV to disrupt IFNβ induction in fibroblasts by controlling pathways leading to the IFNβ enhanceosome(208).This study demonstrates MCMV is capable of inhibiting IFNβ expression, and inhibition is dependent on viral gene expression (does not occur using UV-MCMV). The study also showed IFN inhibition by MCMV leads to

blockage of IkBa degradation and a lack of nuclear IRF3 and ATF-2/c-Jun accumulation in fibroblasts, independently of the IFN-feedback loop.

The MCMV protein M27 has also been shown to modulate IFN-γ signalling by selectively binding and down-regulating *Stat2*(392). M27 modulates ISRE-dependent gene expression by altering *Stat2* phosphorylation, but has little or no effect on *Stat1* activation and signalling. This finding suggests a preference towards modulation of type I IFN signalling by M27. MCMV ORF M45 has also been shown to interact with the innate immune response by inhibiting pro-inflammatory and innate immune pathways through interaction with signalling protein RIP1(230, 364). M45 also has a potent anti-apoptotic function by inhibiting TNFα-induced activation of NF-κB, p38 MAPK. The M45 protein can inhibit TLR3-mediated NF-κB activation and ubiquitination of RIP1, and function as a viral inhibitor of RIP1 signaling(230). The MCMV ORFs m142 and m143 have also been shown to inhibit the protein kinase R (PKR)-mediated antiviral response by blocking PKR-mediated shutdown of protein synthesis during MCMV infection(48, 57, 365).

MCMV also modulates the cell cycle and can arrest cells in G1 and G2 phase during infection (379). This is thought to favour the conditions required for MCMV replication. The ability of MCMV to inhibit apoptosis is well-established and has been reviewed in detail in recent years (10, 119, 244). The many mechanisms by which MCMV interferes with the adaptive immune response have also been covered in recent reviews, particularly in regards to the inhibition of NK-cell function (74, 225, 237, 288).

For HCMV, there is an equally extensive body of literature on immune-evasion (reviewed in (170, 225, 237, 244, 257, 288)). In relation to the IFN response, the HCMV IE2 protein has been shown to block virus-induced IFNβ production(353) and inhibit CCL5 (RANTES) chemokine production(354). HCMV has also been shown to reprogram monocyte differentiation toward an M1 macrophage phenotype (56), and modulate the cell cycle and apoptosis during infection(244). It is notable that several key differences exist between mouse and human cytomegalovirus in

regards to immune evasion in their respective hosts, particularly at immediate early times of infection(243). Overall, however, both viruses encode a number of proteins capable of overcoming immune responses at a variety of different levels.

1.7 The innate immune response to productive versus non-productive viral infection

1.7.1 Principle

The ability to compare the host innate immune response to *productive* (live) versus a *non-productive* (attenuated, replication deficient) virus infection is attractive for a number of reasons. Firstly, an attenuated virus will not express *de novo* viral proteins and will therefore represent an inactive infection. By infecting cells with an attenuated virus, the host response to membrane fusion and viral entry can be measured in the absence of *de novo* protein activity. As a result, the response to structural components of the virion alone can be measured, and the innate antiviral response can be investigated in the absence of viral immune-evasion by *de novo* proteins (the effects of tegument proteins will still be seen). Secondly, by comparing the innate immune response to productive and non-productive viral infection directly, areas of the host response targeted by *de novo* viral proteins can be identified, and aspects of the response differentially regulated between the two conditions can be identified.

Traditionally it has been difficult to measure the innate immune response to a non-productive viral infection without using UV-inactivation, a process whereby viral DNA is cross-linked using UV-radiation, rendering the virus incapable of DNA replication(202). UV-inactivation is considered the “gold standard” technique for attenuating viruses. UV-inactivation has, therefore, been used to attenuate a number of different viruses including HCMV (34, 43, 65, 180, 273, 386), MCMV(18, 48, 373, 379), HSV (231, 263, 275), NDV/HCV(272), SFV(142), SNV(289), VV and Ad (63). The UV-inactivation technique, however, despite being the gold standard, has a number of limitations.

To inactivate a virus using UV-radiation, an increasing dose of UV must be administered until only minimal levels of viral replication are detectable. The inactivation must, therefore, be confirmed using either a measure of viral replication (i.e. plaque assay) or a measure of viral gene expression (i.e. RT-PCR). In both cases, it is difficult to completely ensure that all viral particles are inactivated. Technically, there are also issues related to variability between batches of UV-inactivation, and variability in instruments used to administer the UV-dose. Infectivity between viral stocks can also vary. UV-radiation is known to damage DNA to the point it can no longer replicate, but its effect on other viral structures such as RNA, capsid proteins, and membrane glycoproteins is largely unknown. It may be possible that UV-radiation damages viral proteins in addition to viral DNA, which has been suggested to be the case for Murine Oncornavirus(226). In addition, only a limited number of studies have provided an in-depth phenotypic characterization for an UV-inactivated virus(110, 279).

1.7.2 Literature review of the host response to productive and non-productive viral infection

Despite the above issues, many studies have been conducted measuring the innate immune response to wild-type viruses versus UV-inactivated virions(34, 43, 48, 63, 65, 142, 180, 231, 263, 272, 273, 275, 289, 373, 379, 386). A number of these studies have used microarrays to measure the transcriptional response at the genome-wide level. The response to HCMV versus UV-inactivated HCMV was measured in fibroblasts using microarrays(43), with results indicating considerably more mRNAs induced by UV-HCMV than by HCMV. This suggests a possible suppression of host gene expression by *de novo* HCMV proteins, and amongst the genes suppressed were IFNβ (*Ifnb1*) and pro-inflammatory cytokines (RANTES, interleukin 8, MIG, MIP1a, and MIP3b). An overlapping response to HCMV and UV-HCMV was also reported suggesting common induction of some genes by membrane binding and viral entry. The study was, however, limited by only a single time point measurement, and the use of fibroblasts rather than immune cells to conduct

infections. A very high multiplicity of infection (MOI) of 6 PFU/cell was also used in this study.

The host response to HSV and UV-HSV was measured in human embryonic lung cells in a similar fashion(263), and a suppression of ISGs by productive HSV infection was also reported. A high overlap between the response to UV-HSV and IFNα treatment was observed, and the study found that the establishment of an antiviral state occurred independently of viral replication in response to both HSV and UV-HSV. Again, however, the study was limited to a single time point measurement (24hpi), and the use of non-immune cells. Other studies using HSV-1 mutants lacking the VP16 or VHS (UL41) genes also found significantly higher levels of pro-inflammatory cytokines expressed in response to attenuated HSV-1 strains in comparison to wild-type strains (260, 345). Again, this suggested a suppression of innate immunity by productive viral infection. These studies found more genes up-regulated early in infection by the attenuated viruses, and more genes suppressed late in infection by wild-type HSV(345).

More recent studies have confirmed induction of the innate immune response does not require viral replication(211, 330, 359). Using UV-inactivated Sin Nombre Hantavirus (SNV) in human primary endothelial cells, Prescott *et al.* showed ISGs were induced in response to both live and attenuated SNV between 4hpi and 24hpi(289). In this study, cellular gene expression was measured at multiple time points (24hpi and 72hpi) by microarray analysis, and by qRT-PCR analysis (for MXA and ISG56) at early time points (0-12hpi). In all cases, strong ISG expression was reported in response to both live and UV-inactivated SNV. This study provides considerably more insight into the differential response, and suggests more genes are induced in response to inactivated SNV at early time points (<24hpi), but more genes were induced in response to live SNV at later time points (>24hpi). This was a key observation suggesting host cells respond differently to ongoing and sustained viral activity in comparison to inactive virions alone.

Collins *et al.* later used a range of UV-inactivated viruses to illustrate the innate response to virus entry requires IRF3 but does not require viral replication in fibroblasts(63). Noyce *et al.* then showed the antiviral response and induction of ISG expression could occur independently of IRF3-activation in response to Newcastle Disease Virus (NDV)(272). Other studies find early responses to SNV occur independently of IRF3, PRRs, and viral entry(290). The induction of type I IFN in myeloid dendritic cells (mDC) using UV-inactivated Semliki Forest virus (SFV) was also found by Hidmark *et al.* to require viral fusion, viral entry and IRF3 activation, but not require signalling through MyD88(142). These findings indicate variation in the way different viruses are detected by host cells depending on the context.

Notably, the Hidmark *et al.* study on SFV reported that induction of IFNα/β in dendritic cells (DCs) occurs far more rapidly than in fibroblasts. Furthermore, type I IFN induction in fibroblasts was dependent on viral replication, but in DCs occurred independently of SFV replication. Together, these observations suggest fibroblasts (MEFs) and antigen-presenting cells (DCs) use different mechanisms to sense and respond to viral infection. It also suggests DCs detect viruses more rapidly and with greater sensitivity than fibroblasts. The study on SFV did not include any genome-wide expression profiling analysis.

More recently, Paladino *et al.* conducted a study using HSV, VSV and HCMV showing the initial response to virus particle entry can occur independently of IFN, TLRs and RIG-I(275). This study proposed a model whereby increasing numbers of virus particles (or increasing MOIs) elevate the complexity of the cellular antiviral response from a basal intracellular response which is IFN-independent, to a sustained, heightened response involving IFN signalling, cytokine secretion and attraction of immune cell infiltrates.

Taken together, the body of literature on the host response to productive and non-productive viral infection suggests a) multiple mechanisms of innate viral detection occur within host cells, b) mechanisms of viral detection vary depending on the virus and cell type, and c) activation of the IFN response and induction of an antiviral state

can occur via multiple signalling pathways. Some of the studies also allude to the concept of distinct waves of immune signalling which vary in complexity and intensity based on the amount of virus present. Taken together, these studies have been informative but are individually limited by single time point measurements and the use of non-immune cell types such as fibroblasts.

Perhaps a more relevant study, therefore, is the recently conducted comprehensive gene expression profiling analysis of macrophages infected with wild type and attenuated strains of the intracellular bacterial pathogen Listeria monocytogenes (210). In this study, DNA microarrays were used to monitor the macrophage transcriptional response at 30, 60, 120 and 180 minutes post infection using combinations of host and bacterial mutants. The study found compartment-specific host responses occurring to the different bacterial mutants, despite similar activation of transcription factors between the different conditions. The results suggested combinatorial control of IFNβ induction can occur via recognition of both bacterial DNA and a bacterial cell wall component (muramyl dipeptide) as separate PAMP signals detected at different times and in different cellular locations during infection. The authors further suggest the innate immune system is capable of integrating differential responses from multiple PRRs to define the overall transcriptional response to infection.

An equivalent systems-level study for virus infection, whereby genetic mutants from both host and pathogen are combined with temporal profiling analysis in a highly relevant cell type, has been lacking. The aim of this thesis will be to address this gap in the field, and conduct an in-depth, systems-level analysis of the temporal response to productive and non-productive MCMV infection in macrophages, in greater depth than any other previous studies.

1.7.3 Use of a recombinant MCMV deletion mutant as an alternative to UV-inactivated virus

An alternative method for achieving a non-productive viral infection, in place of UV-inactivation, would be to use a genetic mutant virus that is mechanistically incapable of expressing viral proteins or replicating in the cell type of interest, yet still capable of viral entry and membrane fusion. This way the technical and biological variability and uncertainty introduced by the UV-inactivation procedure would be eliminated. Ideally, this genetic mutant virus would be capable of binding and entering host cells, but incapable of transcribing viral gene products or replicating. An example of this type of mutant is available for murine cytomegalovirus (MCMV), whereby removal of the *immediate early gene 3* was found to render the virus incapable of replication, even at high multiplicities of infection(12). The MCMV *ie3* gene is expressed in abundance at the beginning of the MCMV life cycle and has an essential trans-activator role in the control of down-stream MCMV gene expression. Upon deletion of this gene, the virus is incapable of replicating or expressing viral gene products beyond the immediate early (IE) region (12).

The mutant virus (termed MCMVdie3) is only capable of replication on a complementing cell line where expressing the IE3 protein is expressed in *trans* via a stably co-transfected plasmid. The complementing cell line (termed NIH 3T3-Bam25) was derived from NIH 3T3 cells and was constructed in parallel with the MCMVdie3 virus (12). A revertant virus (MCMVdie3rev), whereby the *ie3* gene was re-inserted into the MCMV genome, was also constructed and shown to be fully restoring of the virus replication cycle. The attenuated MCMVdie3 strain is capable of replicating to high titres in the complementing cell line and can therefore be propagated in large quantities and with consistency across batches. MCMVdie3 provides a unique alternative to the use of UV-inactivated virions for representing non-productive viral infection.

Replication-deficient mutants and complementing cell lines have also been constructed for HCMV genes via the deletion of IE2 86 (320) and IE1(259),

glycoprotein gB (UL55)(163), protein kinase UL97(291), and the UL52 gene(39). Nonviable deletion mutants and complementing cell lines have also been constructed for HSV genes (118, 124) and genes from other viruses (98, 106, 143, 274). More recently, a conditional and reversible fusion protein system was also developed for complementation of essential CMV proteins MCMV IE1 and IE3 and HCMV IE1, IE2, pUL51, and pUL77(117). Despite these efforts, the attenuated viruses have never been used as control reagents to represent non-productive infection in host-response experiments.

1.8 Rationale and predictions of the thesis

The central hypothesis of the thesis is that macrophages respond differently to productive and non-productive MCMV infections at the gene expression and protein level. This is worth investigating as it may help elucidate the ability of macrophages to detect and respond to different infectious conditions *in vivo*, thereby potentially influencing the outcome of downstream immunological events. It also relevant for considering why attenuated vaccines do not always generate effective immunity in comparison to live infections. To test the hypothesis experimentally, mouse bone marrow-derived macrophages (BMDMs) will be infected in parallel with wild-type and attenuated strains of MCMV, then dynamically profiled over a 24 period using a range of different techniques. Particular focus will be made on the transcriptional response to MCMV using time-course microarray profiling.

The main objectives of the study are;

a) Determine if the mutant MCMVdie3 can be used as an alternative to UV-inactivated virions to represent non-productive MCMV infection (Chapter 3)

b) Characterize the macrophage innate immune response to productive and non-productive MCMV infection at the systems-level (Chapter 4)

c) Identify macrophage transcriptional networks targeted for modulation during productive MCMV infection (Chapter 5)

d) Determine the role of type I IFN in regulating the macrophage innate immune response at the genome-expression level (Chapter 6).

Before proceeding to the experimental sections, it is important to first consider the events that may occur during MCMV infection of macrophages. Figure 1.5 shows the events known or predicted to occur during establishment of productive MCMV infection. Firstly, during viral entry, MCMV will activate PRRs either at the cell surface or inside the cell (**a**). This will result in the induction of type I IFN (**b**) and subsequent up- and down-regulation of IFN-dependent genes(**c**). In the cytoplasm, activation of the inflammasome is also predicted to occur via the detection of MCMV genomic dsDNA by AIM2. This will lead to NF-kB activation and induction of pro-inflammatory cytokines independently of type I IFN (**d**). Simultaneously, the MCMV genome will be transcribed and viral proteins will be expressed *de novo*, resulting in the establishment of productive MCMV infection (**e**). The activity of these *de novo* MCMV proteins is then predicted to influence a sub-set of macrophage antiviral genes (**f**). The activity of the *de novo* MCMV proteins is not predicted to influence the expression of all macrophage genes during the innate immune response. There is also predicted to be a secondary macrophage reponse induced by *de novo* MCMV proteins (**g**).

Figure 1.5 - Conceptualization of events known and predicted to occur during the establishment of productive MCMV infection

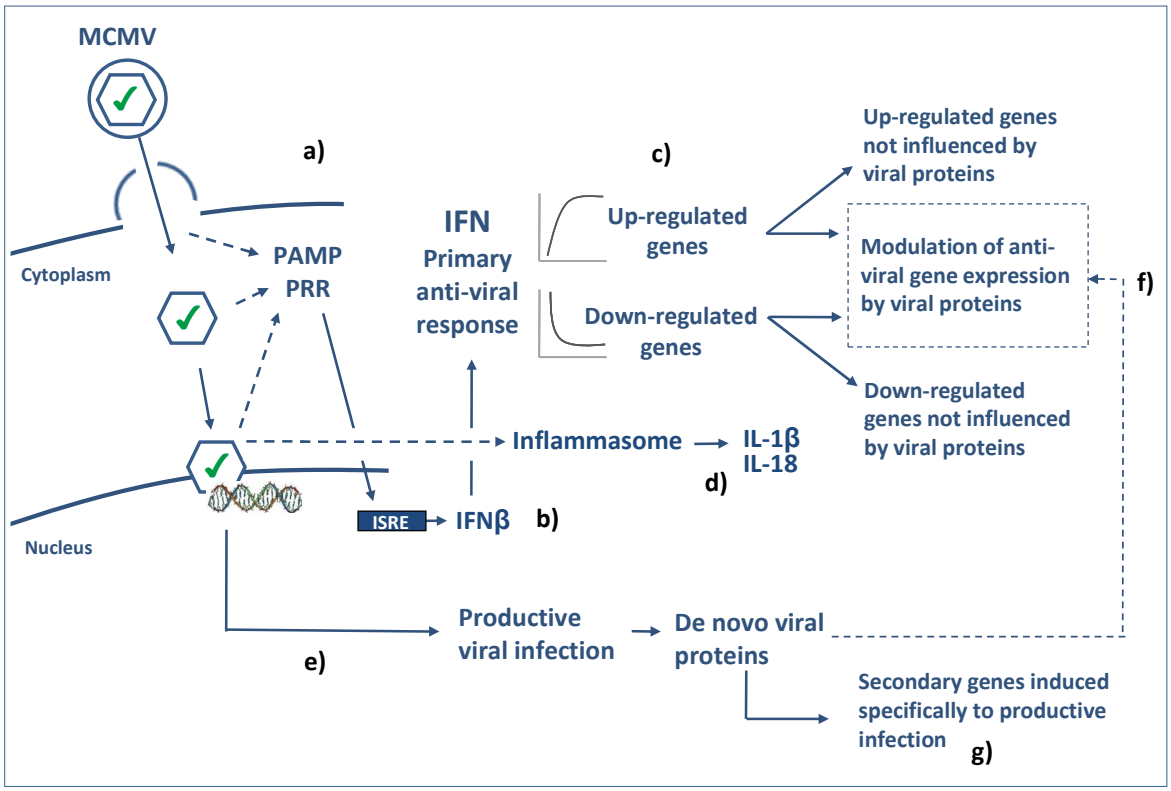

The consequences of infecting macrophages with a non-productive MCMV strain may be somewhat different from those described above. Figure 1.6 shows the events predicted to occur during non-productive MCMV infection using the attenuated MCMVdie3 strain. In a similar fashion to viral entry during productive MCMV infection, the attenuated MCMVdie3 virion is predicted to enter host cells and activate PRR signalling either at the cell surface and/or inside the cell (**a**). The MCMVdie3 virus, however, will be unable to transcribe viral genes or produce *de novo* viral proteins due to the removal of the *ie3* gene (**b**). Therefore the MCMVdie3 strain will be incapable of synthesizing viral proteins and establishing productive infection (**c**). As a result, in response to MCMVdie3, the expression of macrophage antiviral genes is predicted not be modulated by *de novo* viral proteins expressed beyond the IE region (**d**). The effect of tegument proteins packaged in the MCMVdie3 virion will still be functional in MCMVdie3-infected cells.

Figure 1.6 - Conceptualization of events known and predicted to occur during the establishment productive and non-productive MCMV infection.

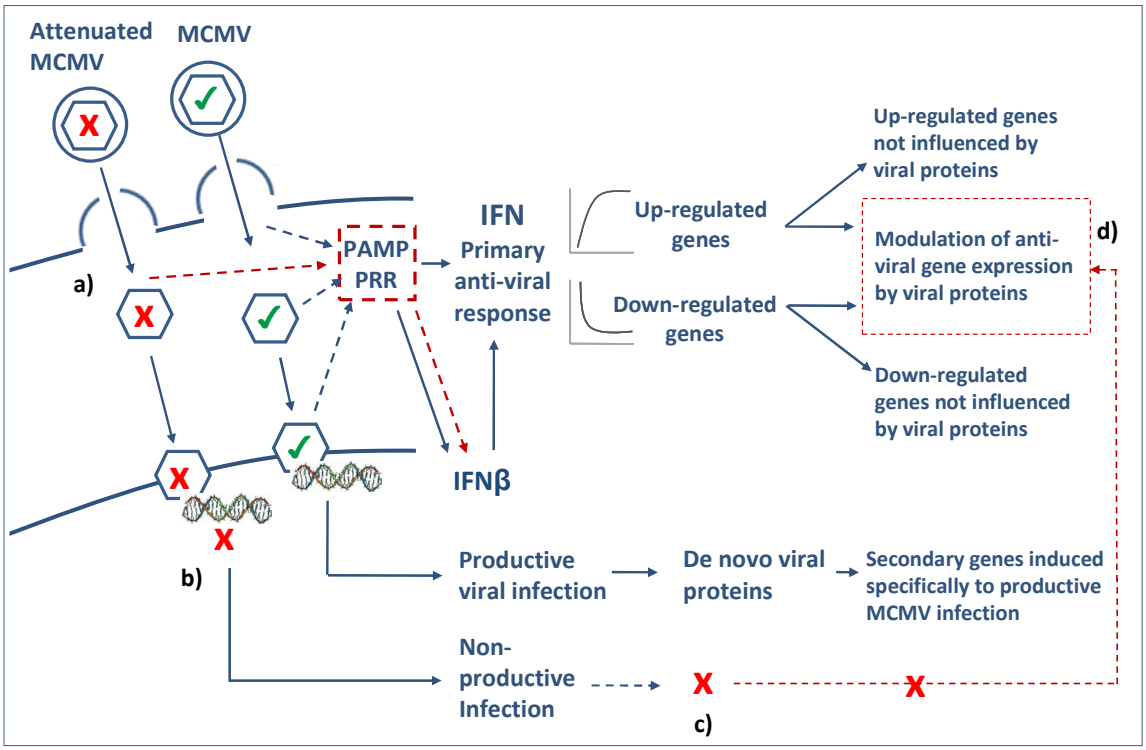

By comparing the macrophage response to productive and non-productive MCMV infection on a genome-wide scale using microarrays, alterations in macrophage gene expression elicited by productive MCMV infection will be identified. Such alterations may involve modulation of macrophage genes by *de novo* MCMV proteins, or host-regulated changes in response to ongoing and sustained MCMV activity. Both of these types of alterations in host gene expression will be informative of the macrophage/MCMV host/pathogen relationship. In addition, genes during the response can be classified into kinetic classes through use of multiple time point measurements, and knock-out cells derived from *Ifnb-/-* and *Ifnar1-/-* mice can be used to identify transcriptional events regulated by type I IFN.

Chapter 6 of the thesis will focus in particular on the role of type I IFN in regulating the macrophage transcriptome during the response to productive and non-productive MCMV infection. This will involve temporal gene expression profiling of wild type, *Ifnb-/-* and *Ifnar1-/-* BMDMs infected in parallel with MCMV and MCMVdie3.

Chapter 2

Materials and methods

2.1 Cell culture

2.1.1 Cell lines

The NIH 3T3 embryonic fibroblast-derived immortalized cell line (ATCC CRL1658 was obtained from American Type Culture Collection (Manassas, VA, USA) and grown in Dulbecco's modified Eagle medium (DMEM) (Lonza, UK) supplemented with 10% calf serum (Invitrogen, UK), 2mM glutamine (Lonza, UK) and 100U of penicillin/streptomycin (Lonza, UK) per ml. The NIH 3T3-Bam25 cell line was derived from NIH 3T3 by co-transfection of the pBAM25 plasmid as described previously(12). NIH 3T3-Bam25 was grown in the same medium as NIH 3T3.

2.1.2 Passaging cell lines

Cell lines were cultured at 37^{o}C and 5% CO_2 in tissue culture flasks (Corning, UK) according to sterile technique. Cells reaching 70-80% confluence were incubated with trypsin/EDTA (Lonza, UK) at 37^{o}C for 1-2 minutes and upon detachment, were transferred to a 15ml tube, mixed with fresh medium and centrifuged at 1000 rpm for 5 minutes. Cell pellets were re-suspended in 2-3ml fresh medium and re-seeded into sterile tissue culture flasks at a factor of 1:2 or 1:3. This process was repeated every 2-3 days up to a maximum of 25 passages.

2.1.3 Cell counting and seeding plates

To count cells after trypsinization and re-suspension, 10µl of suspended cells was diluted in 90µl of Trypan Blue Stain, 0.4% (Invitrogen, UK) to make a 1:10 dilution. 10µl of this dilution was injected directly into a haemocytometer under a cover slip and viable cells counted in the central 16 marked squares. Viable cells in the marked squares were counted, and cells per ml were calculated by multiplying the number of

cells counted by the dilution factor (in this case a factor of 10), by the relative area of the haemocytometer square (10^4 cm^3). Counting cells was repeated on 4-6 replicates for each sample and the average count was taken. Counted cells were then further diluted in warm medium and seeded at specific densities in different sized sterile tissue culture flasks, dishes or plates (Nunc, UK). Seeding densities for NIH 3T3 and NIH 3T3-Bam25 cells in different sized tissue culture plates were as follows;

- 48-well plates - $4x10^4$ cells in 500µl medium per well
- 24-well plates $1x10^5$ cells in 1ml medium per well
- 6-well plates $3x10^5$ cells in 2ml medium per well

2.1.4 Cryopreservation of cells

To preserve NIH 3T3 and NIH 3T3-Bam25 cells for long term storage, cells were centrifuged as previously described and re-suspended in freezing medium containing DMEM 40%, calf serum 50%, and dimethyl sulfoxide (DMSO) 10%. 1ml aliquots were placed in cryovials (Corning, UK) containing $1x10^6$ resuspended cells each. Cells were frozen at –80°C overnight to avoid fast cooling and breaking of the cell membrane and after 24 hours cells were transferred to a liquid nitrogen container (-170°C) for long-term storage.

2.1.5 Thawing cells from liquid nitrogen

For resurrection of frozen cell lines from liquid nitrogen, individual vials of cells were thawed in a water bath at 37°C and added to 10ml of fresh warm growth medium in a sterile 15ml tube. Cells were then centrifuged at 1000 rpm for 5 minutes. Supernatants were discarded and cell pellets re-suspended in 7ml fresh growth medium and transferred to 25 cm^2 tissue culture flasks and propagated as described previously.

2.1.6 Preparation of L929 conditioned media for macrophage differentiation

The L929 cell line was obtained from Sigma, UK (85011425) and is a subclone of the parental cell strain L derived from subcutaneous areolar and adipose tissue. This cell line is used to produce conditioned media containing Macrophage Colony Stimulating Factor 1 (CSF-1) for differentiating bone marrow monocyte progenitor cells into macrophages. CSF-1 is a cytokine secreted by mesenchymal cells that stimulates survival, proliferation and differentiation of bone marrow hematopoietic stem cells into mature monocytes. The L929 cell line is grown in DMEM/F-12 media with GlutaMAX (Invitrogen, UK) containing 10% fetal calf serum (Lonza, UK) and 100 units of penicillin/streptomycin (Lonza, UK) per ml. L929 cells were grown in 175 cm^2 flasks for 14 days at which point the supernatant was removed, aliquotted into 50ml tubes and frozen at -20^oC.

2.1.7 Bone Marrow Derived Macrophages (BMDMs)

2.1.7.1 Mouse bone marrow progenitor cell isolation and macrophage differentiation

Bone marrow monocyte progenitor cells were extracted from mouse femurs from wild type C57BL/6 mice (BRR, University of Edinburgh, UK), and C57BL/6 mice lacking the *Ifnb1* or *Ifnar1* gene (Institute of Animal Breeding and Genetics, University of Vienna, Austria). All mice were aged between 10-12 weeks and male. Mice were sacrificed via cervical dislocation and femurs extracted under sterile conditions by animal technicians. Mouse femurs were cut at both ends and the marrow cavity was flushed with growth medium with cells recovered in a 50ml tube. Bone marrow cells were centrifuged at 1000 rpm for 5 minutes and re-suspended in fresh growth medium. Cells were counted as previously described and seeded in 24-well plates at a density of $2.5x10^5$ cells in 1ml per well. Precursor cells were cultured for a 7-day differentiation period into mature bone marrow-derived macrophages (BMDMs) in the presence of M-CSF in L929 conditioned media, with media changes on days 3 and 5. In the case of knockout mice, femurs were extracted at the Institute of Animal Breeding and Genetics, University of Vienna, Austria and transported on ice overnight to Edinburgh, UK.

2.1.7.2 Characterisation of BMDMs by flow cytometry

To determine the proportion of macrophage-like cells in the BMDM cultures after the seven-day differentiation period, fluorescence-activated cell sorting (FACS) was used to measure the expression of macrophage-specific cell surface protein markers CD11b and F4/80. The FACS procedure consisted of binding specific antibodies to cell surface expressed proteins and adding fluorescently labelled secondary antibodies for detection. Fluorescently labelled cells were sorted one cell at a time based on their individual florescent emission signal to determine the proportion of macrophage-like cells in the heterogeneous cell population.

For flow-cytometry analysis, BMDMs were washed twice with PBS on day seven of the differentiation period, then scraped and removed from tissue culture dishes and transferred to polystyrene FACS tubes (BD Falcon, UK). Tubes were centrifuged at 1000g for 5 minutes at 4°C. After discarding the supernatant, cells were washed with cold PBS and resuspended in 100µl of blocking solution (10% mouse serum) for 30 minutes on ice to avoid non-specific antibody binding. Allophycocyanin (APC) conjugated monoclonal rat-anti-mouse F4/80 (IgG2a·, Caltag Laboratories, UK) and fluorescein isothiocyanate (FITC) conjugated rat-anti-mouse CD11b (IgG2b·, eBiosciences, UK) or their isotype controls were added to the cells (1/100 dilution in blocking solution) and incubated for a further 30 minutes in the dark. Cells were washed with cold PBS, centrifuged and resuspended in 250µl of cold PBS. A FACScan instrument (Becton Dickinson, UK) was used to perform FACS analysis of the samples and the data were analysed using FlowJo software (Treestar, USA). FACs analysis was performed with the assistance of Dr Kevin Robertson from The Division of Pathway Medicine (University of Edinburgh, UK).

2.2 General methods for virology

2.2.1 Viruses

The parental murine cytomegalovirus (MCMV) strain was derived from recombinant bacterial artificial chromosome clone pSM3fr MW97.01 as described previously (250, 370). Recombinant MCMV immediate early (IE) gene deletion mutants for the *ie1* gene (MCMVdie1) and *ie3* gene (MCMVdie3) are also described previously ((12, 113) and reviewed in (49)). Construction of a revertant virus for the *ie3* deletion mutant (MCMVdie3rev) plus deletion mutants for ORFs M27 (MCMVdM27) and M45 (MCMVdM45), and large-scale deletion mutants for MCMV gene blocks 1 (m01-m16), 6 (m144-m157) and 7 (m158-m170) has also been described previously (2, 12, 45, 60, 61, 230). Large deletion mutants were kindly provided by Lars Doelken, Max von Pettenkofer-Institute, Munich, Germany.

2.2.2 Viral stock preparation

To propagate bulk viral stocks for each MCMV strain, confluent 175cm^2 flasks of NIH 3T3 cells were infected at MOI of 0.01 PFU/cell in 17ml of growth medium per flask. Using 6-9 flasks per viral stock, infections were left for 5-7 days until a nearly complete cytopathic effect (CPE) was observed for each virus. At this stage supernatant was harvested from multiple flasks, combined, centrifuged at 1000 rpm for 5 minutes, then separated from cell debris pellets and aliquoted into sterile 50ml tubes and stored at -80^{o}C. This procedure was applied to all viral strains except MCMVdie3 which was propagated in the same way but on the complementing cell line NIH 3T3-Bam25. In some cases viruses were propagated in smaller vessels to increase viral titre of seed stocks before preparation of bulk stocks.

2.2.3 Concentration of viral stocks

To increase the titre of viral bulk stock preparations, viruses were concentrated using high-speed centrifugation on a sorbitol cushion. Frozen viral bulk stocks were thawed slowly for 30 minutes at room temperature then in a water bath at 37^{o}C until

completely thawed. In 30ml centrifuge tubes (Sorvall, UK), 10ml of 20% sorbitol solution (containing 0.01 M Tris-buffered saline (TBS) at pH 7.8) was added gently down the side of each tube followed by 20ml of viral supernatant added carefully above the sorbitol cushion. Tubes were balanced within 0.5 grams of each other and centrifuged at 26,000g for 70 minutes at 4^{o}C in a high-speed centrifuge. After centrifugation, supernatant was removed and pellets re-suspended in 1ml DMEM growth medium containing 3% CS per tube. Re-suspended pellets were pooled together and aliquoted for storage at -80^{o}C.

2.2.4 Titration of virus by plaque assay

To determine the infectivity of viral stocks, plaque assays were performed on NIH 3T3 or NIH 3T3-Bam25 monolayers in 48-well plate format. The plaque assay is the gold standard technique to quantify the infectivity of a virus or measure the amount of infectious virus within a sample. The principle of a plaque assay is to perform serial dilutions or titration of the virus by a factor of ten, and then use the dilutions as innoculums to infect separate monolayers of cells. The infected cell monolayers are then covered with a thick layer of growth media containing agarose in order to prevent spreading of the virus during infection. After four days the number of plaques (individual areas of lysed cells) are counted per dilution and used to calculate the number of plaque forming units (PFU) per ml.

For MCMV, low passage NIH 3T3 or NIH 3T3-Bam25 cells were seeded for 24 hours in growth medium containing 10% CS in 48-well plates at a seeding density of $4x10^{4}$ cells in 500µl per well. A 10-fold serial dilution of the virus was performed in triplicate from 10^{-1} to 10^{-6} in a round-bottom 96-well plate by taking 11µl of virus into 100µl of growth media containing 3% CS over six dilutions. Depending on the expected titre of the virus, 100µl of up to four of the six dilutions were transferred onto confluent cell monolayers in 48-well plates. Infected cells were incubated for an adsorption period of 1.5 hours at 37^{o}C. After the adsorption period, cells were washed with warm growth media. During this time, 2.5% agarose was heated to boiling point in a microwave and then cooled for 60 seconds. 1ml of 2.5% agarose

was added to 9ml of warm growth media (3% CS) in a 15ml tube and mixed vigorously for 10 seconds. The wash media was aspirated from the cell monolayers and replaced with 500µl of the 2.5% agarose-medium mixture which was added very gently down the side of each well. Cells were incubated for four days at 37^{o}C and then number of plaques per well of the 48-well plate were counted on day 4. The number of plaques counted calculates the PFU/ml using the following equation:

PFU/ml = number of plaques counted * individual dilution factor * 10

Plaque counts were averaged over three replicates and over multiple dilutions if plaques appeared at more than one dilution. Once the titre (PFU/ml) for a given virus was calculated, it could be used to determine the infectious dose or multiplicity of infection (MOI) for future experiments. The MOI corresponds to the number of plaque forming units (PFUs) delivered per cell.

2.2.5 Viral growth curves

To monitor rates of MCMV infectivity and viral replication over the course of infection under a given set of conditions, growth curve analysis was performed whereby supernatants were taken periodically from an infected culture of cells and titred using plaque assay. To perform growth curve analysis, confluent cell monolayers for cell-types of interest were infected in 24-well plates. After infection, cells were aspirated, washed with warm media, and replenished with fresh growth media containing 10% CS. 70µl of supernatant was removed from the culture every 24 hours thereafter and stored at -80^{o}C. After 5 or 6 days the infection was ceased and supernatants from each day were titred using plaque assays to determine the relative PFU/ml of virus over the course of the infection. Multi-step growth curves use low MOIs (typically 0.01 PFU per cell) resulting in multiple rounds of viral infection. Single-step growth curves use high MOIs (typically 2 or more PFU per cell) and result in rapid increases in viral titre after only two days of infection.

2.3 Infection / stimulation of cells for downstream molecular analyses

For all MCMV infection experiments involving downstream molecular analysis, cells are first infected with a small volume of virus-containing media (3% CS) for an adsorption period of 1.5 hours at 37^{o}C. This allows sufficient time for viral entry and establishment of infection to occur. At the end of the adsorption period the viral innoculum is removed by aspirator and cells are washed with warm media then replenished with fresh growth medium containing 10% serum. For time course analyses, T_0 or zero hours post infection (0hpi) always corresponds to the *end* of the viral adsorption period (i.e. 90 minutes after first contact). For mock infections, standard growth medium containing 3% serum was used as the innoculum but with no virus added. Mock-infected were washed and replenished with fresh medium as per normal infections.

For drug treatment experiments, cells were pre-treated in the presence of either 50µg/ml cycloheximide (Sigma UK, C7698) or 20µM Ganciclovir (Sigma UK, G2536) for 60 minutes in 10% serum growth medium. During infection, 3% serum medium in the presence of the same concentration of the drug was used. Finally, cells were washed and replenished with fresh medium (10% serum) also containing the same concentration of the drug. For interferon beta (IFNβ) and polycytidylic acid potassium salt (polyIC) stimulation experiments, cells were treated with a regular volume of standard growth medium containing 10 units per ml of recombinant IFNβ (R&D Systems, UK) or 10µg/ml of polyIC (Enzo, UK). The IFNβ and polyIC were left in the growth medium for the duration of the experiment and cells were not washed. In the case of time course analyses, cells were stimulated with IFNβ and polyIC with the same timing as viral infections. This meant that T_0 for IFNβ and polyIC stimulation experiments actually corresponded to 90 minutes after the initial contact of the stimulant with the cells to match the 1.5 hour adsorption period of the virus.

2.4 Nucleic acid purification

2.4.1 RNA extraction

2.4.1.1 Extraction of total RNA using Invitrogen RNA Purification System

To extract RNA, cell monolayers were aspirated to remove all growth medium and cells were lysed directly in the wells of tissue culture plates by adding either 250µl (24-well plates) or 500µl (6-well plates) per well of Trizol reagent (Invitrogen, UK) or RNA lysis buffer containing 1% 2-mercaptoethanol (Invitrogen, UK). Plates were tilted up and down to distribute the lysis reagent evenly and after 5 minutes samples were transferred to sterile 1.5ml microcentrifuge tubes. For 24-well plate experiments, two wells were pooled together into one 500µl sample. All samples were stored at -80^{0}C until RNA extraction began. On the day of RNA extraction, frozen Trizol or RNA lysis buffer samples were thawed to room temperature and flick mixed until homogenous. For Trizol samples, 150µl chloroform was added to each 500µl sample and tubes were capped and mixed vigorously by shaking for 15 seconds. Trizol samples were incubated at room temperature for 2-3 minutes until the aqueous phase began to separate. At this stage Trizol samples were centrifuged at maximum speed (~12,000g) at 4^{o}C for 15 minutes and after centrifugation the clear aqueous phase containing RNA was removed from the thick pink layer of Trizol containing cellular debris and proteins. 200-250µl of the aqueous phase was removed and transferred to a sterile 1.5ml microcentrifuge tube and a second extraction step was performed by adding another 100µl of chloroform and repeating the procedure. The aqueous phase after the second extraction (now generally only around 190µl) was removed and added to another sterile 1.5ml microcentrifuge tube. An equal volume of 70% ethanol (190µl) was added to obtain a final ethanol concentration of 35%. For RNA lysis buffer samples, lysates were thawed, flick mixed and transferred to QIAshredder columns (Qiagen, UK) and centrifuged for two minutes at 12,000g. An equal volume of 70% ethanol (350µl) was added to the samples to obtain a final ethanol concentration of 35%. At this stage, all samples whether derived from Trizol or lysis buffer were mixed by vortex for three seconds and transferred to spin cartridges (Invitrogen, UK) capable of specifically binding RNA. Spin cartridges

were centrifuged at 12,000g for 15 seconds at room temperature to bind RNA then washed twice with 250µl of wash Buffer I (Invitrogen, UK), with centrifugation at 12,000g for 15 seconds at room temperature after each wash. The flow-through was collected in a collection tube beneath the spin cartridge and discarded after each wash. After the second wash, 80µl of DNase mix (Purelink DNase set, Invitrogen, UK) containing 8µl 10X DNase I reaction buffer, 10µl resuspended DNase (~3U/µl) and 62µl RNase-free water per sample was added directly to the membrane of each spin cartridge. Samples were incubated at room temperature for 15 minutes to ensure complete DNase I digestion of genomic DNA. After DNase treatment, spin cartridges were washed twice with Wash Buffer I (250µl) and twice with Wash Buffer II (500µl) by centrifugation at 12,000g for 15 seconds at room temperature after each wash. Flow-through was discarded and the spin cartridge is reinserted back into the same collection tube after each wash. After the wash steps, spin cartridges were centrifuged at 12,000g for one minute at room temperature to dry the membrane with attached RNA. The collection tube was discarded and the spin cartridge inserted into a sterile 1.5ml recovery tube and eluted with 38µl of RNase-free water added directly to the centre of the membrane. After incubation at room temperature for one minute to elute the RNA, the spin cartridge was centrifuged with the recovery tube for 2 minutes at 12,000g at room temperature. Eluted, purified RNA was assessed for concentration and quality measures by spectophotometer before being stored at -80^{o}C.

2.4.1.2 Extraction of viral RNA/DNA from cell-free samples

The PureLink Viral RNA/DNA Kit (Invitrogen, UK) is designed to isolate viral nucleic acids from cell-free samples through the use of higher lysis temperatures, proteinase K and selective binding of viral nucleic acids by carrier RNA (yeast tRNA). The addition of carrier RNA increases binding of viral nucleic acids to a silica matrix and reduces viral nucleic acid degradation. This kit could be used to extract viral RNA/DNA from 200µl samples of viral stocks or from any 200µl cell-free tissue culture samples from viral infections. In each viral RNA/DNA preparation, 25 µl of proteinase K was added to a sterile microcentrifuge tube to

which 200µl of the cell-free sample was added. To lyse samples, 200µl of Lysis Buffer (containing 5.6 µg Carrier RNA) was added before the tube was vortexed for 15 seconds and incubated at 56^{o}C for 15 minutes. 250µl of 100% ethanol was added and mixed by vortexing for 15 seconds then incubated at room temperature for five minutes. The lysate was transferred to a Viral Spin Column in a collection tube and centrifuged at 6,800g for one minute. The flow-through was discarded and the spin column placed into a new Wash Tube. The column was washed twice with 500µl Wash Buffer (W5) with ethanol by centrifugation for one minute at 6,800g. The flow through and collection tube were discarded and the spin column was placed in another clean Wash Tube. Spin columns were centrifuged at maximum speed for one minute to remove any residual Wash Buffer (W5) then placed in a clean 1.7-ml Recovery Tube and eluted with 10-50µl sterile RNase-free water added to the centre of the cartridge membrane. After incubation at room temperature for one minute, spin cartridges were centrifuged at maximum speed for one minute to elute the nucleic acids.

2.4.1.3 Quality assessment of total RNA

RNA concentration and purity were determined using a Nanodrop ND-1000 spectrophotometer (Nanodrop Technologies, Germany). 1.5µl of purified RNA sample was loaded onto the spectrophotometer which places the sample between two optical surfaces, passes UV light through the sample and determines the emission path length at 230, 260 and 280nm. The absorption ratio at 260/280nm indicates RNA purity, and the ratio at 260/230nm indicates presence of organic (phenol, chloroform) contaminants within the sample. RNA samples with a 260/280 ratio <1.8 or a 260/230 <1.5 were deemed poor quality and excluded from further downstream analysis. To assess RNA integrity, the 2100 Bioanalyzer (Agilent, CA, USA) was also used to run an automated denaturing agarose gel on 1µl of purified RNA sample

2.4.2 DNA extraction

For DNA extraction, cells were washed twice with ice cold PBS and scraped thoroughly in the second PBS wash. Scraped cells were transferred to sterile 1.5ml microcentrifuge tubes and centrifuged at 1000rpm for 5 minutes. PBS was removed and cell pellets were re-suspended in 200µl of NP-40 lysis buffer (Sodium Chloride 150 mM, NP-40 1%, Tris, pH 8.0 50 mM) and incubated on ice for 20-30 minutes. After lysis, samples were centrifuged at maximum speed for 10 minutes at 4^{o}C to remove cell debris. Supernatants were transferred to sterile 1.5ml tubes and stored at -80^{o}C. To extract viral DNA from total DNA samples, the PureLink Viral RNA/DNA Kit (Invitrogen) was used as described in 2.4.1.3.

2.5 Quantitative Polymerase Chain Reaction (qPCR)

2.5.1 Quantification of viral genome copy number using qPCR

A custom qPCR assay was developed to measure the quantity of MCMV genomes in infected cell samples and viral bulk stocks. The assay was used to complement the gold standard plaque assay as a measure of viral infectivity, but also provided a more sensitive and quantitative measure of viral genome copy number within samples. The principle of the assay was to use qPCR to amplify a common MCMV sequence found in both target MCMV samples and in a reference DNA plasmid of known size, quantity and molecule number. Assuming that the plasmid was roughly equivalent to a viral genome in the context of a qPCR reaction, the relative abundance of MCMV genomes in target samples could compared to the reference plasmid based on Ct values from a qPCR standard curve.

2.5.2 Construction of recombinant plasmid DNA containing the MCMV m115 gene

To measure MCMV genome copy number, a reference DNA plasmid containing the MCMV m115 (gL) gene was constructed. Cloning the plasmid was originally performed by Even Fossum at The University of Edinburgh (for detailed methodology see (99)). Briefly, the MCMV m115 (gL) gene (nts 166387-167208 GenBank accession no. NC_004065) was amplified from pC3X (250) using nested

PCR primers incorporating the attB1 and attB2 recombination sites and cloned into the GATEWAY recombinatorial cloning entry vector pDONR207 (Invitrogen, CA, USA). The pDONR207 vector plasmid is 5585nt in length, with a region of 2243nt removed between positions 413-2656nt. Into this region, the m115 gene (825nts) was inserted.

Total plasmid length = pDONR207 length – region removed + insert length
= 5585 – (2656-413) + 825
= 4167nt

To generate large quantities of plasmid DNA, the pDONR207-MCMVm115 plasmid was re-transformed into competent bacterial cells (DH10D). 1µl of plasmid was mixed with 50µl cells, electroporated (2mm, 2.5kv), re-suspensded in lysogeny broth (LB) and incubated at 37^{o}C for 60 minutes with shaking at 900rpm. Gentamicin (15ug/ml) was added to the bacteria/plasmid/LB solution and 100µl was then spread across gentamicin agar plates which were incubated overnight at 37^{o}C. The next day a single colony was selected and placed in a beaker of LB with gentamicin and incubated overnight at 37^{o}C shaking at 220rpm. To purify high-quality plasmid DNA from the preparation, the PureYield Plasmid Midiprep System (Promega, UK) was used according to manufacturer's instructions. To determine purity of the plasmid, 2µl of DNA was digested (BamHI) and run on a 1% agarose gel at 120v, 400mA, 99W for 35min.

The concentration of purified DNA was determined using NanoDrop spectrophotometer (NanoDrop Technologies, DE, USA). The plasmid size (4167nt) and the DNA concentration (1200ng/µl) were used together to calculate DNA copy number per µl in the purified plasmid stock using the online tool at http://www.uri.edu/research/gsc/resources/cndna.html. This tool makes a calculation based on the assumption that the average weight of a base pair (bp) is 650 Daltons meaning that one mole of a bp weighs 650g. It also assumes that the molecular weight of any double stranded DNA template can be estimated by taking the product of its length (in bp) and 650. Using Avogadro's number (6.022x10^{23} molecules/mole) the number of molecules of the template per gram can be calculated using the following formula:

number of copies = (amount * 6.022x10^{23}) / (length * 1x10^{9} * 650)

The number of molecules per gram can then be to converted to molecules per ng by multiplying by $1x10^9$ then multiplying by the amount of template (in ng). For an alternative description of this approach see (331). The final number of calculated DNA copies in the pDONR207-MCMVm115 purified plasmid stock was $2.6x10^{11}$ molecules per µl.

Once the number of molecules in the reference plasmid DNA had been calculated, qPCR could then be used to compare against the quantity of MCMV genomes within a sample of interest by amplifying the same 82bp fragment of the m115 (gL) gene. To perform qPCR, the purified pDONR207-MCMVm115 plasmid first had to be linearized by restriction digest. 2µl plasmid DNA was added to 0.5µl BSA, 5µl BamII enzyme, 3µl buffer and 19.5µl RNase-free water. In this digestion the plasmid DNA was diluted by a factor of 1/15 (2µl DNA in a 30µl volume). This meant the molecule number per µl had to be adjusted accordingly to $2.6x10^{11}$ x (1/15) = $1.7x10^{10}$ molecules per µl. After linearization, the plasmid DNA was diluted in a 10-fold series in RNase-free water from 10^{-1} to 10^{-8}. Only dilutions spanning 10^{-3} to 10^{-7} were used in qPCR reactions (corresponding to $1.7x10^7$, $1.7x10^6$, $1.7x10^5$, $1.7x10^4$ and $1.7x10^3$ molecules per µl). qPCR reactions were performed in 96-well PCR plates (Applied Biosystems, CA, USA), each in technical duplicate with 1µl of diluted plasmid DNA used per reaction. Total reaction volume was 20µl containing 10µl 2x Brilliant QRT-PCR Buffer (Stratagene, CA, USA), 8µl RNAse-free water, 1µl plasmid DNA, and 1µl of Taqman FAM labelled custom probe/primer premix 20x (Applied BioSystems, CA, USA). Mastermix containing 10x buffer, RNAse-free water and Taqman primer/probe mix was made up to scale for the appropriate number of reactions (wells) required plus an additional 10%. 19µl of mastermix was pipetted into each well of the 96-well plate, followed by 1µl of the diluted plasmid DNA which was added to the side of individual wells before plates were sealed with MicroAmp Optical Caps (Applied Biosystems, CA, USA) and centrifuged at 1500rpm for 2 minutes. qPCR was performed on the MXPRO3000P cycler (Stratagene, CA, USA). In each reaction, the 82bp fragment from the m115 (gL) gene was amplified using a custom Taqman gene expression assay (Applied BioSystems, CA, USA) with primer sequences 5' GAGCTCAACGACGAGTTCCT 3' (forward) and 5' GCATCAGCGTCAGCAGAAC 3' (reverse). The thermal cycle

used was 10 minutes at 95^{o}C, then 40 cycles of the following; 30 seconds at 95^{o}C, 60 seconds at 60^{o}C, 30 seconds at 72^{o}C.

The qPCR data from the pDONR207-MCMVm115 reference plasmid dilution series was used to generate a standard curve with cycle threshold (Ct) values plotted on the y axis against molecule numbers on the x axis (see Figure 2.1), deriving the following equation; Y = -3.444*LOG(X) + 38.95 (Y = Ct value, X= molecule number), the equation can then be rearranged to; X=10^((Y-38.95)/-3.444). At this stage Ct values derived from any sample could be inserted into the formula (as Y) to calculate molecule number per µl compared to the reference plasmid.

Figure 2.1 Amplification plots (2.1a) and standard curve (2.1b) for the pDONR207-MCMVm115 reference plasmid DNA.

a)

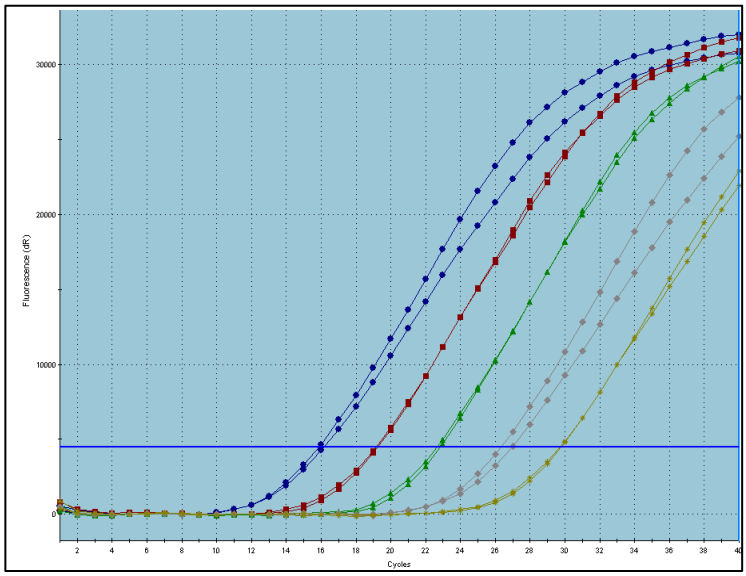

b)

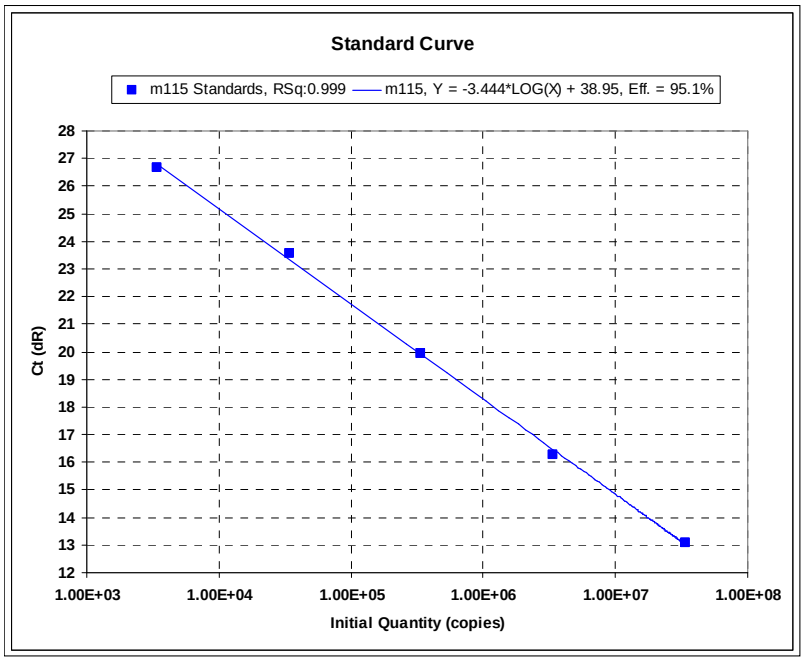

2.5.3 Measurement of MCMV genome copy number in viral stocks

Once the pDONR207-MCMVm115 reference plasmid and standard curve equation had been derived, comparisons against viral DNA extracted from MCMV viral stocks could be made. Viral DNA was isolated from 200µl of each viral stock using the PureLink Viral RNA/DNA Kit (Invitrogen, CA, USA) as described previously. The extracted DNA was eluted in 10µl of RNase-free water, and 2µl of this DNA was taken into a 10-fold serial dilution with dilutions spanning 10^{-1} to 10^{-5} used in qPCR reactions performed alongside the pDONR207m155 plasmid standard. In each qPCR reaction the same 82 bp fragment of the m115 (gL) gene was amplified and the same reaction volume, mastermix conditions, and primer sequences used as described previously for the reference plasmid. qPCR reactions were performed in technical duplicate and average Ct values were inserted into the standard curve formula to calculate genome copy number at each dilution for the target DNA samples. Calculations at the five different dilutions plus standard deviations for genomic MCMV DNA were averaged to calculate the final genome copy number (for raw data and calculations see Supplementary File 1). Once genome copy number per µl of DNA from viral stocks had been calculated, the number of viral genomes per PFU in the stocks could also be determined. As each viral DNA sample was extracted from 200µl of viral bulk stock and eluted in 10µl of water, the number of genomes per µl could be multiplied by 10 to determine the total number of viral genomes in the 10µl extracted DNA. This could then be converted into total genomes per samples, genomes per ml of viral stock, and genomes per PFU.

2.5.4 Quantification of intracellular MCMV genome copies in infected cell samples

In addition to DNA extracted from viral stocks, DNA could also be extracted from MCMV infected cells and assayed for viral genome copy number. DNA was extracted from 24-well plates as previously described with each sample representing a single well containing $3.5x10^5$ cells. DNA was eluted in 25µl RNase-free water and 10µl of this was then taken into a 10-fold serial dilution from 10^{-1} to 10^{-8}. Dilutions spanning 10^{-2} to 10^{-7} were used in qPCR reactions in parallel with the pDONR207m115 standards as previously described. Genome copy number

calculations were made in the same way to calculate the number of MCMV genomes per µl of extracted DNA. This figure could then be multiplied by the total volume of extracted DNA (25µl) to calculate the total number of MCMV genomes per sample, which also corresponded to the number of MCMV genomes per $3.5x10^5$ cells in any given sample (for raw data and calculations see Supplementary File 2).

2.6 Quantitative *Real-Time* Polymerase Chain Reaction (qRT-PCR)

To measure the relative abundance of mRNA transcripts between samples, mRNA is reverse-transcribed into cDNA before being amplified using qPCR in a process termed qRT-PCR. After reverse transcription and PCR amplification, the relative quantity of cDNA between samples can be measured by comparative analysis of Ct values from PCR amplification plots. This is a standard technique for measuring relative gene expression.

2.6.1 qRT-PCR detection of cellular transcripts

2.6.1.1 One-Step qRT-PCR using Taqman 96-well format

For qRT-PCR measurement of mRNA transcripts in 96-well format, the Brilliant II One-step qRT-PCR kit (Stratagene, CA, USA) and Taqman probe/primer system (Applied Biosystems, CA, USA) were used. The reverse-transcriptase step is performed immediately prior to qPCR in the same plate in the same instrument, hence a 1-step reaction. The Brilliant II Master Mix contains reverse transcriptase (RT) enzyme plus oligonucleotides and magnesium to allow the formation of cDNA and the PCR amplification product in the same sample, rather than having to perform the RT step separately. Taqman gene expression assays can be bought off-the-shelf and contain a mixture of pre-optimized forward/reverse primers and sequence-specific probes for a target gene of interest.

PCR reaction volumes used in 96-well plates were 19µl per well with the following components; 10µl 2x Brilliant QRT-PCR Buffer (Stratagene, CA, USA), 0.1µl RT/Block Enzyme (Stratagene, CA, USA) 6.9µl RNAse-free water, 1µl of Taqman

FAM- labelled custom probe/primer premix 20x (Applied BioSystems, CA, USA) and 1µl template RNA per reaction. Mastermixes containing 10x buffer, RT enzyme and Taqman primer/probe mix were made up to scale for the appropriate number of reactions (wells) plus an additional 10%. 18µl of mastermix was pipetted manually into individual wells of MicroAmp Optical 96-well reaction plates (Applied Biosystems, CA, USA). 25ng/µl or 50ng/µl of RNA was used per reaction depending on the abundance of the target transcript. 1µl of diluted RNA was added to the side of each individual well before plates were sealed with MicroAmp Optical Caps (Applied Biosystems, CA, USA) and centrifuged at 1500rpm for 2 minutes. qPCR was performed on the MXPRO3000P cycler (Stratagene, CA, USA) with a 30 minute reverse transcription step at 50^{o}C followed by a hot-start step of 10 minutes at 95^{o}C, then 40 cycles of the following; 30 seconds at 95^{o}C, 60 seconds at 60^{o}C, 30 seconds at 72^{o}C. Target transcript levels were normalized to the housekeeping gene Glyceraldehyde 3-phosphate dehydrogenase (*Gapdh*) which is abundantly expressed and stable across a range of experimental conditions. Gapdh levels were measured using a pre-validated *Gapdh* Taqman assay (Stratagene, CA, USA) under the same PCR conditions. For a list of Taqman primer/probes used see Supplementary File 3.

2.6.1.2 Two-step qRT-PCR using Roche Universal Probe Library 384-well format

To scale up the capacity of qPCR analysis, a high-throughput system was developed using an automated liquid handling robot, 384-well plate format and 10µl reaction volumes. Using the 384-well format, four times more reactions could be performed per plate with only half the amount of reagent used per reaction. In addition, by using an automated liquid-handling robot, pipetting error was significantly reduced. The high-throughout qPCR assay was optimized at the Centre for Systems Biology Edinburgh (CSBE), University of Edinburgh with the kind technical assistance of Lorraine Kerr and Eliane Salvo-Chirnside. The LightCycler480 instrument (Roche, Switzerland) was used with the Roche Universal Probe Library (UPL) (Roche, Switzerland) in 2-step qPCR reactions. The Roche UPL is a library of 165 real-time PCR probes with individual sequences that when combined with gene-specific primers, cover over 99% of the mouse genome. Using the Roche online assay design

tool (https://www.roche-applied-science.com/sis/rtpcr/upl/index.jsp?id=uplct_030000) 20-24nt primer sequences were designed for target genes of interested and matched to corresponding UPL probes. The assays are specifically designed to have a melting temperature (Tm) of 59-60^{o}C, G-C content of ~50% and amplicon length of ~70-100nt. Primer and probe concentrations were optimized manually for each assay by performing standard curves. UPL assays were designed for a range of cellular and viral genes (for complete list of all UPL primer sequences and probe numbers see see Supplementary File 4). Forward and reverse primers were ordered from Invitrogen, UK and diluted in RNase-free water to a concentration of 100nM.

For 2-step UPL qPCR reactions, 1ug of extracted RNA was reverse-transcribed into cDNA using the Roche Transcriptor First Strand cDNA Synthesis Kit (Roche, Switzerland) as per manufactures instructions. Then in a separate reaction (hence 2-step qPCR) the cDNA for each sample was diluted 1:5 and run in qPCR reactions. Total reaction volumes for 384-well plates were 10µl per well with the following components; 5µl LC480 Universal Probes 2x Buffer (Roche, Switzerland), 0.05µl Forward Primer (100 µM), 0.05µl Reverse Primer 1 (100 µM), 0.2µl Roche UPL Probe (10 µM) (Roche, Switzerland), and 3µl RNAse-free water. Mastermixes without cDNA were made up for the required number of reactions plus 10% extra. 9µl of mastermix was pipetted into each well of a 384-well PCR plate (Roche, Switzerland) followed by 1µl of diluted cDNA using the Freedom Evo-2 150 liquid handling platform (Tecan, Switzerland). Prior to qPCR, plates were covered with plastic coating and centrifuged at 1500rpm for 2 minutes. qPCR was performed on the LightCycler480 (Roche, Switzerland) with a hot-start of 15 minutes at 95^{o}C, followed by 50 cycles of the following; 5 seconds at 95^{o}C, 10 seconds at 60^{o}C, 30 seconds at 72^{o}C. Relative expression levels were normalized to the cellular housekeeping gene beta actin (*ActB*) which was also measured using UPL probes (Roche, Switzerland) and custom primers (Invitrogen, UK).

2.6.2 Analysis of qRT-PCR data

Ct values were exported from MXPro software (Stratagene, CA, USA) or Roche LC480 software (Roche, Switzerland). For each condition three biological replicate samples were used, with averaged Ct values from technical duplicate qPCR reactions. This generated three raw data points per condition (three Ct values per target gene and three Ct values per reference). *Gapdh* or *ActB* were used as reference genes. From the Ct values, the relative transcript abundance for each gene of interest was calculated using the ΔΔC(T) method (224). This method calculates the ratio of Ct values of the gene of interest to the Ct value of a housekeeping gene to give a normalised value per sample (see below). The method also incorporates the qPCR efficiency of a given probe/primer assay if known.

Ratio = (($Efficiency_{target}$) ^ ΔCT_{target}(control-treated)) /

(($Efficiency_{reference}$) ^ $\Delta CT_{reference}$(control-treated))

or

Ratio = $(Eff_t)^{(\Delta CT_t)}/(Eff_r)^{(\Delta CT_r)}$

The calculated ratio represents relative fold difference in transcript abundance between a control and treated sample. These ratios can be averaged over biological replicates to calculate an average fold change between conditions and standard deviations. In the case of Taqman probe/primers, PCR efficiency was assumed to be 2. For UPL probe/primers, PCR efficiency was calculated by prior standard curve analysis to be between 1.8-2.2. After the relative abundance ratios including standard deviations were calculated, an independent two-sample Student's t-test could be applied to determine whether the difference in transcript levels was statistically significant ($p<0.05$).

$$t = \frac{\bar{x}_1 - \bar{x}_2}{\sqrt{\frac{s_1^2}{n_1} + \frac{s_2^2}{n_2}}} \quad \mapsto \quad \frac{\text{difference between means}}{\frac{\text{variance}}{\text{sample size}}}$$

where $\bar{x}_1$ = mean of sample 1

$\bar{x}_2$ = mean of sample 2

n_1 = number of subjects in sample 1

n_2 = number of subjects in sample 2

$$s_1^2 = \text{variance of sample 1} = \frac{\Sigma(x_1 - \bar{x}_1)^2}{n_1}$$

$$s_2^2 = \text{variance of sample 2} = \frac{\Sigma(x_2 - \bar{x}_2)^2}{n_2}$$

2.7 Microarray gene expression analysis

Microarrays are a commonly used tool for the global measurement of mRNA expression based on sequence-specific DNA oligonucleotide probes printed on specialized slide surfaces which bind target material (generally fluorophore-labelled cRNA or cDNA). The target material hybridizes to corresponding probe(s) and is quantified by fluorescence signal to determine relative abundance of nucleic acid sequences in the target.

2.7.1 Analysis of viral gene expression using custom MCMV microarrays

2.7.1.1 Design and annotation of custom MCMV array

To measure genome-wide viral transcripts in MCMV, a custom oligonucleotide DNA microarray platform was developed. This array was designed, fabricated and optimized at the Division of Pathway Medicine, University of Edinburgh, and is based on the complete genome sequence of the MCMV Smith strain (299). The array consists of 55-mer oligonucleotide probes designed against each of the 170 viral open reading frames (ORFs) in the MCMV genome (299). Probes are desinged in both sense and antisense orientation for each ORF region. 192 positive control probes were also included against 192 mouse genes stably expressed and unchanging in NIH 3T3 fibroblasts during MCMV infection (unpublished data). 97 negative control probes were also designed against yeast sequences with no homology to the mouse or MCMV genomes. Positive and negative control probes were used for normalization purposes and to determine thresholds of detection for target probe signals. Probe sequences were originally designed by José J García-Ramírez, University of Edinburgh. ORFs, strand, position, length, MW, HCMV homologue name and annotations were taken from Rawlinson *et al.* (299). Additional annotations for MCMV ORFs were taken from wherever possible in the literature and referenced (for complete list of probe sequences and annotations see Supplementary File 5).

2.7.1.2 Fabrication, printing, hybridization and scanning of MCMV microarray*

*This work was performed by Alan Ross, Division of Pathway Medicine, University of Edinburgh, UK.

Custom MCMV 55mers oligonucleotides (synthesized by Invitrogen, UK) were diluted in 50% glycerol, 0.01% triton to a concentration of 60uM using a RapidPlate liquid handler (Qiagen, Hilden, Germany). Microarrays were inkjet printed using a SuperMarathon Aj120 (Arrayjet, UK) onto Corning GAPII, aminosilane coated glass slides. Six identical sub-arrays were printed per slide and arrays were baked for 2 hours at 70^{o}C on a hotplate and then UV crosslinked at 300kJ. Slides were blocked using preheated 1% BSA, 5% SSC, 1% SDS for 45 minutes at 42^{o}C, washed and spun dry. Print QC was tested using cyanine 3 labelled random 9-mers which were hybridised to a set of test arrays. The target RNA was labelled using the Agilent low input fluorescent linear amplification protocol (Agilent, CA, USA). A primer containing poly dT and T7 polymerase promoter was annealed to the polyA+ RNA. Reverse transcriptase was added to synthesize the first and second strands of cDNA from which cRNA was synthesized using T7 RNA polymerase which simultaneously incorporates cyanine 5. For hybridization 3ug of each of the Cyanine 5 labelled target cRNAs was hybridised to microarray slides for 18 hours at 60^{o}C in a rotating oven, washed in Agilent (CA, USA) wash solutions (1) 6% SSPE , 0.005% N-lauroylsarcosine (2) 0.06% SSPE , and 0.01% N-lauroylsarcosine. Arrays were scanned using an excitation wavelength of 630 nm and Cyanine 5 detection filter in an Agilent (CA, USA) microarray scanner (G2505B). Quantarray version 3.1 (Packard BioChip Technologies, MA, USA) was used to feature extract the data from images. Each sample was hybridized to one slide containing six identical sub-arrays with positive control, negative control and target MCMV probes printed in triplicate per array.

2.7.1.3 MCMV microarray analysis, statistics and bioinformatics

After background subtraction (subtraction of pre-hybridization signals), data from each set of triplicate probes was median-summarized to form raw data points. As each array was printed six times per slide, this gave six raw data points per sample

per slide. Raw data was quality controlled and normalized between samples based on a subset of positive control probes highly correlated across the data set (Pearson r<0.90). On/off calls for normalized probe intensities were determined using receiver operating characteristic (ROC) set at 70% sensitivity (31) where the gold standard per condition is defined by the sets of known positive and negative controls. Statistical testing by empirical Bayes (336) was applied between mock and infected groups to identify the most highly significant MCMV ORFs. Technical replicates were included in the model as consensus correlation estimates. Statistical analysis was performed by Thorsten Forster, Division of Pathway Medicine, University of Edinburgh, UK.

2.7.2 Analysis of host gene expression using Affymetrix whole-genome microarrays

2.7.2.1 Affymetrix Mouse Exon 1.0ST microarray (16-sample dataset)

The Affymetrix Mouse Exon 1.0ST microarray provides full coverage of the mouse coding transcriptome and contains multiple probes for each mouse gene designed across the entire length of transcripts, without any 3' bias. The Affymetrix Mouse Exon 1.0ST microarray platform was used to analyze global gene expression in 16 samples from infected wild-type C57BL/6 BMDMs. The GeneChip Whole Transcript (WT) Sense Target Labeling Assay protocol (Affymetrix, CA, USA) was followed according to manufacturer's instructions, and modified only by using a starting RNA input of 300ng per sample. Briefly, the four-day protocol consists of 1st cycle cDNA synthesis, 1st cycle cRNA *in-vitro* transcription and amplification, clean-up of antisense cRNA, 2nd cycle cDNA synthesis, hydrolysis of cRNA, cleanup of sense strand DNA, fragmentation, terminal labelling, overnight hybridization, washing, scanning, and feature extraction. For detailed methodology see GeneChip Whole Transcript (WT) Sense Target Labeling Assay Manual (http://www.partnerchip.fr/doc/File/wt_sensetarget_label_manual.pdf)

2.7.2.2 Affymetrix microarray data analysis (16-sample dataset)

Quality control of Affymetrix Mouse Exon 1.0ST microarray data was performed using Affymetrix Expression Console (Affymetrix, CA, USA) following standard procedures. All arrays passed the quality control metrics and raw data was imported into Partek Genomics Suite (MO, USA) for downstream analysis. All probesets from the 'core' set of exons (188,596 probes) were imported and normalized using the gcRMA algorithm. Transcript-level summarization was performed using the mean of all probesets across each transcript based on the “core” set of exons to give gene-level expression data for 16,761 mouse genes. Normalized expression data was visualized using boxplots, Principle Component Analysis (PCA) and sample histograms. An expression level filter was applied to exclude any genes with a maximum normalized antilog signal intensity below 100 over all arrays. This reduced the dataset to 7,890 genes expressed to a high confidence level. The filtered data was used to identify genes changing significantly over the time course either within or between conditions by performing a statistical analysis based on EDGE(213) (http://www.genomine.org/edge/0) with 500 iterations. Fold changes between conditions at each time point were also determined by ANOVA testing. For clustering analysis, identifiers and annotation (nodeclass) columns were loaded into BioLayout Express3D (103) and an all-versus-all Pearson correlation matrix was calculated based on the expression profile of all filtered probesets. Pearson correlations greater than $r = 0.9$ were stored and network graphs were constructed using this threshold. Graphs consisted of nodes representing transcripts connected by edges representing expression correlations above Pearson>0.9. The MCL algorithm was then used to cluster the data into network graphs according to the connectivity between nodes as defined by a mathematical bootstrapping procedure. Network graphs were explored for clusters which changed markedly over time or were altered between conditions.

2.7.2.3 Affymetrix Mouse Gene 1.0ST Microarray (72-sample dataset)

The Affymetrix Mouse Gene 1.0ST microarray consists of a sub-set of probes from the Exon 1.0ST Array and also provides full-length transcript coverage for all mouse genes. The Mouse Gene 1.0ST microarray was used to analyze global gene expression in 72 samples from infected and immune-stimulated BMDMs from wild type, *Ifnb1-/-* and *Ifnar-/-* C57/BL6 mice. The processing and data analysis procedures for the Mouse Gene 1.0ST array are similar to the Exon 1.0ST array, however for this large study the array processing and hybridization was out-sourced to a contract research company (Gen-Probe Life Sciences Ltd, UK). An updated cDNA synthesis and labelling protocol was performed by Gen-Probe based on the Ambion WT Expression Kit (Ambion, UK) (for details see http://www.ambion.com/techlib/prot/fm_4411973.pdf).

2.7.2.4 Affymetrix microarray data analysis (72-sample dataset)

Quality control, normalization and importing of microarray data was performed as previously described. Normalized data was filtered to include only genes with a maximum expression value of above 150 across the data set (19,118 probes) to identify only genes expressed to a high confidence level. All control probes and un-annotated probes were removed from the analysis reducing the dataset to 13,244 probes. The 13,244 remaining probes were imported into BioLayout Express3D and arranged in a network graph using the threshold of Pearson>0.9. 3,517 probes formed a graph as this level. The data was then clustered at MCL=1.5 with a minimum cluster number of n=15. This arranged the data into 24 clusters containing a total of 2,325 probes which were used for subsequent analysis.

2.7.3 Functional annotation of Affymetrix microarray data

2.7.3.1 Database for Annotation, Visualization, and Integrated Discovery (DAVID).

The DAVID online annotation tool (79) takes annotation classes from various different databases (e.g. NCBI, PIR, SWISS-PROT, GO, OMIM, PubMed, KEGG, BIOCARTA, AffyMetrix, TIGR, Pfam, BIND, MINT, DIP, etc.) and measures for

over-representation of annotation terms within an input gene list. Over-representation or *enrichment* statistics are determined using a modified Fisher Exact test with P-values ranging from 0 to 1, indicating the likelihood of enrichment compared to that occurring by chance alone. If the Fisher Exact test detects perfect enrichment of the gene list with a given term, the P-value will equal 0. Annotation categories with bonferroni-corrected $p < 0.005$ were considered significantly enriched.

2.7.3.2 Ingenuity Pathway Analysis (IPA)

IPA is a commercial software tool and database incorporating molecular interaction data from experiments and from the literature. Using an input genelist, IPA will find associations, relationships and interactions between input genes, or with other genes as secondary interaction partners, and build networks of highly connected genes with related function. IPA will also incorporate chemical interaction data, cellular phenotypes, gene ontologies and disease processes to annotate an input genelist.

2.7.3.3 Innate DB analysis

InnateDB is a database of molecular interactions designed specifically to facilitate systems level analysis of the innate immune response in human and mice(229). It is a manually-curated database of genes, proteins, interactions, pathways and signalling responses involved in the mammalian innate immune response. The interactions are from publicly available sources and manually curated with contextual annotations including reference publications, interaction detection methods, and cell type information. InnateDB can either be mined as a knowledgebase or batch-searched to return all interactions or pathways associated with a list of genes. Interaction networks can also be visualized in the Cerebral java plugin for Cytoscape visualization software. InanteDB can also be used to statistically test for over-representation of pathway or annotation terms within an input genelist based on an hypergeometric algorithm and benjamini Hochberg p-value correction.

2.8 Protein methods

2.8.1 Whole-cell lysis

For protein extraction, cells were seeded in 6-well plates. Before lysis, cells were washed twice with ice cold PBS and then lysed directly in the wells by adding 100µl of NP-40 lysis buffer containing phosphatase inhibitors (Sigma, UK). Cells were scraped in the lysis buffer with a plastic scraper, transferred to sterile 1.5ml tubes and incubated on ice for 20-30 minutes. After lysis, cells were centrifuged at max speed at 4˚C for 10 minutes to remove cell debris and supernatants were transferred to fresh 1.5ml tubes and stored at -80ºC.

2.8.2 Measurement of whole-cell protein concentration

Total protein concentration was determined using the Micro BCA protein assay (Pierce, UK) according to manufacturer's instructions. Along with standards, 20µl of each target sample was loaded into a 96- well plate in duplicate wells. Protein concentration per sample was obtained via measurement of absorbance at 562 nm on the POLARstar OPTIMA Multifunction Microplate Reader (BMG LabTech, UK).

2.8.3 Western blotting*

* Western blots were performed by Christopher Millward under the supervision of Paul Lacaze at the Division of Pathway Medicine, University of Edinburgh, UK

After determining protein concentration, equal amounts of protein for each sample were mixed with 2X Laemmli Sample Buffer, containing 10% of DTT and loaded onto 10% SDS-PAGE gels with 6µl of molecular weight marker (Prestained Protein Marker Broad Range, New England Bioloabs, UK). Gels were run for 45 minutes at 200 V using a BioRad PowerPac 200 Power Supply. Filter papers (BioRad, UK) were soaked in transfer buffer along with fiber pads and polyvinylidene difluoride (PVDF) membranes were cut to the dimension of the gel (maximum size 7.5 cm x 10 cm). Membranes were soaked in methanol for 10 seconds, then washed in distilled water and soaked in transfer buffer. After electrophoresis, the cassette was disassembled and the gel was placed on a transfer sandwich on the top of the PVDF

membrane. The gel sandwich was placed in the TransBlot module with the cooling unit and cold water. The tank was filled with transfer buffer and run for 1 hour at 100V/constant. When transfer was finished, the cassette was disassembled and the PVDF membranes were blocked with 20 ml of blocking buffer at room temperature with gentle shaking. The membrane was washed three times for 15 minutes in washing buffer. The primary antibody was diluted into primary antibody dilution buffer and the membrane was incubated with the primary antibody overnight at 4^{o}C with gentle rocking. After primary antibody incubation membranes were washed and then incubated with the secondary antibody, diluted in blocking solution for one hour at room temperature. The membrane was washed again and laid onto a mixture of detection reagents (ECL Plus Western Blotting Detection Reagents, Amersham Biosciences, UK) for 5 minutes. Membrane exposure was performed using the VersaDoc imaging system 4000. MCMV antibodies CROMA101 and CROMA103 were provided by Prof. Stipan Jonjinc (Faculty of Medicine Rijeka University, Croatia)

2.8.4 Enzyme-linked immunosorbent assay (ELISA)

Cytokines in the supernatant of tissue culture samples were measured using ELISA. TNF levels were measured using the mouse TNF DuoSet ELISA Development kit (R&D Systems, Europe) according to manufacturer's instructions. This kit is designed to detect TNF in the range of 32.5-2000 pg/ml. IFNβ levels were measured using the Mouse Interferon Beta ELISA Kit v1.2 (PBL Biomedical Laboratories, NJ, USA) according to manufacturer's instructions with an assay Range of 15.6-1000 pg/ml. Briefly, ELISAs were performed in 96-well plates coated with capture antibody incubated overnight, washed and blocked the following day. A series of standards prepared after blocking were added with 100µl of each sample to the plate. Standards and samples were left for one hour at room temperature, after which the plate was washed three times and incubated with the detection antibody. The plate is washed again before Streptavidin-horseradish peroxidase (HRP)-conjugated solution was added at the recommended working concentration. The plate was incubated in the dark at room temperature for 20 minutes, then washed and 100µl of substrate solution was added. The plate was again incubated in the dark for 20 minutes and

stop solution was added. Protein concentration was determined by reading absorbance at 450 nm using the POLARstar OPTIMA Multifunction Microplate Reader (BMG LabTech, UK).

2.8.5 Multiplex detection of cytokines using Luminex assay

To detect multiple cytokines in BMDM tissue culture supernatants, the Bio-Plex system (BioRad, USA) was used according to manufacturer's instructions (for overview see Figure 2.2 and detailed protocol see http://www.bio-rad.com/webroot/web/pdf/lsr/literature/4110004F.pdf). Briefly, the basic principle is based on sandwich immunoassay technique where antibody-coated beads are incubated with samples and standards, then washed and incubated further with detection antibodies. Streptavidin-PE is then added before beads are resuspended and measured for fluorescence signal using a lazer-based instrument. Protein quantities (in pg/ml) can then be calculated based on comparison to the internal standards using the Bioplex software (BioRad, USA). The mouse cytokines measured were IL-6, IL-10, MIP-1b, RANTES, TNFa, MIG, and MIP-2.

Figure 2.2 - Experimental workflow for multiplex bead-based Bioplex ELISA assay for detection of multiple cytokines in tissue culture supernatants.

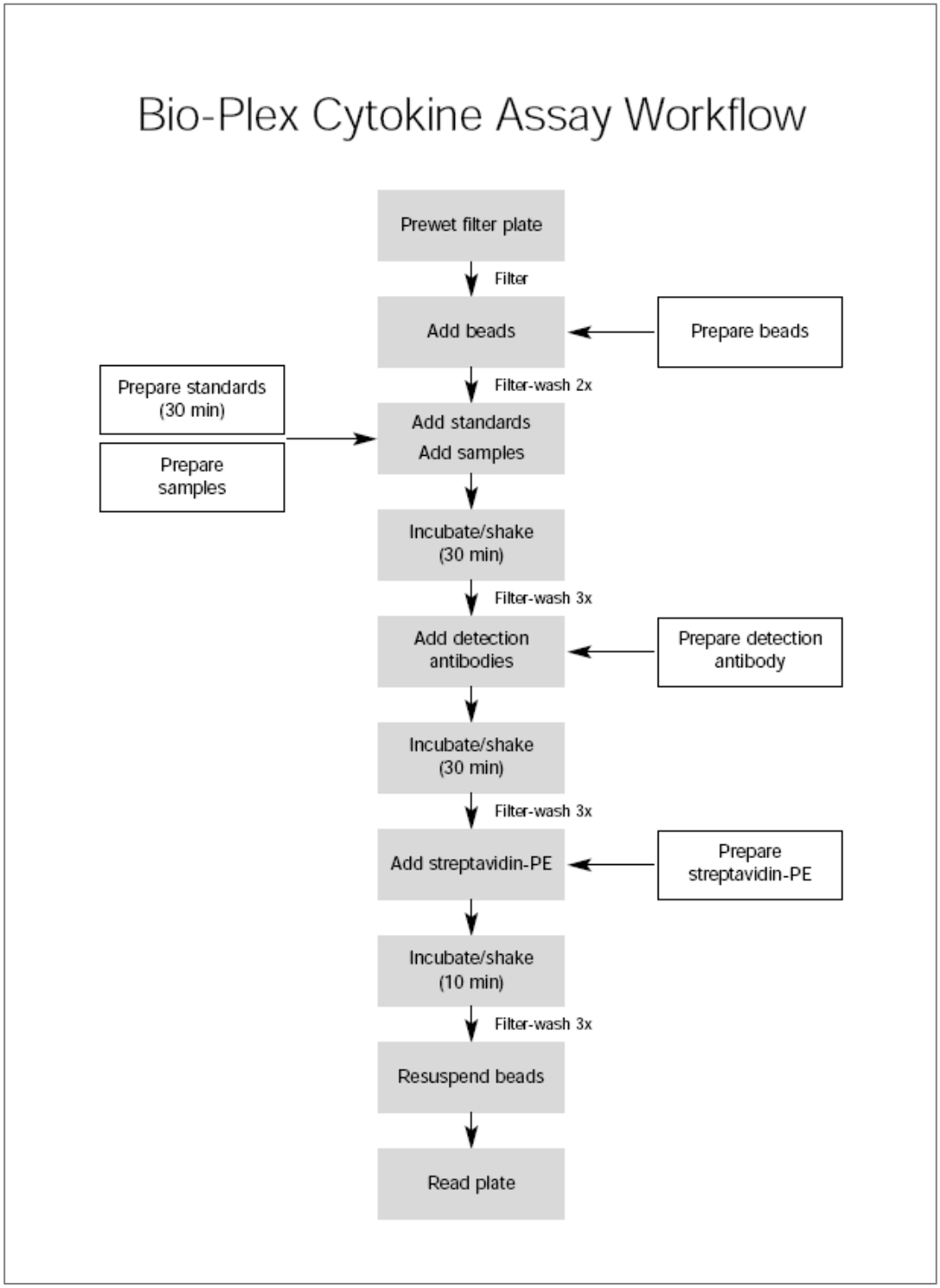

2.9 Sanger sequencing

For DNA sequencing of the MCMV MIEP region for the MCMVdie3 strain, viral DNA was extracted from 200µl of the MCMVdie3 viral stock as previously described. The entire MCMVdie3 MIEP region (NC_004065, 182,796-184,368C, 1572bps) was then amplified by PCR in three separate reactions using the Roche Expand Superscript System (Roche, Switzerland) using the following primer sequences (forward 5' TCCGATGCGCTTCAGTAGCC 3' and reverse 5' GCAAGCACACTGAGTCAAATGG 3'). The three amplified PCR products were then sent to a sequencing service facility (The Gene Pool, University of Edinburgh, UK) and sequenced by capillary analysis using the Sanger sequencing method on the ABI3730 instrument (Applied Biosystems, CA, USA). The MIEP region was sequences in two separate contigs with the following two sets of primers;
Contig 1 - forward 5'TCCGATGCGCTTCAGTAGCC 3' and reverse 5'CCGAGCCCAATGCAACCTTACC
Contig 2 - forward 5' CCCTATTGACTCACCCACATTG 3' and reverse 5' GCAAGCACACTGAGTCAAATGG 3'.
Sequence assembly was performed using Scied Clone Manager software (NC, USA).

Chapter 3

Functional characterization of a non-productive virus

Introduction

The main question to be addressed in the first results chapter will be whether the MCMV deletion mutant MCMVdie3 can be used as a reliable control reagent to represent non-productive viral infection. Specifically, it will be tested whether the MCMVdie3 mutant strain is a) replication deficient, b) capable of viral entry, c) transcriptionally inactive, and d) incapable of promoting *de novo* viral protein synthesis. The characterization work will allow subsequent experiments in macrophages to be designed whereby the host response to productive and non-productive viral infection can be measured comparatively by infecting in parallel with MCMV and MCMVdie3.

At the outset of this work, the MCMVdie3 mutant had been characterized for the purpose of studying *ie3* function (12). This involved growth analysis and limited analysis of viral gene expression measuring MCMV genes *ie1*, M54, M55 and M115, with detectable expression limited to the *ie1* gene(12). The MCMVdie3 virus had also been used in an investigation of *ie3* in G1 and G2 cell cycle arrest in infected cells(379). The MCMVdie3 strain, however, had never been previously used as a control reagent to represent non-productive infection. For this reason, the mutant required more extensive phenotypic characterization, especially regarding its transcriptional status. This chapter outlines the functional and phenotypic characterization undertaken to determine if MCMVdie3 was indeed a replication-deficient, transcriptionally inert and non-productive virus capable of representing a non-productive viral infection.

Results

3.1 MCMVdie3 is a replication-deficient virus in fibroblasts and BMDMs

To corroborate previously published reports for the attenuated growth phenotype of MCMVdie3, as well as assess the growth characteristics of revertant (MCMVdie3rev), wild-type (MCMV) and *ie1* deletion mutant (MCMVdie1) viruses, growth curve analyses were performed for each virus in NIH 3T3 fibroblasts and in the complementing cell line (NIH 3T3-Bam25). A multi-step growth curve at a low multiplicity of infection (MOI) of 0.05 PFU/cell, and a single-step growth curve at a high MOI of 2 PFU/cell were conducted for each virus. One PFU (plaque forming unit) corresponds to one infectious unit as determined by titration of virus by plaque assay on NIH 3T3 cells (see Methods).

Consistent with previous reports (12, 113, 232), the MCMVdie1 and MCMVie3rev strains grew identically to the parental MCMV strain in cell culture, resulting in productive infection and reaching titres of around $1x10^6$ PFU/ml after four days (see Figure 3.1a). Also consistent with previous reports(12), no viral growth for the MCMVdie3 mutant was detectable in NIH 3T3. The growth curves were repeated at the same MOIs in the complementing cell line (NIH 3T3-Bam25) where IE3 is expressed in *trans* (Figure 3.1b), and growth of the MCMVdie3 was recovered to wild type levels. This indicated the MCMVdie3 virus is still functional if the IE3 protein is provided in *trans*.

Figure 3.1 - MCMVdie3 is a replication-deficient virus in fibroblasts (NIH 3T3) but viral growth is recovered to wild-type levels in the complementing cell line (NIH 3T3-Bam25) NIH 3T3 (**3.1a** and **3.1b**) or NIH 3T3-Bam25 (**3.1c** and **3.1d**) cells were infected at an MOI of 0.05 PFU/cell (**3.1a** and **3.1c**) or MOI of 2 PFU/cell (**3.1b** and **3.1d**) with MCMV, MCMVdie1, MCMVdie3rev and MCMVdie3. At indicated days post infection (dpi), supernatants from infected cultures were harvested and titered on NIH 3T3-Bam25 monolayers. Error bars indicate standard deviation from three separate cultures. Red indicates data from NIH 3T3 and green indicates data from the NIH 3T3-Bam25 complementing cell line. The astericks mark the MCMVdie3 deletion mutant.

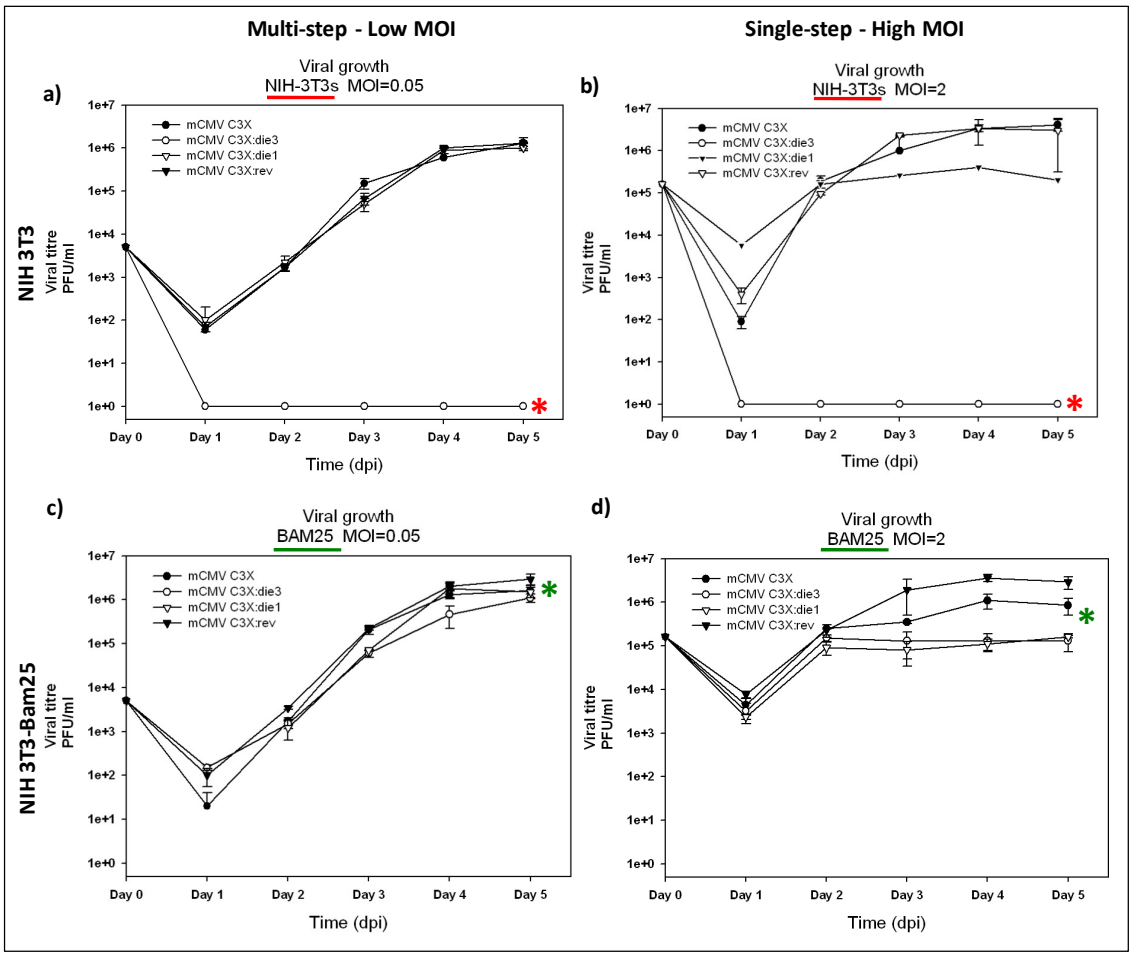

Next, to evaluate viral replication of the MCMVdie3 strain in macrophages, growth curve analyses were repeated in mouse bone marrow-derived macrophages

(BMDMs) at low and high MOIs (Figure 3.2). Again, no viral growth was detected for the MCMVdie3 mutant at either MOI.

Figure 3.2 MCMVdie3 is a replication-deficient virus in BMDMs. BMDMs were infected at MOI of 0.1 and 1 PFU/cell with MCMV and MCMVdie3. Every 24 hours, supernatants from infected cultures were harvested and titered on NIH 3T3-Bam25 monolayers. CSF-1 was present in the BMDM media at all times during the infection. Error bars indicate standard deviation from three cultures. The asterick marks the MCMVdie3 deletion mutant.

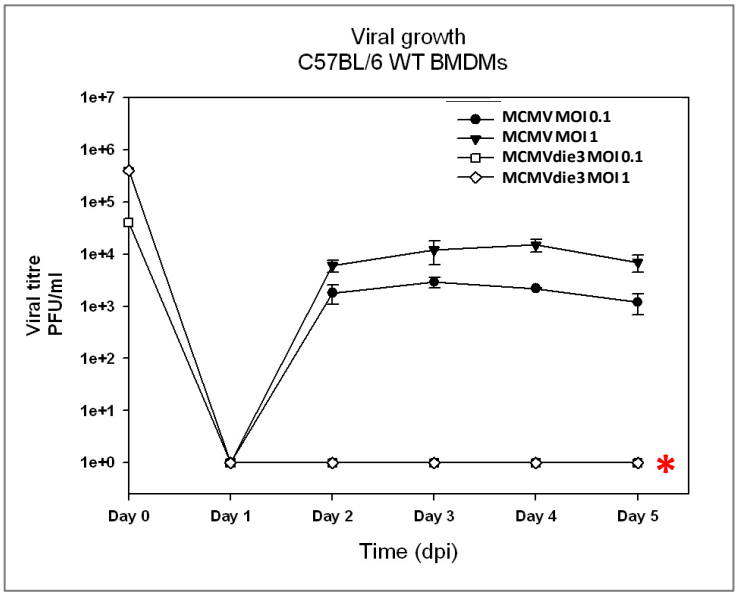

3.2 Molecular characterization of the MCMVdie3 mutant

3.2.1 MCMVdie3 is capable of viral entry but not viral replication in BMDMs

Due to the limited sensitivity of the plaque assay, it was still possible that MCMVdie3 could be replicating at low levels below the threshold of detection. In addition, and perhaps more importantly, the plaque assay did not indicate whether MCMVdie3 and MCMV particles were actually entering host cells in an equivalent manner. To test these factors, a more sensitive assay based on qPCR detection of intracellular MCMV genomes was developed (for details see Methods section 2.5.1). The assay was used to quantify the number of MCMV genome copies within infected

cells at different stages post-infection, relative to plasmid reference DNA. Cells were washed free of supernatant, viral DNA was extracted and viral genome propagation in infected cells over the course of infection was measured (Figure 3.3). A possible caveat of this approach is that residual viral particles may still be bound to cells prior to DNA extraction and qPCR analysis at early time points. To avoid this, cells were washed thoroughly twice with PBS after the adsorption period, however the retention of viral particles on the cell surface can not be excluded.

Figure 3.3 No propagation of MCMV genomes occurs during MCMVdie3 infection of BMDMs. Confluent BMDM monolayers were infected in 24-well plates at day 7 at MOI of 1 PFU/cell with parental MCMV, MCMVdie3 and MCMVdie3rev viruses. DNA was harvested from triplicate cultures at 2, 6, 24, 48 and 72 hpi and qPCR amplification of the m115 (gL) gene from genomic MCMV DNA was measured against reference plasmid DNA to calculate MCMV genome copy number per sample. Each sample represents $3.5x10^5$ cells. Error bars indicate standard deviation from three samples. The level of detection (dotted line) represents non-specific PCR signals from mock-infected cells.

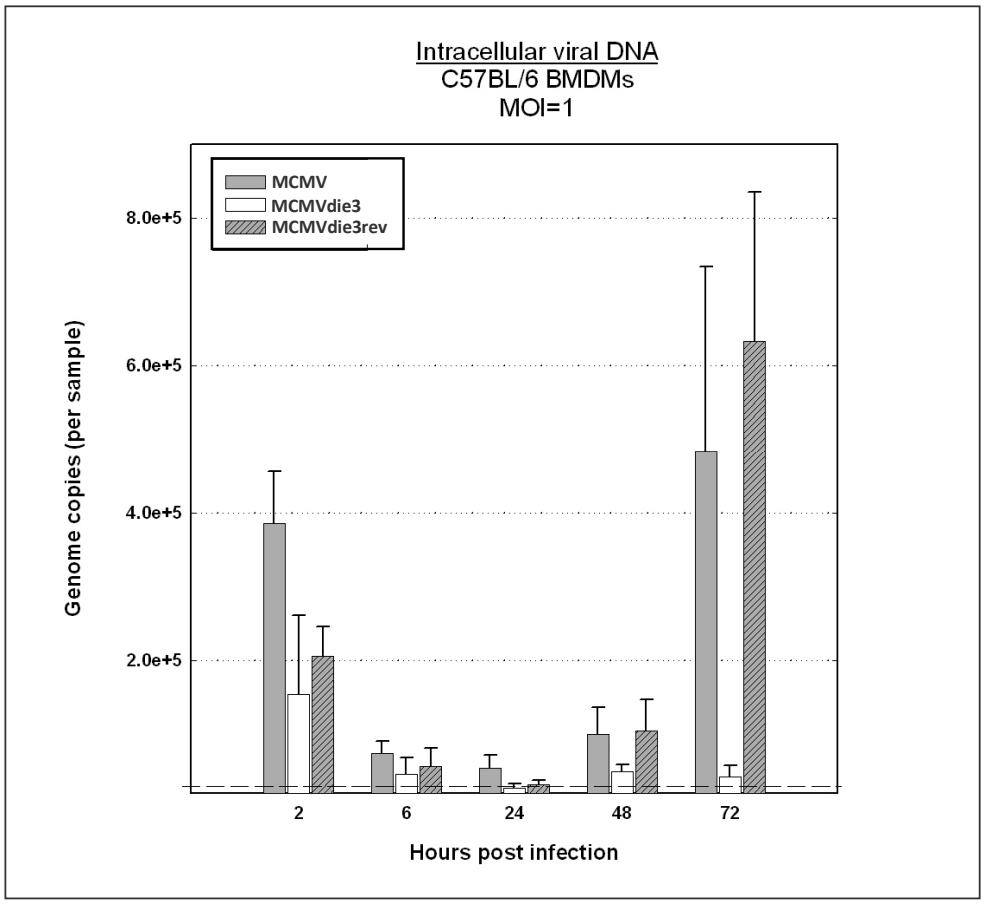

The results of the qPCR assay show comparable numbers of MCMV and MCMVdie3 genomes detectable in BMDMs at 2hpi, however they are low compared to the initial MOI (roughly equating to only one viral genome copy per cell at $3.5x10^5$ cells per sample). This suggests viral entry occurs in an equivalent manner in both conditions at MOI of 1, but that only few viral genomes enter host cells. This suggests the level of infection at MOI of 1 in BMDM cultures is particularly low at the initial stages of infection.

Consistent with the growth curve analysis, there was no synthesis of MCMVdie3 genomes during the 72 hours of infection in BMDMs, further indicating MCMVdie3 is a replication-deficient virus. As the infection progresses over 24, 48 and 72 hpi, the number of viral genomes propagated in the parental and revertant MCMV infections rises exponentially, indicating productive viral infection.

3.2.2 MCMV genome/PFU ratios are equivalent between viral stocks

To determine the number of viral particles (genomes) delivered per PFU for the different viruses, the qPCR assay was used to measure viral genomes in DNA extracted from MCMV and MCMVdie3 virus stocks. This provided an indication of how many viral genomes were delivered per PFU in MCMV and MCMVdie3 infections, and whether propagating MCMVdie3 on a complementing cell line had drastically altered the number of non-infectious or defective viral particles produced per PFU. To conduct the analysis, viral DNA was extracted from 200µl of each viral stock and subjected to qPCR alongside the reference plasmid DNA (for details see Methods 2.5.1). The result shows the number of viral genome copies developed per PFU for the MCMVdie3 virus was not statistically different from the number developed by the wild-type MCMV strain (Student t-test pvalue=0.26) (Table 3.1). This ensured the amount of viral genomes delivered per PFU for subsequent experiments using MCMV and MCMVdie3 would be equivalent, despite the low level of infection. The MCMVdie1 and MCMVdie3rev viruses were also measured and had similar genome copy number/PFU ratios.

Table 3.1. Viral titres and viral genome/PFU ratios are not statistically different between four MCMV strains. Viral DNA was extracted from 200µl of viral stock from each strain and the number of MCMV genome copies per ml was measured using qPCR (for details see Methods section 2.5.1). Using the number of MCMV genome copies per ml for each virus, combined with the viral titre (PFU/ml), the number of MCMV genomes per PFU could also be calculated. The difference between MCMV genomes per PFU in MCMV and MCMVdie3 stocks was not statistically significant (* Students t-test >0.05).

	Titre (PFU/ml)	Genomes per ml in viral stocks	Genomes per PFU in viral stocks
MCMV	6.8×10^6	$2.2 \pm 0.3 \times 10^7$	166.2 ± 3.4*
MCMVdie1	3.0×10^6	$1.7 \pm 0.8 \times 10^7$	283.3 ± 137.9
MCMVdiie2	1.3×10^7	$4.4 \pm 0.8 \times 10^7$	146.7 ± 18.8
MCMVdie3	1.1×10^7	$4.0 \pm 0.2 \times 10^7$	183.2 ± 2.4*

These calculations indicate between ~150-200 viral genomes per PFU in the MCMV and MCMVdie3 virus stocks. This means, in theory, that at least 100 viral genomes should be delivered per cell in BMDM infections at MOI of 1 (according to these calculations). In the previous qPCR analysis of intracellular viral DNA (Figure 3.3) however, only ~1 viral genome was detectable per cell at 2hpi using MOI of 1. This suggests only ~1/100 viral particles actually enter BMDMs and the initial level of infection in BMDM cultures at MOI of 1 is particularly low (actual MOI of ~0.01 PFU/cell).

To obtain a better indication of the level of infection in BMDM cultures at MOI of 1 using an alternate technique, data from BMDMs infected with a MCMV-GFP reporter virus was used. The MCMV-GFP virus has a GFP reporter under the control of the major immediate early promoter which can be used to identify GFP-positive cells(49). Flow cytometry analysis of MCMV-GFP infected BMDMs at MOI of 1 PFU/cell indicates that only around 12% of cells are GFP-positive (expressing viral genes) at 6hpi (1214 ± 652 GFP-positive cells per 10,000 over six experiments). This data was generated by Muhamad Fairus Noor Hassim (University of Edinburgh, *personal communications*). The Flow cytometry data suggests only a fraction of

delivered MCMV particles successfully enter cells and establish productive infection in BMDMs by 6hpi at MOI of 1. Some cells may become abortively (non-productively) infected despite receiving viral particles, and some cells may establish a state of latent infection in BMDM cultures, however the data indicates a low level of initial infection at MOI of 1 PFU/cell, consistent with the qPCR analysis.

3.3 MCMV viral gene expression does not occur beyond the IE region in MCMVdie3

3.3.1 Global detection of MCMV transcripts by custom MCMV microarray

Experiments to this stage show MCMVdie3 to be a replication-deficient virus, however, it remained uncertain whether the mutant virus was still capable of transcribing viral genes at higher levels of infection. Previous reports found *ie1* expression from the MCMVdie3 template but reported no viral gene expression beyond the IE region in fibroblasts(12). To further evaluate whether MCMVdie3 was a transcriptionally inert virus beyond the IE region, a custom DNA microarray was used to measure global MCMV gene expression from all 170 MCMV open reading frames (ORFs) in infected NIH 3T3 fibroblasts. NIH 3T3 cells were used for this analysis rather than BMDMs to achieve higher levels of infection and improve microarray signals.

NIH 3T3 fibroblasts were infected in parallel at MOI of 1 PFU/cell with MCMV, MCMVdie3, MCMVdie3rev and MCMVdie1, and viral gene expression was profiled using a custom MCMV microarray. The MCMV microarray contains 55mer oligonucleotide probes designed against all 3' coding ORFs regions from the MCMV genome(299). The array was designed, developed and optimized at the Division of Pathway Medicine, University of Edinburgh. For details on array design, fabrication, and printing see Methods section 2.7.1.2.

Total RNA was harvested for microarray analysis at 0.5, 6.5 and 48hpi, with RNA from mock-infected cells. The *ie1* deletion mutant (MCMVdie1) was included in this analysis as *ie1* has a putative function as both a viral transcriptional regulator (53,

126, 249) and a modulator of host factors (267, 351) making its viral transcriptional profile of general interest. Figure 3.4 shows the comparative activation of viral transcriptomes of the four MCMV strains, and indicates a complete lack of detectable viral gene expression in MCMVdie3 at 0.5, 6.5, or 48hpi (empirical Bayes $p<0.05$).

Figure 3.4 - Viral gene expression does not occur beyond the IE region in MCMVdie3. NIH 3T3 fibroblasts were infected in parallel at MOI of 1 PFU/cell with MCMV, MCMVdie3*, MCMVdie3rev and MCMVdie1. Total RNA was harvested for microarray analysis at 0.5, 6.5 and 48hpi, along with RNA from mock-infected cells. **3.4a** Volcano plots compare microarray signals from mock and infected samples using p-value (y-axis) and fold change (x-axis) comparisons derived from empirical Bayes testing with two biological replicates per group. **3.4b** Hierarchical clustering of significantly expressed MCMV probes with each row representing a single probe per-gene normalized to its mean value across the data set to show relative expression with yellow indicating increased expression and blue decreased expression relative to the mean. Genes are clustered based on the similarity of their expression profile across the dataset, with similar genes being connected at the hierarchical tree on the left. Data in columns represents mean values at different time points from two biological replicates per sample.

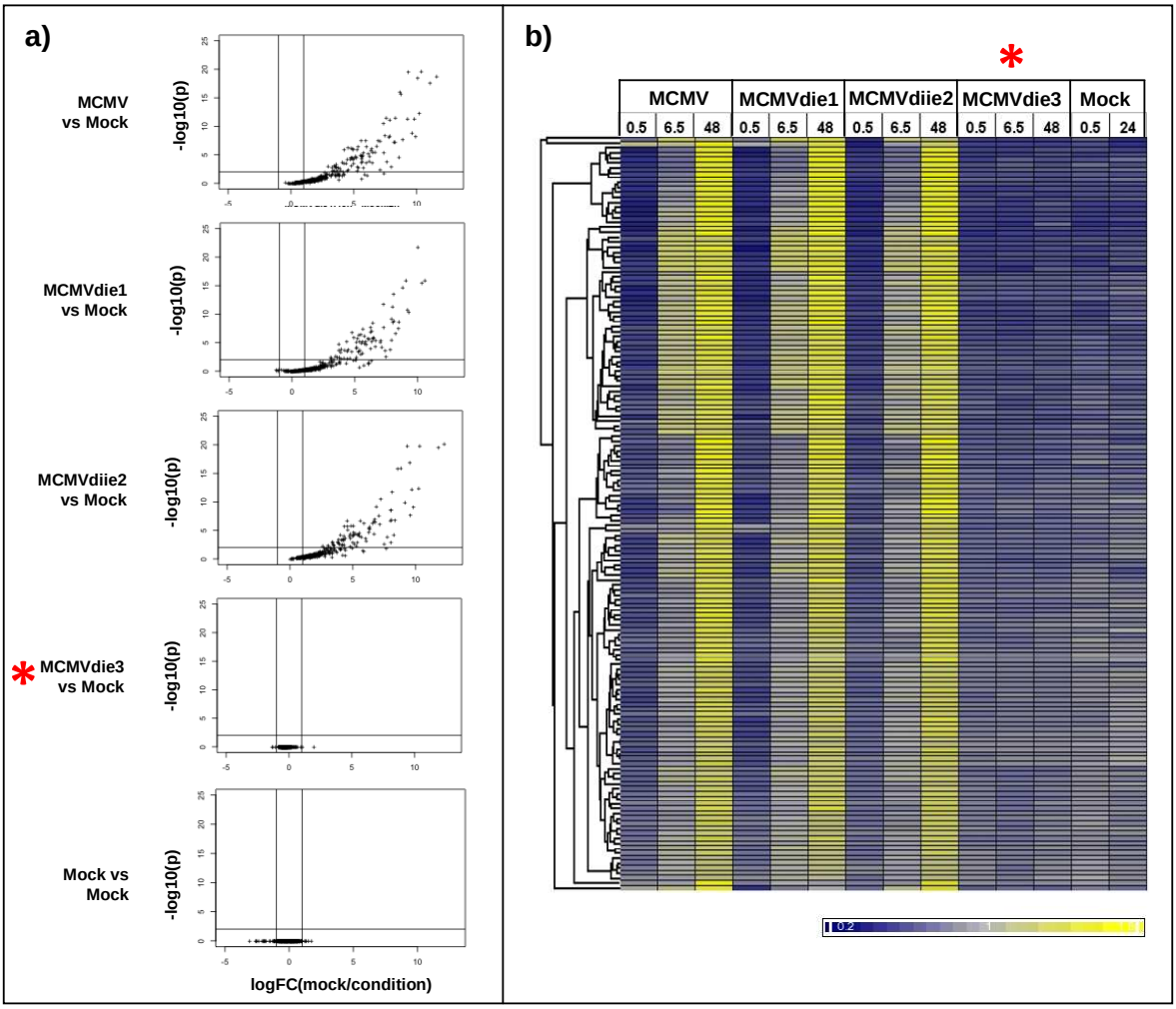

The MCMV microarray gene expression data is consistent with MCMVdie3 being a transcriptionally inactive virus incapable of transcribing viral genes beyond the IE region. Low levels of *ie1* and *ie2* transcripts were detected in MCMVdie3-infected cells, but were not expressed significantly above mock levels (empirical Bayes $p>0.05$). The transcriptomes of MCMVdie1 and MCMVdie3rev were expressed with similar dynamics to the parental MCMV strain over the 48-hour period. At the end of the infection (48hpi), there were equivalent numbers (within 10%) of MCMV probes detectable from MCMVdie1 (103 ORFs), MCMVdie3rev (114 ORFs) and the wild-type MCMV strain (113 ORFs). The level of similarity in expression profiles shared between the MCMVdie1, MCMVdie3rev and wild-type MCMV strains suggests that *ie1* and *ie2* have a redundant or negligible transcriptional regulatory role in controlling downstream MCMV gene expression during fibroblast infection.

Hierarchical clustering (Figure 3.4b) further indicates few, if any, differences in the global gene expression profiles of MCMVdie1 and MCMVdie3rev compared to the parental strain, and again shows no MCMV transcripts detectable from the MCMVdie3 strain.

Note: The MCMV microarray gene expression analysis revealed a number of interesting and novel observations regarding the gene expression programme of MCMV, including the presence of non-coding and antisense transcripts. These results have been published (Journal of Virology, *in press*) and can be found in Appendix I.

3.3.2 Immediate early gene expression is attenuated in MCMVdie3

Previous studies using MCMVdie3 report equivalent *ie1* expression levels in MCMV and MCMVdie3 during fibroblast infection(12). This is consistent with the current knowledge of the MCMV major immediate early region, whereby *ie1* and *ie2* genes are transcribed independently of *ie3* from the same promoter(49, 249). For this reason, the *ie1* and *ie2* transcripts should be expressed by the MCMVdie3 virus. In the MCMV microarray experiments however, *ie1* and *ie2* were considerably lower in MCMVdie3-infected cells compared to wild-type MCMV. To further investigate this, and to measure the expression of *ie1* and *ie3* with increased sensitivity, qRT-PCR analysis was used to measure *ie1* and *ie3* levels in MCMV and MCMVdie3 infected NIH 3T3 cells at immediate early time points; -0.5hpi (within the absorption period), 0.5hpi and 1.5hpi (see Figure 3.5a).

Figure 3.5 - *Immediate early gene 1* expression is attenuated in MCMVdie3
Triplicate cultures of NIH 3T3 cells were infected at MOI of 1 PFU/cell with MCMV and MCMVdie3. Transcripts levels were measured by qRT-PCR for *ie3* (**i**) and *ie1* (**ii**) at -0.5hpi (ie. within the absorption period), 0.5hpi and 2.5hpi. Fold induction is shown on the Y axis relative to the parental MCMV strain. The level of detection (dotted line) represents non-specific PCR signals from mock-infected cells.

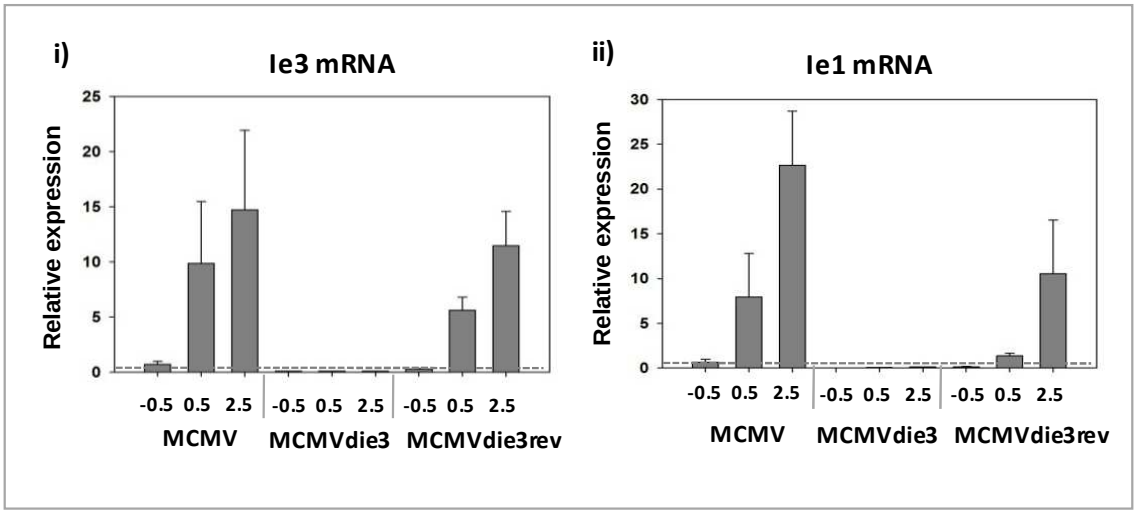

The qRT-PCR analysis indicated no *ie3* expression was detectable from the deleted *ie3* locus in MCMVdie3 (Figure 3.5 a i), and also revealed a considerably lower level of *ie1* transcription in the MCMVdie3 strain compared to wild-type MCMV (Figure 3.5 a ii). The reduction was 1-2 orders of magnitude lower (Figure 3.5a), however *ie1* transcripts were still detectable at very low levels (above mock). Although this was encouraging in the sense that MCMVdie3 was more transcriptionally inert than previously reported, the result was not consistent with previously published studies and warranted further investigation.

In order to test whether the reduced *ie1* levels in MCMVdie3 were due to the lack of a *de novo* MCMV protein, the infections were repeated in the presence of 50ug/ml cyclohexmide, a chemical inhibitor of protein synthesis. This would block viral protein synthesis in the wild-type MCMV infection and determine whether the reduction in IE transcript levels in the MCMVdie3 infection had any link to *de novo* IE3 protein synthesis (IE3 had previously been reported to regulate the MCMV MIEP promoter(12)).

Figure 3.6 - *Immediate early gene 1* expression is attenuated in MCMVdie3 in both the presence and absence of cycloheximide Triplicate cultures of NIH 3T3 cells were infected at MOI 1 PFU/cell with MCMV and MCMVdie3 in the presence and absence of 50ug/ml cyclohexmide (+/-CHX). Transcripts levels were measured

by qRT-PCR for *ie3* (**a**) and *ie1* (**b**) at 2.5hpi (**i**) and 15hpi (**ii**). Fold induction is shown in log scale relative to parental MCMV strain in the absence of CHX. The level of detection (dotted line) represents non-specific PCR signals from mock-infected cells.

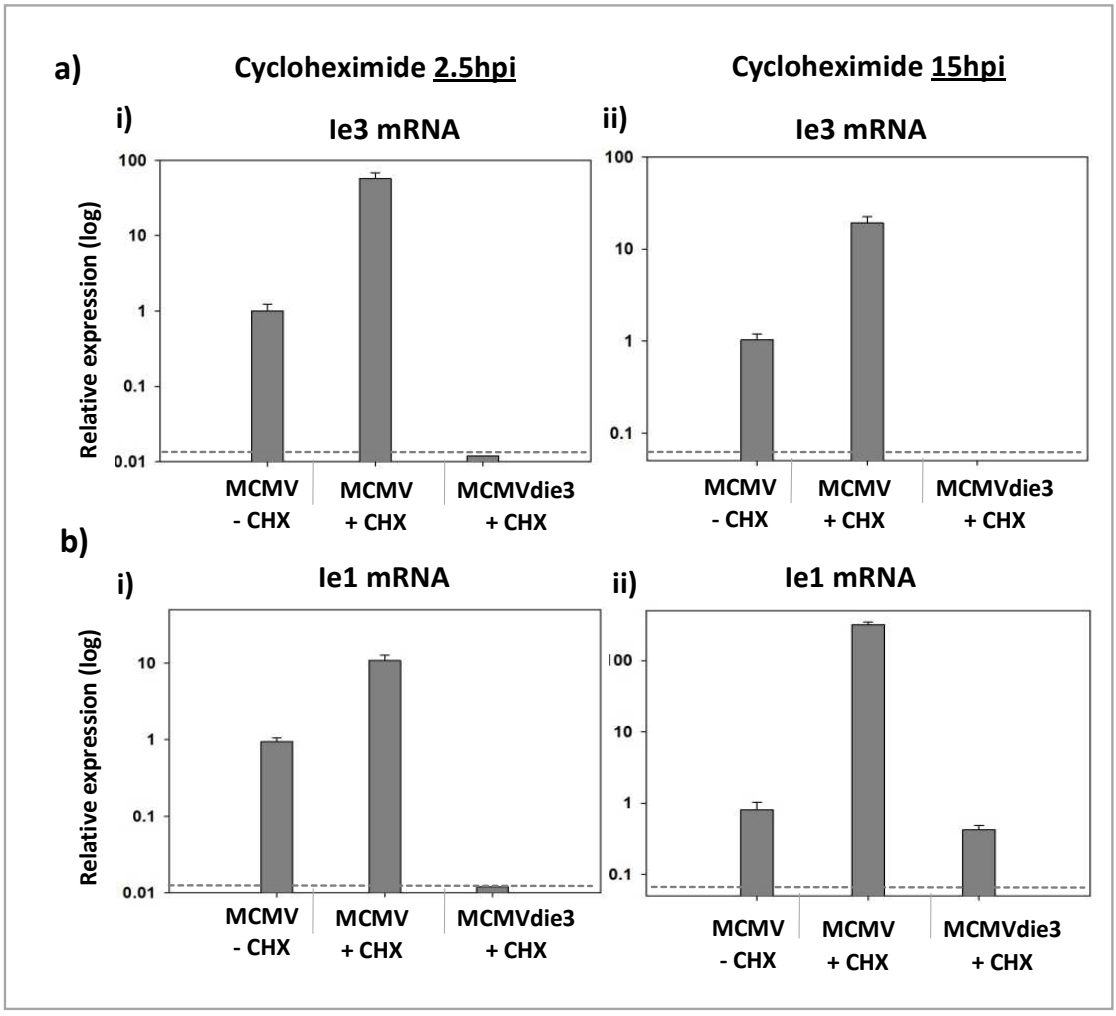

In the presence of cycloheximide, the *ie1* transcript levels from MCMVdie3 compared to the parental strain were still attenuated by over two orders of magnitude at both 2.5hpi and 15hpi (Figure 3.6 b). The *ie1* gene was however, still expressed in MCMVdie3 (Figure 3.6 b ii), but to significantly attenuated levels. This result indicated attenuated *ie1* gene expression in MCMVdei3 was not due to factors relating to viral protein function, and ruled out any positive auto-regulation by the IE3 protein. At this stage, it appeared the attenuated MCMVdie3 *ie1* gene expression may be due to a secondary mutation in the genomic sequence of the

MCMVdie3 strain, possibly within the MIEP regulatory region. This mutation may have been masked by the IE3 protein provided in *trans* in the complementing cell line in which the MCMVdie3 strain was grown.

3.4 Sequencing of the MCMVdie3 Major Immediate Early Promoter region

The reduced levels of *ie1* transcripts from MCMVdie3 in the presence of cycloheximide gave reason to believe the MCMVdie3 enhancer region may be mutated beyond the deleted *ie3* region, possibly by a secondary site mutation within the MIEP causing attenuated *ie1* expression. In order to test this, and to determine if any major aberrations had occurred in the MCMVdie3 MIEP region during passage in a complementing cell line, the MIEP region (NC_004065, 182,796-184,368C, 1572bps) from MCMVdie3 was amplified by PCR and sequenced using the Sanger method (for details see Methods). The resulting sequence was aligned against the reference MCMV MIEP sequence from the parental MCMV strain (299). The alignment showed no major deletions or rearrangements within the MCMVdie3 MIEP region at the level of 70% identity (Figure 3.7), however the sequence quality was poor and not sensitive enough to detect changes at the single base-pair level.

Figure 3.7 - Sequence alignment map of the MCMVdie3 MIEP region. The MCMV MIEP region from the MCMVdie3 strain (NC_004065, 182,796-184,368C, 1572bps) was amplified by PCR in triplicate reactions and sequenced using the Sanger method. To cover the 1572 bp region, two contigs were sequenced, Region 1(**a**); 182,796-183,923 and Region 2 (**b**); 183,743-184,368. The sequences were aligned against a reference MCMV MIEP sequence from the parental strain (299). The alignment shows sequence identify at 70% with a mis-match penalty of 2.

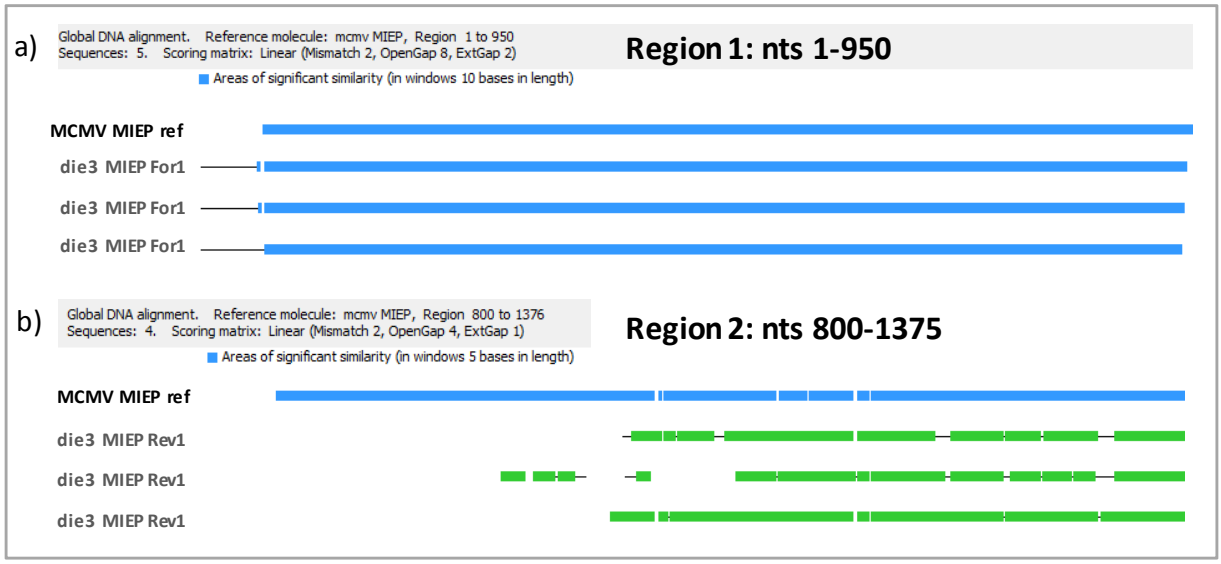

The results of the sequencing analysis suggest the MCMVdie3 MIEP region had not been affected by any *major* mutations at the level of 70% identity. The transcriptional silencing of the *ie1* gene in MCMVdie3 must therefore have been due to another factor, possibly a mutation further within an exonic region, or by epigenetic factors. Regardless, the final outcome, was that the MCMVdie3 strain was even more transcriptionally silenced than first reported**.**

3.5 Viral protein expression does not occur past the IE region in MCMVdie3

Finally, to assess whether productive MCMV infection occurred in BMDMs at MOI of 1 PFU/cell despite the low level of initial infection, BMDMs were infected with MCMV or MCMVdie3 at MOI of 1 and viral protein expression was measured using Western Blots. MCMV immediate early (IE1), early (E1) and late (M6) proteins were measured. The result indicated that MCMV is capable of establishing productive infection in BMDMs within 4hpi, and showed that early and late viral protein expression does not occur in MCMVdie3-infected cells (Figure 3.8). Low levels of IE1 expression were, however, detectable in MCMVdie3-infected cells.

Figure 3.8 - Viral protein expression in MCMVdie3 does not occur beyond the IE region in BMDMs. BMDMs were infected at MOI 1 with MCMV (lanes 3 and 5) and MCMVdie3 (lanes 4 and 6) and whole cell lysates were harvested at 2hpi (lanes 3 and 4) and 4hpi (lanes 5 and 6). Western blots were performed for immediate early protein IE1, early protein E1, and late protein M6 with β-actin used as a loading control. Protein from heavily infected fibroblasts was used as a positive control (lane 1) and protein from mock infected cells was used as a negative control (lane 2). *Western blots were performed by Christopher Millward under the supervision of Paul Lacaze at the Division of Pathway Medicine, University of Edinburgh, UK

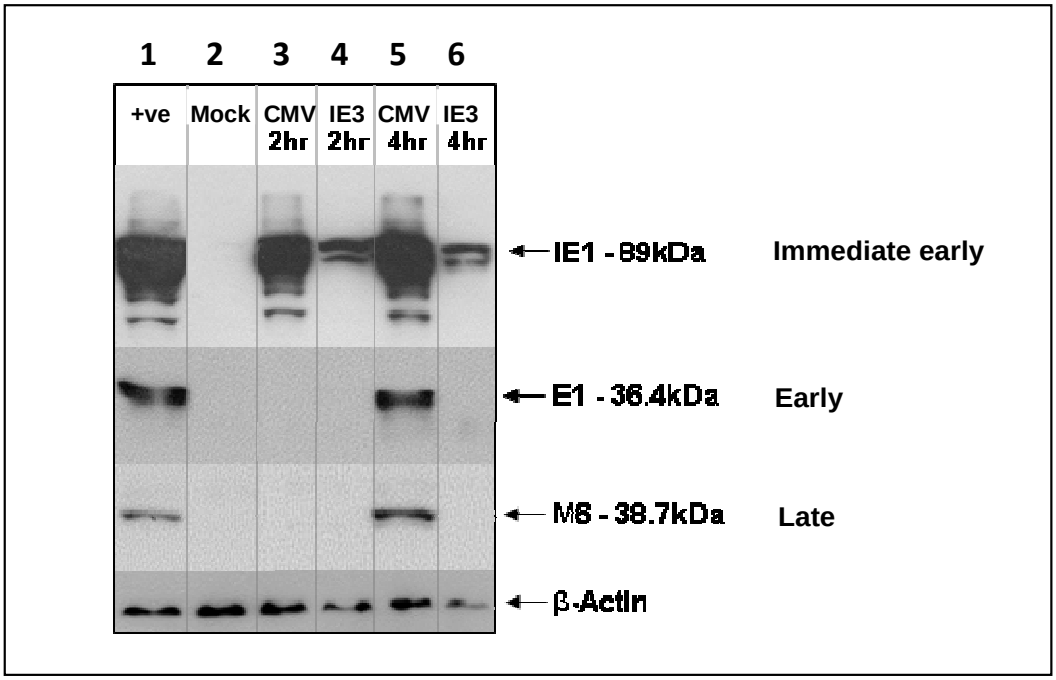

The Western blot indicated that IE1 was still expressed by MCMVdie3 at low levels. Other immediate early proteins may also be expressed in this same manner. Taking this into account, the potential effect of immediate early proteins on immune signalling in MCMVdie3-infected cells had to be considered for future experiments. This is significant given the role of IE1 in interacting with host factors during MCMV infection (49, 126, 188, 351). The MCMVdie3 virus, therefore, cannot be considered completely inactivated but rather only attenuated in viral gene expression beyond the IE region.

Discussion

The objective of the work in this chapter was to functionally and phenotypically characterize the MCMVdie3 mutant strain and ensure it is a non-productive, replication deficient and transcriptionally attenuated virus, capable of entering host cells but incapable of productive viral infection. Characterization of this phenotype meant the mutant strain could be used as an alternative approach to UV-inactivated MCMV virions to represent non-productive infection. The characterization was achieved using a range of virologic and molecular techniques, each of which was informative of the mutant phenotype in a different way.

Firstly, viral growth was measured using plaque assays to show MCMVdie3 was replication deficient in permissive fibroblast cells (NIH 3T3s) and mouse BMDMs, both at low and high multiplicities of infection. Furthermore, as viral growth was completely recoverable in the complementing cell line, it showed the mutant was still functional and capable of replication if the IE3 protein is provided in *trans*. These preliminary results were all consistent with previous characterization work on the MCMVdie3 strain(12, 49).

Secondly, a qPCR assay was developed to measure equivalency of infection between MCMV strains at the genomic level. This assay was valuable in establishing equivalent doses of viral particles delivered at the genomic level between infections, and equivalent genome/PFU ratios in each viral stock. The assay was also used to determine the number of viral genomes inside differentially infected cells, and revealed that only a small portion of delivered viral genomes successfully enter BMDMs at MOI of 1 PFU/cell. This result was supported by flow cytometry data generated using a MCMV-GFP reporter virus, indicating only around 12% of BMDMs are GFP-positive at 6hpi using MOI of 1 PFU/cell. The outcome of these findings indicates the initial level of infection in BMDM cultures at MOI of 1 is very low. Despite this, the numbers of MCMV genomes detectable in MCMV and MCMVdie3-infected cells were comparable at 2hpi, indicating levels of viral entry between the strains were comparable (albeit low). Further, it showed that deletion of the *ie3* gene did not affect viral entry for the mutant virus.

The development of the qPCR assay also provided a more sensitive and accurate method for the detection of MCMV particles in infected cells and viral stocks compared to the 'gold standard' plaque assay technique. The plaque assay only provides a measure of infectious plaque-forming units (PFUs), as indicated by regions of lysed cells of NIH 3T3 monolayers, rather than providing a quantitative measure of MCMV genomes in infected BMDMs. Therefore, development of the qPCR assay was important in providing a more sensitive and flexible technique for the detection of MCMV in different experimental settings. The assay also showed the initial level of infection in BMDM cultures at MOI of 1 PFU/cell is very low. Similar approaches based on qPCR have been used elsewhere(331), however this assay will now be of direct future benefit for the study of MCMV genome copy numbers.

The gene expression phenotypes of the different MCMV strains were investigated using a custom DNA oligonucleotide microarray for global detection of MCMV transcripts. This analysis indicated MCMVdie3 is a transcriptionally attenuated virus in comparison to the parental MCMCV strain in fibroblasts. qRT-PCR analysis of immediate early viral gene expression in MCMVdie3 revealed that *ie1* was still expressed by MCMVdie3, but at considerably lower level compared to the wild-type virus. This result was contrary to previous reports(12) and seen in both the presence and absence of cycloheximide.

For the purpose of this study, the attenuated IE transcriptional phenotype of the MCMVdie3 strain did not compromise further experiments. In contrast, it made the strain even more transcriptionally inactive, and therefore, even more appropriate for use as a control reagent to represent non-productive MCMV infection. For future studies focusing on *ie3* function, however, the MCMVdie3 strain will have to be used with extreme caution, or else re-propagated from the original C3X-die3 BAC plasmid.

The attenuated *ie1* levels in MCMVdie3 were investigated further by sequencing of the MCMVdie3 MIEP region to determine if a secondary site mutation had occurred.

The sequencing, however, did not identify any major deletions or re-arrangements in the MCMVdie3 MIEP region. The sequencing analysis, which was outsourced to a sequencing service company and performed using the Sanger method, did not yield high quality sequence data. The sequencing was repeated three times using independent samples, but sequence quality remained poor. This could be due to technical issues related to the Sanger sequencing instrumentation, however, is more likely due to the high degree of sequence repeats and high GC content within the MCMV MIEP region(199). Repeats can lead to problems associated with primer design, both for PCR primers and for sequencing primers, leading to non-specific PCR products and/or non-identical sequences reads, resulting in poor sequence quality. To avoid non-specific PCR amplification and sequencing, different combinations of primers were used, and PCR products were run on gels after each reaction to confirm size. The sequence quality, however, remained poor and, therefore, the only conclusion that could be made from the data was that no major mutations or rearrangements had occurred, based on alignments at 70% identity.

Finally, viral protein expression was measured in MCMV and MCMVdie3 infected BMDMs using Western blots. No viral protein expression beyond the IE region was detected in MCMVdie3-infected BMDMs. The Western blots also indicated productive MCMV infection occurs within four hours of infection in BMDMs using the wild-type MCMV strain. This suggested productive MCMV infection is still established in BMDMs at MOI of 1 PFU/cell, despite low levels of infection as indicated by qPCR and MCMV-GFP reporter virus.

The only modification to the MCMVdie3 characterization work which, in hindsight, could be improved on would be performing direct comparisons of UV-inactivated MCMV virions with the MCMVdie3 virus. This would provide a direct comparison of the two conditions, and would indicate how similar and inter-changeable they might be from an experimental perspective. This comparison would have been particularly useful in the early stages, and if equivalency between the two conditions was shown, UV-inactivated MCMV virions could be excluded from subsequent

analyses. This, however, was not done due to technical complications with UV instrumentation early in the study.

Another issue to consider is that MCMVdie3 virions still contain tegument proteins enclosed within the viral particle. Up to 38 different MCMV proteins have been detected in the MCMV virion by mass spectrometry(184), and many of these proteins are predicted to have immune-modulatory functions(181, 182). Tegument proteins, however, will be functional in both MCMVdie3 and UV-inactivated virions. At least in the case of MCMVdie3, immune-evasion as a result of *de novo* MCMV proteins can be ruled out. The effect of immediate early viral proteins, such as IE1, also cannot be ruled out in MCMVdie3 infections.

Overall, the characterization work provided an essential foundation on which future work could be built, and meant that future experiments based on the host-response to productive versus non-productive MCMV infection could be conducted using MCMVdie3 as a control reagent instead of UV-inactivated virions. The MCMVdie3 strain was shown to be capable of entering host cells, but incapable of replication, and considerably attenuated in viral gene and protein expression beyond the IE region. These characteristics made it an appropriate tool for non-productive viral infection for subsequent BMDM experiments.

Chapter 4

Systems analysis of the host response to productive and non-productive MCMV infection in macrophages

Introduction

In the previous chapter, a mutant MCMV strain (MCMVdie3) was characterized and shown to be capable of entering host cells, but incapable of viral replication. The MCMVdie3 virus was also shown to be attenuated in viral gene and protein expression beyond the IE region. The MCMVdie3 strain was, therefore, deemed appropriate for use as a genetic tool and control reagent to represent non-productive viral infection. In the work described in this chapter, macrophages are infected in parallel with wild-type MCMV and MCMVdie3, and the innate immune response to both viruses is analyzed at the systems-level. These experiments address the central hypothesis of the thesis, and determine whether macrophages are capable of responding differentially to productive and non-productive MCMV infection.

In considering the macrophage innate immune response to productive and non-productive MCMV infection, there are a number of possible outcomes that could occur regarding differential activation of signalling pathways and regulation of downstream genes in response to the two conditions. Firstly, activation of signalling pathways in response to MCMV and MCMVdie3 could be induced to roughly equivalent levels, resulting in an overlapping, or indistinguishable response. This outcome would suggest macrophages respond in an equivalent manner to productive and non-productive MCMV infection, and would refute the hypothesis of this study. Secondly, activation of innate immune signalling and downstream gene expression could be induced to greater levels in response to productive MCMV infection, and be curtailed or suppressed in response to the inactive MCMVdie3 virion. This outcome

would support the hypothesis of the study, and suggest macrophages respond differently to productive MCMV infection. The third possible outcome, however, is that macrophages respond to the attenuated MCMVdie3 virus with higher levels of innate immune signalling and pro-inflammatory gene expression. If this is the case, it suggests *de novo* MCMV proteins suppress the innate immune response in macrophages during productive infection. This outcome would refute the hypothesis, however, would be consistent with most previous studies using fibroblasts and UV-inactivated virions to measure the response to productive and non-productive virus infection. Most of these studies report higher levels of type I IFN and ISG expression in response to UV-inactivated virions compared to productive viruses(43, 142, 260, 263, 289, 345).

In order to determine the outcome of macrophage infection with productive and non-productive MCMV, the innate immune response to both conditions was profiled temporally in BMDMs using a range of different techniques. The results presented in this chapter will provide a comprehensive account of the similarities and differences in the macrophage innate immune response to the two conditions.

Results

4.1 Characterization of bone marrow-derived macrophages (BMDMs)

Before proceeding with macrophage host-response experiments, first the BMDM system required characterization. To determine the proportion of macrophage-like cells in BMDM cultures after the seven-day differentiation period, fluorescence-activated cell sorting (FACS) was used to measure expression of macrophage-specific cell surface protein markers CD11b and F4/80. Figure 4.1 shows 99.5% of gated cells were positive for both F4/80 and CD11b, indicating differentiation of macrophages in the M-CSF conditioned medium yielded a homogenous population of mature BMDMs after 7 days. L929 conditioned growth medium and FCS used to culture BMDMs were also routinely tested for exdotoxin (<0.02 ng/ml) and mycoplasma.

Figure 4.1 Phenotypic characterization of BMDMs by flow cytometry

The level of expression of F4/80 and CD11b and their isotypes was analysed by flow cytometry. A) Dot blot showing gating of cells in forward scatter (FSC) and side scatter (SSC). B). Scatter plot showing double-staining signals for F4/80 (y-axis) and CD11b (x-axis) plotted against each other. C) Histogram of percentage enrichment of CD11b (Fitc) positive cells within the gated population. D) Histogram of percentage enrichment of F4/80 (PE) positive cells within the gated population.

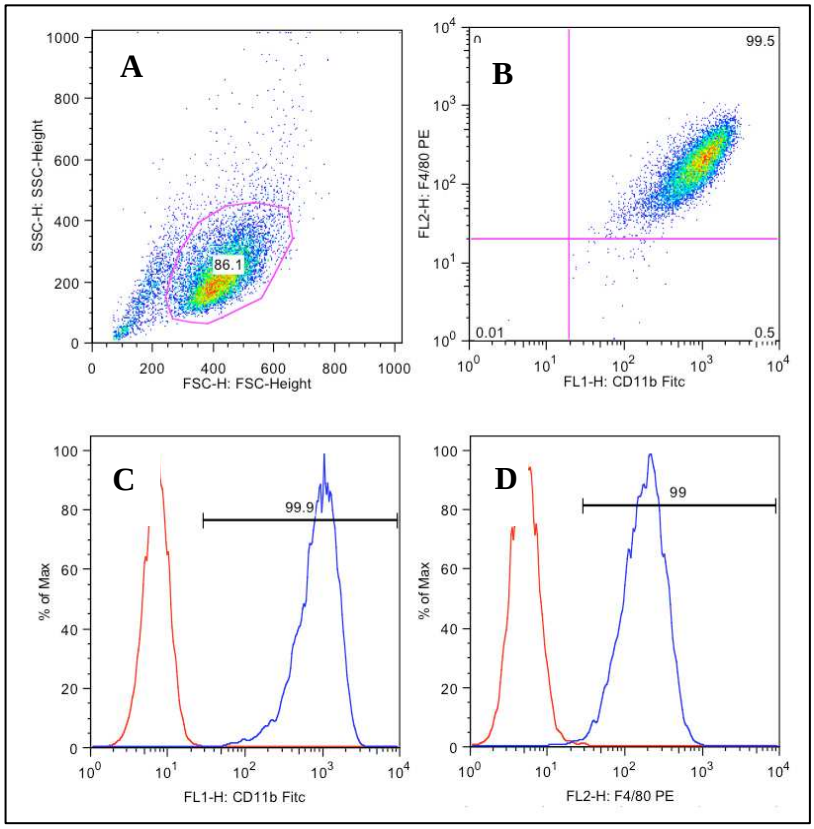

4.2 Experimental overview: Macrophage host response to productive and non-productive MCMV infection

To measure the temporal, dynamic macrophage host response to productive and non-productive MCMV infection, BMDMs were infected on day seven of culture at MOI of 1 PFU/cell with MCMV or MCMVdie3 and a time course analysis was undertaken with cell culture supernatants and total RNA harvested at 0, 2, 4, 6, 8, 10, 12 and 24hpi, from three replicates cultures per condition per time point. The first time point (0hpi) corresponded to the end of the 1.5 hour viral adsorption period after cells had been washed free of viral innoculum and replenished with fresh medium. This means at the 0hpi time point cells have already been in contact with viral particles for 1.5 hours. Mock infected samples were taken at each time point over the course of the experiment (for an overview see Figure 4.2).

Figure 4.2 Experimental overview: Macrophage antiviral host response. Bone-marrow progenitor cells from male C57BL/6 mice were flushed from mouse femurs and differentiated in conditioned medium containing M-CSF1 for seven days, and re-fed on days 3 and 5. Confluent BMDM monolayers were infected on day 7 with MCMV and MCMVdie3 in parallel and triplicate cell culture supernatants and total RNA were harvested every two hours between 0-12hi and at 24 hpi.

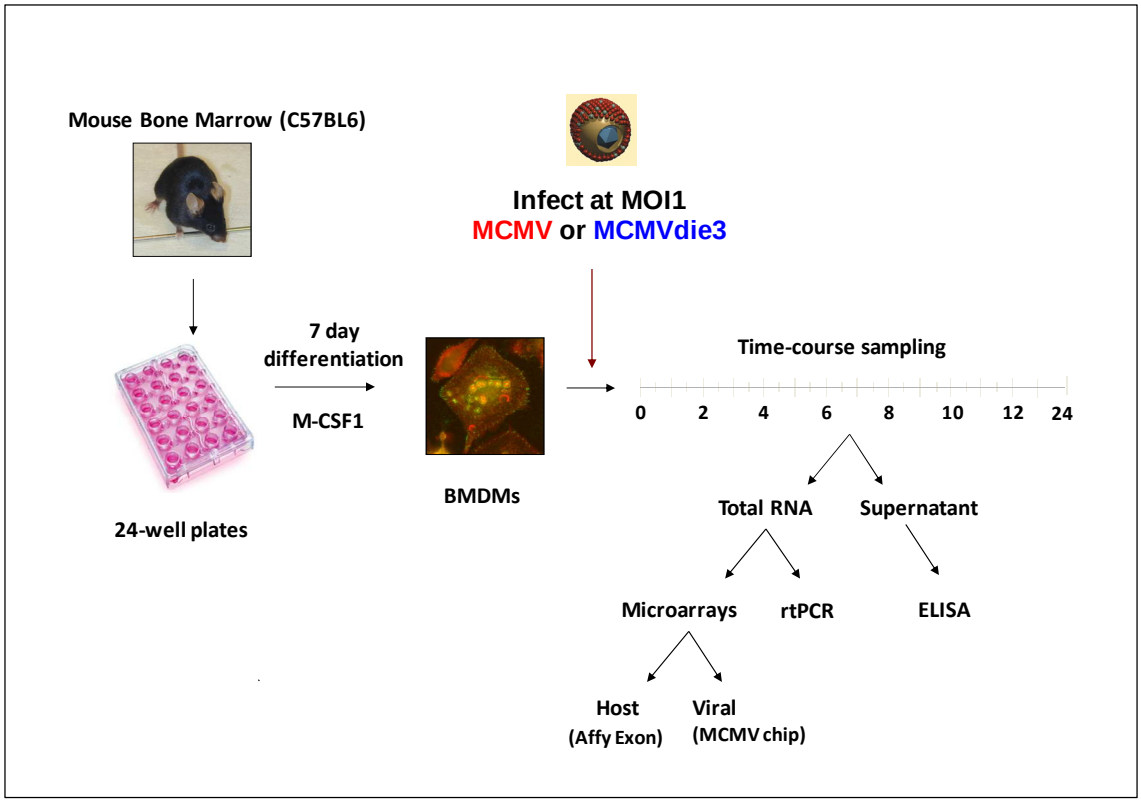

4.3 IFNβ induction occurs more rapidly in response to productive MCMV infection

The first question regarding the differential innate immune response to productive and non-productive MCMV infection in macrophages was whether IFNβ was induced equivalently in response to the two conditions. The induction of IFNβ is a key signalling event in the innate immune response and occurs directly after PRR activation (38). Several studies report IFNβ to be induced to higher levels in response to UV-inactivated virions compared to wild-type virus, including one study using MCMV(208).

Ifnb1 transcripts were measured using qRT-PCR at 0, 2, 4, 6, and 8hpi in both MCMV and MCMVdie3 infected BMDMs (Figure 4.3). IFNβ is a single-exon gene, therefore all RNA samples were DNase-treated prior to qRT-PCR to avoid non-specific amplification of genomic DNA. Furthermore, to ensure equivalency of infection between the two conditions (i.e. that equivalent number of MCMV genomes were delivered per cell) the viral genome copy number per PFU for MCMV and MCMVdie3 viral stocks was measured (see previous chapter Table 3.1). In addition, the number of MCMV genome copies detectable inside infected BMDMs at 2hpi was measured and found to be equivalent (see previous chapter Figure 3.3).

As seen in Figure 4.3, *Ifnb1* transcripts were induced in response to both conditions, suggesting the attenuated MCMV virion was still capable of inducing IFNβ in BMDMs. Notably, however, this induction was more rapid in response to productive MCMV infection by a period of 2-4 hours. The regulation of *Ifnb1* expression in response to MCMV and MCMVdie3 was similar, but peak levels occurred at different time points. There was a two-fold or greater difference in *Ifnb1* transcript abundance between the conditions at 0hpi, 2hp and 6hpi.

Figure 4.3 Transcriptional induction of *Ifnb1* occurs more rapidly in response productive MCMV infection. BMDMs were infected at MOI of 1 PFU/cell and *Ifnb1* transcripts were measured at 0-8hpi in response to MCMV (solid lines) and MCMVdie3 (dotted lines) using Taqman qRT-PCR gene expression assays. The 0hpi time point represents the end of the 1.5 hour viral adsorption period. Transcript levels were normalized to the housekeeping gene *Gapdh* and calibrated to mock levels to show relative expression. Error bars indicate standard deviation from three separate cultures. Asterisks indicate a two-fold or greater difference between conditions.

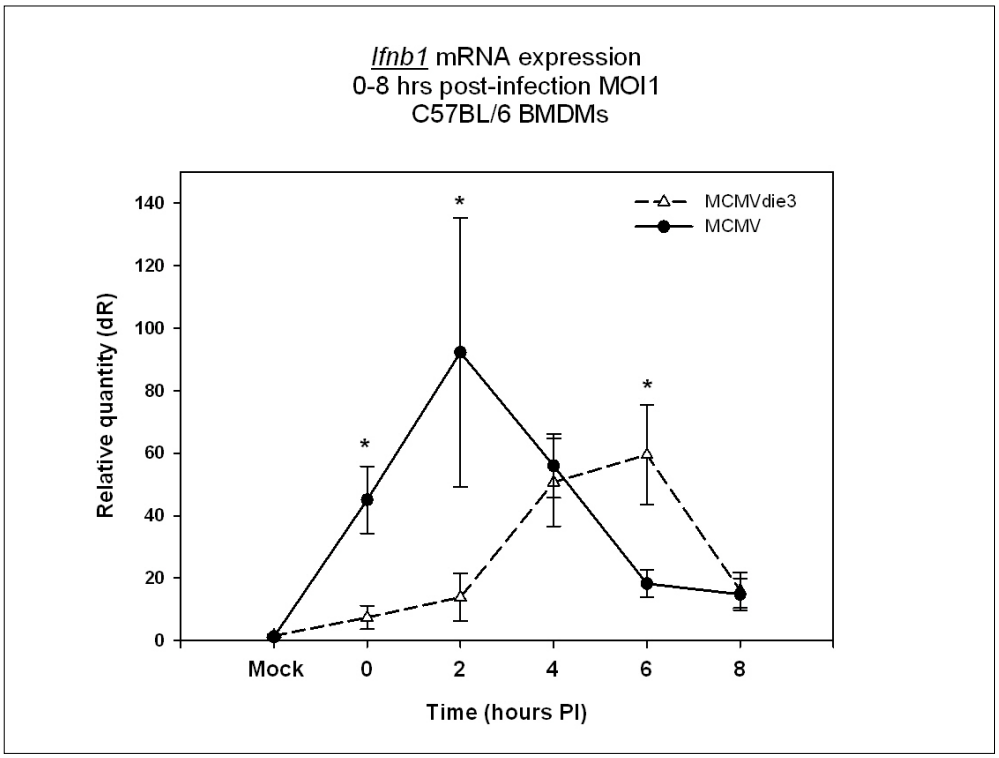

Next, to assess whether the more rapid induction of IFNβ was also detectable at the protein level, secreted IFNB1 protein was measured in cell culture supernatants using ELISA at 2-10hpi. This indicated a more rapid induction of IFNβ in response to productive MCMV infection at the secreted protein level. Differences in IFNβ induction at both the gene expression and protein level between MCMV and MCMVdie3 are shown in Figure 4.4.

Figure 4.4 Induction of IFNβ at the gene expression and protein level occurs more rapidly in response productive MCMV infection. BMDMs were infected at a MOI of 1 PFU/cell. Induction of IFNβ in response to MCMV (solid lines) and MCMVdie3 (dotted lines) was measured at the transcript level using Taqman qRT-PCR gene expression assays (orange lines) and secreted protein level using ELISA (blue lines). The 0hpi time point represents the end of the 1.5 hour viral adsorption period. Error bars indicate standard deviation from three separate cultures.

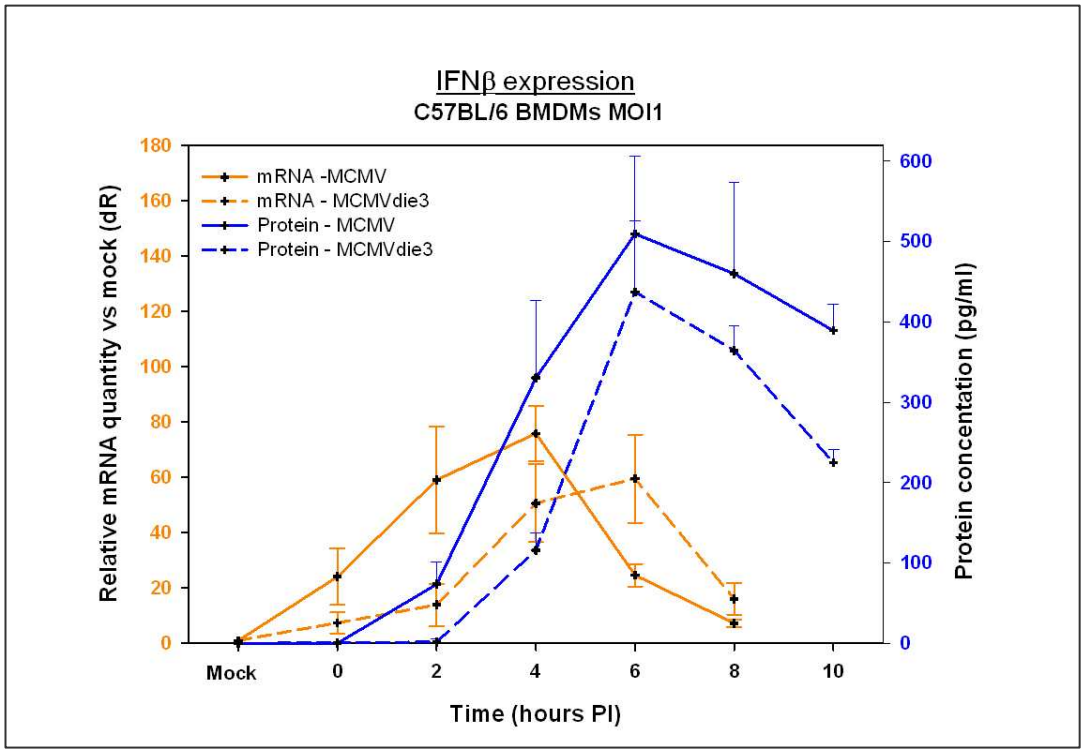

To validate the observation regarding IFNβ induction, the time course experiment was repeated using BMDMs from a different set of mice. *Ifnb1* transcripts levels were again measured using qRT-PCR at 0-8hpi in response to MCMV and MCMVdie3. In the repeat experiment, *Ifnb1* transcripts were again induced more rapidly in response to productive MCMV infection, with a greater than two-fold difference at 2hpi (Figure 4.5a). Results from an additional microarray experiment performed under the same conditions are also shown in Figure 4.5b, and show the same effect.

Figure 4.5 - Transcriptional induction of *Ifnb1* occurs more rapidly in response productive MCMV infection (repeat experiments). BMDMs were infected at MOI of 1 PFU/cell. *Ifnb1* transcript levels were measured in response to MCMV (solid lines) and MCMVdie3 (dotted lines) at 0-8hpi using Taqman qRT-PCR gene expression assays. The 0hpi time point represents the end of the 1.5 hour viral adsorption period. Transcript levels were normalized to the housekeeping gene *Gapdh*. Error bars indicate standard deviation from three separate cultures. Asterisks indicate a greater than two-fold difference between conditions.

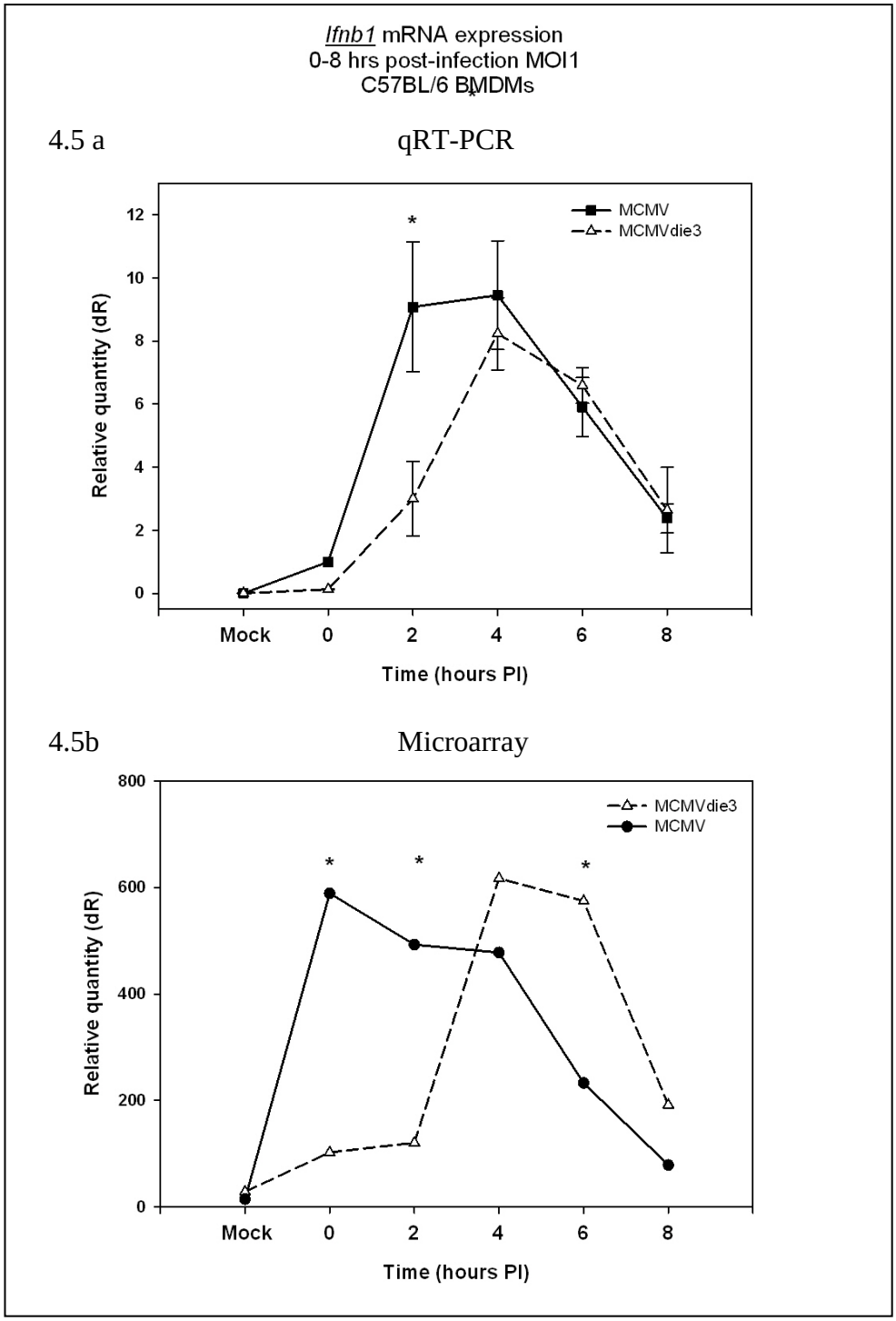

4.4 Induction of TNFα gene expression occurs in an equivalent manner in response to productive and non-productive MCMV infection

Next, to test if the rapid induction of IFNβ in response to productive MCMV infection was a specific effect, or extended to other cytokines, TNFα (*Tnf*) transcript levels were measured at 0-6hpi in response to the two MCMV strains. TNFα is a pro-inflammatory cytokine induced by mechanisms independent of IFN during the antiviral response(92). Difference in the kinetics TNFα induction were not seen at the gene expression level, as *Tnf* transcripts were induced with equivalent kinetics and to equivalent peak levels in response to MCMV and MCMVdie3 (Figure 4.6). This result indicated the more rapid induction seen for IFNβ did not apply to the pro-inflammatory cytokine TNFα. It did, however, show the inactive MCMVdie3 virion is capable of inducing a pro-inflammatory response, as well as a type I IFN response, at the transcriptional level in BMDMs.

Figure 4.6 Induction of TNFα gene expression is equivalent in response to MCMV and MCMVdie3. BMDMs were infected at MOI of 1 PFU/cell. *Tnf* transcript levels in response to MCMV (solid lines) and MCMVdie3 (dotted lines) were measured at 0-6hpi using Taqman qRT-PCR gene expression assays. The 0hpi time point represents the end of the 1.5 hour viral adsorption period. Transcript levels were normalized to the housekeeping gene *Gapdh* and calibrated to mock samples to show relative expression. Error bars indicate standard deviation from three cultures.

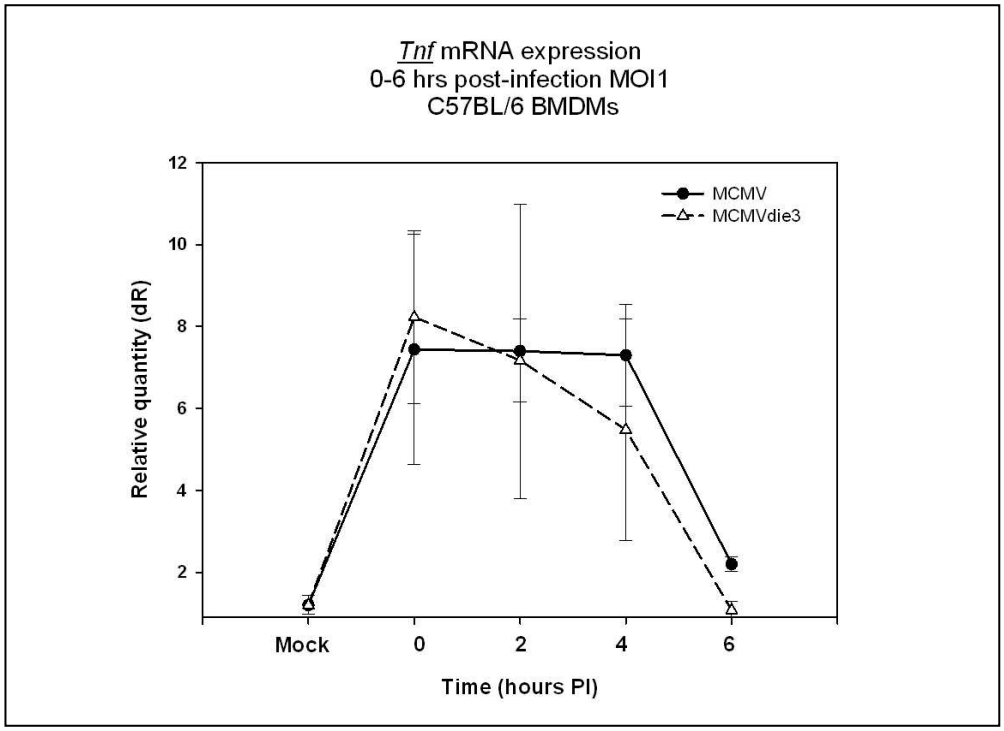

4.5 Global gene expression profiling of the macrophage response to productive and non-productive MCMV infection

4.5.1 Microarray data processing

The next step was to assess differences in macrophage gene expression in response to productive and non-productive MCMV infection at the genome-wide level. To achieve this, time-course microarray profiling of BMDMs was conducted. The objective of this analysis was to identify differentially regulated genes in response to the two conditions, and find genes induced specifically in response to productive MCMV infection. Total RNA from the BMDM time-course experiment was extracted from MCMV and MCMVdie3-treated BMDM cultures at 0, 2, 4, 6, 8, 10, and 24hpi and hybridized to Affymetrix Mouse Exon 1.0ST microarrays. Mock-infected samples at 0 and 24hpi were also included in the microarray analysis. 0hpi corresponded to the end of the 1.5 hour viral adsorption period.

Microarray data from the exon-level microarray probes was quality controlled, log transformed and normalized according to standard Affymetrix workflows (for details see Methods section 2.7.2). All samples passed quality control measures and gene-level data were obtained for a total of 16,761 annotated mouse genes. To remove genes not expressed across the dataset, a filter was applied to exclude any gene with a maximum normalized intensity of less than 100 across all samples. This value corresponded to the mean of all negative control probes plus two standard deviations. This filter reduced the dataset to 7,890 genes expressed to a high confidence level.

To determine if microarray measurements were equivalent to those made previously by qRT-PCR, the expression of *Ifnb1* was assessed in the microarray data. The previously reported delay in *Ifnb1* induction in response to MCMVdie3 was also detectable in the microarray in an equivalent manner as it was using qRT-PCR (see Figure 4.5b).

To determine how many genes were changing statistically in response to either the MCMV or MCMVdie3 infection over the time course, the EDGE tool was used(213). EDGE is open-source software specifically designed for the statistical analysis of time-series microarray data, and is based on using permutations to determine significance of gene changes over time based on a longitudinal model. Using *time course* function with 500 iterations, natural cubic spline and a Q-value cut-off of 0.001, 980 genes were found to be differentially expressed in response to MCMV over the time course (for details see Methods). Using the same settings, 1044 genes were found to be differentially expressed in response to the attenuated MCMVdie3. This indicated the total number of genes statistically changing in response to productive (n980) or non-productive (n1044) MCMV infection in BMDMs was similar over the 24 hours of infection (for complete lists of EDGE genes see Supplementary Files 6 and 7).

4.5.2 Hierarchical clustering analysis

Next, in order to obtain an unbiased overview of the microarray data, and determine which samples were correlated based on their overall gene expression profile, unsupervised hierarchical clustering analysis of the 7,890 filtered genes was performed. The objective of this was to determine similarities between samples, and between groups of genes across the data set. The hierarchical clustering analysis generated a heatmap based on gene-to-gene correlation (y-axis) and sample-to-sample correlation (x-axis). Genes with similar expression profiles were arranged together as rows into distinct groups or clusters. Similarly, individual samples sharing correlated expression profiles were clustered together as columns. This technique provided a qualitative assessment of the similarities and differences between genes and samples in the dataset (Figure 4.7).

Figure 4.7 - Unsupervised hierarchical clustering of 7,890 genes and 16 microarray samples in response to productive and non-productive MCMV infection. BMDMs were infected at MOI of 1 PFU/cell with MCMV or MCMVdie3 and transcript levels were measured using Affymetrix Mouse Exon 1.0ST microarrays. Hierarchical clustering was performed on 7,890 filtered genes, with

each gene represented as a row and per-gene normalized to its mean value to show relative expression. Yellow indicates an increase relative to the mean for each gene and blue indicates a decrease. Genes are clustered on similarity of expression profile with similar genes connected by the hierarchical tree on the left. Samples (columns) are also clustered based on correlation and are connected by the hierarchical tree at the top. Samples are labelled at the bottom of the figure and colour-coded by green (mock), red (MCMV) and blue (MCMVdie3).

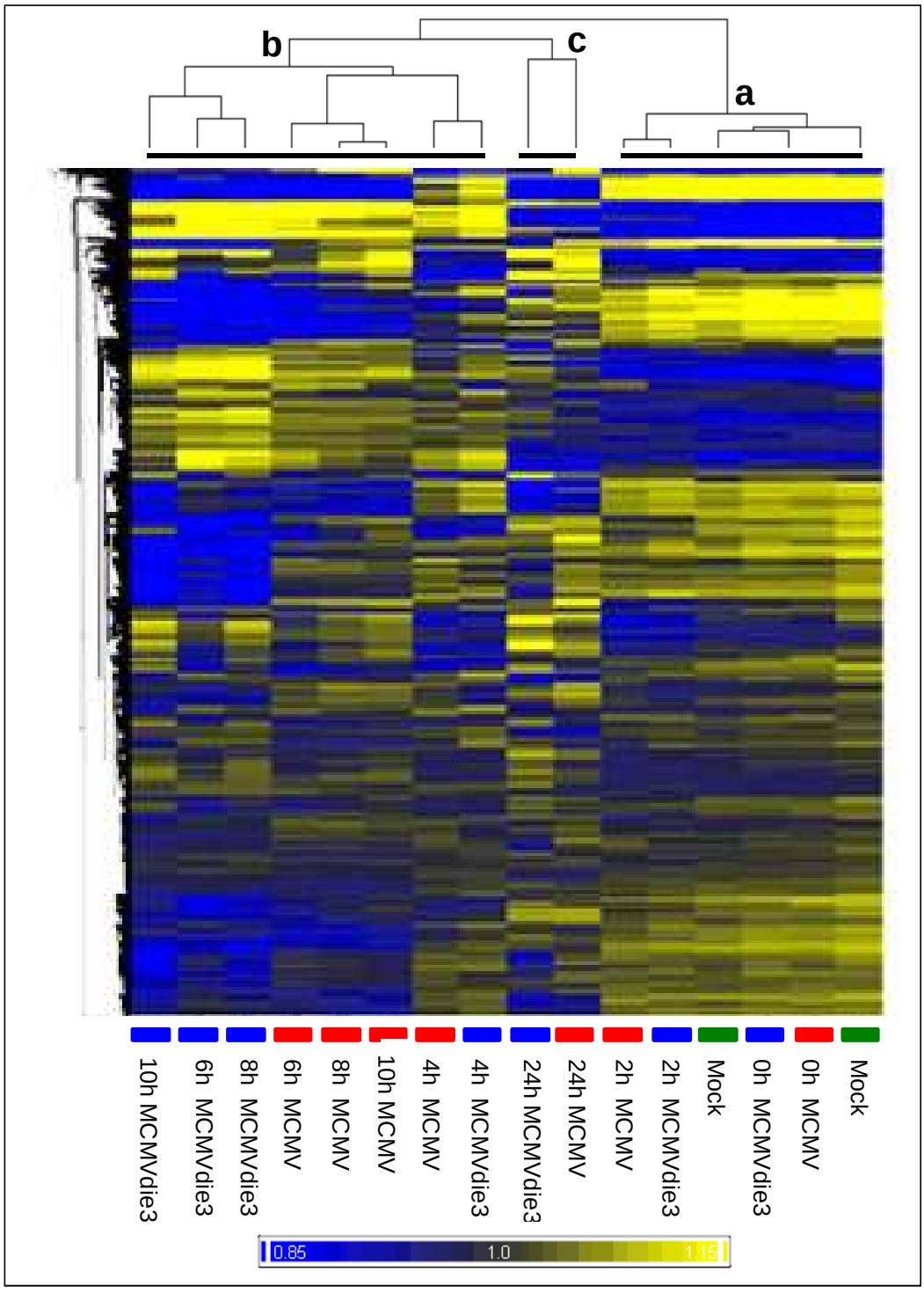

Figure 4.7 shows the clustering of 7,890 genes and 16 microarray samples across the dataset. Based on the hierarchical tree at the top of the heatmap, the 16 samples are separated into three distinct clusters or groups based on the similarity of gene expression across the 7,890 genes (labelled **a, b, c**). The 16 samples fall into three distinct groups based on the kinetics of the response. Firstly, on the far right side of the heatmap (**a**), the Mock, 0hpi and 2hpi samples from both MCMV and MCMVdie3 conditions have clustered together. This indicates that only few gene expression changes have occurred at these early time points (0hpi, 2hpi) relative to Mock. It also indicates that there have been only few gene expression differences between the MCMV and MCMVdie3 responses at these early time points (0-2hpi).

On the left side of the heatmap (**b**), there is a second group of samples which is larger and consists of 4hpi, 6hpi and 8hpi samples from both MCMV and MCMVdie3. This larger group of samples is split into three sub-groups consisting of the two 4hpi samples together on the right, then the MCMV 6hpi, 8hpi, 10hpi samples, then finally the MCMVdie3 6hpi, 8hpi, 10hpi samples on the far left. These sub-groups indicate the macrophage transcriptional response to MCMV and MCMVdie3 is diverging kinetically between 6-10hpi. It also suggests MCMV and MCMVdie3 samples are different during these time points as they have clustered into separate sub-groups. Upon close inspection of the heatmap, the differences between MCMV and MCMVdie3 samples between 6-10hpi are both kinetic and quantitative, indicating differential immune responses occurring in response to the different conditions. These differences will be expanded on in later sections of the thesis.

Finally, the third overall group of samples are the two 24hpi samples found in the centre of the heatmap (**c**). These two 24hpi samples cluster together to form their own sub-group. This again shows kinetic changes in macrophage gene expression occurring. Despite the 24hpi MCMV and MCMVdie3 samples clustering together, they are visibly different from each other, suggesting some transcriptional divergence at the late 24hpi time point.

Next, to examine global patterns of transcriptional regulation across the data set in a supervised manner, the hierarchical clustering approach was repeated on genes only. This meant the gene-to-gene correlation was still performed, but samples were not clustered, and instead were kept in their original temporal order and separated by condition. The heatmap in Figure 4.8 provides a visualization of global gene expression changes in response to MCMV and MCMVdie3 over the temporal course of infection. This supervised approach identified specific areas of differential gene expression between the conditions.

Figure 4.8. Hierarchical clustering of the macrophage transcriptional response to MCMV and MCMVdie3. Hierarchical clustering was performed on 7,890 filtered genes, with each gene represented as a row. Genes were per-gene normalized to their mean value to show relative expression. Genes are clustered on similarity of expression profile with similar genes connected by the hierarchical tree on the left. Samples are arranged in temporal order, separated by condition and labelled at the bottom of the heatmap; MCMV (red) and MCMVdie3 (blue). 0hpi corresponds to the end of the 1.5 hour viral adsorption period, meaning cells had been in contact with viral particles for 1.5 hours by 0hpi.

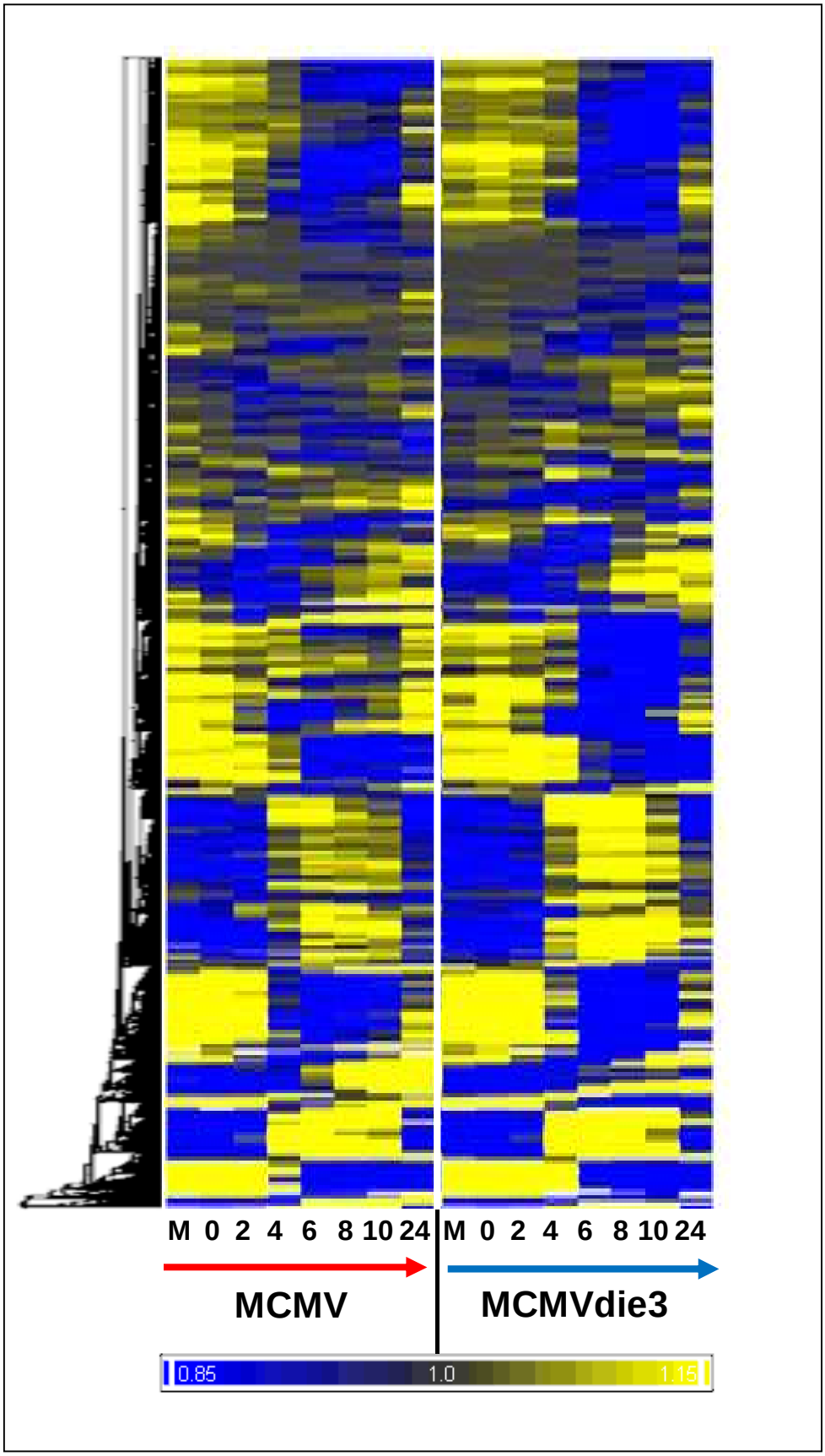
M 0 2 4 6 8 10 24
M 0 2 4 6 8 10 24
MCMV
MCMVdie3
0.85
1.0
1.15

4.6 Genes regulated in an equivalent manner in response to productive and non-productive MCMV infection

4.6.1 Identification of genes regulated in an equivalent manner in response to MCMV and MCMVdie3

As indicated by the similarities between the left (MCMV) and right (MCMVdie3) side of the heatmap in Figure 4.8, the macrophage transcriptional response to MCMV and MCMVdie3 was quite similar overall at the gene expression level. In particular, this was the case during the first four hours of infection, whereby many genes were up-regulated in an equivalent manner and with similar kinetics in response to both MCMV and MCMVdie3. Overall, the similarity in gene expression profiles induced by MCMV and MCMVdie3 indicates an overlapping transcriptional response to productive and non-productive MCMV infection in BMDMs at the gene-expression level.

Stat1 (signal transducer and activator of transcription 1) was induced in an equivalent manner in response to MCMV *and* MCMVdie3. To find other genes that also shared this profile (i.e. up-regulated in an equivalent manner in response to MCMV *and* MCMVdie3), a clustering analysis was performed whereby any gene with an expression profile highly correlated to *Stat1* (Pearson>0.9) was identified. This was not designed to identify genes regulated by *Stat1*, but was merely a strategy to identify genes in the macrophage transcriptome induced with equivalent kinetics by MCMV and MCMVdie3 infection. 131 genes were highly correlated with *Stat1* over the time course and induced equivalently by MCMV and MCMVdie3 infection (Figure 4.9) (for gene list see Supplementary File 8).

Figure 4.9 - Genes up-regulated equivalently in response to MCMV *and* MCMVdie3. BMDMs were infected at MOI of 1 PFU/cell with either MCMV or MCMVdie3 and transcript levels were measured using Affymetrix Mouse Exon 1.0ST microarrays. Pearson correlation was used to identify genes with expression profiles highly correlated with either *Stat1* (r>0.9) commonly up-regulated by both MCMV and MCMVdie3. Each gene is represented by a row on the heatmap and is per-gene normalized to its mean value to show relative expression. Yellow indicates increased expression relative to the mean and blue indicates decreased expression. The 0hpi time point represents the end of the 1.5 hour viral adsorption period.

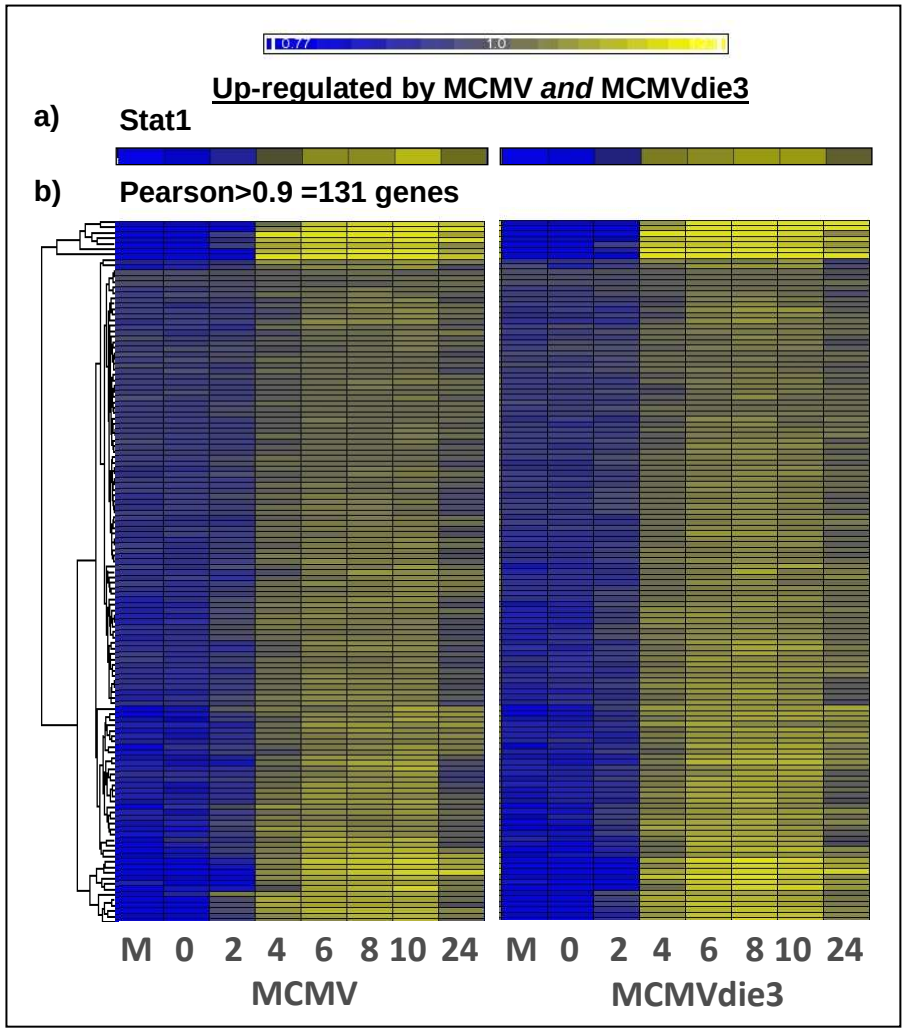

Next, to find genes down-regulated equivalently by both MCMV and MCMVdie3, the same approach was taken using a different marker gene; *Rasgrp3* (RAS guanyl releasing protein 3). This gene was chosen as a down-regulated marker based on its

expression profile in previous MCMV data sets (Sing *et al*. *personal communications*). *Rasgrp3* is a member of the RAS subfamily of GTPases involved in signal transduction and acquisition of GTP(301). 362 genes were found to have a highly correlated expression profile with *Rasgrp3* and commonly down-regulated in response to both MCMV and MCMVdie3 conditions (Figure 4.10) (for complete list see Supplementary File 9).

Figure 4.10 - Genes down-regulated in response to MCMV and MCMVdie3. Pearson correlation was used to identify genes with expression profiles highly correlated with either *Rasgrp3* (r>0.9) down-regulated by MCMV and MCMVdie3. The 0hpi time point represents the end of the 1.5 hour viral adsorption period.

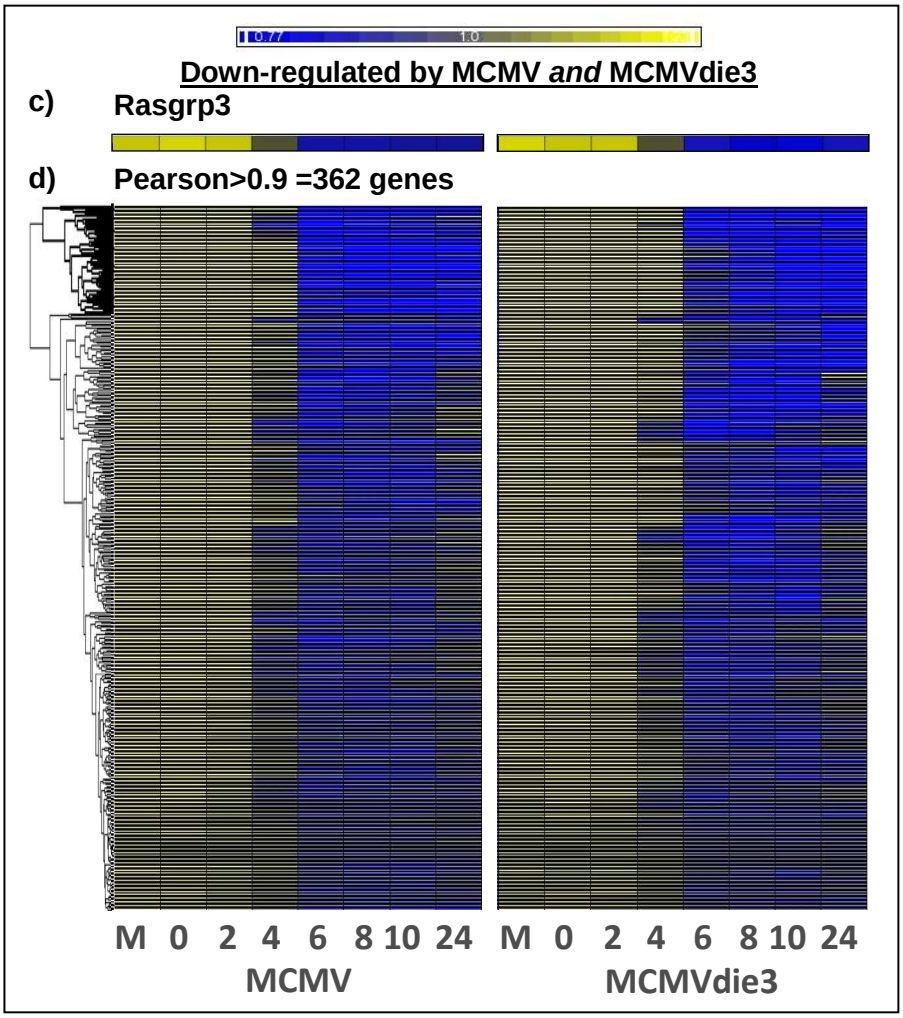

4.6.2 Functional annotation of genes regulated in an equivalent manner in response to MCMV and MCMVdie3

To determine the functional annotation of genes up-regulated or down-regulated in an equivalent manner in response to MCMV *and* MCMVdie3, the DAVID annotation tool(79) was used. This tool takes annotation classes from various different databases to measure over-representation of annotation terms within an input gene list (for details see Methods). If a particular annotation term is over-represented, or enriched, within a list of genes (above the levels of chance alone), a low p-value will be assigned to that annotation term as determined by a Fisher's exact test (for details see Methods). Databases accessed by the DAVID tool include Gene Ontology(1), which provides standardized and controlled vocabulary for gene attributes, Interpro(159), which provides a resource for protein family, domain, region and site information, and the Protein Information Resource (PIR)(381), which provides classification of proteins into family, superfamily, domain and motif groups based on structural and functional features.

Genes up-regulated equivalently by MCMV and MCMVdie3 contained over-represented annotation terms associated with *immune response, 2-5-oligoadenylate synthetase,* and *purine nucleotide binding* (Table 4.1). The group also contained interferon-stimulated genes including guanylate binding proteins (*Gbp2, Gbp4, Gpb6*), 2'-5' oligoadenylate synthetase genes (*Oas1a, Oas1b, Oas2, Oasl1, Oasl2*), interferon induced genes (*Ifi204, Ifi205, Ifi35, Ifi44, Ifit2, Isg20*), regulators of interferon signalling (*Ifr7, Stat2*), proteosome components (*Psmb8, Psmb9, Tap1, Tap2*) chemokines (*Cxcl9 MIG*), pattern recognition receptors (*Ddx58 RIG-I, Zbp1*) and MHC class II genes (*H2-gs10, H2-t10, HS-t22*) (for complete gene list see Supplementary File 8). This indicated an overlapping transcriptional response induced by both the MCMV and MCMVdie3 virions related to type I IFN.

The group of genes down-regulated in an equivalent manner by MCMV and MCMVdie3 group contained 362 members, many of which were involved in cell cycle control including cyclin-dependent kinases *(Ccna2, Cdc2a, Cdc45l, Cdca2, Cdca3, Cdca5, Cdca8, Cdk4, Cdkn2c),* spindle checkpoint genes (*Bub1,Bub1b)* and

topoisomerases (*Top1, Top2a, Topbp1*). Genes involved in cholesterol metabolism were also found to be down-regulated in this manner (*Insig1, Mvd, Srebf1, Srebf2, Sqle*). Over-represented functional annotation classes within the down-regulated group included *cell cycle, mitosis, nuclear division* and *chromosome* (Table 4.1b), suggesting a repression of the cell cycle during the macrophage response to MCMV *and* MCMVdi3 (for complete gene list see Supplementary File 9). The down-regulation of this group indicates BMDMs are proliferating at the point of infection, but cease to proliferate after contact with virus.

Table 4.1 Functional annotation of genes regulated equivalently in response to MCMV *and* MCMVdie3. 131 genes were highly correlated with *Stat1* (Pearson>0.9) and induced equivalently by both MCMV and MCMVdie3 **(a)**. 362 genes were highly correlated with *Rasgrp3* (Pearson>0.9) and down-regulated equivalently by both MCMV and MCMVdie3 (**b**). Genes from these two groups were annotated using DAVID tool to find over-represented functional annotation classes. The *Category* column indicates the number of genes in the input list with annotation for that particular annotation category. The *Term* column indicates the annotation term of significance and the *count* column indicates the number of genes within the gene list associated with that term, also represented by a percentage (%). The unadjusted (*PValue*) and adjusted (*Bonferroni*) p-values columns represent the Fishers exact test results for over-representation. The top ten annotation classes for each list are shown with a cut-off of Bonferroni p<0.005.

a) Commonly up-regulated genes n=131

Category	Term	Count	%	PValue	Bonferroni
GOTERM_BP 84/131	GO:0006955~immune response	25	19.7	3.22E-16	1.88E-13
INTERPRO 116/131	IPR006117:2-5-oligoadenylate synthetase, conserved site	5	3.9	1.14E-07	3.33E-05
SP_PIR_KEYWORDS 114/131	immune response	11	8.7	2.62E-07	4.36E-05
GOTERM_MF 88/131	GO:0017076~purine nucleotide binding	32	25.2	3.72E-07	8.77E-05
GOTERM_MF 88/131	GO:0032555~purine ribonucleotide binding	31	24.4	5.27E-07	1.24E-04
GOTERM_MF 88/131	GO:0032553~ribonucleotide binding	31	24.4	5.27E-07	1.24E-04
INTERPRO 116/131	IPR018952:2'-5'-oligoadenylate synthetase 1, domain 2/C-terminal	5	3.9	1.14E-06	3.32E-04
INTERPRO 116/131	IPR006116:2-5-oligoadenylate synthetase, ubiquitin-like region	5	3.9	1.59E-06	4.62E-04

GOTERM_BP 84/131	GO:0019882~antigen processing and presentation	8	6.3	9.67E-07	5.44E-04
GOTERM_CC_FAT 67/131	GO:0042824~MHC class I peptide loading complex	4	3.1	1.15E-05	0.001556

b) Commonly down-regulated genes n=362

Category	Term	Count	%	PValue	Bonferroni
SP_PIR_KEYWORDS 349/362	cell cycle	58	16.0	2.93E-30	7.93E-28
SP_PIR_KEYWORDS 349/362	cell division	44	12.2	7.09E-28	1.92E-25
SP_PIR_KEYWORDS 349/362	phosphoprotein	223	61.6	8.38E-28	2.27E-25
SP_PIR_KEYWORD 349/362S	mitosis	38	10.5	1.85E-27	5.01E-25
GOTERM_BP_FAT 278/362	GO:0051301~cell division	44	12.2	1.15E-25	1.76E-22
GOTERM_BP_FAT 278/362	GO:0000087~M phase of mitotic cell cycle	37	10.2	1.48E-24	2.27E-21
GOTERM_CC_FAT 246/362	GO:0000775~chromosome, centromeric region	29	8.0	1.06E-23	3.11E-21
GOTERM_BP_FAT 278/362	GO:0007049~cell cycle	60	16.6	2.58E-24	3.97E-21
GOTERM_BP_FAT 278/362	GO:0000278~mitotic cell cycle	40	11.0	4.81E-24	7.40E-21
GOTERM_BP_FAT 278/362	GO:0000280~nuclear division	36	10.0	8.76E-24	1.35E-20

4.7 Genes differentially regulated between the MCMV and MCMVdie3 responses

4.7.1 Genes induced specifically by productive MCMV infection at 24hpi

Next, to identify differences, rather than similarities in the macrophage response to MCMV and MCMVdie3, the 24 hour time point was examined in more detail. The 24hpi time point was found to have the most variability and most gene expression changes between MCMV and MCMVdie3 (illustrated in Figure 4.11). It also appeared some genes were induced specifically by productive MCMV infection but not by MCMVdie3 at 24hpi only.

Figure 4.11. The transcriptional response to MCMV and MCMVdie3 is most different at 24hpi. a) Hierarchical clustering of 7,890 expressed genes in response to MCMV and MCMVdie3 as shown previously. **b)** Differences in the expression profiles induced by MCMV and MCMVdie3 are marked at the 24hpi time point.

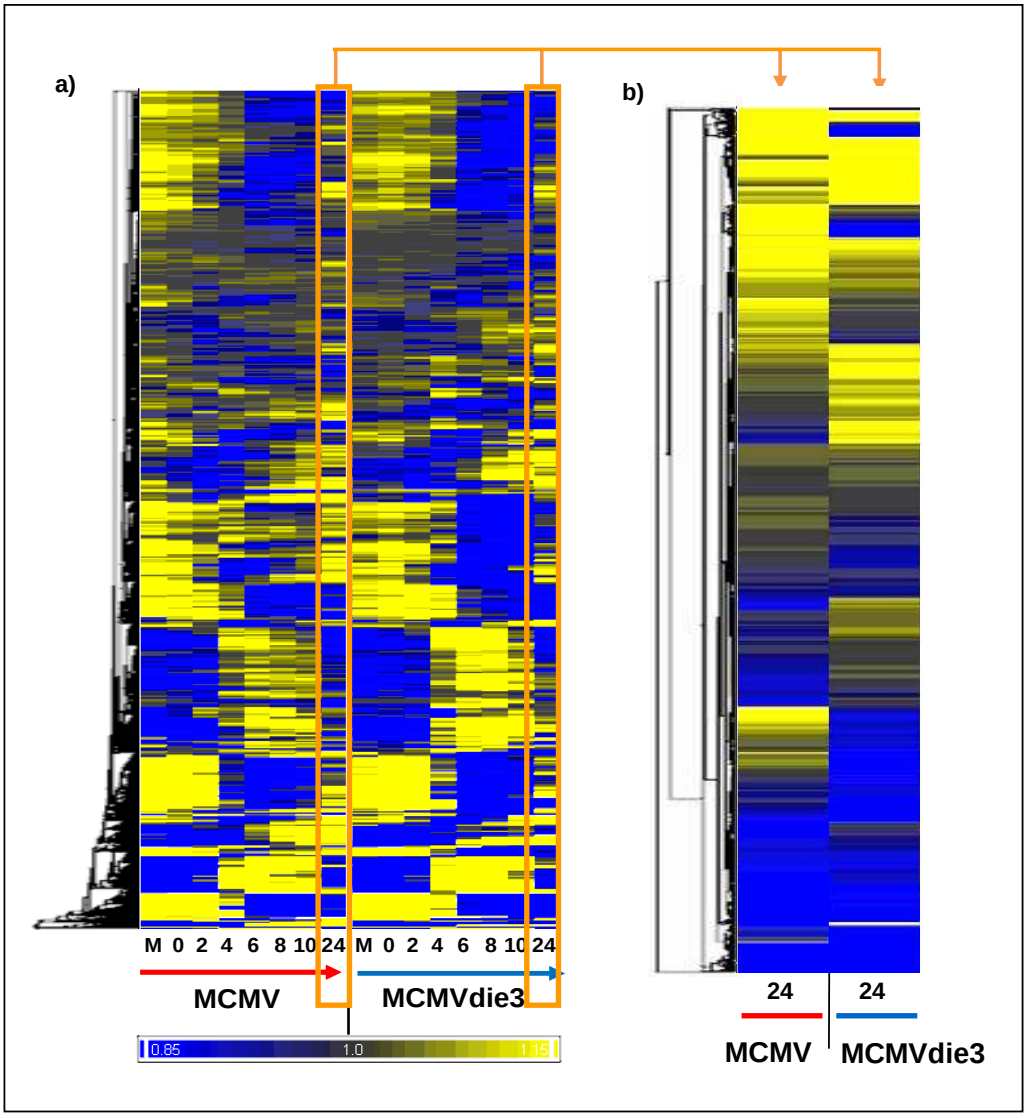

To focus on the more pronounced differences in gene expression occurring late in the response at 24hpi, and to identify genes up-regulated specifically in response to productive MCMV infection, a filter was applied to the data whereby only genes with a 1.5-fold or higher gene expression level in MCMV-infected cells samples between 10-24hpi were identified. This resulted in 283 genes with a 1.5-fold or higher gene expression level in MCMV-infected cells above that of both mock and MCMVdie3 levels at both 10hpi and 24hpi (for complete list see Supplementary File

10). These 283 genes represented a transcriptional response occurring specifically in response to productive MCMV infection. These genes were not induced by the inactive MCMV virion alone (Figure 4.12).

Figure 4.12 A sub-set of macrophage genes is induced specifically by productive MCMV infection between 10-24hpi. 283 genes were induced specifically in response to productive MCMV infection by a factor of 1.5-fold or higher above mock and MCMVdie3 levels at 10hpi and 24hpi. The heatmap shows hierarchical clustering of these genes with each row representing an individual gene that has been per-gene normalized to its mean value to show relative expression. Each column represents a different time point as indicated beneath the heatmap.

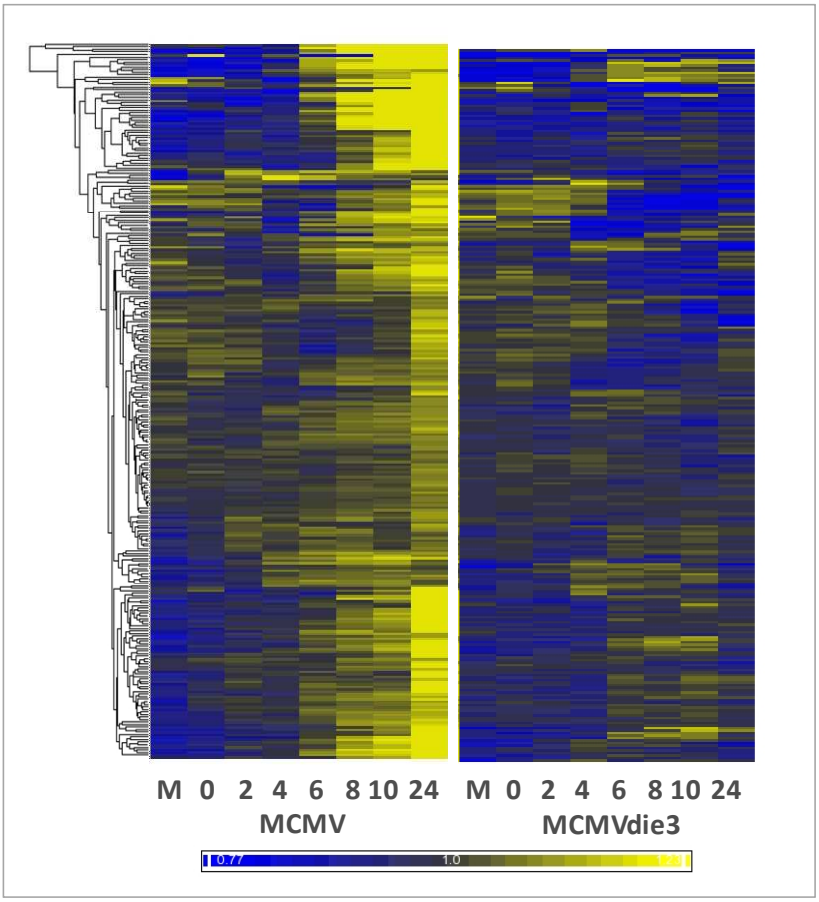

To determine the functional annotation of the 283 genes induced specifically by productive MCMV infection, annotation was performed again using DAVID(79), and also using InnateDB(229). InnateDB is a manually-curated public database of

genes, proteins, interactions, and pathways designed specifically to facilitate systems level analysis of the innate immune response. Over-representation of annotation terms was determined using a corrected p-value<0.01 (for details see Methods). Significant over-representation of GO annotation terms included *plasma membrane* (GO:0044459 Bonferroni p=0.009) and *glutathione transferase activity* (GO:0004364 Bonferroni p=0.01). Using InnateDb, pathways involved in *glutathione metabolism* (KEGG p=0.001) and *glutathione conjugation* (REACTOME p=0.001) were identified as over-represented. No significant annotation was found associated with the innate immune response or IFN signalling in this group of genes, suggesting regulation via an alternative pathway (for a complete list of the genes in this group see Supplementary File 10).

To validate the expression of some of the genes induced specifically by productive MCMV infection at 10-24hpi, the experiment was repeated in cells from a different set of mice, and three marker genes were chosen for validation using qRT-PCR. The genes chosen were *Elovl4* (elongation of very long chain fatty acids), *Alox15* (arachidonate 15-lipoxygenase), and *Crabp1* (cellular retinoic acid binding protein). These genes were chosen due to their high expression levels (>2000 antilog) and fold changes (>2) in the microarray data set. For each of the three marker genes, significant up-regulation was again found in response to productive MCMV infection, and no induction was seen in response to the inactive MCMVdie3 virion at 24hpi (Figure 4.12). The qRT-PCR data confirmed induction of these genes is specific to productive MCMV infection, and does not occur in response to MCMVdie3.

Figure 4.13 *Elovl4, Alox15* and *Crabp1* are induced specifically in response to productive MCMV infection at 24hpi. BMDMs were infected at MOI of 1 PFU/cell and total RNA was harvested at 24hpi. Transcript levels were measured for three marker genes (*Elovl4, Alox15* and *Crabp1*) using qRT-PCR. Transcript levels were normalized to the cellular housekeeping gene *Gapdh* and calibrated to the MCMV 24hpi samples to show relative expression. Error bars indicate standard deviation from three separate cultures.

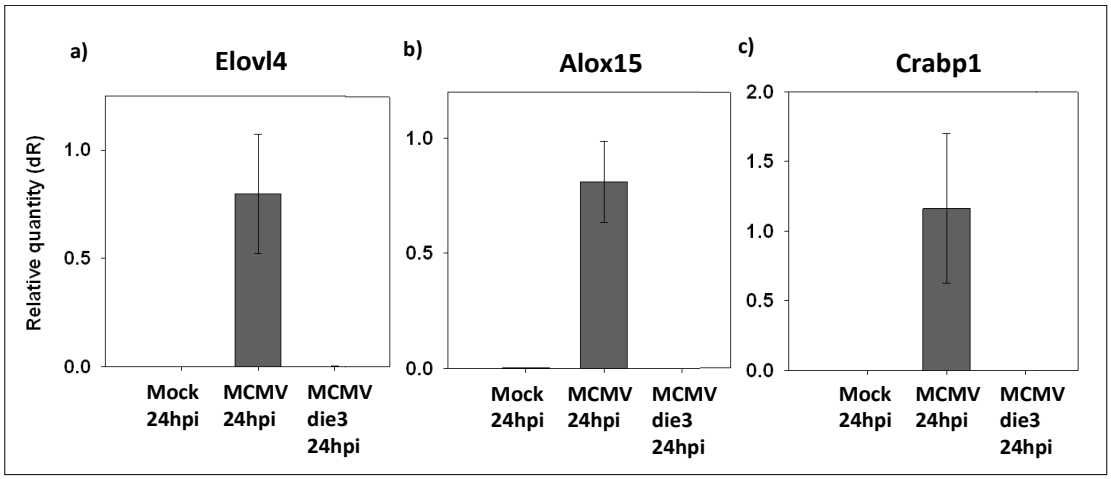

Next, to determine if up-regulation of these marker genes was also dependent on viral DNA replication, the experiment was repeated in presence of 20uM Ganciclovir (GCV); a licensed antiviral drug capable of inhibiting the activity of CMV DNA polymerase, thereby terminating the elongation of viral DNA and inhibiting viral DNA replication(245). In the presence of Ganciclovir, *Elovl4* was induced to wild-type levels (Figure 4.13a) and other marker genes (*Alox15* and *Crabp2*) were also induced, but slightly attenuated in their expression (Figure 4.14b-c). This result suggests viral DNA replication is not required for the transcriptional induction of *Elovl4, Alox15* and *Crabp1* at 24hpi in BMDMs. The induction of these genes may instead be driven by *de novo* MCMV proteins, independently of viral DNA replication.

Figure 4.14 - Induction of *Elovl4, Alox15* and *Crabp1* in response to productive MCMV infection occurs in the presence of Ganciclovir. BMDMs were infected at MOI of 1 PFU/cell in the presence and absence of 20uM Ganciclovir. Transcript

levels were measured at 24hpi for three marker genes (*Elovl4*, *Alox15* and *Crabp1*) using qRT-PCR. Samples were calibrated to the MCMV 24hpi condition to show relative expression. Error bars indicate standard deviation from three cultures.

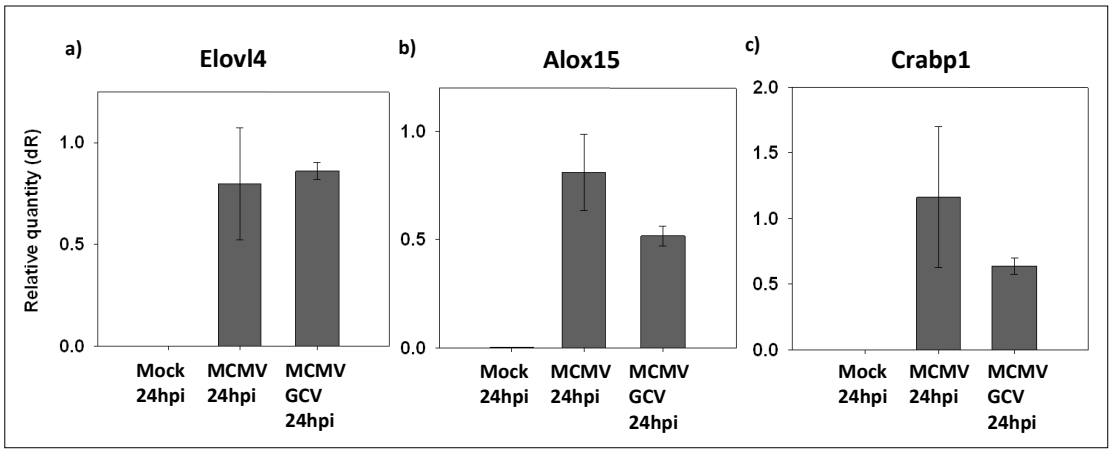

4.8 Cytokine secretion is markedly different in response to productive and non-productive MCMV infection in macrophages

Although differences at the gene expression level had been measured in response to MCMV and MCMVdie3, the differences did not necessarily reflect the functional immune-activation status of the differentially infected macrophages. Therefore, in order to address the hypothesis more directly, and to obtain a more definitive and functional measure of immune activation, cytokine secretion was measured in supernatants from MCMV and MCMVdie3 infected BMDMs at 2hpi, 6hpi, and 10hpi. This was done using a multiplexed bead-based ELISA assay to simultaneously measure pro-inflammatory cytokines (TNFα, IL-6) chemoattractant cytokines (RANTES, MIG, MIP-2) and the anti-inflammatory cytokine IL-10 in response to MCMV and MCMVdie3 infection. The cytokines were chosen based on their known roles in the innate immune response, their transcriptional profiles which were of interest from in the microarray data, and their availability as part of a commercially available multiplexed ELISA platform (for details see Methods). Measuring cytokine secretion was intended to provide a more functional and definitive output for determining the final immunological status of the differentially infected BMDMs.

Figure 4.15 - Chemoattractant cytokines are secreted to higher levels in response to productive MCMV infection in macrophages. BMDMs were infected at MOI of 1 PFU/cell with either MCMV or MCMVdie3 and secreted protein levels were measured in cell culture supernatants; RANTES (**a ii**), MIG (**b ii**), and MIP-2 (**c ii**). Error bars indicate standard deviation from three separate cultures. The response to MCMV is shown in light grey and MCMVdie3 in dark grey. Asterisks indicate a significant difference between conditions (Student's t-test, *p<0.05, **p<0.001). RNA microarray profiles for each gene are also shown on the left side for reference.

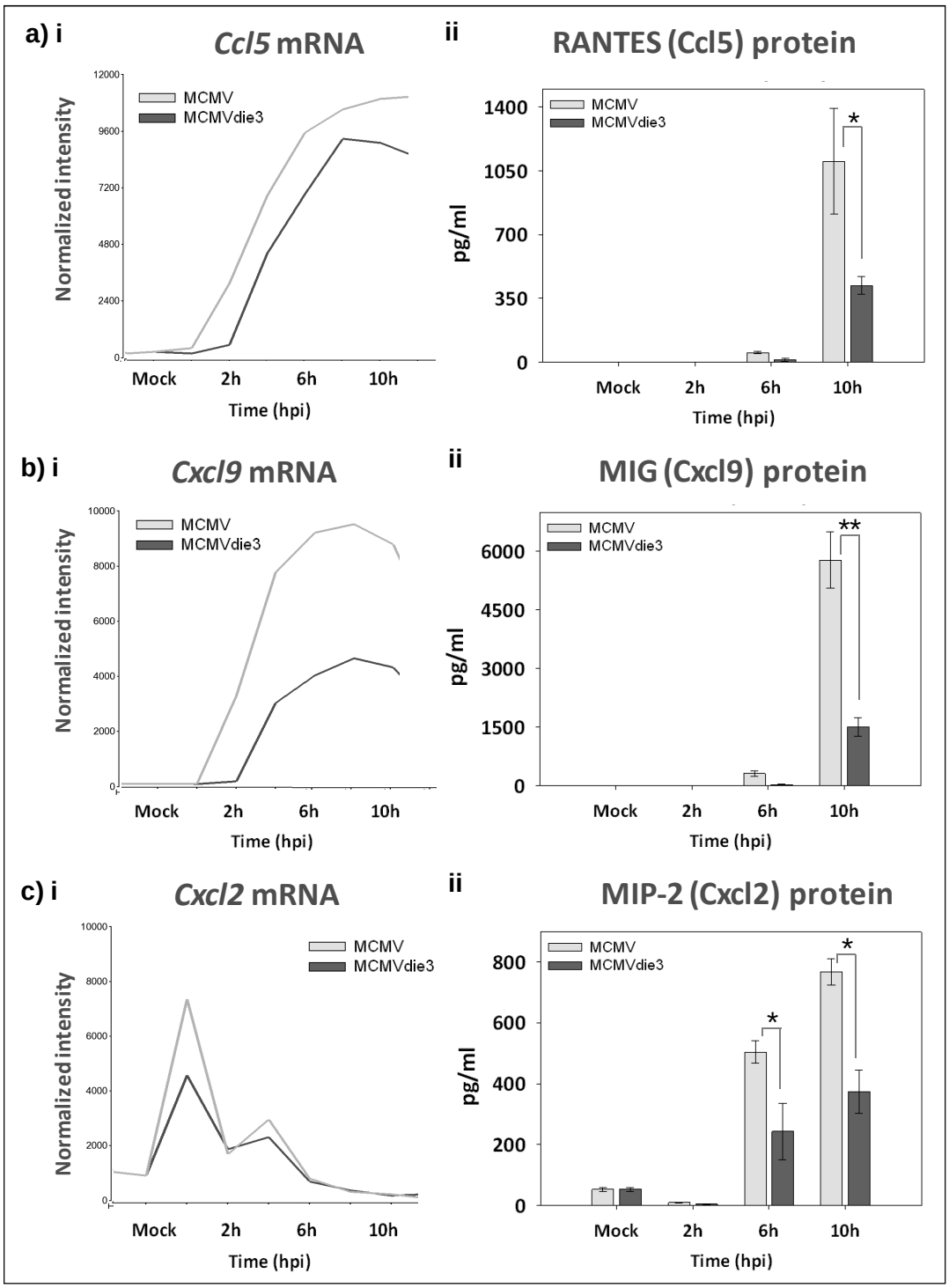

As seen in Figure 4.15, chemoattractant cytokines RANTES, MIG and MIP-2 were secreted to significantly higher levels in response to productive MCMV infection compared to MCMVdie3 at the protein level (Figure 4.14 a ii, b ii, c ii). This was particularly significant for MIG ($p<0.001$). The result suggests a higher level of innate immune activation occurring in response to productive MCMV infection, based on the known roles of chemoattractant chemokines in the recruitment of immune cells to the site of infection(255). The difference at gene expression level, however, was only significantly detectable for MIG (*Cxcl9*).

Figure 4.16 - Pro-inflammatory cytokines are secreted to higher levels in response to productive MCMV infection. BMDMs were infected at MOI of 1 PFU/cell with MCMV and MCMVdie3 and secreted protein levels were measured in cell culture supernatants for TNF (**a ii**) and IL-6 (**b ii**). The response to MCMV is shown in light grey and the response to MCMVdie3 is shown in dark grey with error bars indicating standard deviation from three separate cultures. Asterisks indicate a significant difference between conditions (Student's t-test, *$p<0.05$, **$p<0.001$). mRNA microarray profiles are also shown on the left side for reference.

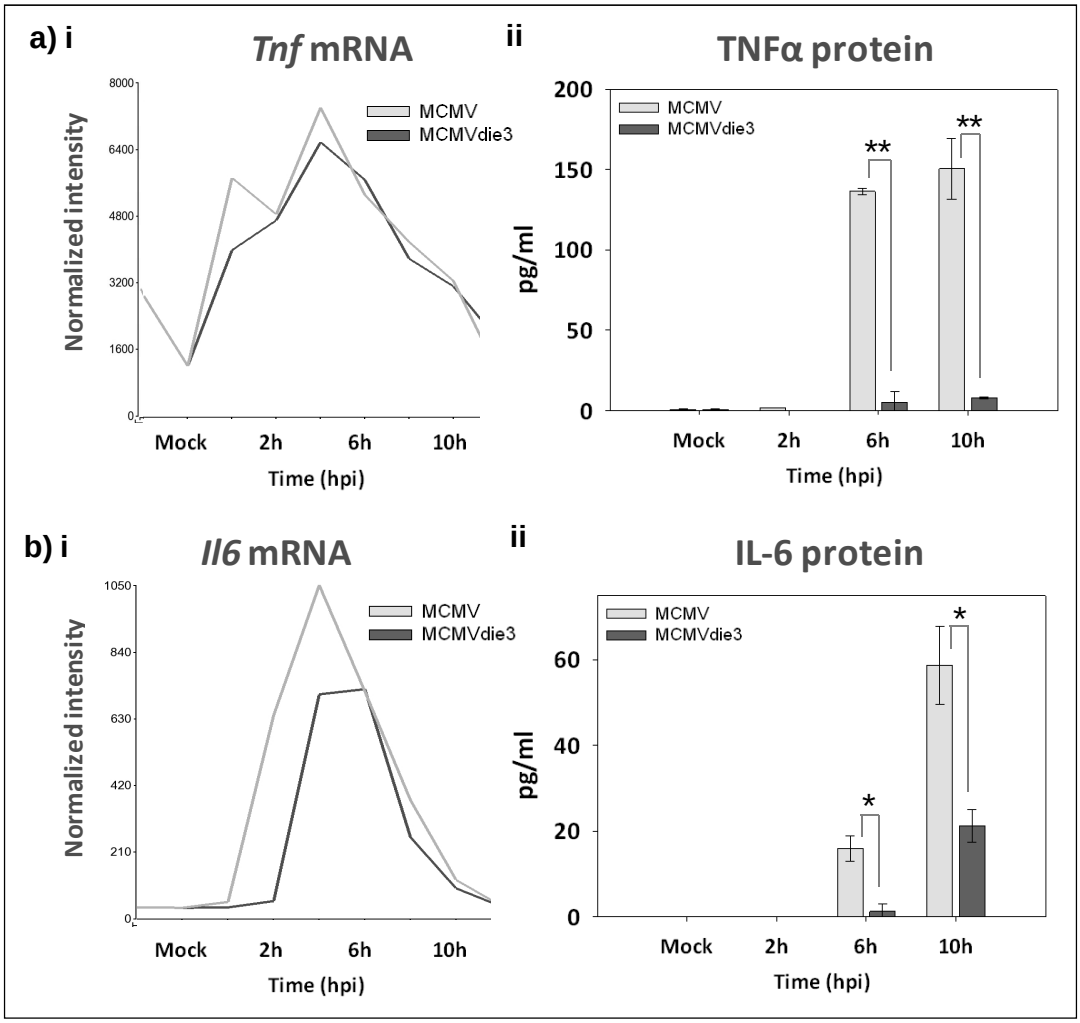

The secretion of pro-inflammatory cytokines TNF and IL-6 was found to be significantly higher in response to productive MCMV infection compared to MCMVdie3 (Figure 4.16). This difference was particularly significant for TNF, which was found to be secreted only in response to productive MCMV infection. This result indicated an increased amount of pro-inflammatory immune activation occurring in response to productive MCMV infection, and not in response to the inactive MCMVdie3 virion. The difference was not detectable at the gene expression level for TNF.

The only cytokine secreted to higher levels in response to MCMVdie3 was IL-10, an anti-inflammatory cytokine with immunosuppressive properties(25, 322). IL-10 was secreted to significantly higher levels in response to MCMVdie3 at 10hpi (Figure 4.17).

Figure 4.17 - IL-10 secretion is lower in response to productive MCMV infection in macrophages. BMDMs were infected at MOI of 1 PFU/cell with either MCMV or MCMVdie3 and secreted protein levels were measured in cell culture supernatants for IL-10 (**ii**). The response to MCMV is shown in light grey and the response to MCMVdie3 is shown in dark grey with error bars indicating standard deviation from three separate cultures. Asterisks indicate a significant difference between conditions (Student's t-test, *p<0.05). The mRNA microarray profile for the *Il-10* gene is also shown on the left side for reference.

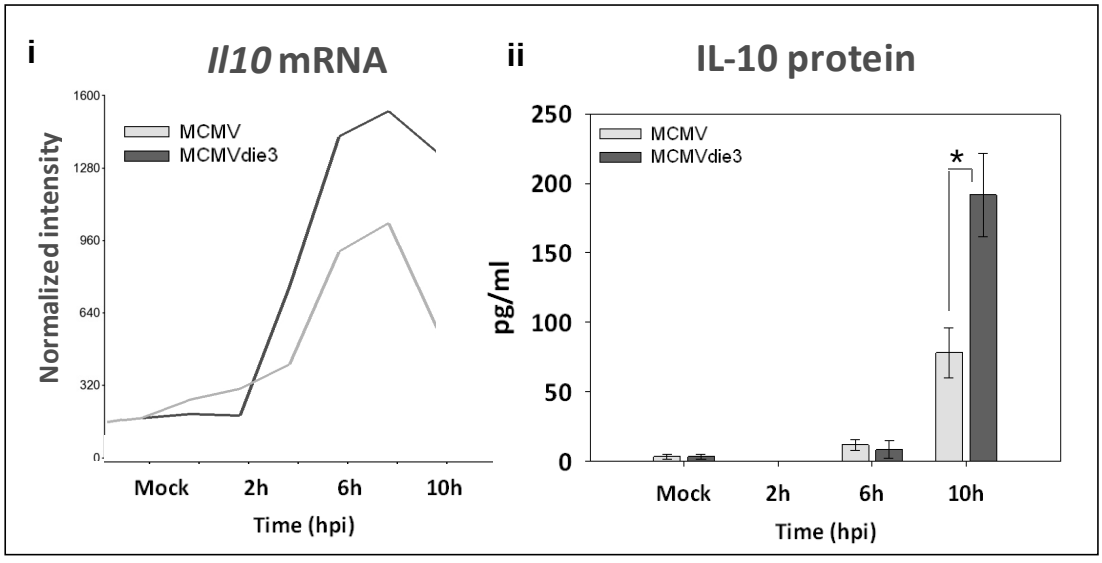

Overall, the most significant difference between MCMV and MCMVdie3 for the six cytokines measured was for TNFα ($p<0.0005$). TNFα was secreted specifically in response to wild-type MCMV at both 6hpi and 10hpi, but barely detectable in response to the attenuated MCMVdie3 virion (Figure 4.16a ii). This result was surprising given *Tnf* mRNA levels were induced equivalently in response to MCMV and MCMVdie3 at the gene expression level (Figure 4.16a i). To further investigate this observation, and to verify the result independently, the entire experiment was repeated again twice under the same conditions using BMDMs from a different set of mice. TNFα secretion was measured in BMDM supernatants at the same time points as the previous experiment, using individual TNFα ELISAs.

In the repeat experiments, again no TNFα protein was detectable from MCMVdie3 infected cells, but secretion occurred in response to wild-type MCMV at multiple time points (Figure 4.18). This result further suggested post-transcriptional regulation of TNFα occurs only in response to productive MCMV infection, and not in response to the inactive MCMVdie3 virion. This result indicated that BMDMs respond with a heightened level of pro-inflammatory innate immune signalling as a result of productive MCMV infection.

Figure 4.18 - TNFα secretion in BMDMs only occurs in response to productive MCMV infection (repeat experiments). BMDMs were infected at MOI of 1 PFU/cell and secreted cytokine levels for TNFα were measured in cell culture supernatants from two repeat experiments (**a**) and (**b**) using standard ELISA assays (R&D Systems, UK). Error bars indicate standard deviation from three separate cultures. The response to MCMV is shown in white and the response to MCMVdie3 shown in black.

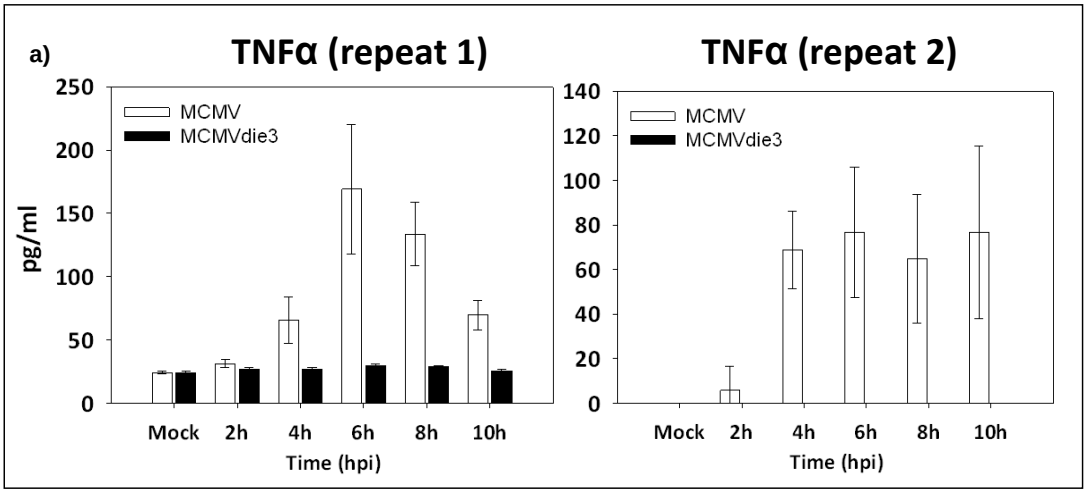

Discussion

A number of findings were presented in this chapter regarding similarities and differences in the macrophage innate immune response to productive and non-productive MCMV infection. Some of the key findings were; a) IFNβ is induced more rapidly in response to productive MCMV infection, b) sub-sets of genes are regulated in an equivalent manner in response to MCMV and MCMVdie3, c) sub-sets of genes are up-regulated specifically in response to productive MCMV infection between 10-24hpi, and d) pro-inflammatory and chemoattractant cytokines are secreted to significantly higher levels in response to productive MCMV infection. These findings identify new aspects to consider in light of the hypothesis, and in light of the existing literature on the innate immune response to productive and non-productive viral infection.

IFNβ induction occurs more rapidly in response to productive MCMV infection

Although IFNβ was induced to equivalent peak levels in MCMV and MCMVdie3 infections, the induction was more rapid in response to wild-type MCMV by a period of 2-4 hours (Figure 4.3). This difference was detectable at both the gene expression and protein level, and across multiple experiments (Figures 4.4 and 4.5). A similar kinetic shift in IFNβ induction is not reported in literature for most comparable studies, however one study did report wild-type strains of polioviruses are more potent inducers of type I IFN than attenuated strains in human leukocytes (284). Most studies using UV-inactivated virions report higher expression of type I IFNs and ISGs in response to attenuated viruses compared to wild-type strains(43, 133, 263, 289). Many of these studies have used fibroblasts or other permissive cell types, rather than macrophages, for their analyses.

There are a number of possible reasons why a more rapid type I IFN induction might occur in response to productive MCMV infection than MCMVdie3 in BMDMs. Firstly, a difference in the number of incoming MCMV and MCMVdie3 virions may account for the kinetic shift in *Ifnb1* induction between the conditions. This may

possibly be caused by variation in the genome/PFU ratio between the two viral stocks, although this factor was tested for in the optimization stages using qPCR (Figure 3.3, Table 3.1).

Another factor to consider in light of the differences in IFNβ induction between the conditions is the low level of infection in BMDMs at MOI of 1 PFU/cell. Based on previous MCMV-GFP reporter virus data in Chapter 3, the proportion of infected cells at MOI of 1 PFU/cell is only around 15%. This suggests paracrine induction of IFNβ may play a major role in defining the innate immune response at MOI of 1 in BMDM cultures at this low level of infection. Differences in paracrine signalling effects may potentially contribute to the kinetics of IFNβ induction.

Another possible explanation for the differences in IFNβ induction between MCMV and MCMVdie3 is that a viral PAMP signal is produced during the initial stages of the productive infection, but not during the non-productive infection. One candidate PAMP signal produced at this time may be a viral-transcribed RNA capable of activating a PRR and rapidly inducing the IFNβ response. Previous experiments in Chapter 3 identified substantial differences in the overall amount of mRNA transcribed at immediate early times between MCMV and MCMVdie3 infections (Figures 3.5 and 3.6). In addition, double-stranded viral RNA (dsRNA) has previously been shown to be transcribed during MCMV infection(48), however only at late stages of infection. To test the possibility that viral-derived RNA produced during MCMV infection could contribute to the activation of IFNβ, an experiment was designed whereby 1250ng total RNA extracted from MCMV-, MCMVdie3- and mock-infected BMDMs was transfected into new BMDMs monolayers. The type I IFN response was then measured using the Mx2 marker gene, however, transfection of RNA from MCMV-, MCMVdie3-, and mock-infected BMDMs all induced the type I IFN response to equivalent levels (for data see Supplementary File 11).

The overlapping transcriptional response to productive and non-productive MCMV infection

Regardless of difference in IFNβ induction, many ISGs and innate immune response genes were regulated with equivalent kinetics and to equivalent peak expression levels in response to MCMV and MCMVdie3 (Figure 4.9). In addition, whole-genome microarrays uncovered widespread overlapping macrophage gene expression at the genome-wide level (Figure 4.8). The overlapping transcriptional response was particularly similar between 0-8hpi, reflecting the activation of common signalling pathways by structural components of the incoming MCMV virions. The transcriptional overlap, which was characterized by up-regulation of innate immune response genes, is consistent with a number of other studies using live and UV-inactivated viruses(63, 142, 211, 289, 330, 359). The common induction of these transcripts is likely to be induced by viral membrane fusion and/or viral entry(211, 330, 359). Down-regulation of cell cycle and mitosis genes also occurred in an equivalent manner in response to MCMV and MCMVdie3 infection (Figure 4.10). This down-regulation indicates incoming structural components of the MCMV virion are sufficient to repress macrophage gene expression.

Another factor to consider in light of the overlapping transcriptional response to MCMV and MCMVdie3 is the high level of autocrine and paracrine signalling in BMDM cultures compared to other cell types. Even small numbers of infected macrophages induce widespread signalling responses via secretion of cytokines, such as IFNβ, with potent ability to induce signalling in neighbouring and un-infected cells(261). Paracrine responses can therefore potentially induce widespread gene expression changes in both infected and un-infected cells, and may blur the distinction between specific responses induced to productive and non-productive MCMV infection. This factor would be less pronounced in fibroblasts and cell lines with higher levels of infection and lower levels of cytokine secretion. In this sense it is difficult to differentiate between macrophage gene expression induced directly by the virus, compared to that induced indirectly by paracrine signalling. This effect is more pronounced given the low level of infection at MOI of 1 PFU/cell.

Other important differences exist between this study in BMDMs compared to other studies using fibroblasts and more permissive cell types(43, 133, 263, 289). For example, macrophages express a far broader range of PRRs in comparison to fibroblasts, and therefore have the ability to respond to virus infection with increased sensitivity. This may explain why IFNβ was induced so rapidly in response to both MCMV and MCMVdie3 infection in BMDMs, as discussed previously. In addition, macrophages have been shown to have a higher endocytotic capacity than fibroblasts(346), which may contribute to rates of viral uptake at the initial stages of infection. However the qPCR data on viral genome entry does not support this. Differences in the sensitivity of pDCs in comparison to fibroblasts have been illustrated in the context of SFV infection, and pDCs were shown to respond significantly more rapidly than fibroblasts (MEFs) in response to SFV infection(142).

Highly permissive cell types and high MOIs used in combination with UV-inactivated virions has been the approach for most previous studies comparing the innate immune response to productive and non-productive virus infection(43, 63, 142, 260, 263, 272, 289, 345). This has its advantages, as it results in very high levels of infection, high levels of viral protein activity, and strong suppression of the innate immune response. This approach was not taken in the current study. Instead, primary BMDMs were used as a physiologically relevant cell type to conduct an extensive analysis of macrophage gene expression during the innate immune response. In addition, a modest MOI of 1 PFU/cell was used. For these reasons, suppression of the innate immune response by MCMV was less pronounced and more difficult to detect.

Genes induced specifically by productive MCMV infection

At later time points during the response to MCMV (10-24hpi), a secondary wave of macrophage genes were induced specifically in response to productive MCMV infection (Figure 4.12). This group consisted of 283 genes up-regulated specifically by MCMV, and not in response to the inactive MCMVdie3 virion. This response

begins at 8hpi and increases in intensity by 24hpi. The induction of these genes suggests important biological differences occurring between 8-24hpi in productively versus non-productively infected BMDMs at MOI of 1 PFU/cell, despite the low levels of initial infection. Genes induced in this manner were associated with cellular metabolism and *glutathione*, rather than innate immunity. It is unclear whether genes up-regulated in this manner are part of a secondary antiviral response, or up-regulated by the virus as pro-viral genes. The possibility these genes are also merely a metabolic bi-product of lytic infection also cannot be ruled out. The genes could also be related to the ER stress response, or the unfolded protein response to CMV infection(165). The functional annotation of these genes only provides a limited insight into the overall function of these genes in relation to MCMV infection. siRNA screening approaches are currently being used to determine the relative contribution of these genes to MCMV replication in fibroblasts.

Despite the limitations of functional annotation analysis, significant annotation classes were found associated with *glutathione transferase activity, glutathione metabolism,* and *glutathione conjugation* for genes up-regulated specifically in response to productive MCMV infection. The glutathione synthetase gene (*Gss*) and six different glutathione S-transferase genes (*Gsta4, Gstk1, Gstm4, Gstm5, Gstp2, Gstt1*) were also up-regulated as part of this group. Glutathione is an intracellular anti-oxidant found in millimolar concentrations in all mammalian cells(382) and is involved in a range of physiological processes. The ratio of reduced and oxidized glutathione (GSH:GSSG) can serve as a representative marker of the antioxidative capacity of a cell(101), and deficiencies in glutathione levels can put cells at risk for oxidative damage. Glutathione has also been reported to have antiviral properties against HSV1(277) and HIV1(276) replication (70, 104), and has been used as an antiviral therapy(101). Glutathione has also been reported to influence the immunomodulatory properties of macrophages in relation to Th1/Th2 responses(102).

This suggests there may be a relationship between glutathione and the antiviral response, or at least a link between glutathione metabolism and genes up-regulated

specifically in response to productive MCMV infection between 10-24hpi in BMDMs. Caution must be given, however, to the functional annotation analysis which only provides an indication as to the real function of this group of genes. Preliminary siRNA screening experiments suggests that genes up-regulated in this group are pro-viral and required for efficient MCMV replication in fibroblasts, however results are only preliminary (Kai Kropp and Mathieu Blanc, *personal communications*).

The expression of three marker genes within this group (*Elolv4*, *Alox15* and *Crabp1*) were measured in the presence and absence of Ganciclovir, a drug inhibiting viral DNA polymerase activity, in response to MCMV and MCMVdie3 infection (Figure 4.13), in order to determine if their up-regulation was dependent on viral DNA replication. Up-regulation of these genes, however, was found to occur independently of Ganciclovir treatment, suggesting MCMV viral DNA replication is not required for the induction of these genes (Figure 4.14). This result provided some insight into how these genes are regulated during the MCMV replication cycle, and suggested their induction may be regulated by *de novo* MCMV proteins, rather than as a result of viral DNA replication. Further experimentation, however, will be required to uncover the MCMV proteins responsible for regulation at this level.

Some additional experimentation strategies may be useful for future investigation of these genes. For example, other viruses could be used to determine if up-regulation of these genes is specific to productive infection with MCMV, or occurs in response to infection with other viruses. The antiviral role of the genes could also be investigated further using a siRNA screening approach, with individual genes suppressed using RNAi and MCMV replication subsequently measured. In addition, the regulation of these genes could be measured in other cell types, including fibroblasts, to determine if induction is macrophage-specific.

Differences in cytokine secretion in response to MCMV and MCMVdie3

To conduct a more comprehensive analysis beyond the level of gene expression, a protein-level technique was required to provide a more functional measurement of the BMDM response. Protein-level data would also complement the extensive amount of gene expression data generated in the microarray analysis. To achieve this, a number of different techniques were considered such as mass spectrometry, Western blotting, multiplexed immunoblotting and ELISA analysis. The most reliable, cost effective and tractable method for gaining the most protein-level data regarding the macrophage innate immune response was a multiplex bead-based ELISA assay to measure secreted cytokine levels BMDM supernatants in response to MCMV and MCMVdie3 infection.

This analysis revealed a number of important differences in response to productive and non-productive MCMV infection at the secreted protein level. Significantly higher levels of chemoattractant (RANTES, MIG, MIP-2) and pro-inflammatory (IL-6, TNF) cytokines were secreted in response to productive MCMV infection compared to MCMVdie3 (Figures 4.15 and 4.16). This indicated important immunological differences occurring in productively and non-productively infected BMDMs at MOI of 1 PFU/cell, despite low levels of initial infection. The cytokine data also provided strong evidence in support of the central hypothesis of the study that macrophages respond differently to productive and non-productive MCMV infection through differential innate immune signalling.

The difference was particularly significant for the secretion of TNF, which occurred specifically in response to productive MCMV infection and not in response to the MCMVdie3 virion (Figures 4.16 and 4.18). The difference in TNF regulation was only seen at the secreted protein level, and was not seen in the levels of *Tnf* mRNA which were induced to equivalent levels by MCMV and MCMVdie3 (Figure 4.16). This result indicates that productive MCMV infection results in a significantly higher level of TNF secretion compared to non-productive infection, and that differential regulation of TNF secretion must occur at the post-transcriptional level.

The post-transcription regulation of TNF is a complex process involving several mechanisms. *Tnf* mRNA contains adenine/uridine-rich elements (AREs) in the 3'-untranslated region which can be regulated post-transcriptionally via cis-acting factors(9, 389). Regulation of ARE elements can influence the rate of degradation and translation of TNF mRNA into protein. For example, cis-acting factors HuR and AUF1 can bind with opposing effects, stabilizing or destabilizing ARE-containing transcripts(9). ARE-mediated post-transcriptional regulation has been reported for TNF and other pro-inflammatory cytokines including IL-1β(314) and IL-6(390). Specifically for TNF, the ERK and p38 pathways have been shown to be involved in regulation of mRNA stability (197, 246) by a proteasome-dependent mechanism(78).

TNF can also be regulated at the level of membrane protein cleavage by the TNF-alpha converting enzyme (TACE) to affect the level of secretion(67). The TACE enzyme cleaves the precursor form of TNF protein into a mature form which can be secreted from the cell. The precursor TNF is located close to the cell membrane, and cleavage results in secretion of mature TNF protein into extracellular space. In the context of the current study, it is likely that this post-translational cleavage event is regulated differentially in response to productive and non-productive MCMV infection in BMDMs, given equivalent levels of TNF mRNA are detectable inside MCMV and MCMVdie3-infected cells. To determine if the difference in TNF regulation was due to differences in intracellular TNF production, or alternatively due to differences in cleavage and secretion, intracellular TNF staining experiments are now being conducted. These experiments will determine if the amount of intracellular TNF produced in MCMV- and MCMVdie3-infected cells is equivalent, or whether differential regulation of cleavage is occurring.

The increased level of TNF secretion in response to productive MCMV infection could also account for the increased level of IL-6 secretion (Figure 4.16b), and possibly the decreased level of IL-10 secretion (Figure 4.17) in response to productive infection. The regulation of other cytokines by TNF has been reported(314), and could occur as a result of paracrine signalling in BMDM cultures.

In order to explain why there would be an increased amount of pro-inflammatory and chemoattractant cytokine secretion in response to productive MCMV infection and not in response to MCMVdie3, there are two possible explanations. Firstly, the macrophage may be capable of sensing *de novo* virus activity during productive infection, leading to a heightened pro-inflammatory response. Alternatively, *de novo* viral proteins may induce TNF secretion and pro-inflammatory cytokine signalling. The MCMV immediate early enhancer region has been shown to be TNF-inducible (158, 331), suggesting the virus may use pro-inflammatory signalling to drive immediate early viral gene expression.

The differences regarding cytokine secretion in response to productive infection have important implications if considered in light of potential downstream immunological outcomes at the site of a primary infection *in vivo*. Higher levels of chemoattractant and pro-inflammatory cytokines from macrophages at a primary site of infection will lead to increased inflammation and immune cell infiltrate, potentially resulting in a more robust systemic response. In contrast, lower levels of chemoattractant and pro-inflammatory cytokine secretion, or higher levels of anti-inflammatory cytokine secretion, will result in a reduced response with less inflammation and less immune cell infiltrate.

The only cytokine to be secreted to higher levels in response to the non-productive MCMVdie3 infection was IL-10, an anti-inflammatory cytokine with known immunosuppressive properties(25, 322). IL-10 has been shown to reduce inflammatory cytokine production in macrophages(73, 96) and down-regulate the production of TNF and IL-6(83, 347). IL-10 has also been shown to suppress TNF and IL-6 production during the response to MCMV infection *in vivo*(348). This raises the question of whether the increased IL-10 levels in response to MCMVdie3 are responsible for the suppression of pro-inflammatory cytokines IL-6, TNF in MCMVdie3-infected cells, or vice versa?

HCMV encodes an IL-10 viral homolog with potent immunosuppressive function(337) but MCMV does not encode this homolog. MCMV has been shown induce IL-10 to down-regulate MHC class II expression on macrophages(303). These factors indicate there is an important relationship between IL-10 regulation and the response to CMV infection. It is difficult, in this case however, to distinguish whether IL-10 is being targeted by the virus for modulation, or being regulated directly by the host via TNF or another mechanism.

Overall, the data in this chapter supports the hypothesis of the thesis and suggests macrophages respond differently to productive and non-productive MCMV infections. In the next chapter, the activity of the virus rather than the host will be investigated in more depth during the same period of infection. New questions will be asked in relation to whether *de novo* MCMV proteins are capable of modulating macrophage gene expression during productive infection.

Chapter 5

Modulation of transcriptional networks during macrophage infection by MCMV

Introduction

In the previous chapter, the macrophage innate immune response to productive and non-productive MCMV infection was examined. In this chapter, a more targeted analysis of macrophage gene expression networks potentially modulated by MCMV during productive infection will be conducted. Particular focus will be made on the ability of *de novo* MCMV proteins to modulate macrophage gene expression between 4-10hpi in BMDMs.

Understanding how CMV modulates the innate immune response in macrophages is important given the efficiency with which CMV infects macrophages both *in vitro* and *in vivo*(271, 334, 335). HCMV has also been reported to replicate more efficiently in differentiated macrophages than in immature monocytes(132), and even reprogram monocyte differentiation toward an activated M1 macrophage phenotype to favour viral replication(56). MCMV and HCMV have also been reported to use macrophages as a reservoir for latency (172, 256, 286).

The primary objective of this chapter will be to identify macrophage gene expression networks modulated by MCMV during productive infection, and identify which networks are targeted and why. This will be done by re-analyzing the microarray data from the previous chapter using an alternative analysis approach. The second objective of the chapter will be to determine which MCMV proteins (ORFs) might be responsible for modulating the macrophage innate immune response.

Results

5.1 Interferon-stimulated genes (ISGs) are expressed to lower levels in response to productive MCMV infection

Previous studies using UV-inactivated virions suggest strong inhibition of ISGs in response to productive virus infection in comparison to UV-inactivated virions (43, 263, 289). To determine if productive MCMV infection also resulted in a similar suppression of ISGs in macrophages, BMDMs were infected in parallel with MCMV and MCMVdie3 and nine ISGs related to IFN signalling were measured using qRT-PCR analysis. Measurements were made from triplicate BMDM cultures with the intention of having increased sensitivity than microarray analysis.

The ISGs measured included pattern recognition receptors involved in the detection of viruses (*Ddx58* RIG-I and *Tlr9,)* interferon regulatory factors (*Irf1*, *Irf7*), antimicrobial effectors (*Oasl1*, *Mx2*), and chemokines (*Ccl3, Ccl4, Cxcl10*). These genes, based on their varying function and relationship to MCMV, were predicted to be candidates for potential suppression by MCMV at the gene expression during productive MCMV infection.

Of the ISGs measured, *Tlr9* and *Irf1* have been shown to play a direct role in the antiviral defence against MCMV(95, 344). *Ddx58* (RIG-I) is a cytosolic sensor of RNA viruses(385), *Mx2* has a confirmed antiviral role against VSV(396), *Irf7* is a well-established regulator of type I IFN genes(213) with a limited antiviral role against MCMV(339), *Oasl1* is a member of the IFN-induced 2′-5′-oligoadenylate synthetase ubiquitin-like family(32), however has been reported to have an inactive function in mouse(91), and *Ccl3*, *Ccl4*, and *Cxcl10* are chemokines involved in immune cell recruitment during the response HCV infection(206, 388).

Figure 5.1 - Interferon-stimulated genes (ISGs) are expressed to lower levels in response to productive MCMV infection. BMDMs were infected at MOI of 1 PFU/cell and total RNA was harvested at 4hpi and 8hpi. Transcript levels were measured for nine ISGs in response to MCMV (light grey) and MCMVdie3 (dark grey) using qRT-PCR. Transcript levels were normalized to the cellular housekeeping gene *Gapdh* and calibrated to the first 4hpi MCMV sample to show relative expression. Error bars indicate standard deviation from three separate cultures. Asterisks indicate statistically significant differences between the conditions (Students t-test *p<0.05, **p<0.01).

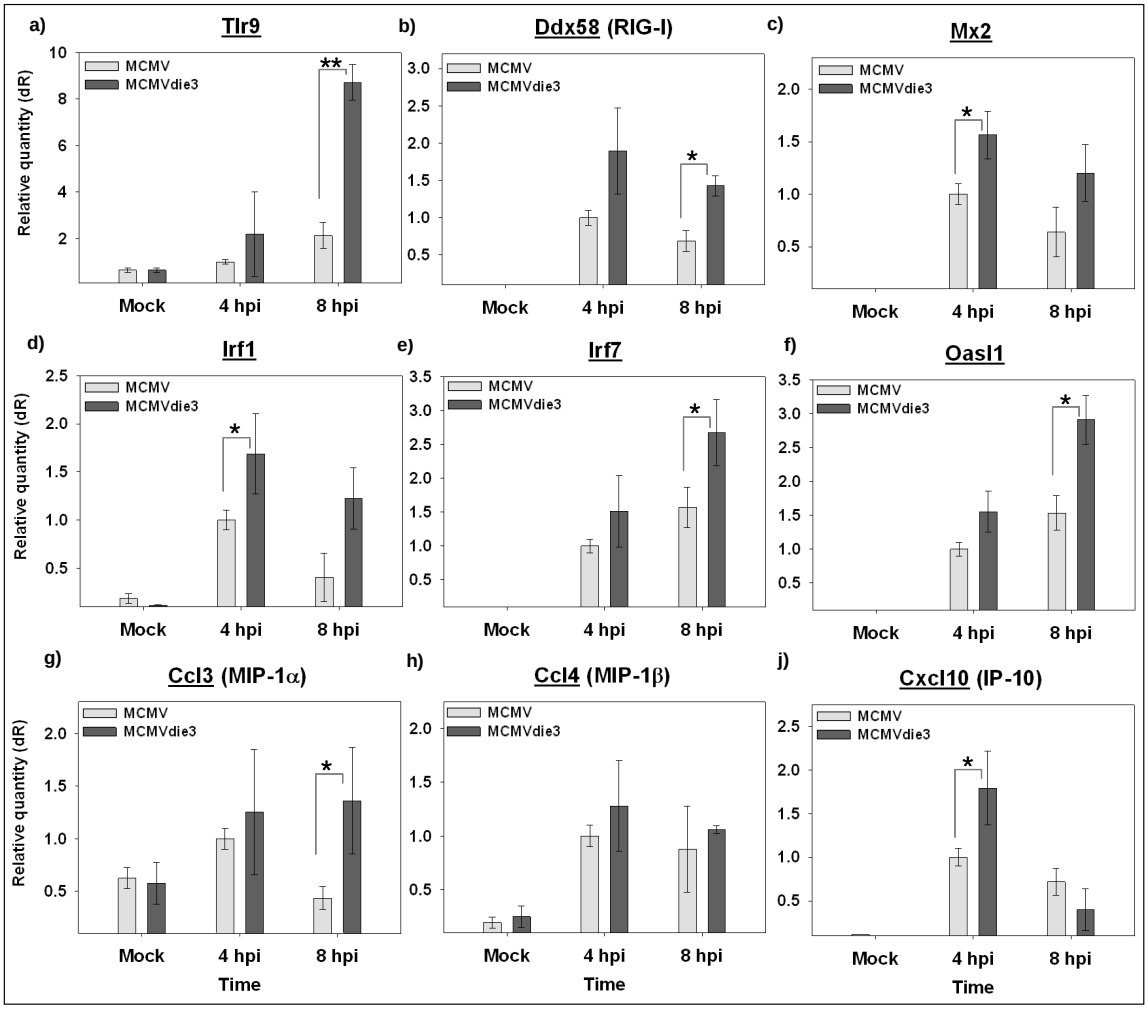

The qRT-PCR data show expression of ISGs is mildly, but consistently lower in response to productive MCMV infection (Figure 5.1). A statistically significant difference in transcript abundance was found for eight of the nine genes measured, at

one or more time point (Students t-test $p<0.05$). In every case the difference was a decrease in transcript abundance in response to productive MCMV infection relative to MCMVdie3, rather than an increase (Figure 5.1). This result suggested a possible suppression of some ISGs by *de novo* MCMV proteins .

Of the nine ISGs measured, toll-like receptor 9 (*Tlr9*) had by far the most significant difference between the conditions ($p< 0.0003$) (Figure 5.1a). Transcript levels for the *Tlr9* gene were over three-fold lower in response to productive MCMV than to MCMVdie3. This suggested, in particular, that suppression of *Tlr9* occurs during productive MCMV infection in BMDMs.

5.2 Genome-wide identification of macrophage gene networks differentially regulated by productive MCMV infection

The suppression of ISGs in response to productive MCMV infection provided justification to explore similar trends occurring throughout the macrophage transcriptome. It was particularly striking that the phenotype was still detectable despite the low levels of infection at MOI of 1 PFU/cell (discussed in the previous two chapters). The time course microarray data described in Chapter 4 was re-visited (for experimental overview see Figure 4.2). The objective of re-analyzing the data was to identify macrophage gene expression networks (i.e. groups of co-regulated genes) potentially modulated by MCMV during productive infection, in a similar way to the ISGs previously measured by RT-PCR.

5.2.1 Statistical identification of differential gene expression between the MCMV and MCMVdie3 responses

The first approach for identifying genes regulated differentially in response to MCMV and MCMVdie3 over the time course was to determine a statistical measure of differential gene expression between the MCMV and MCMVdie3 conditions. For this, an EDGE analysis was applied using *condition*, rather than *time*, as the class

variable. The EDGE tool(213) has a specific function for detecting differential gene expression between two microarray time courses. Using a Q-value cut-off of 0.001, the EDGE analysis identified 196 genes differentially expressed between MCMV and MCMVdie3 conditions, based on temporal profiles.

Upon inspection of these genes, however, it was apparent that the EDGE algorithm was only identifying genes with anti-correlated expression profiles between the two conditions. Any gene that had a correlated gene expression profile between the two conditions (i.e. a gene that was induced with similar kinetics in both conditions but to different peak expression levels) was not identified. This was a problem, as the target genes of interest (ISGs) were predicted to be up-regulated by both MCMV and MCMVdie3, and therefore correlated in their expression, but induced to different peak levels. Therefore, in order identify genes correlated in their expression, but also differentially expressed between the MCMV and MCMVdie3 conditions, an alternative approach was required.

5.2.2 Co-expression network analysis of differential gene expression between the MCMV and MCMVdie3 responses

Using an alternative strategy, a filter was applied to the data whereby any gene with a 1.5 fold or greater difference between MCMV and MCMVdie3 conditions in at least three consecutive time points between 4-10hpi was identified. Using this approach, genes differentially expressed, but also correlated in their expression profiles, would still be identified. 952 genes passed the filter and had a 1.5 fold or greater difference between MCMV and MCMVdie3 at three or more consecutive time points between 4-10hpi. Genes with an increase or decrease in gene expression in MCMV relative to MCMVdie3 were included.

Once the 952 differentially expressed genes had been filtered, the next step was to identify groups of genes that were co-regulated, or affected in the same way, by productive MCMV infection relative to MCMVdie3. The objective of this analysis

was to identify groups of co-regulated genes, rather than individual genes, possibly targeted for modulation by MCMV during productive infection.

In order to identify co-regulated groups of genes, the time-course gene expression data for the 952 genes was imported into BioLayout Express 3D(103). This tool performs gene-to-gene Pearson correlation on every possible pair of input genes, and calculates rates of correlation for each gene pair (for details see Methods section 2.7.2.2). The result is a large cross-correlation matrix of all Pearson correlation values for every possible gene-to-gene correlation. By using the most highly correlated gene pairs (Pearson>0.9), highly correlated genes can be arranged into a three-dimensional network based on the similarity of their gene expression profiles. A network graph is then generated, with nodes representing individual genes. Any two genes (nodes) sharing a highly correlated expression profile (Pearson>0.9) will be connected by a straight line (edge) in the graph.

Once the network graph has been constructed in three dimensions, it can then be visualized and further clustered (sub-divided) into smaller groups based on a more stringent measures of co-expression (Markov MCL clustering). The clusters, or sub-groups, will then represent tightly co-expressed groups of genes regulated in the same manner across the data set. Any genes not passing the Pearson and MCL clustering measures will be excluded from the analysis.

Applying this process to the 952 genes from the previous filter, a network graph of 459 highly correlated genes was formed based on Pearson>0.9 (Figure 5.2). The graph contained genes differentially expressed between the MCMV and MCMVdie3 conditions, and correlated in their expression profiles across the data set. This approach identified transcriptional networks, or groups of genes, possibly targeted by MCMV during productive macrophage infection in the same manner. The resulting network graph was separated into four distinct clusters of co-expression based on MCL clustering. Each cluster represents a different class of genes with a different expression profile in relation to MCMV and MCMVdie3.

Figure 5.2 - Co-expression analysis of differential gene expression between the MCMV and MCMVdie3 responses. 952 genes were identified as having a 1.5 fold of greater difference in gene expression levels between MCMV and MCMVdie3 conditions at three or more consecutive time points between 4-10hpi. These genes were arranged into a network graph based on co-expression using BioLayout Express 3D (Pearson>0.9). Each node (ball) represents an individual gene. Any two nodes connected by a straight line (edge) are highly correlated in their expression profile across the time course (Pearson>0.9). The network graph contains 459 highly correlated genes in four distinct clusters of co-expression, each shown with a different colour, and each differentially expressed between MCMV and MCMVdie3.

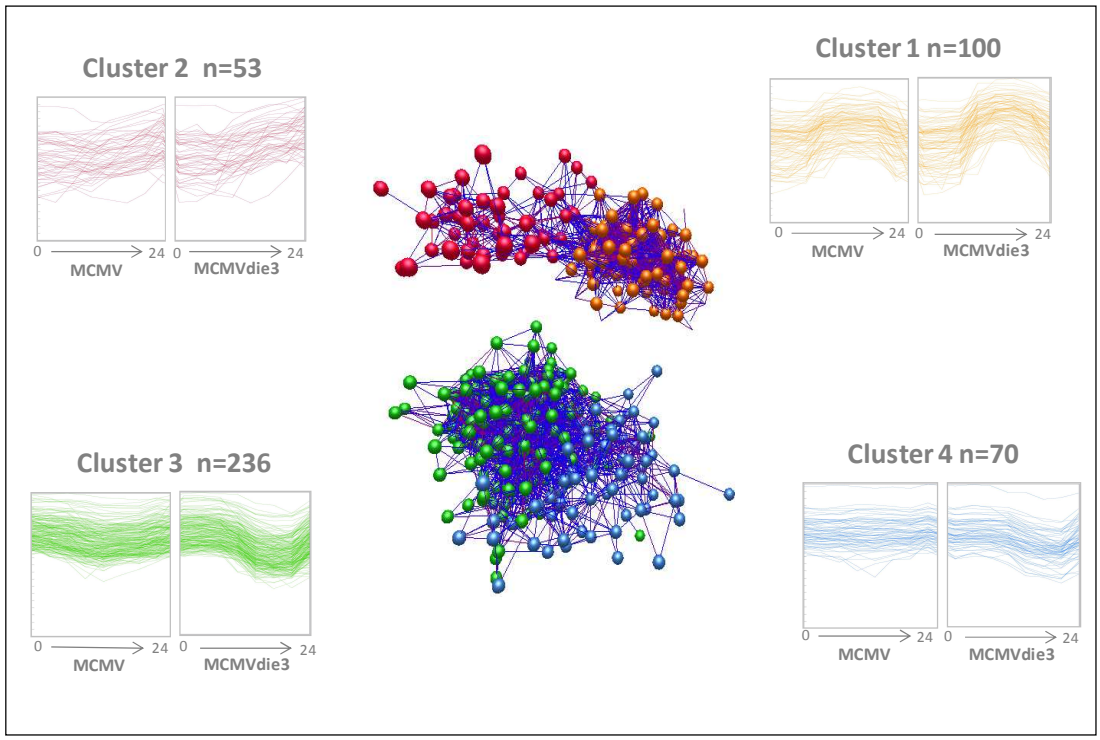

As shown in Figure 5.2, the co-expression analysis identified two up-regulated and two down-regulated gene expression clusters. Each of these clusters contained genes differentially regulated by a factor of 1.5 fold or higher between MCMV and MCVMdie3 over three or more consecutive time points between 4-10hpi. To further illustrate the differences between MCMV and MCMVdie3 responses for these clusters, in Figure 5.3 they are shown as relative expression heatmaps and mean (average) expression profiles to improve the interpretation.

Figure 5.3 - Co-expressed networks of macrophage genes differentially regulated in response to productive MCMV infection. (**i**) Four clusters are shown as heatmaps to illustrate differences between MCMV and MCMVdie3 and to show relative expression. Each gene is represented by a row and per-gene normalized to its mean value. Yellow indicates increased expression relative to the mean and blue indicates a decrease. Each column represents a different time point as indicated below the heatmaps. (**ii**) Mean expression profiles show the average for all genes within the cluster in response to MCMV (light grey) and MCMVdie3 (dark grey). Red arrows emphasize the overall difference between the MCMV and MCMVdie3 responses. The 0hpi time point represents the end of the 1.5 hour viral adsorption period.

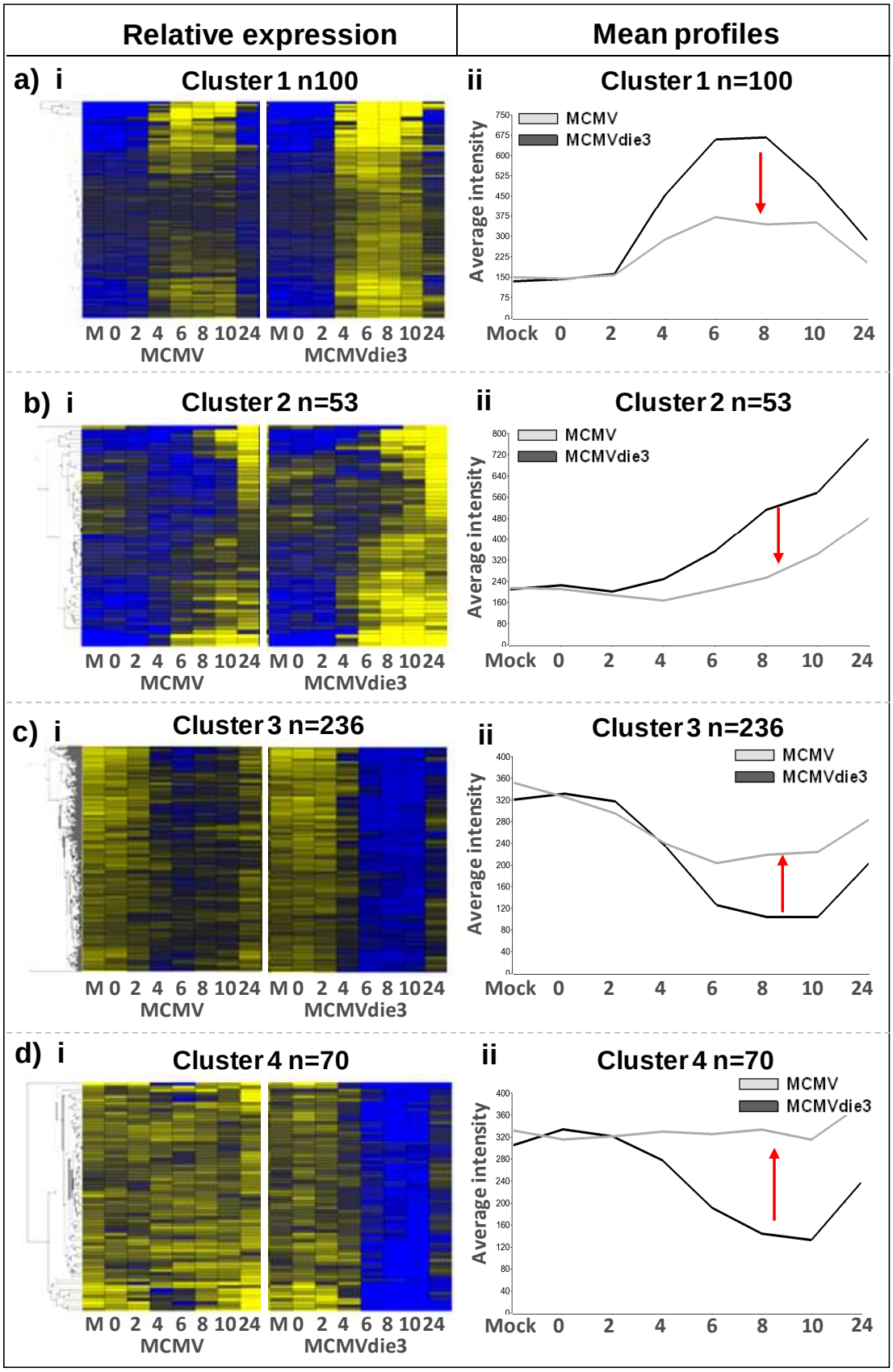
Relative expression
Mean profiles
a) i
Cluster 1 n100
M 0 2 4 6 8 1024 M 0 2 4 6 8 1024
MCMV
MCMVdie3
ii
Cluster 1 n=100
MCMV
MCMVdie3
Average intensity
Mock 0 2 4 6 8 10 24
b) i
Cluster 2 n=53
M 0 2 4 6 8 1024 M 0 2 4 6 8 1024
MCMV
MCMVdie3
ii
Cluster 2 n=53
MCMV
MCMVdie3
Average intensity
Mock 0 2 4 6 8 10 24
c) i
Cluster 3 n=236
M 0 2 4 6 8 1024 M 0 2 4 6 8 1024
MCMV
MCMVdie3
ii
Cluster 3 n=236
MCMV
MCMVdie3
Average intensity
Mock 0 2 4 6 8 10 24
d) i
Cluster 4 n=70
M 0 2 4 6 8 1024 M 0 2 4 6 8 1024
MCMV
MCMVdie3
ii
Cluster 4 n=70
MCMV
MCMVdie3
Average intensity
Mock 0 2 4 6 8 10 24

As shown in Figure 5.3, the genes up-regulated in Clusters 1 and 2 are induced by both MCMV and MCMVdie3 infection, but are expressed to lower levels (i.e. possibly suppressed) in response to productive MCMV infection (Figure 5.3a-b). Clusters 3 and 4 are down-regulated during the macrophage response to MCMV and MCMVdie3, but are seemingly blocked, or inhibited, in their down-regulation by productive MCMV infection (Figure 5.3c-d).

Before proceeding with further analysis, at this point it was important to consider the possibility that host factors, rather than viral factors, could account for the changes in gene expression observed in Clusters 1-4. For example, if key negative regulators were expressed differentially between the MCMV and MCMVdie3 conditions, it could account for changes in downstream gene expression seen in Clusters 1-4. This would particularly be the case if negative regulators of the innate immune response were expressed to higher levels during productive MCMV infection, leading to a suppressive effect that would appear to be the result of *de novo* viral proteins. To determine if such an effect was occurring, a list of negative regulators of toll-like receptor-mediated signalling was obtained from Liew *et al*(217). The expression levels of the mouse homologs of these negative regulators was used to give an indication of whether or not host factors were contributing to the regulation of genes in Clusters 1-4 at 4hpi. Table 5.1 shows the expression levels of negative regulator genes in mock, MCMV and MCMVdie3 infected BMDMs at 4hpi, corresponding to the beginning of the time period analyzed in section 5.2.2.

Table 5.1 –Expression level of negative regulators of Toll-like receptor-mediated signalling in response to MCMV and MCMVdie3 (normalized microarray intensity)

Gene	Alias	Mock	MCMV 4hpi	MCMVdie3 4hpi	Fold change MCMVdie3/ MCMV 4hpi
Socs1		107.6	1338.0	1434.84	1.07
Socs2		21.5	250.5	212.3	-1.17
Socs3		10.6	81.4	134.2	1.65*
Tnfaip3	A20	193.8	1060.9	1131.2	1.06
Tollip		700.4	784.1	652.3	-1.20
Pik3r1	PI3K	403.9	255.6	343.4	1.52*
Nod2		38.6	107.9	162.9	-1.15
Tmed1	St2L	96.0	162.4	140.7	1.02
Irak3	Irak-m	Below detection threshold			Irak-m
Sigirr		Below detection threshold			

Overall, the expression level of negative regulators in this list was similar between the MCMV and MCMVdie3 conditions (less than 1.5 fold difference at 4hpi). The only negative regulators in the list to have a 1.5 fold or greater difference in gene expression between MCMV and MCMVdie3 at 4hpi were *Socs3* and *Pik3r1* (a sub-unit of PI3K). Although *Socs3* is a well known negative regulator of innate immune signalling(82), the expression level of *Socs3* and *Pik3r1* was higher in response to MCMVdie3 than in response to MCMV, the opposite of what this exercise was trying to identify. This suggests, if anything, that *Socs3* and *Pik3r1* were suppressed during productive MCMV infection at 4hpi, and not expressed to higher levels during productive MCMV infection. This analysis suggested that at the beginning of the time period analyzed in section 5.2.2, the expression of negative regulators of the innate immune response is comparable in MCMV and MCMVdie3 conditions.

5.2.3 Functional annotation of co-expressed networks differentially regulated between MCMV and MCMVdie3

Functional annotation of genes within Clusters 1-4 was conducted to help identify biological processes potentially affected by *de novo* viral proteins during productive MCMV infection. Within Cluster 1, innate immune signalling genes were found such as interleukins 10 and 18 (*Il10, Il18*), interleukin receptor components (*Il18rap, Il21r, Il2ra, Il4ra*), antimicrobial effector genes (*Oas1b, Naip5*) and members of the TNF superfamily (*Tnfsf4, Tnfsf8*). The negative regulator of IFN signalling *Socs3* was also in Cluster 1, as described above. In Cluster 2, genes involved in immune cell trafficking and leukocyte recruitment were found (*Ccl8, Ccr1l1, Ccr2, Ccr3, Ccr5, Cd5l*), as well as members of the Schlafen family (*Slfn1, Slfn10*), and toll-like receptors (*Tlr9, Tlr13*). The lower level of expression for these genes in the productive MCMV infection suggests possible suppression by *de novo* MCMV proteins. Genes in Cluster 1 were up-regulated early and transient in their expression, whereas genes in Cluster 2 were up-regulated late and sustained in their expression, indicating different kinetic classes of genes (Figure 5.3a-b). For a complete list of gene in Clusters 1 and 2, see Supplementary File 12.

The down-regulated genes in Clusters 3 and 4 were seemingly blocked, or inhibited, in their down-regulation during productive MCMV infection (Figure 5.3c-d). This blocking, or inhibition effect was more pronounced in Cluster 4 (Figure 5.3d). Genes down-regulated in this manner were not associated with the innate immune response but were more associated with the cell cycle. In Cluster 3 (Figure 5.3c), there were a number of genes linked to cell cycle control (*Ccdc21, Cdc35a, Chek2, Clock, Mcm3*) and DNA/RNA polymerase activity (*Pold2, Poldip2, Pole2, Polh, Polr1b, Polr3e*). In Cluster 4 (Figure 5.3d) there were genes associated with ribosomal RNA processing (*Rrp1b, Rrp8*) and ATP/GTP-binding (*Abcb6, Gtpbp4, Mtg1*). For a complete list of gene in Clusters 3 and 4, see Supplementary File 13.

To determine over-representation of annotation classes and biological processes for genes in the four co-expressed clusters, InnateDB(229) and Ingenuity Pathway

Analysis (IPA) were used. These tools identify functional links and associations between genes based on molecular and chemical interactions, cellular phenotypes, gene ontologies and disease processes. InnateDB is a manually-curated public database of interactions and pathways designed specifically to facilitate systems level analysis of the innate immune response. IPA is a commercial database and resource of molecular interactions from experimental platforms and from the literature. Both tools build interaction networks between genes based on their annotated molecular relationships. For the InnateDB and IPA analyses, the two up-regulated (*induced*) Clusters 1 and 2 were combined together into a single list, and the two down-regulated (*suppressed*) *C*lusters 3 and 4 were combined together into a single list to simplify the interpretation.

Using InnateDB, annotation of the up-regulated networks identified a highly significant over-representation of the *Cytokine-cytokine receptor interaction* pathway (KEGG map04060)(corrected p-value 6.91E-05). This suggests genes involved in this pathway are co-regulated in macrophages, and expressed to lower levels in response to productive MCMV infection. Using IPA, 27/153 of the genes in Clusters 1 and 2 were found to have an association with the inflammatory response and 21/153 with infectious disease. Genes with roles in the recruitment of leukocytes (*Adora3, Ccr2, Ccr3, Ccr5, Hds, Il18, Kitlg, Txn*), and genes involved in the IL10 pathway (*Il10, Ccr5, IL4r, Socs3*) were also found.

An interaction network for all genes in the up-regulated Clusters 1 and 2 was constructed using InnateDB. This network included all interactions between genes within the input list, and also incorporated secondary interactions with other genes in the genome that were highly connected to the network (Figure 5.4).

Figure 5.4 InnateDB interaction network of genes from Clusters 1 and 2.
A network of interactions based on molecular and chemical interactions, cellular phenotypes, gene ontologies and disease processes was constructed using 153 highly correlated genes induced by MCMV and MCMVdie3 but expressed to lower levels in response to productive MCMV infection. Interactions between these genes, as well as interactions with secondary genes are shown.

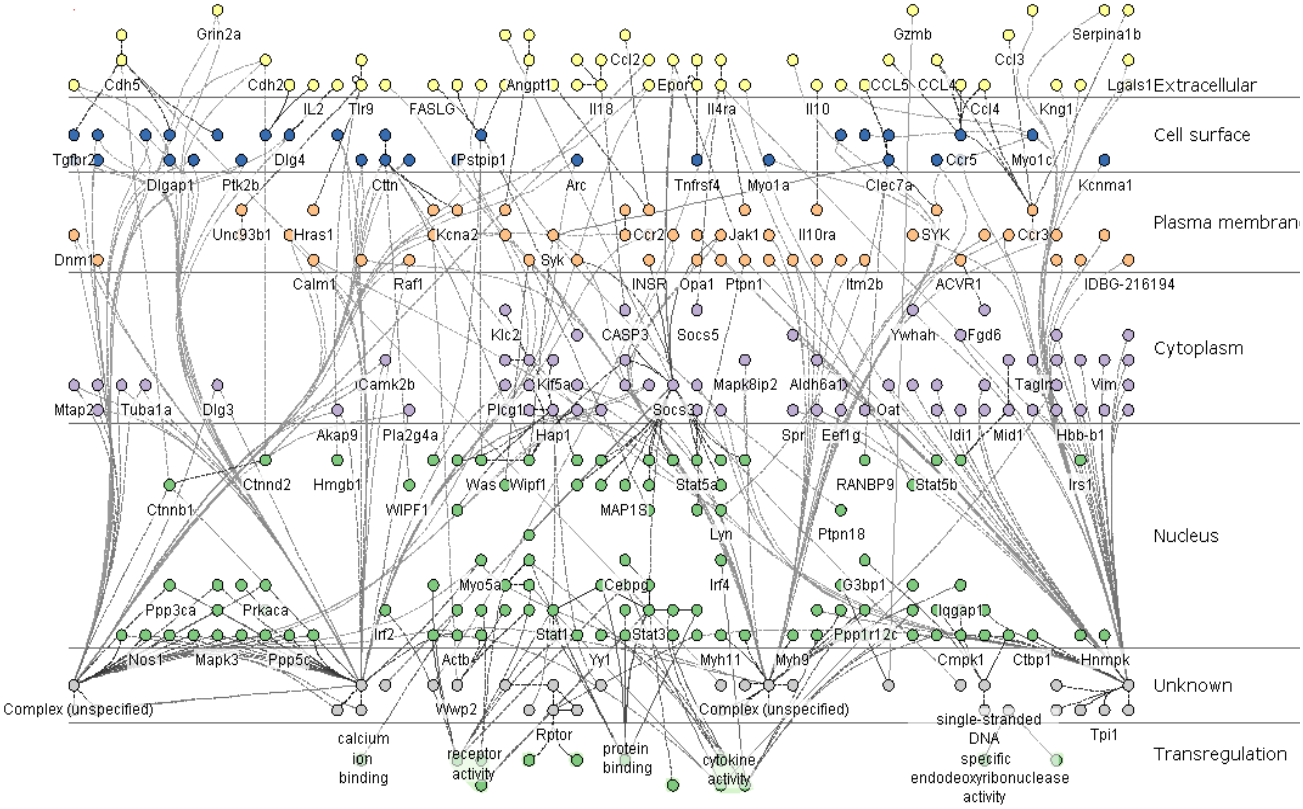

The interaction network shown above suggests a high degree of connectivity between the genes within Clusters 1 and 2, and indicates a number of 'hub' genes with many interactions to other genes in the network.

Next, to identify a more focused network of genes from Clusters 1 and 2 representing a more defined area of biology, IPA was used to derive a network of 34 highly associated genes (Figure 5.5) involved in *immune cell trafficking* and *leukocyte recruitment*.

Figure 5.5 - Immune cell trafficking and leukocyte recruitment; Focused molecular interaction network from Clusters 1 and 2. IPA was used to build an interaction network based on molecular and chemical interactions, cellular phenotypes, gene ontologies and disease processes. The most significant network constructed by IPA was associated with *immune cell trafficking* and *leukocyte recruitment*. Genes that were part of the original input list are shown in grey, and secondary interacting partners are shown in white.

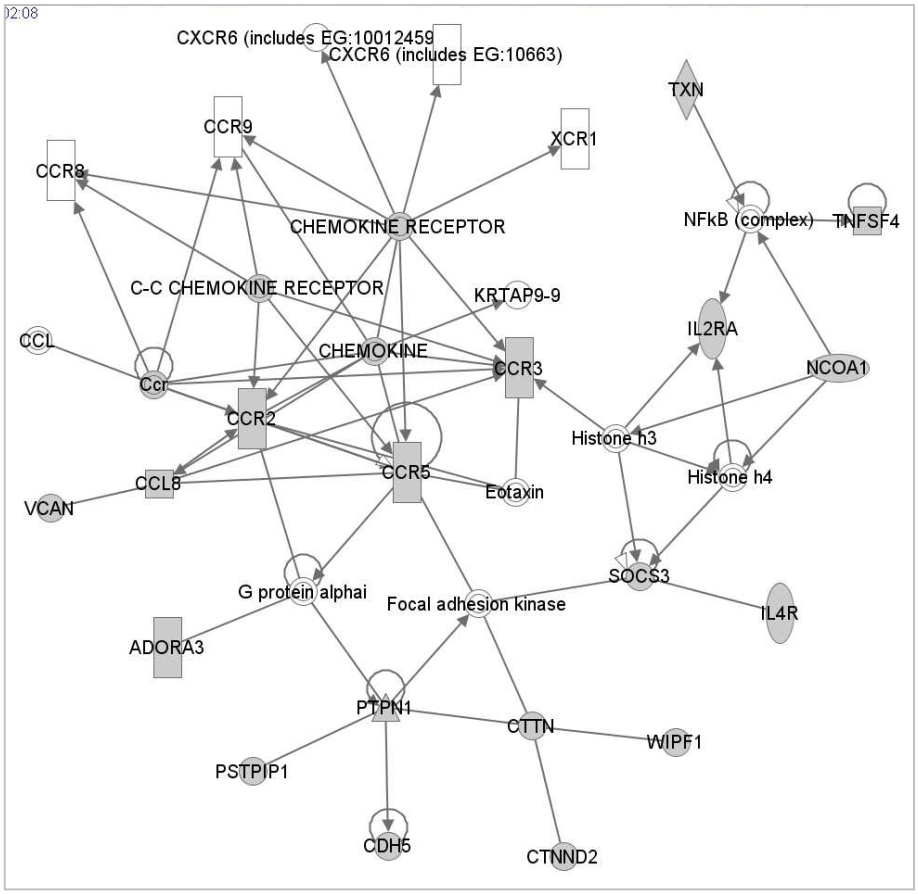

Next, a similar network analysis was performed on down-regulated genes from Clusters 3 and 4 that were seemingly blocked, or inhibited, by productive MCMV infection. InnateDB identified a number of significantly over-represented down-regulated pathways including *Metabolism of folate and pterines* (p0.001), *TRNA Aminoacylation* (p0.002), *Cell Cycle, Mitotic* (p0.005), *Activation of the pre-replicative complex* (p0.005), *Cytosolic tRNA aminoacylation* (p.006), and *DNA*

replication (p0.007). InnateDB was used to construct an interaction network for all down-regulated genes in Clusters 3 and 4. This network included all interactions between genes in the input list and secondary interactions with other genes in the genome (Figure 5.6).

Figure 5.6 InnateDB interaction network of genes from Clusters 3 and 4.
A network of interactions based on molecular and chemical interactions, cellular phenotypes, gene ontologies and disease processes was constructed using 306 genes down-regulated by MCMV and MCMVdie3 but block, or inhibited, in their down-regulation by productive MCMV infection. Interactions between these genes, as well as interactions with secondary genes throughout the genome are shown.

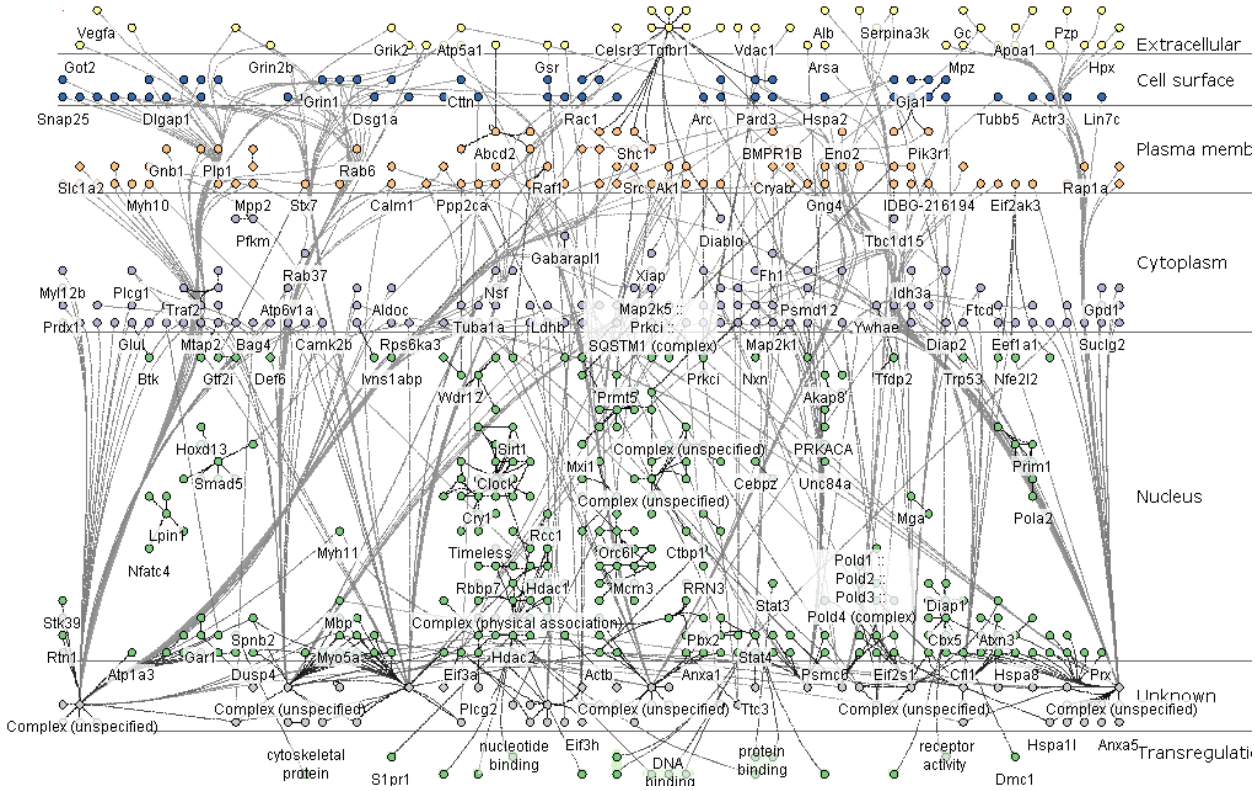

The interaction network above shows a high degree of connectivity between genes blocked, or inhibited, in their down-regulation during productive MCMV infection. In particular, many genes within the nucleus involved in the cell cycle were found to have a high degree of connectivity in this network.

To identify a more focused network of genes from Clusters 3 and 4 associated more with a common biological process, IPA was used to derive a network of highly associated genes (Figure 5.7). This network was highly enriched with annotation terms associated with *cell cycle* and *DNA replication.*

Figure 5.7 - Cell cycle and DNA replication; Focused molecular interaction network of down-regulated genes in Clusters 3 and 4. IPA was used to build an interaction network based on molecular and chemical interactions, cellular phenotypes, gene ontologies and disease processes from genes in Clusters 3 and 4. The most significant network constructed by IPA was associated with *cell cycle* and *DNA replication*. Genes part of the original input list are shown in grey, and secondary interacting partners are shown in white.

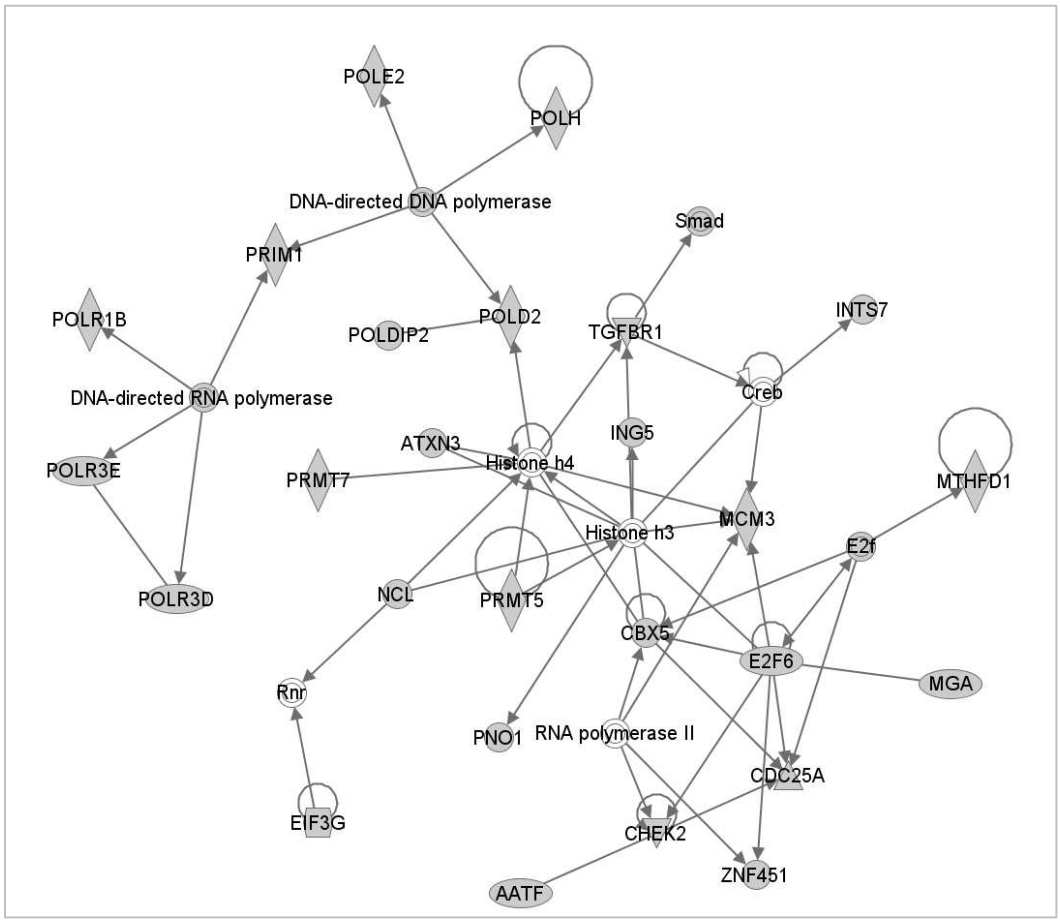

5.3 Identification of MCMV proteins capable of modulating macrophage gene expression during productive MCMV infection

5.3.1 Detection of MCMV genes expressed at 12hpi in BMDMs

After identifying macrophage gene expression networks differentially regulated during productive MCMV infection, the next step was to identify which MCMV proteins (or open reading frames) might be responsible for the modulation. For this analysis, the large MCMV genome of ~170 open reading frames (ORFs) was reduced down in any way possible to create a smaller candidate list of potential MCMV ORFs responsible. The first step in this process was to determine which MCMV ORFs were expressed in BMDMs in the relevant time frame. To do this, BMDMs were infected at MOI of 1 PFU/cell and total RNA was harvested from triplicate cultures at 6, 12 and 24hpi and hybridized to the custom MCMV gene expression microarray to measure genome-wide MCMV transcript abundance (for details see Methods section 2.7.1.1).

To identify only high-confidence MCMV ORFs expressed in BMDMs at12hpi, a stringent expression-level cut-off of a normalized log intensity value of 9 was used. This reduced the false positive rate and ensured only MCMV ORFs expressed to high confidence levels were identified. 70 MCMV ORFs were detectable at 12hpi to this level and were used to form the initial candidate list of MCMV proteins (Table 5.2).

Table 5.2 - High confidence MCMV ORFs detectable in BMDMs at 12hpi. Total RNA was extracted from MCMV-infected BMDMs at 12hpi and was hybridized to a custom oligonucleotide MCMV microarray. Target probe intensities for MCMV ORFs were log transformed and normalized using a sub-set of positive control probes (for details see Methods section 2.7.1.1).

Probe ID	MCMV ORF	Microarray intensity (log)		Probe ID	MCMV ORF	Microarray intensity (log)
vMC003	m03	9.79		vMC086	M88	9.32
vMC004	m04	11.59		vMC092	M94	10.87
vMC006	m06	13.35		vMC096	M97	9.22
vMC008	m08	10.24		vMC100	M102	12.69
vMC013	m13	9.44		vMC103	M105	9.06
vMC016	m16	10.39		vMC108	M113	11.00
vMC017	m17	11.80		vMC109	M114	9.64
vMC018	m18	12.47		vMC114	M118	12.19
vMC020	m20	9.67		vMC115	m119	9.50
vMC026	M25	10.53		vMC116	m119.1	10.63
vMC027	m25.1	10.84		vMC117	m119.2	11.77
vMC030	M28	11.34		vMC118	m119.3	9.36
vMC034	M31	11.34		vMC121	m120	9.06
vMC035	M32	9.06		vMC127	m124	11.13
vMC037	M34	10.12		vMC132	m128 Ex3	9.42
vMC038	M35	9.46		vMC136	m132 Ex2	12.71
vMC039	M36 Ex1	9.24		vMC137	m132 Ex1	10.31
vMC040	M36 Ex2	12.58		vMC141	m137	11.67
vMC041	M37	12.68		vMC142	m138	13.19
vMC042	M38	10.43		vMC143	m139	9.07
vMC045	m41	11.72		vMC146	m142	11.57
vMC046	m42	10.73		vMC149	m145	9.06
vMC047	M43	11.40		vMC151	m147	11.59
vMC049	M45	11.97		vMC156	m152	10.10
vMC055	m48.2	11.06		vMC158	m154	11.61
vMC056	M49	9.52		vMC159	m155	10.28
vMC061	M54	9.59		vMC163	m159	9.34
vMC064	M57	9.05		vMC164	m160	9.10
vMC067	M69	9.96		vMC167	m163	10.44
vMC070	M71	9.34		vMC168	m164	10.42
vMC071	M72	10.68		vMC170	m166	11.58
reM73c	M73	9.28		vMC173	m169	13.00
vMC077	M78	11.34		vMC176	m132 Ex2	12.80
vMC079	M80	10.30		vMC180	m163	12.04
vMC080	M82	9.48		vMC184	M45	9.18

5.3.2 Use of large-scale MCMV deletion mutants to identify MCMV ORFs capable of modulating macrophage gene expression during productive infection

For experimental purposes, the list of 70 MCMV ORFs identified in the MCMV microarray analysis (Table 5.2) was still too long to test individual ORFs for their macrophage immune-modulating properties. Therefore, to further reduce the list of potential candidate ORFs, an alternative approach was taken through the use of large-scale MCMV deletion mutants. The large-scale MCMV deletion mutants have large blocks of the MCMV genome deleted (60, 177), each of which contains a region of ~15 ORFs predicted to have role in immune-evasion. These deleted regions are removed from terminal ends of the MCMV genome which are not part of the essential conserved herpesvirus region. Their deletion, therefore, does not result in attenuation of viral growth in cell culture(60). Table 5.3 shows the three large-scale deletions mutants and the corresponding genomic regions deleted in each strain. Between the three strains, a total of 43 MCMV ORFs are deleted.

Table 5.3 - MCMV deletion mutants with large regions of the genome removed.

Strain name	**Genomic region deleted**	**MCMV ORFs deleted**
MCMVdel1	Gene block 1	m01, m02, m03, m04, m05, m06, m07, m08, m09, m10, m11, m12, m13, m14, m15,m16
MCMVdel6	Gene block 6	m144, m145, m146, m148, m149, m150, m151, m152, m153, m154, m155, m156, m157
MCMVdel7	Gene block 7	m158, m159, m160, m161, m162, m163, m164, m165, m166, m167, m168, m169, m170

To determine if MCMV ORFs responsible for modulating macrophage gene expression were located within the deleted regions of the MCMV mutants, a marker gene approach was used. The marker gene chosen was the toll-like receptor 9 gene (*Tlr9)* which would provide a representation of macrophage genes induced by MCMV and MCMVdie3, but expressed to lower levels in response to productive MCMV infection (i.e. potentially suppressed). *Tlr9* had been previously identified as

being significantly suppressed in response to productive MCMV infection compared to MCMVdie3 in qRT-PCR experiments (over 3-fold at the mRNA level - see Figure 5.1). *Tlr9* was also found in Cluster 2 of the co-expression network analysis (Figure 5.3b), and *Tlr9* is of high biological relevance given its direct role in the detection of MCMV dsDNA during infection (42, 148, 169, 200, 344). The *Sectm1* gene (secreted and transmembrane 1) was also chosen for as a secondary marker for similar purposes.

If *Tlr9* was suppressed during infection with the large-scale MCMV deletion mutants relative to MCMVdie3, as it was during infection with wild-type MCMV, it would mean the viral ORF responsible for the suppression would not be located in the deleted regions. Alternatively, if the viral ORF responsible for the suppression was within the deleted region, the expression of *Tlr9* should be de-repressed as was seen in response to MCMVdie3. If the ORF responsible for the suppression phenotype was not located within any of the three deleted regions, then at least a total of 43 MCMV ORFs located within the deleted regions could be ruled out of the analysis.

BMDMs were infected in parallel with MCMV, MCMVdie3, MCMVdel1, MCMVdel6, MCMVdel7 at MOI of 1 PFU/cell and total RNA was extracted from triplicate cultures at 10hpi. A deletion mutant for MCMV ORF M45 (MCMVd45) was also included in the analysis, given the known role of M45 in modulating the innate immune response during MCMV infection(45, 230, 364). *Tlr9* transcript levels were then measured in response to each virus at 10hpi. Figure 5.8 shows the level of expression for *Tlr9* at 10hpi in response to the each of the MCMV mutant strains, and in response to mock infection.

Figure 5.8 Suppression of *Tlr9* expression still occurs in response to MCMV large deletion mutant strains. BMDMs were infected at MOI of 1 PFU/cell with six different MCMV strains and total RNA was harvested at 10hpi. Transcript levels for *Tlr9* (**a**) and *Sectm1a* (**b**) were measured in response to each strain using qRT-PCR. Transcript levels were normalized to the cellular housekeeping gene *Gapdh* and calibrated to the first MCMV condition to show relative expression. Error bars indicate standard deviation from three separate cultures. Red arrows emphasize the suppression by wild-type MCMV.

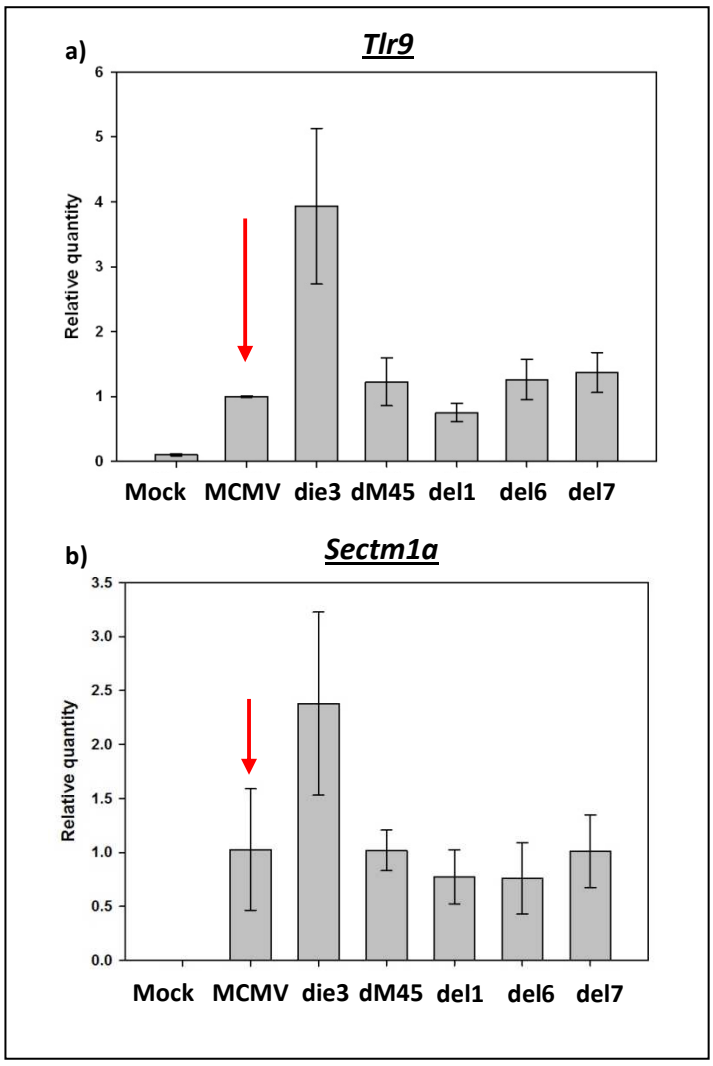

As shown in Figure 5.8, *Tlr9* and *Sectm1a* were suppressed by wild-type MCMV infection (as emphasized by the red arrows), and expressed to higher levels in response to MCMVdie3. In response to the large-scale deletion mutants, however, the expression of the marker gene was equivalent to wild-type MCMV levels. This

indicated viral ORF responsible for the suppression of *Tlr9* and *Sectm1a* was not located within the deleted genomic regions. It also ruled out M45 as a possible candidate for the phenotype.

Taking this information into account, the list of candidate MCMV ORFs could now be shortened from 70 to 51 by removing any ORFs located within the three deleted regions from MCMVdel1, MCMVdel6 and MCMVdel7, and by removing M45. Also, any MCMV ORFs known to be encoding tegument proteins or structural components of the virion (i.e glycoproteins etc) were also removed at this stage, reducing the list to 42 ORFs.

Table 5.4 Remaining 42 candidate MCMV ORFs Of the 70 MCMV ORFs detectable at 12hpi during BMDM infection, 28 could be excluded from the analysis due to their location within one of the deleted genomic regions of the three large-scale MCMV deletion mutant strains. This left a remaining 42 candidate ORFs.

Probe ID	MCMV ORF	Microarray intensity (log)		Probe ID	MCMV ORF	Microarray intensity (log)
vMC018	m18	12.47		vMC086	M88	9.32
vMC020	m20	9.67		vMC096	M97	9.22
vMC027	m25.1	10.84		vMC100	M102	12.69
vMC030	M28	11.34		vMC103	M105	9.06
vMC034	M31	11.34		vMC108	M113	11.00
vMC037	M34	10.12		vMC109	M114	9.64
vMC038	M35	9.46		vMC114	M118	12.19
vMC039	M36 Ex1	9.24		vMC115	m119	9.50
vMC040	M36 Ex2	12.58		vMC116	m119.1	10.63
vMC041	M37	12.68		vMC117	m119.2	11.77
vMC042	M38	10.43		vMC118	m119.3	9.36
vMC045	m41	11.72		vMC121	m120	9.06
vMC046	m42	10.73		vMC127	m124	11.13
vMC047	M43	11.40		vMC132	m128 Ex3	9.42
vMC056	M49	9.52		vMC136	m132 Ex2	12.71
vMC064	M57	9.05		vMC137	m132 Ex1	10.31
vMC070	M71	9.34		vMC141	m137	11.67
vMC071	M72	10.68		vMC142	m138	13.19
reM73c	M73	9.28		vMC143	m139	9.07
vMC077	M78	11.34		vMC146	m142	11.57
vMC079	M80	10.30		vMC176	m132 Ex2	12.80

Any further investigation to identify the MCMV ORF(s) responsible for modulation of macrophage gene expression was at this stage deemed beyond the scope of the study.

Discussion

The primary objective in this chapter was to identify macrophage gene expression networks modulated during productive MCMV infection and determine their biological relevance to the macrophage innate immune response. This was achieved through temporal gene-expression profiling of macrophages infected with productive and non-productive MCMV, followed by a network clustering and functional annotation analysis. The secondary objective of the chapter was to identify MCMV ORFs responsible for immune-modulation in macrophages at the gene expression level between 4-10hpi. This secondary objective was not achieved, however a candidate list of 42 possible MCMV ORFs responsible for the phenotype was formulated.

Suppression of ISG expression in response to productive MCMV infection

Initially, nine ISGs were measured by qRT-PCR analysis in response to MCMV and MCMVdie3 infection. The ISGs were chosen due to their known or predicted role in the antiviral innate immune response to virus infection. Although the expression of almost all of ISGs measured was found to be lower in response to productive MCMV infection (Figure 5.1), the differences, overall, were quite small for many of the genes (fold change <2, p-values>0.02). This is likely due to the low level of infection achieved at MOI of 1 PFU/cell, and possibly due paracrine signalling in non-infected (bystander) cells in BMDM cultures. In addition, there was no direct evidence that the lower level of expression for the ISGs was actually due to direct viral activity, as opposed to host factors. To investigate this point, the expression of negative regulator genes involved in innate immune suppression was assessed at 4hpi, and found to be similar (below 1.5 fold) between the MCMV and MCMVdie3 conditions (Table 5.1)

Tlr9 was expressed to significantly lower levels in response to productive MCMV infection compared to MCMVdie3. Transcript levels for *Tlr9* were over three-fold lower in response to productive MCMV infection at 8hpi, even despite the low levels

of infection. This was by far the most significant difference detected for any of the nine ISGs measured by qRT-PCR analysis. This result suggested *Tlr9* was suppressed with some degree of specificity by *de novo* MCMV proteins during productive MCMV infection. This result was of high biological relevance given the role of *Tlr9* in the context of MCMV infection. *Tlr9* has been shown by a number of studies to be involved in the direct recognition of CMV viral DNA in infected cells (42, 148, 169, 200, 344), and has also been shown to be a highly significant susceptibility factor for MCMV infection in *Tlr9* knockout mice(344). In murine macrophages, the *Tlr9* gene has been shown to be regulated by the PU.1 and ICSBP transcription factors(325), by interferon-regulatory factors (IRFs) 1 and 2(269), and by a distal regulatory region(127). Suppression of *Tlr9* expression would represent an immune evasion mechanism previously not described for MCMV. Direct evidence of the mechanism involved, and identification of the MCMV ORF responsible is still lacking. Recently, an EBV latent protein has been shown to suppress TLR9 mRNA in human primary B cells(93), suggesting targeting of TLR9 may be conserved in other herpesviruses.

Genome-wide identification of co-expressed gene networks differentially regulated in response to productive MCMV infection

Many previous studies investigating the host response to productive and non-productive viral infection in fibroblasts and other non-immune cells report a strong suppression of type I IFN and ISGs expression in response to productive virus infection(43, 133, 263, 289). This is likely due to high levels of viral infection and an attenuated innate immune response in fibroblasts and non-immune cell types. In the current study, however, due to the use of BMDMs, only a subtle modulation of the innate immune response was observed in response to productive MCMV infection. As a result, less conventional approaches were required to identify the subtle modulations in macrophage gene expression caused by MCMV activity. In addition, this study had the added objective of identifying co-regulated networks of genes, rather than individual genes, targeted on a genome-wide scale.

The approach used was to identify genes differentially expressed between MCMV and MCMVdie3 over the time course, then cluster these genes based on co-expression. This lead to identification of four distinct groups, or clusters, of genes co-regulated and differentially expressed between MCMV and MCMVdie3 (Figure 5.2). Subsequently, the four clusters of co-expressed genes (termed Clusters 1, 2, 3 and 4) were investigating further using functional annotation and molecular interaction network analyses to determine the relationship of the genes to the macrophage response.

Clusters 1 and 2 contained genes induced by MCMV and MCMVdie3, but expressed to lower level in response to productive MCMV infection (Figure 5.3a-b). Over-representation of annotation categories for genes in these clusters included *immune cell trafficking* and *leukocyte recruitment*. This suggested MCMV may target these areas of biology for suppression during productive macrophage infection. Down-regulated Clusters 3 and 4 contained genes involved in the *cell cycle* and *DNA replication*. Genes within these clusters were down-regulated by MCMV and MCMVdie3, but their down-regulation was inhibited (or blocked) by productive MCMV infection (Figure 5.3c-d). These genes were highly associated with the *cell cycle* and *mitosis.*

Considering the annotation of the clusters in a biological context, the inhibition of leukocyte recruitment to a site of primary virus infection has clear benefits in giving the virus an overall replication advantage. Suppression of genes in Cluster 1 and 2 may therefore reflect the ability of MCMV to inhibit immune cell recruitment during primary infection *in vivo* (237, 288), an observation which is consistent with a number of other studies(24, 27, 257).

In relation to Clusters 3 and 4, the inhibition of apoptosis has been well described as an immune-evasion strategy for CMV(10, 119, 244, 379). Annotation of genes within these two clusters would be consistent with this activity (i.e. *cell cycle* and *DNA replication*). Inhibiting apoptosis has obvious advantages during lytic

infection(105), and modulation of the cell cycle by CMV, in particular halting the cell cycle in G1 and G2 phase, has also been shown(10, 119, 244, 379).

The adenosine A3 receptor (*Adora3*) was also up-regulated during the macrophage response to MCMV and MCMVdie3 but suppressed by productive MCMV infection. *Adora3* has been shown to play an important role in haematopoiesis(146) and macrophage function(20, 21, 137, 238) in a number of different contexts. Interleukin 10 (*Il-10*) and other members of the IL-10 signalling pathway (*Il10, Ccr5, IL4r, Socs3*) were also found to be induced by MCMV but suppressed by productive MCMV infection.

Although the biological process reflected by the four co-expressed clusters are consistent with previously documented mechanisms of CMV immune evasion, there is still the possibility that genes within these clusters are regulated purely by host factors, and not affected by direct MCMV activity. This, in fact, was a major limitation of the line of experimentation used in this chapter. More mechanistic studies of MCMV proteins and their direct interaction with host factors will be required to directly link the activity of the virus to modulation of these genes.

One such study that has already been conducted, is an investigation of *Stat2* modulation by the MCMV protein M27(392). This study showed M27 was capable of modulating the *Stat2* transcription factor during the IFNγ antiviral signalling response. In relation to the four co-expressed gene clusters potentially modulated in BMDMs, it is possible that MCMV may target a specific transcription factor in a similar manner, and achieve coordinate modulation of many downstream co-expressed genes. The possibility of M27 modulation of *Stat2* in BMDMs is currently being investigated using a M27 deletion mutant virus, and experiments are ongoing.

Identification of candidate MCMV proteins capable of modulating macrophage gene expression during productive infection

After identifying macrophages genes potentially modulated by productive MCMV infection, an attempt was made to find which viral proteins might be responsible. This objective was always challenging given more than 170 ORFs are encoded in the MCMV genome, many of which have no annotation. The first step in this process was to identify MCMV ORFs expressed to high confidence levels in BMDMs at 12hpi. This was done using a custom MCMV gene expression microarray with probes designed against coding MCMV ORFs. Although this exercise was valuable in narrowing down the number of potential ORFs responsible, it was also subject to limitations associated with the sensitivity and specificity of the MCMV microarray. The variation in probe efficiency and arbitrary cut-off used to determine detection thresholds meant there was a high possibility of false negatives (i.e. MCMV ORFs expressed in the infected cell but not detected by the microarray). The MCMV microarray analysis did, however, effectively rule out a number of candidate ORFs from the analysis (Table 5.2).

Next, three large-scale MCMV deletion mutants were used to screen the MCMV genome for deleted regions that were rich in immune-evasion genes (Table 5.3). This approach was promising in principle, but the ORF responsible for the suppression of marker genes *Tlr9* and *Sectm1a* was not found within any of the deleted regions (Figure 5.8). The final combined analysis left 42 remaining MCMV ORFs as potential candidates for the macrophage immune-modulation phenotype, excluding structural, virion-associated or tegument proteins (Table 5.4).

Although the approach undertaken to identify the MCMV ORF responsible for the immune-modulation was somewhat informative, it was also flawed for a number of reasons. Firstly, it did not account for the fact that multiple MCMV ORFs could target macrophage transcriptional networks simultaneously, rather than just a single ORF. The capacity for functional redundancy within the MCMV genome is substantial given its size, and it is also possible that different MCMV ORFs target the

four different networks individually. In this case, a single marker gene approach may not be valid. There is also the possibility that small non-coding RNAs, such as miRNAs were responsible for the phenotype, rather than a protein-coding MCMV ORF. This in fact, is quite possible given the important role of miRNAs during MCMV infection(46, 47, 84, 85, 321).

For the reasons outlined above, the investigation to identify the MCMV ORF responsible was deemed beyond the scope of the study. Ideally, a siRNA library would have been designed against all the remaining 42 MCMV ORFs, or indeed against the whole MCMV genome, and used to screen for the suppression of *Tlr9*. A siRNA screening approach, in this case, would be more systematic and tractable to identify candidate ORFs, however, was not possible due to the difficulty in transfecting primary BMDMs with siRNA without inducing apoptosis and/or the IFN response.

Overall, in this chapter, macrophage gene expression networks were identified as potentially modulated by MCMV during productive infection. The mutant MCMVdie3 strain was again valuable in making this process possible. Some new aspects of macrophage biology may have been identified in relation to MCMV immune evasion at the gene expression level, however further experimentation will be required to confirm the significance of these findings. The complexity of the host/pathogen relationship has also been illustrated in this chapter, and some results suggest MCMV is capable of targeting macrophage genes with specificity. Furthermore, it was found that MCMV appears to target the *Tlr9* gene for suppression with particular specificity, potentially meaning MCMV suppresses the expression of its own pattern recognition receptor during productive macrophage infection.

In the next chapter, aspects of host regulatory control of the macrophage transcriptome will be investigated, particularly in relation to the role of type I IFN in regulating the macrophage antiviral response to productive and non-productive MCMV infection at the gene expression level.

Chapter 6
Interferon control of the macrophage transcriptome

Introduction

The type I IFN pathway plays a key role in regulating the macrophage antiviral response, and controls the downstream expression of hundreds of antiviral genes during innate immunity. In the previous two chapters, macrophage gene expression networks have been identified representing different aspects of the macrophage response to productive and non-productive MCMV infection. The main objective of this chapter will be to determine the relative contribution of the type I IFN receptor in regulating each of these networks at the gene expression level. This will be done through transcriptional profiling of BMDMs derived from knockout mice lacking the *Ifnar1* gene.

The second objective of the chapter will be to conduct an exploratory analysis of gene expression in IFN-deficient BMDMs. This will involve use of BMDMs from from mice lacking the type I IFN receptor (*Ifnar1-/-*) and mice lacking the IFNβ gene (*Ifnb1-/-*), in comparison to wild-type BMDMs. Macrophages will be infected in parallel with productive and non-productive MCMV, or stimulated with polyIC, a the synthetic dsRNA inducer of type I IFN(242). Temporal gene expression profiling of the transcriptional responses to these stimuli will be performed, followed by a clustering analysis of the microarray data. This analysis will provide an insight into the kinetic regulation of IFN-dependent and IFN-independent gene expression during the macrophage antiviral response.

Although gene expression profiling analyses of the LPS response in *Ifnb1-/-* macrophages(355) and the response to Listeria monocytogenes in *Ifnar1-/-* macrophages(210) has been conducted previously, the analysis presented here will provide the first account of macrophage temporal gene expression in response to virus infection in both *Ifnb1-/-* and *Ifnar1-/-* BMDMs.

Results

6.1 Experimental design

To conduct a system-level temporal analysis of the macrophage innate immune response to productive and non-productive MCMV infection in wild type and IFN-deficient macrophages, BMDMs were cultured in parallel from wild type mice (WT) and mice lacking either the IFNβ (*Ifnb1-/-*) or type I IFN receptor (*Ifnar1-/-*) gene. All mice were the same genetic background (C57BL/6), male and aged 10-12 weeks. On day 7, triplicate BMDM monolayers were either mock infected, infected with MCMV, infected with MCMVdie3, or stimulated with 10ug/ml synthetic polyinosinic-polycytidylic acid potassium salt (polyIC). Cell culture supernatants, total RNA samples, and whole cell lysates were harvested in triplicate every two hours between 0-10hpi and at 24hpi (for experimental overview see Figure 6.1). 0hpi corresponds to the end of the 1.5 hour viral adsorption period.

Figure 6.1 Experimental overview Bone-marrow progenitor cells from male wild-type, *Ifnb1-/-* or *Ifnar1-/-* C57BL/6 mice were flushed from mouse femurs and differentiated in parallel for seven days using conditioned medium containing M-CSF1. Confluent BMDM monolayers were infected on day 7 with MCMV or MCMVdie3 at MOI 1 pfu/cell, or stimulated with 10ug/ml polyIC. Triplicate cell culture supernatants, cell lysates and total RNA samples were harvested every two hours between 0-12hi and at 24 hpi.

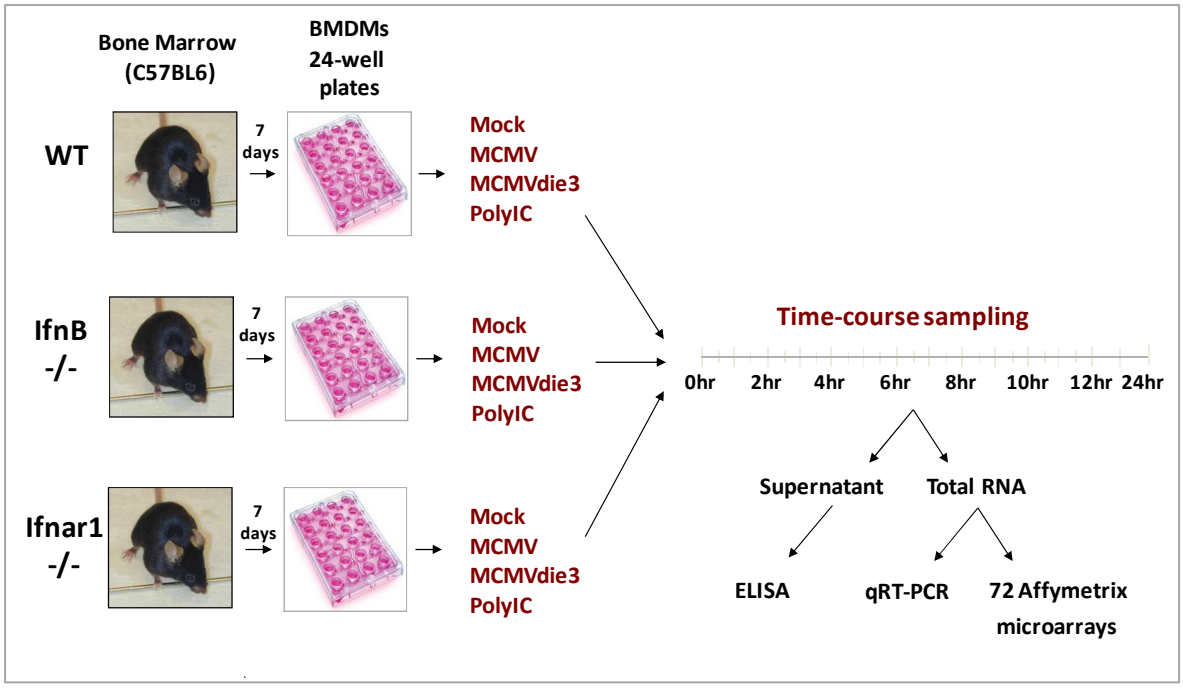

6.2 Microarray data processing and preliminary analysis

Total RNA samples were harvested for each condition/cell type at 0, 2, 4, 6, 8, 10 and 24hpi and hybridized to Affymetrix Mouse Gene 1.0ST arrays. A total of 72 samples were hybridized with mock-infected samples taken at 0hpi and 24hpi for each cell type. An additional three MCMV-infected samples at -1 hpi (within the adsorption period) were also hybridized to complete the 72 sample data set.

Quality control and normalization of raw microarray data was performed using standard Affymetrix analysis methodologies (see Methods section 2.7.2.3). A total of 35,556 probes on the array were filtered based on their maximum expression level across the data set. The threshold of detection used for filtering genes was set 150 (antilog), slightly above the threshold used for previous analyses. This was to ensure only high-confidence genes would be included in the final analysis. The value of 150 corresponded to roughly the mean of all negative control probes plus three standard deviations. 19,118 probes had intensities above the detection threshold (above 150 in one or more samples across the data set) and were deemed 'expressed'. The list of 19,118 probes was further reduced to 13,244 annotated mouse genes by removing control probes and un-annotated probes.

6.2.1 Expression of control probes and housekeeping genes in wild type, *Ifnb1-/- and Ifnar1-/-* BMDMs

The first step before proceeding to downstream microarray data analysis was to verify basal levels of gene expression in the different samples were equivalent between wild-type, *Ifnb1-/- and Ifnar1-/-* BMDMs. To do this, a cross-correlation matrix was generated based on 157 Affymetrix control probes. The Affymetirx controls consist of negative control probes designed again non-mouse genes, and positive controls probes designed against mouse genes (for complete list of control probes see Supplementary File 14). The control probes were used to generate a measure of sample-to-sample correlation between the 72 samples in the data set. A cross-correlation matrix plot is generated indicating the level of similarity for each

sample-to-sample comparison based on the 157 control probes. Pearson correlation is used to determine the rate of correlation between any two given samples. As seen in Figure 6.2, all samples within the data set were correlated to a high level (Pearson>0.934), indicating the expression of the 157 control probes was equivalent across all 72 samples. The level of correlation was particularly high between *Ifnb1-/-* and *Ifnar1-/-* samples (Pearson>98).

Figure 6.2 - Sample-to-sample cross-correlation plot based 157 Affymetrix control probes. Correlation between 72 microarray samples was performed using Pearson correlation on sample-to-sample comparisons based on 157 Affymetrix control probes. Each square represents an individual sample-to-sample comparison and increasing intensity of colour represents a higher degree of correlation.

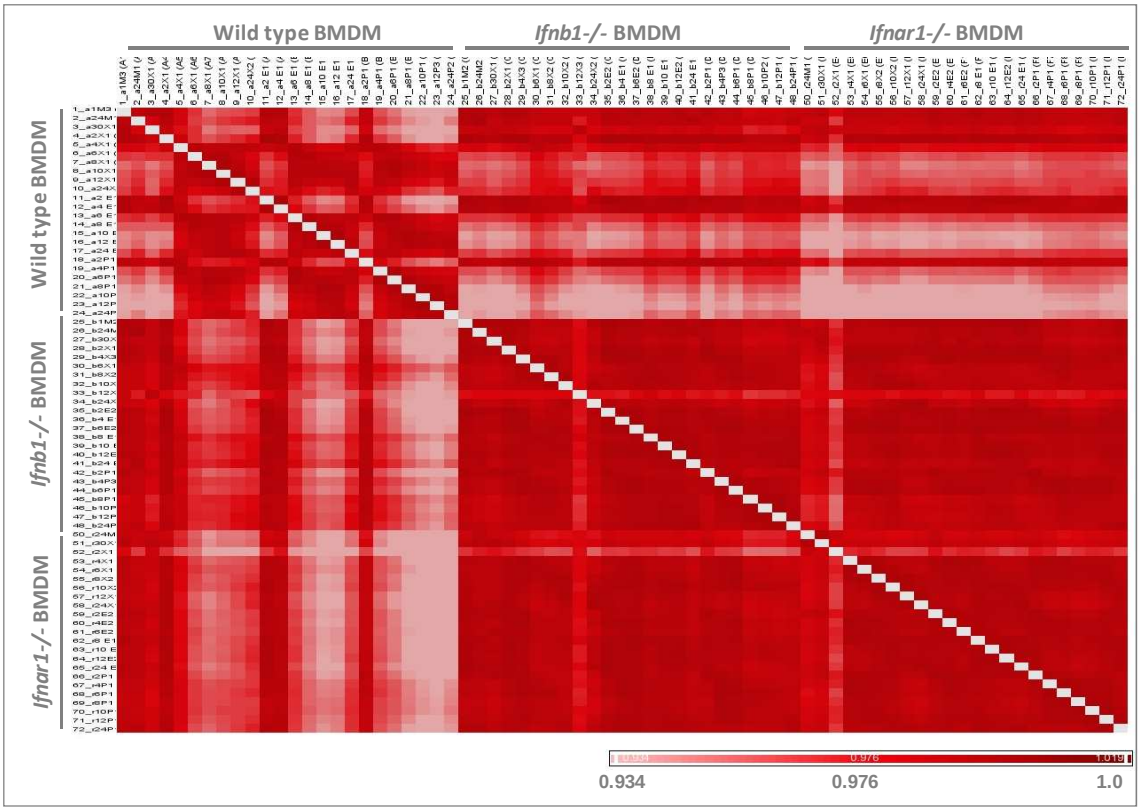

The cross-correlation matrix indicates 157 Affymetrix control probes were expressed to equivalent levels and highly correlated amongst all samples in the data set. This suggests array performance was consistent, and there were no outlier samples. It also suggests the basal level of transcription occurring in wild type, *Ifnb1-/-* and *Ifnar1-/-* BMDMs, based on the 157 control probes, was equivalent.

Next, in order to check the expression of individual housekeeping genes (i.e genes required for maintenance of basal cellular function), three commonly used housekeeping genes; Beta actin (*Actb*), glyceraldehyde 3-phosphate dehydrogenase (*Gapdh*) and lactate dehydrogenase A (*Ldha*) were assessed. These genes were found to be expressed stably and consistently in wild type, *Ifnb1-/-* and *Ifnar1-/-* BMDMs (Figure 6.3), indicating transcription of housekeeping genes was comparable across wild type and IFN-deficient BMDMs.

Figure 6.3 Housekeeping genes are expressed to equivalent levels in wild type, *Ifnb1-/-* and *Ifnar1-/-* macrophages. The expression profiles of *Actb* (**a**), *Gapdh* (**b**), and *Ldha* (**c**) are shown with normalized microarray intensity on the Y axis. Samples are arranged in temporal order on the X axis. The 0hpi time point represents the end of the 1.5 hour viral adsorption period.

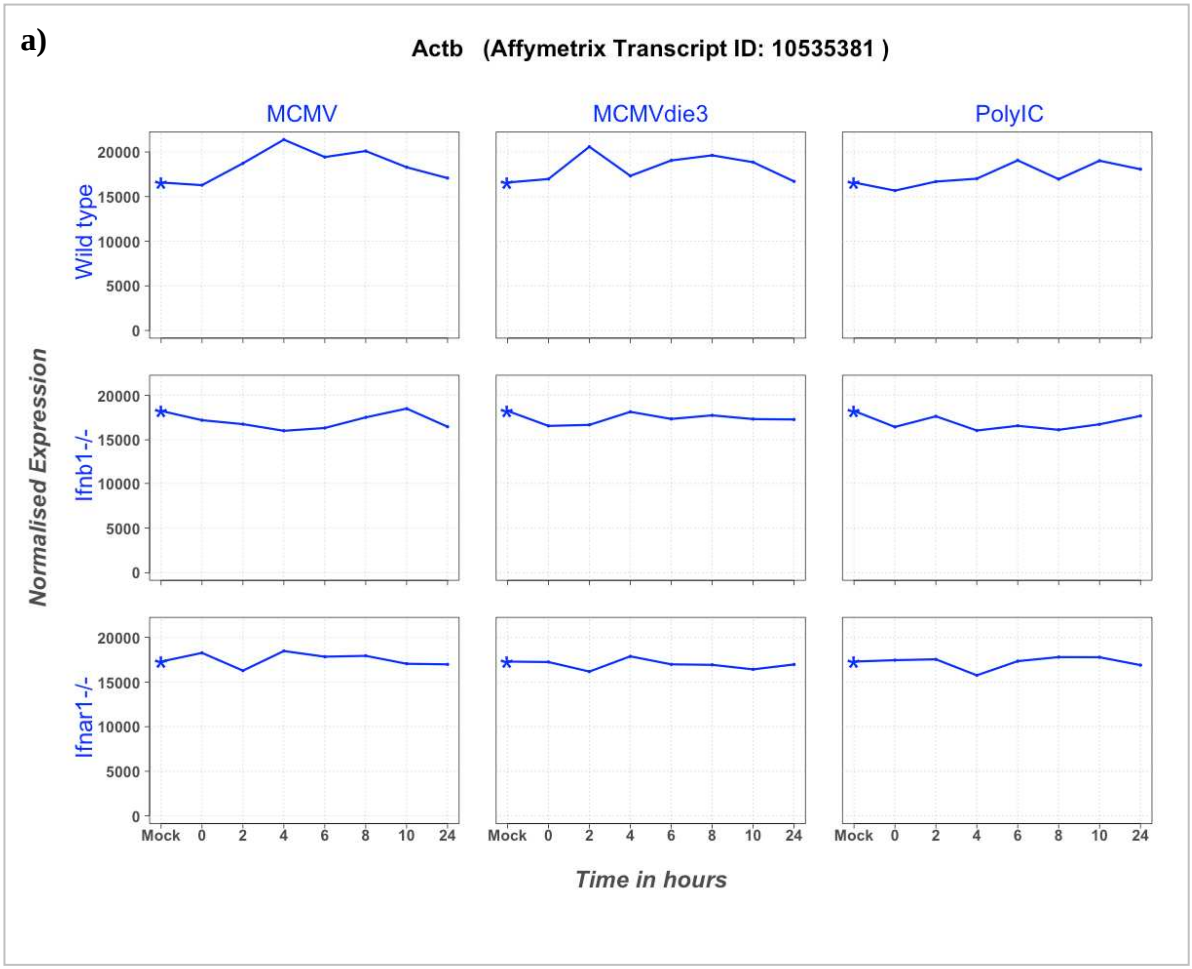

b)

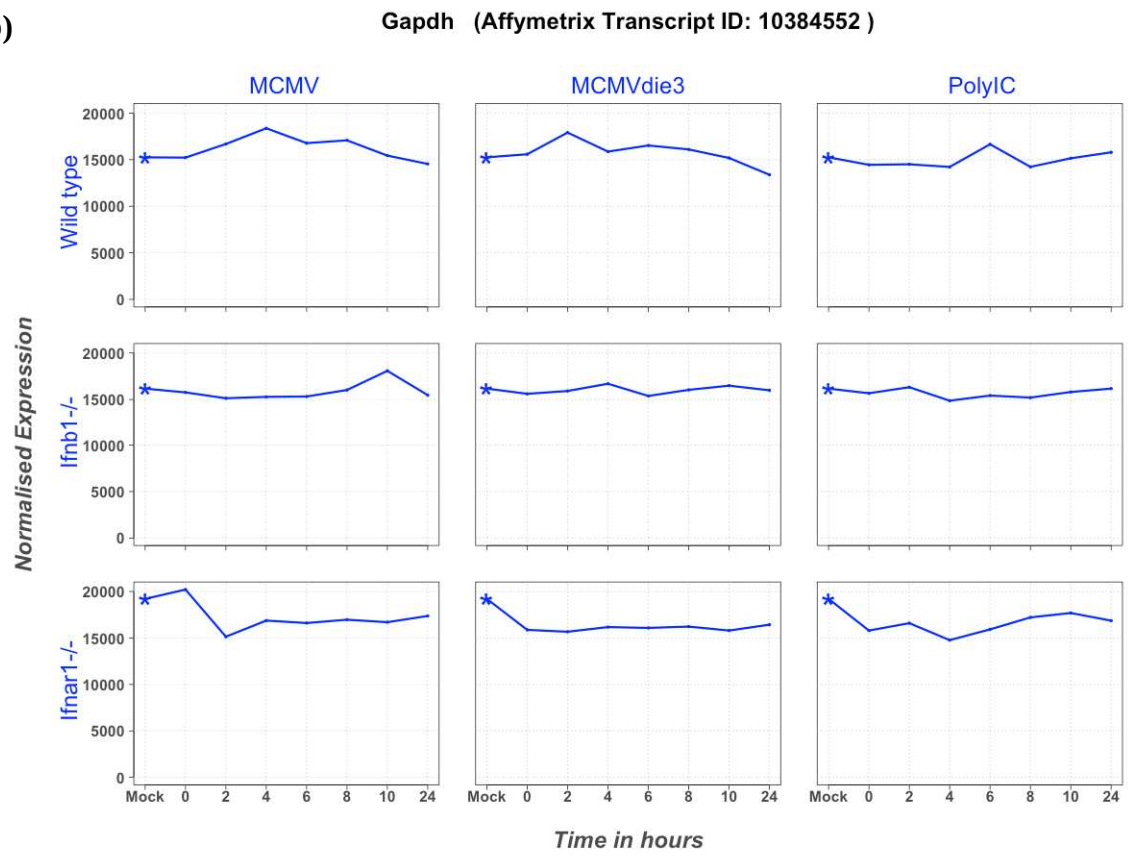
Gapdh (Affymetrix Transcript ID: 10384552)
MCMV
MCMVdie3
PolyIC
Wild type
Ifnb1-/-
Ifnar1-/-
Normalised Expression
20000
15000
10000
5000
0
Mock 0 2 4 6 8 10 24
Time in hours

c)

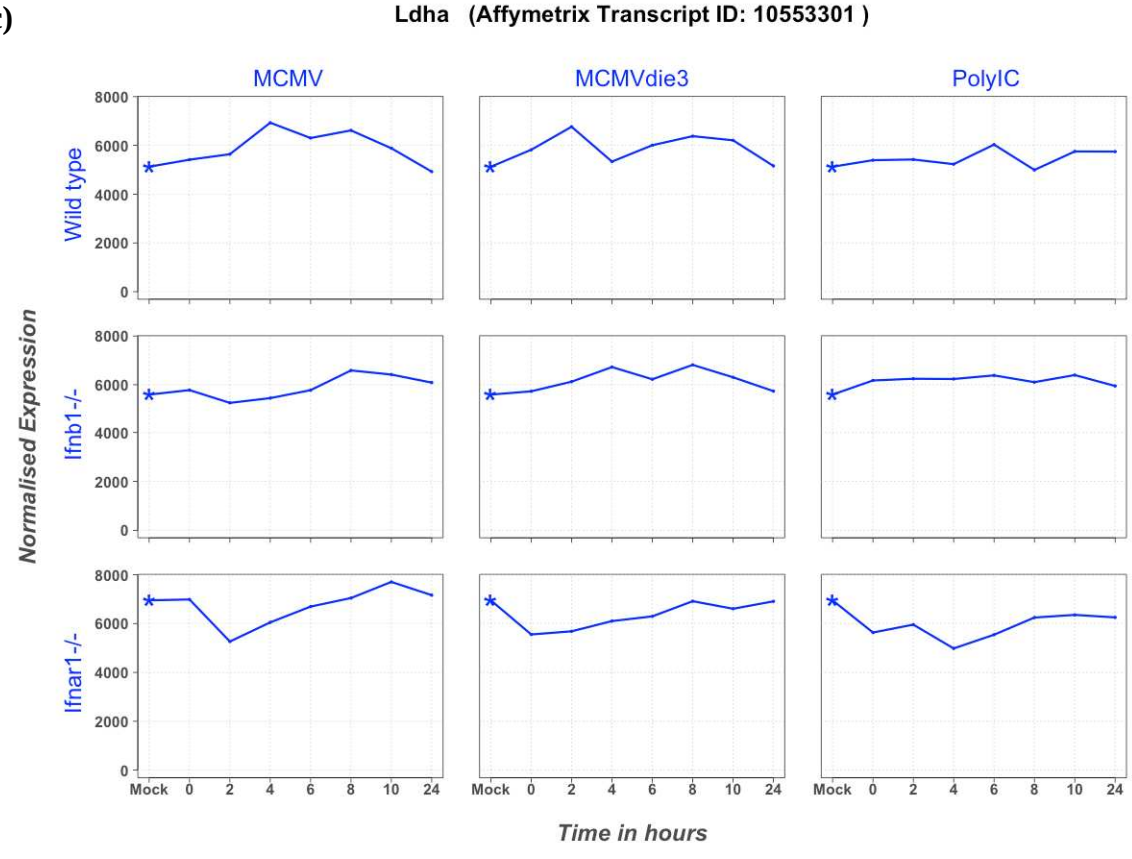
Ldha (Affymetrix Transcript ID: 10553301)
MCMV
MCMVdie3
PolyIC
Wild type
Ifnb1-/-
Ifnar1-/-
Normalised Expression
8000
6000
4000
2000
0
Mock 0 2 4 6 8 10 24
Time in hours

The next step was to assess the levels of basal endogenous type I IFN signalling in wild type versus *Ifnar1-/-* BMDMs. Deficiency in basal type I IFN signalling, both at the level of ISG expression and STAT1 phosphorylation, have been reported previously for *Ifnar1-/-* BMDMs compared to wild type (97). Fleetwood *et al* showed that basal expression of ISGs (i.e. *Mx1, Mx2, Ifi203, Ccl5, Stat1, Stat2, Socs1* and *Tlr3*) was significantly higher in wild-type BMDMs compared to *Ifnar1-/-* due higher STAT1 phosphorylation and higher basal endogenous type I IFN expression. To determine if this was also the case in the current study using MCMV, expression levels of ISGs were compared in mock-infected wild type and *Ifnar1-/-* BMDMs at basal levels (Table 6.1) . Consistent with the Fleetwood *et al* study (97), the expression of a number of key ISGs was considerably higher in wild-type BMDMs than in *Ifnar1-/-* at basal levels. This included *Oas1a, Oas2, Ifit1, Ifit3, Irf7, Mx1, Gbp2* and *Stat1* which were all expressed two-fold or higher in wild-type BMDMs than in *Ifnar1-/-* (Table 6.1). This finding indicated the level of endogenous type I IFN signalling in wild type BMDM cultures was considerably higher than in *Ifnar1-/-* BMDMs, an observation which was taken into consideration for the interpretation of all further data from this experiment.

Table 6.1 - Genes expressed to higher levels in wild type BMDMs compared to *Ifnar1-/-* BMDMs (top 25 by fold change)

Transcript ID	Gene Symbol	WT Mock	Ifnar1-/- Mock	Fold change Ifnar/WT	Gene_assignment
10434778	**Rtp4**	2276.34	33.655	67.64	receptor transporter protein 4
10524621	**Oasl2**	2432.63	55.0992	44.15	2'-5' oligoadenylate synthetase-like 2
10533198	**Oas2**	1700.09	50.9889	33.34	2'-5' oligoadenylate synthetase 2
10533246	**Oas1g**	1350.52	51.5578	26.19	2'-5' oligoadenylate synthetase 1G
10462618	**Ifit3**	1558.78	59.7945	26.07	interferon-induced protein with tetratricopeptide repeats
10462623	**Ifit1**	1047.62	43.982	23.82	interferon-induced protein with tetratricopeptide repeats
10533256	**Oas1a**	688.952	29.6007	23.27	2'-5' oligoadenylate synthetase 1A
10379615	**Slfn5**	1200.32	52.0819	23.05	schlafen 5
10399710	**Rsad2**	967.367	55.6612	17.38	radical S-adenosyl methionine domain containing 2
10541307	**Usp18**	785.061	46.0682	17.04	ubiquitin specific peptidase 18
10533213	**Oas3**	947.919	68.261	13.89	2'-5' oligoadenylate synthetase 3
10351873	**Pyhin1**	852.603	67.7622	12.58	pyrin and HIN domain family, member 1
10569102	**Irf7**	969.818	94.8496	10.22	interferon regulatory factor 7
10376324	**Gm12250**	374.562	39.8051	9.41	predicted gene 12250
10402347	**Ifi27l2a**	1848.07	199.737	9.25	interferon, alpha-inducible protein 27 like 2A
10455954	**Gm4951**	459.809	59.6455	7.71	predicted gene 4951
10467979	**Scd1**	738.094	99.0497	7.45	stearoyl-Coenzyme A desaturase 1
10360382	**Ifi204**	3045.58	444.128	6.86	interferon activated gene 204
10378068	**Xaf1**	610.539	103.433	5.90	XIAP associated factor 1
10395039	**Cmpk2**	250.572	42.9269	5.84	cytidine monophosphate (UMP-CMP) kinase 2, mitochondrial
10450675	**H2-T24**	631.623	109.148	5.79	histocompatibility 2, T region locus 24
10389143	**Slfn8**	977.722	169.253	5.78	schlafen 8
10496592	**Gbp2**	632.635	110.125	5.74	guanylate binding protein 2
10441233	**Mx1**	260.413	45.3525	5.74	myxovirus (influenza virus) resistance 1

6.2.2 Induction of innate immune response genes in *Ifnb1-/-* and *Ifnar1-/-* BMDMs

To determine if the *Ifnb1-/-* and *Ifnar1-/-* BMDMs were still capable of inducing the innate immune response following the three treatments, *Tnf* transcript levels were assessed across the data set. *Tnf* is an IFN-independent innate immune response gene activated upon viral infection(92). *Tnf* was up-regulated to equivalent levels in wild-type, *Ifnb1-/-* and *Ifnar1-/-* BMDMs, however expression was sustained for a longer period in wild-type BMDMs. This indicated that IFN-deficient BMDMs were still capable of mounting an innate immune response to virus infection at the gene expression level (Figure 6.4). *Icam1* (intercellular adhesion molecule 1) was also up-regulated in all three treatments independently of IFN and provided further evidence of an intact IFN-independent innate immune response in *Ifnb1-/-* and *Ifnar1-/-* BMDMs at the gene expression level.

Figure 6.4 - *Tnf and Icam1* are induced *in Ifnb1-/-* and *Ifnar1-/-* BMDMs in response to MCMV, MCMVdie3 and polyIC. The expression profiles of *Tnf* (**a**) and *Icam1* (**b**)) are shown with normalized microarray intensity on the Y axis. Individual samples are arranged in temporal order on the X axis. The 0hpi time point represents the end of the 1.5 hour viral adsorption period.

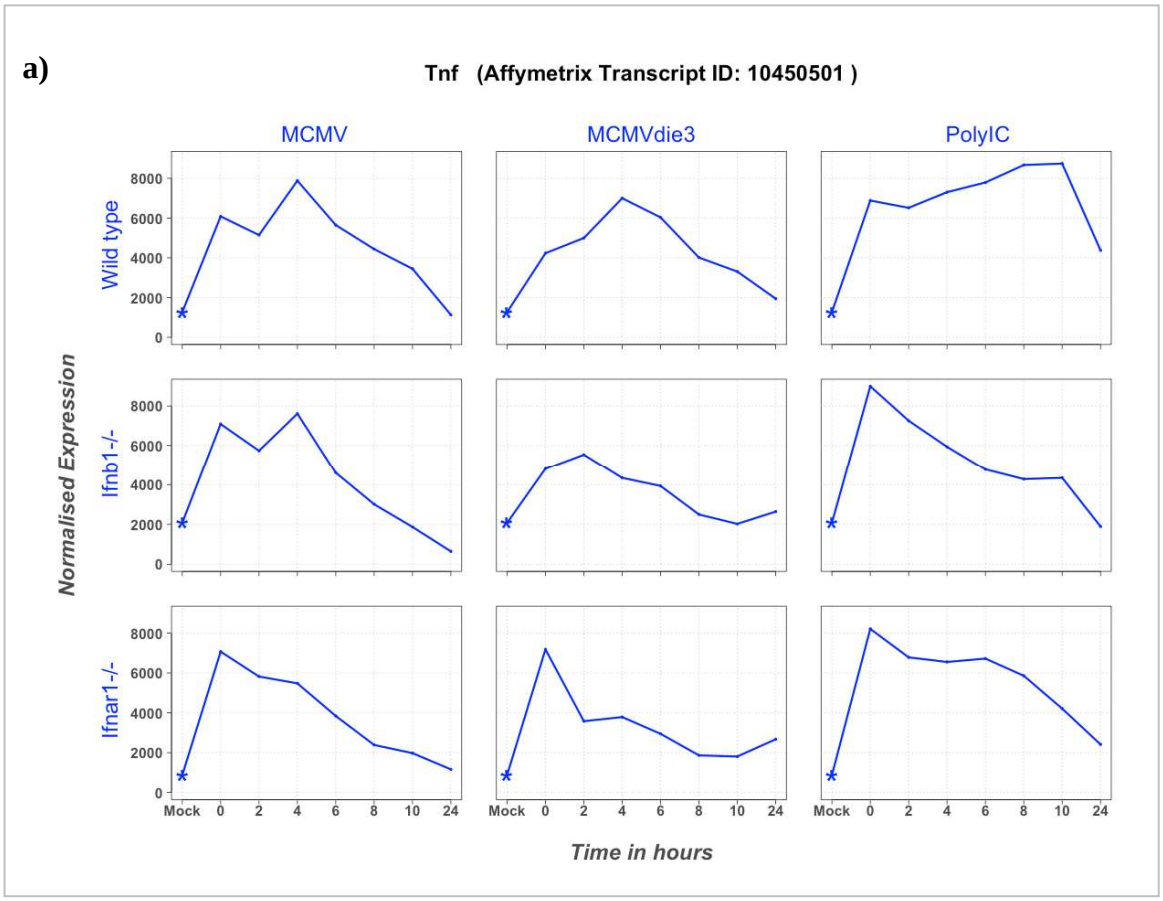

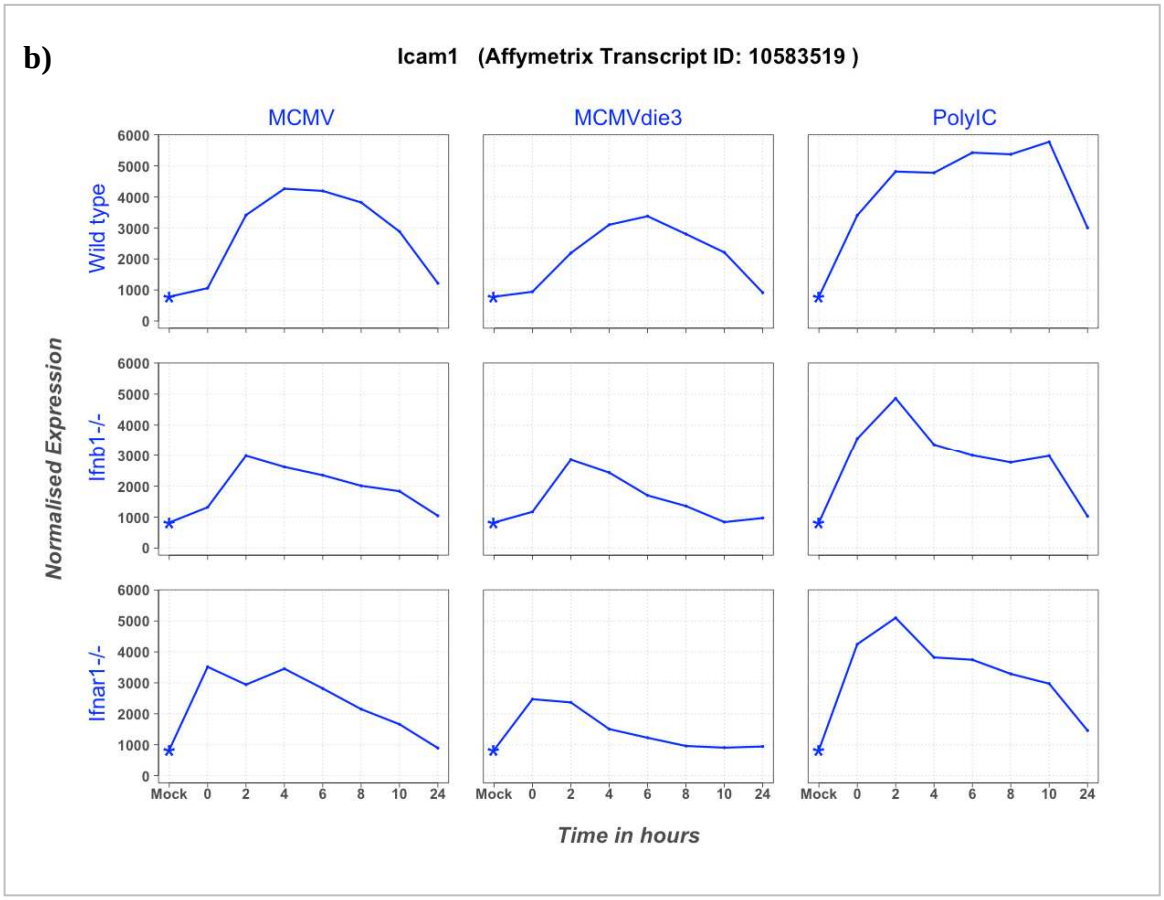

6.2.3 Expression of type I IFNs

Next, IFNβ (*Ifnb1*) transcript levels were assessed across the dataset in response to the three stimuli (Figure 6.5). As expected, no *Ifnb1* expression was detectable from *Ifnb1-/-* BMDMs. In wild-type BMDMs *Ifnb1* was induced in response to all three stimuli (MCMV, MCMVdie3 and polyIC). In agreement with the published literature(242), the synthetic ligand polyIC was found to be a potent and rapid inducer of IFNβ, and induced *Ifnb1* transcripts over two-fold higher than MCMV infection at 0hpi. The transcriptional induction of IFNβ was diminished in response to MCMVdie3 compared to MCMV in wild-type BMDMs. Low levels of *Ifnb1* just above the limit of detection were observed in BMDMs lacking the type I IFN receptor (*Ifnar1-/-*) in response to MCMV and polyIC. The attenuated *Ifnb1* levels in *Ifnar1-/-* BMDMs was further evidence of a lower level of basal endogenous type I

IFN signalling in *Ifnar1-/-* BMDM cultures, and evidence for an absence of the type I IFN positive feedback loop.

Figure 6.5 - Expression profile of *Ifnb1* in response to MCMV, MCMVdie3 and polyIC in wild type, *Ifnb1-/-* and *Ifnar1-/-* macrophages. The expression profile of *Ifnb1* is shown with normalized microarray intensity on the Y axis. Individual samples are arranged in temporal order on the X axis. The 0hpi time point represents the end of the 1.5 hour viral adsorption period.

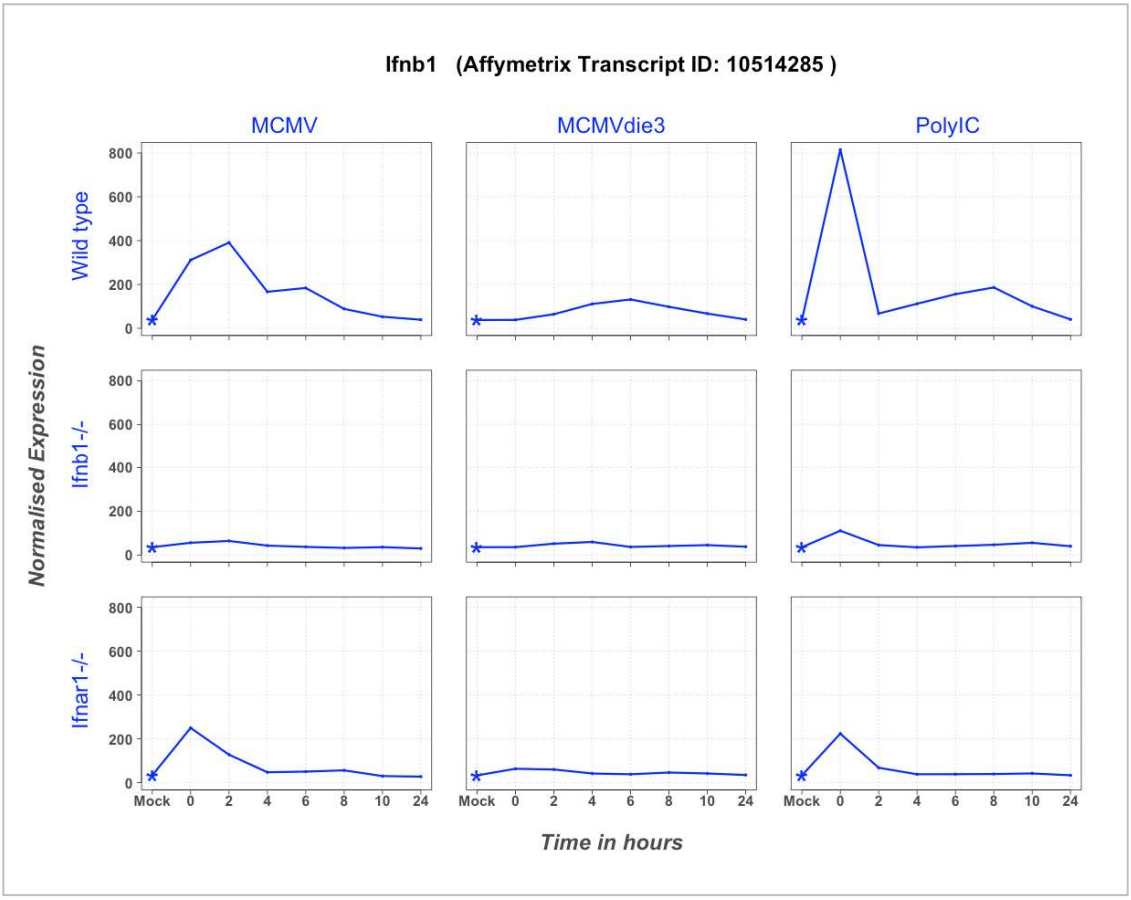

To further investigate the role of *Ifnb1* and *Ifnar1* in the regulation of other type I IFNs, the expression levels for other type I IFNs on the array (other than *Ifnb1)* were assessed. The type I IFNs (other than *Ifnb1*) expressed above the limit of detection on the array were *Ifna1*, *Ifna2*, *Ifna5* and *Ifna7*. Interestingly, none of these genes were found to be induced in *Ifnb1-/-* or *Ifnar1-/-* BMDMs, despite strong induction by MCMV and polyIC in wild type cells (Figure 6.6). This result also indicates the attenuated capacity for type I IFN signalling in *Ifnb1-/-* and *Ifnar1-/-* BMDMs.

Figure 6.6 - The transcriptional induction of IFNα genes (*Ifna1*, *Ifna2*, *Ifna5*, *Ifna7*) is dependent on IFNβ signalling. The expression profiles of *Ifna1* (**a**), *Ifna2* (**b**), *Ifna5* (**c**) and *Ifna7* (**d**) are shown with normalized microarray intensity on the Y axis. Individual samples are arranged in temporal order on the X axis. The 0hpi time point represents the end of the 1.5 hour viral adsorption period.

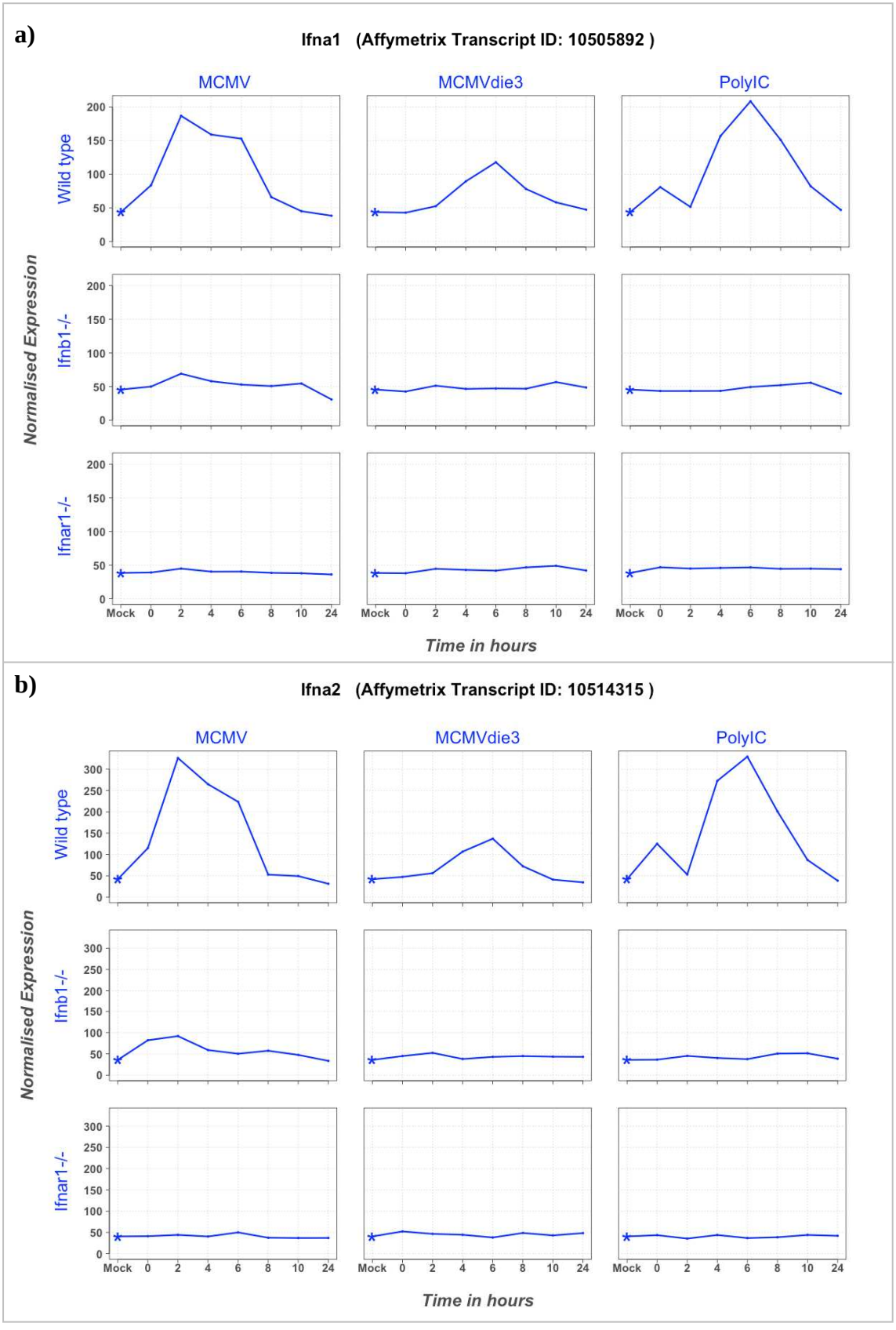

c)

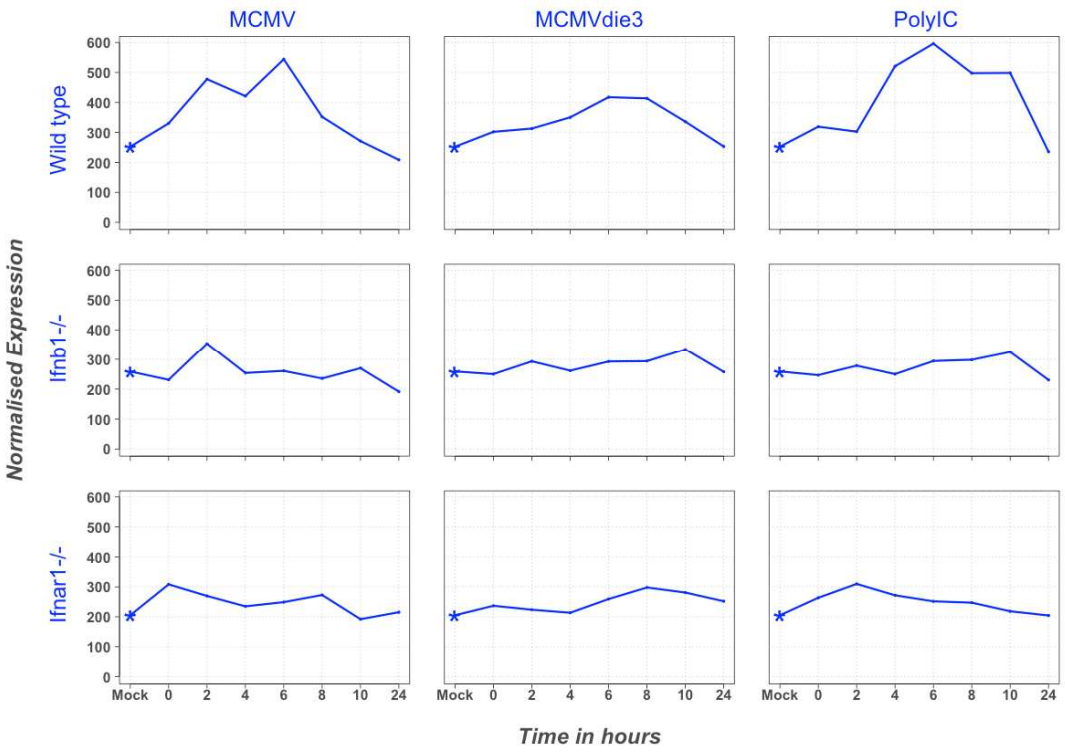
Ifna5 (Affymetrix Transcript ID: 10505888)
MCMV
MCMVdie3
PolyIC
Wild type
Ifnb1-/-
Ifnar1-/-
Normalised Expression
Mock 0 2 4 6 8 10 24
Time in hours

d)

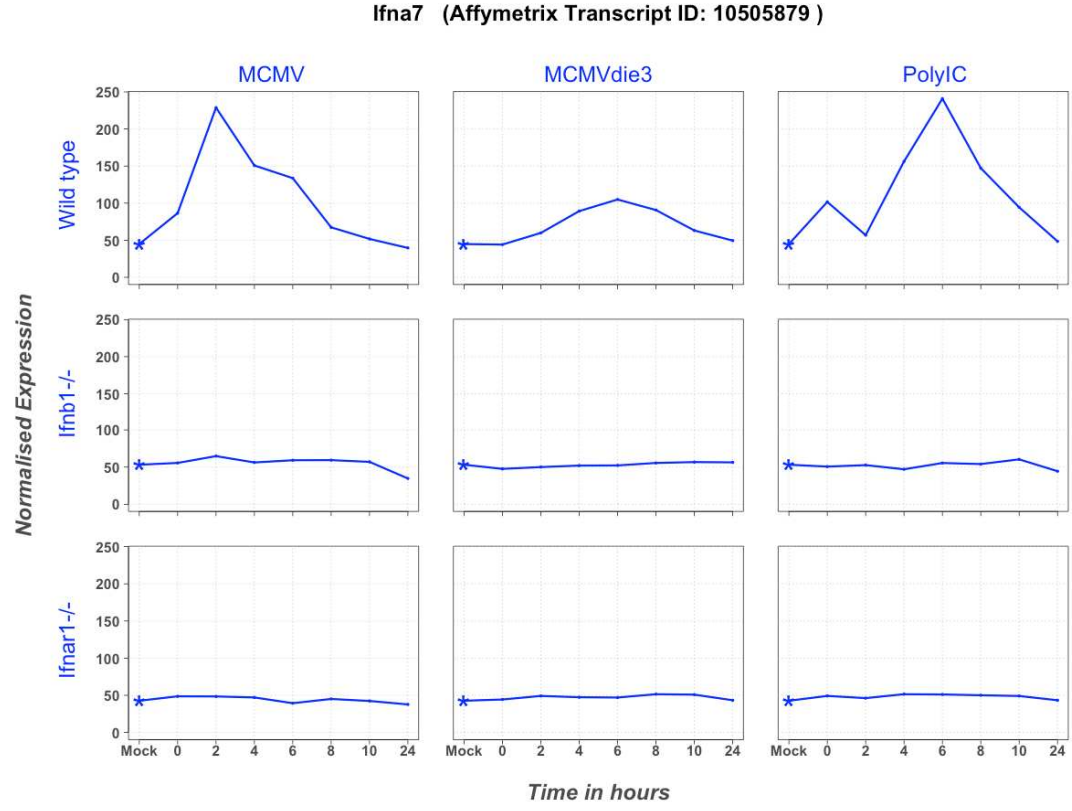
Ifna7 (Affymetrix Transcript ID: 10505879)
MCMV
MCMVdie3
PolyIC
Wild type
Ifnb1-/-
Ifnar1-/-
Normalised Expression
Mock 0 2 4 6 8 10 24
Time in hours

6.2.4 Expression of CMV pattern recognition receptors

The transcriptional regulation of pattern recognition receptor genes involved in detection of CMV was of general interest. Figure 6.7 shows the expression of *Tlr3*, *Tlr9*, *Zbp1* and *Aim2* in wild-type, *Ifnb1-/-* and *Ifnar1-/-* BMDMs. These genes are all inducible by MCMV infection and have a strong dependency on type I IFN receptor for their induction.

Figure 6.7 - Pattern recognition receptors involved in the detection of MCMV are regulated in an IFN-dependent manner. The expression profiles of *Tlr3* (**a**), *Tlr9* (**b**), *Zbp1* (**c**) and *Aim2* (**d**) are shown with normalized microarray intensity on the Y axis. Individual samples are arranged in temporal order on the X axis. The 0hpi time point represents the end of the 1.5 hour viral adsorption period.

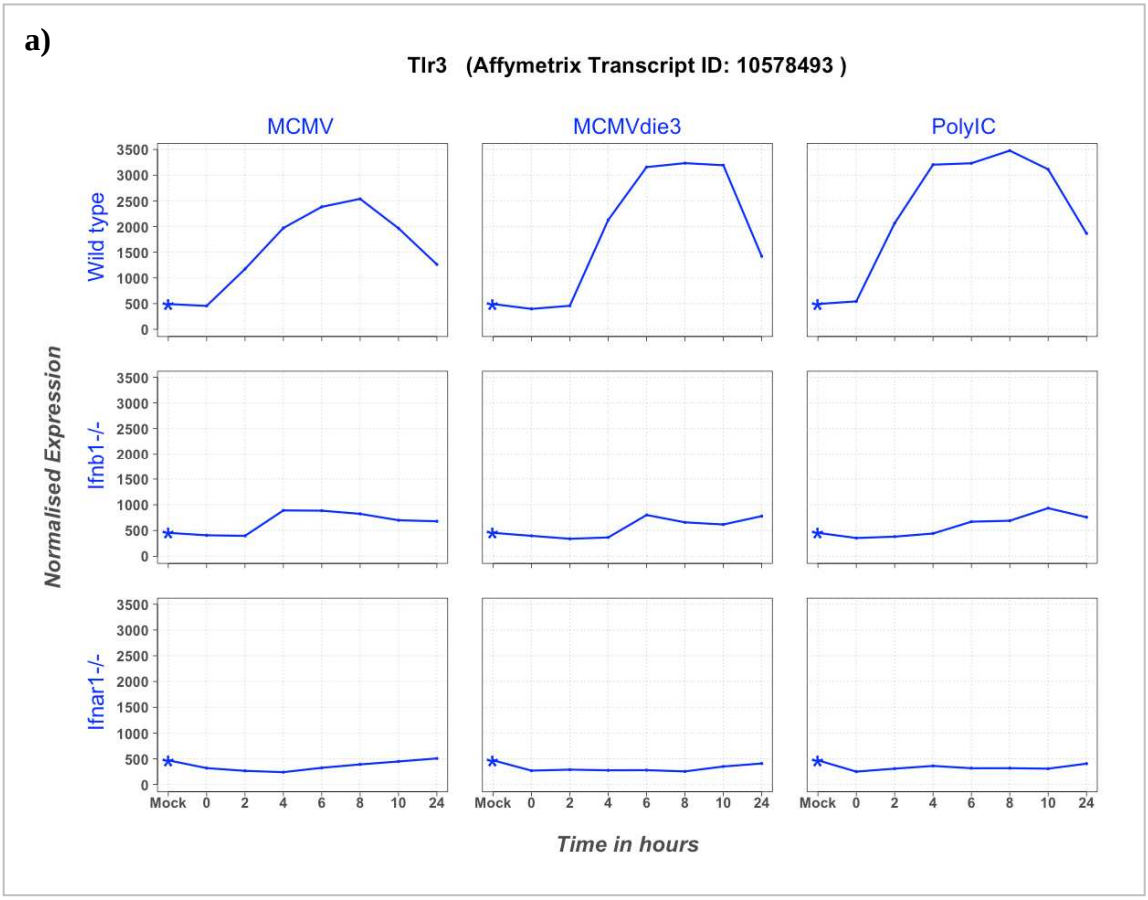

b)

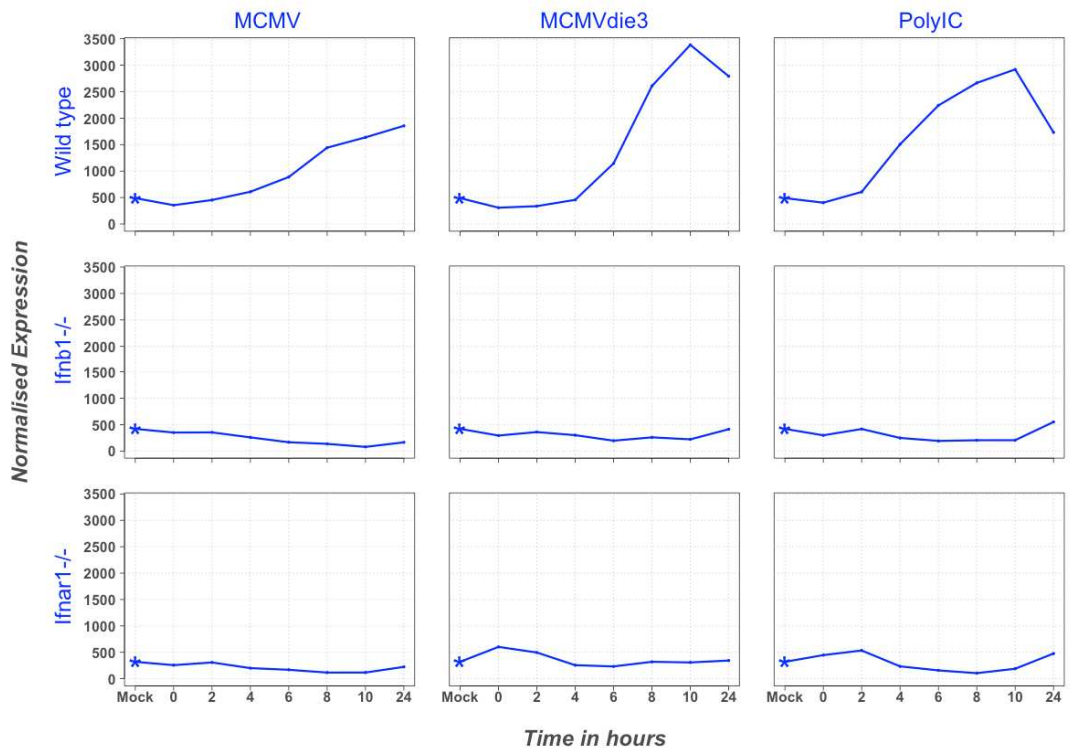
Tlr9 (Affymetrix Transcript ID: 10588479)
MCMV
MCMVdie3
PolyIC
Wild type
Ifnb1-/-
Ifnar1-/-
Normalised Expression
Time in hours
Mock 0 2 4 6 8 10 24

c)

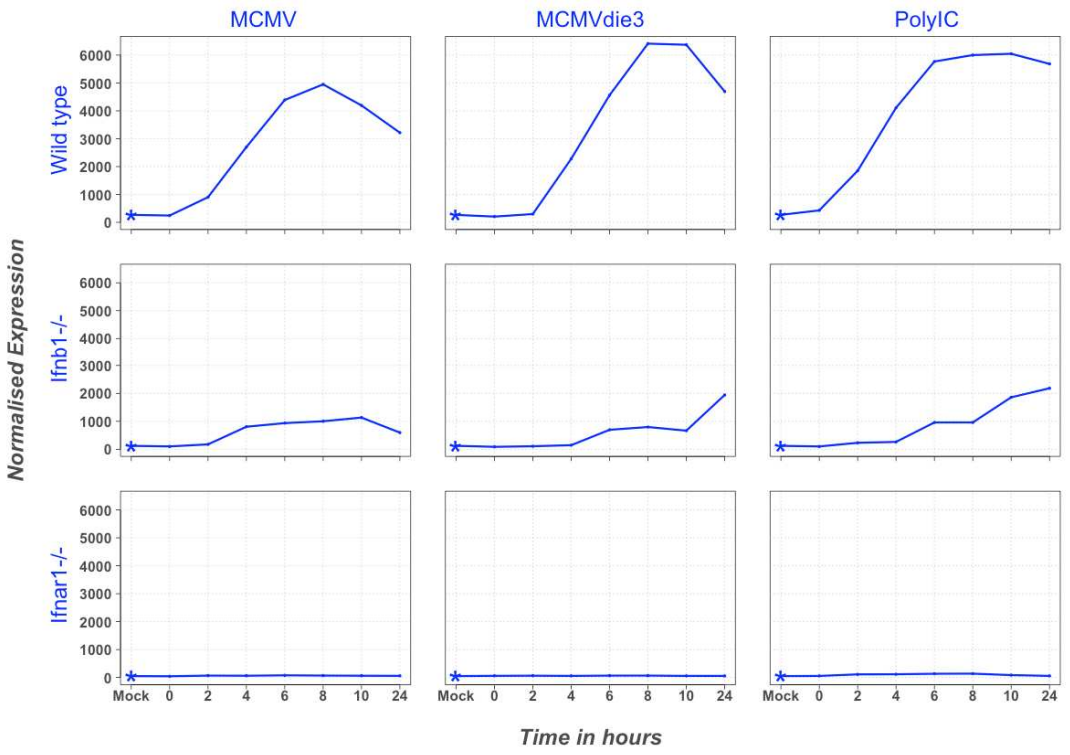
Zbp1 (Affymetrix Transcript ID: 10490150)
MCMV
MCMVdie3
PolyIC
Wild type
Ifnb1-/-
Ifnar1-/-
Normalised Expression
Time in hours
Mock 0 2 4 6 8 10 24

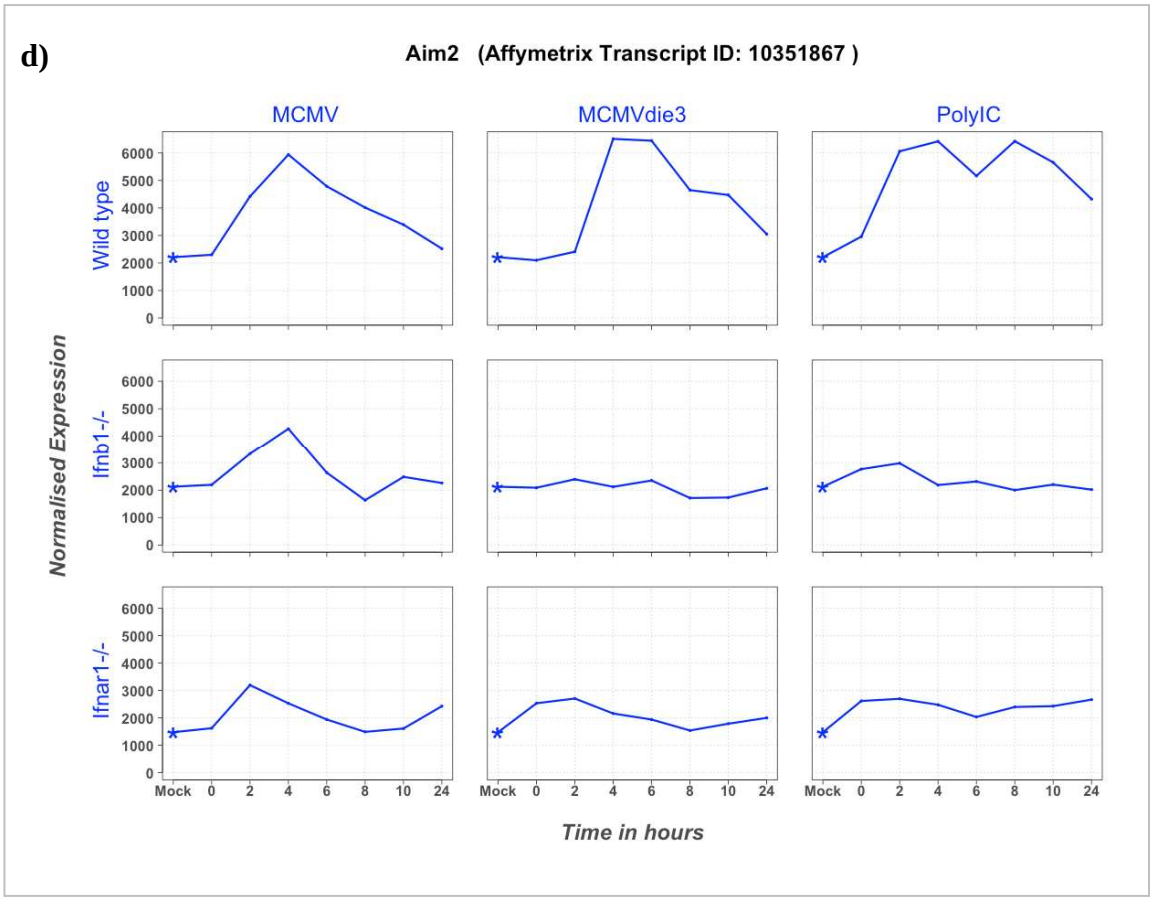
d)
Aim2 (Affymetrix Transcript ID: 10351867)
MCMV
MCMVdie3
PolyIC
Wild type
Ifnb1-/-
Ifnar1-/-
Normalised Expression
0
1000
2000
3000
4000
5000
6000
Mock
0
2
4
6
8
10
24
Time in hours

6.3 Focused analysis of previously identified macrophage gene expression networks in the presence and absence of type I IFN signalling

The main objective of this chapter is to determine the role of type I IFN in the regulation of macrophage gene expression networks identified in previous chapters. To do this, expression profiles in BMDMs derived from *Ifnar1-/-* mice were compared directly alongside wild-type BMDMs. In the data presented below, the *Ifnb1-/-* BMDMs and polyIC samples have been excluded from the analysis to simplify the interpretation and allow a straightforward comparison between wild-type and *Ifnar1-/-* BMDMs.

The networks of interest from previous chapters are summarized in Table 6.2. Genes from each of the networks were overlaid onto the new data set using unique Affymetrix probe IDs.

Table 6.2 - Previously identified macrophage gene expression networks

Chapter presented	Network description	No. of Genes	Predicted function and relationship to type I IFN
4	Genes up-regulated in response to MCMV and MCMVdie3	129	PRR response, non-specific, IFN-dependent?
4	Genes down-regulated in response to MCMV and MCMVdie3	362	Non-specific, down-regulation of cell cycle
4	Genes up-regulated specifically in response to productive MCMV infection at 24hpi	283	Antiviral? Proviral? Metabolic?
5	MCMV-modulated "*Cluster 1*" Up-regulated early, transient, Suppressed by productive MCMV	100	Antiviral? Specific to MCMV? partially IFN-dependent?
5	MCMV-modulated "*Cluster 2*" Up-regulated late, sustained Suppressed by productive MCMV	53	Antiviral? Specific to MCMV? partially IFN-dependent?
5	MCMV-modulated "*Cluster 3*" Down-regulated, partially blocked by productive MCMV	236	Antiviral? down-regulation of cell cycle, apoptosis-related, IFN-independent?
5	MCMV-modulated "*Cluster 4*" Down-regulated, completely blocked by productive MCMV	70	Antiviral? down-regulation of cell cycle, apoptosis-related, IFN-independent?

The expression of each network listed above will now be shown in wild-type and *Ifnar1-/-* BMDMs. The networks will be presented as heatmaps to show relative expression, and as mean expression profiles to show the average difference between the MCMV and MCMVdie3 conditions. The expression levels in wild-type BMDMs will provide independent validation of the previous microarray experiment, and the expression levels in *Ifnar1-/-* BMDMs will indicate if type I IFN contributes to regulation at the gene expression level.

6.3.1 Genes regulated in an equivalent manner in response to MCMV and MCMVdie3 infection

The first gene networks to be assessed for their expression in IFN-deficient BMDMs were those induced or suppressed in an equivalent manner in response to MCMV and MCMVdie3 infection (as presented in Chapter 4). These networks represent the initial macrophage response to incoming structural components of the MCMV virion, and are regulated equivalently in response to MCMV and MCMVdie3 infection. The networks consisted of 129 genes up-regulated in an equivalent manner, and 362 genes down-regulated in an equivalent manner. Figure 6.8 shows expression of the two networks in both wild type and *Ifnar1-/-* BMDMs.

Figure 6.8 - Expression of genes up-regulated and down-regulated in an equivalent manner in response to MCMV and MCMVdie3. (**i**) Heatmaps show the relative expression of genes in wild-type and *Ifnar1-/-* BMDMs with each gene represented by a row and per-gene normalized to its mean value to show relative expression. Yellow indicates an increase in expression relative to the mean and blue indicates a decrease. Genes are clustered based on similarity of expression profiles with similar genes connected at the hierarchical tree on the left. Columns represent different time points as indicated beneath the heatmap, and MCMV and MCMVdie3 conditions are separated. Wild-type and *Ifnar1-/-* cells are also shown separately. (**ii**) Mean expression profiles show the average expression level of the network in response to MCMV (light grey) and MCMVdie3 (dark grey) in both wild-type and *Ifnar1-/-* BMDMs.

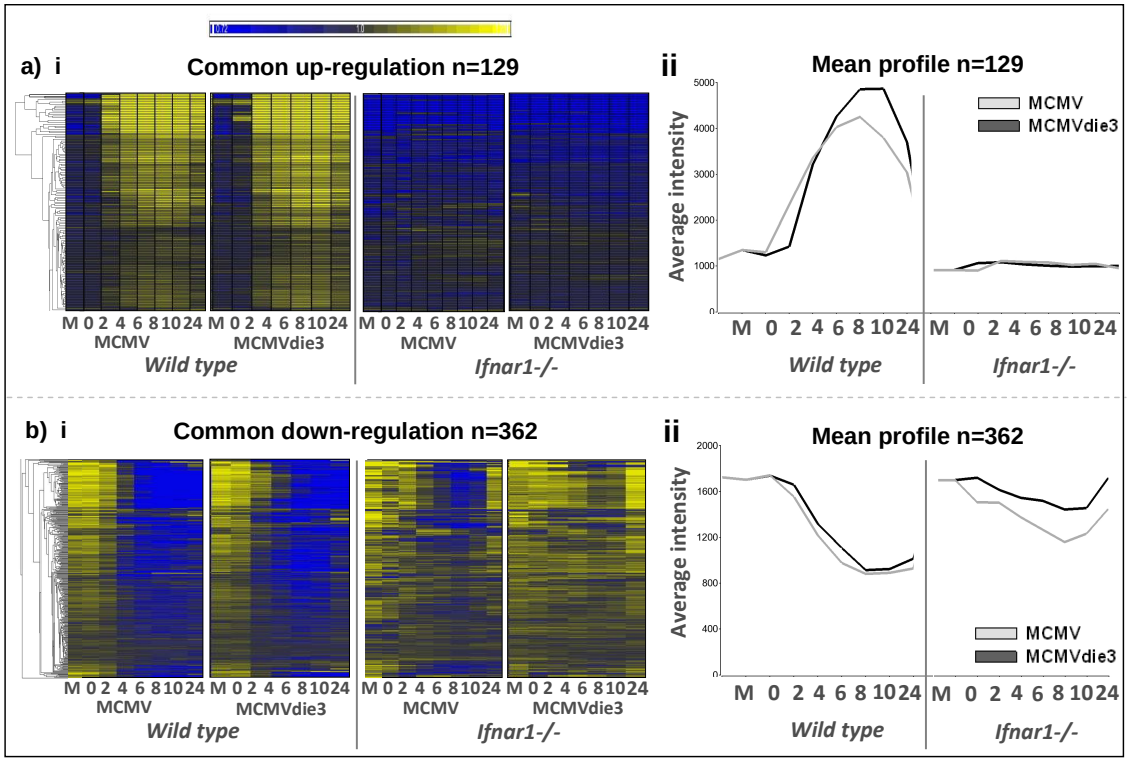

As shown in Figure 6.8a i, the up-regulation of this network of genes is completely dependent on the type I IFN receptor. This result indicates genes up-regulated in an equivalent manner by MCMV and MCMVdie3 are IFN-dependent. For the network down-regulated genes, a partial dependence on type I IFN receptor was observed

(Figure 6.8b). This suggests type I IFN contributes to the down-regulation of these genes in response to MCMV and MCMVdie3.

6.3.2 Genes differentially expressed between productive and non-productive MCMV infection

Next, the four clusters identified in Chapter 5 as potentially MCMV-modulated were assessed for their regulation by type I IFN (Figure 6.9). The objective of this analysis was to determine if MCMV was targeting IFN-dependent or IFN-independent genes for modulation during productive infection.

Figure 6.9 - Expression of gene networks modulated by productive MCMV infection. (**i**) Heatmaps show the relative expression of genes in wild-type and *Ifnar1-/-* BMDMs with each gene represented by a row and per-gene normalized to its mean value to show relative expression. Yellow indicates an increase in expression relative to the mean and blue indicates a decrease. Genes are clustered based on similarity of expression profiles with similar genes connected at the hierarchical tree on the left. Columns represent different time points as indicated beneath the heatmap, and MCMV and MCMVdie3 conditions are separated. Wild-type and *Ifnar1-/-* BMDMs are also shown separately. (**ii**) Mean expression profiles show the average expression level of the network in response to MCMV (light grey) and MCMVdie3 (dark grey) in both wild-type and *Ifnar1-/-* BMDMs. Red arrows emphasize the overall difference between MCMV and MCMVdie3.

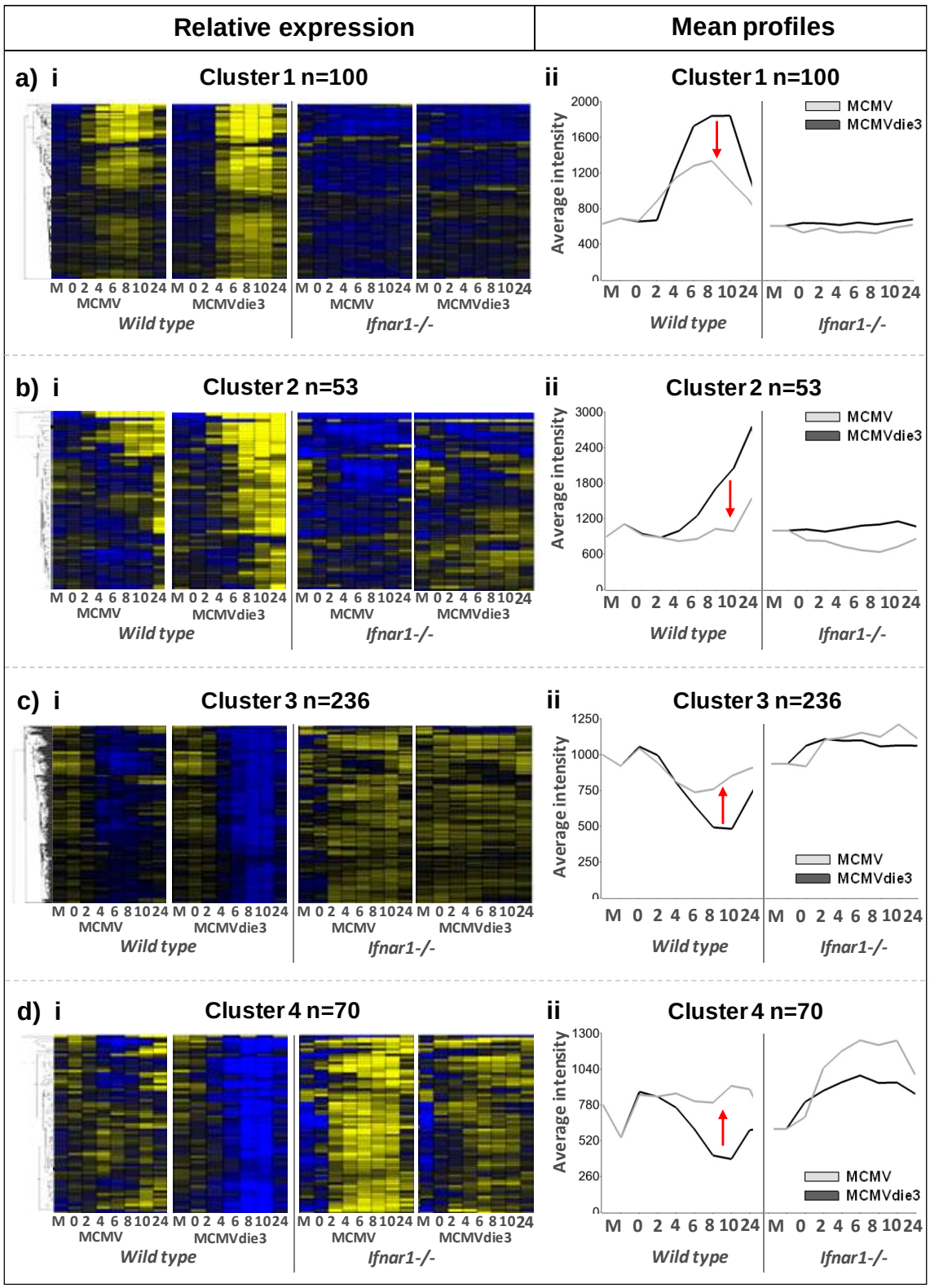
Relative expression
Mean profiles
a) i
Cluster 1 n=100
ii
Cluster 1 n=100
M 0 2 4 6 8 10 24
MCMV
MCMVdie3
Wild type
Ifnar1-/-
Average intensity
2000
1600
1200
800
400
0
MCMV
MCMVdie3
b) i
Cluster 2 n=53
ii
Cluster 2 n=53
3000
2400
1800
1200
600
0
c) i
Cluster 3 n=236
ii
Cluster 3 n=236
1250
1000
750
500
250
0
d) i
Cluster 4 n=70
ii
Cluster 4 n=70
1300
1040
780
520
260
0

As shown in Figure 6.9a, Cluster 1 was again induced by both MCMV strains in wild-type BMDMs, but expressed to lower level in response to productive MCMV infection, relative to MCMVdie3. Strikingly, the induction of almost every gene in Cluster 1 was completely dependent on the type I IFN receptor, as genes in the cluster were non-inducible in *Ifnar1-/-* BMDMs. This suggests MCMV may be capable of suppressing IFN-regulated genes during productive infection. Cluster 2 also had a strong dependency on the type I IFN receptor, with only few genes inducible in *Ifnar1-/-* BMDMs (Figure 6.9b i). This provides further evidence MCMV may target IFN-regulated gene expression for suppression during productive macrophage infection. The toll-like receptor 9 gene (*Tlr9*) was part of Cluster 2.

Clusters 3 and 4 were down-regulated in response to MCMV and MCMVdie3, but blocked, or inhibited, in their down-regulation by productive MCMV infection in wild type BMDMs (Figure 6.9c-d). This effect was more apparent in Cluster 4, whereby the down-regulation of genes was almost completely blocked by productive MCMV infection (Figure 6.6d i). Surprisingly however, both of these down-regulated clusters were found to have a strong dependence on the type I IFN receptor for their down-regulation.

6.3.3 Genes up-regulated specifically in response to productive MCMV infection

The final macrophage network to be assessed in the *Ifnar1-/-* BMDMs was the cluster of genes induced specifically in response to productive MCMV infection between 10-24 hpi, as identified in Chapter 4 (Figure 4.12). Assessing the expression of this group of genes in *Ifnar1-/-* BMDMs would determine if type I IFN played a role in the regulation of a late, secondary macrophage response to productive MCMV infection.

Figure 6.10 - Genes induced specifically by productive MCMV infection in wild-type and *Ifnar1-/-* BMDMs. (**i**) Heatmaps show the relative expression of genes in wild-type and *Ifnar1-/-* BMDMs with each gene represented by a row and per-gene normalized to its mean value to show relative expression. Yellow indicates an increase in expression relative to the mean and blue indicates a decrease. Genes are clustered based on similarity of expression profiles with similar genes connected at the hierarchical tree on the left. Columns represent different time points as indicated beneath the heatmap, and MCMV, MCMVdie3 and polyIC conditions are separated. Wild-type and *Ifnar1-/-* BMDMs are also shown separately. (**ii**) Mean expression profiles show the average expression level of the network in response to MCMV (light grey) and MCMVdie3 (dark grey) in both wild-type and *Ifnar1-/-* BMDMs. Red arrows emphasize the overall difference between MCMV and MCMVdie3.

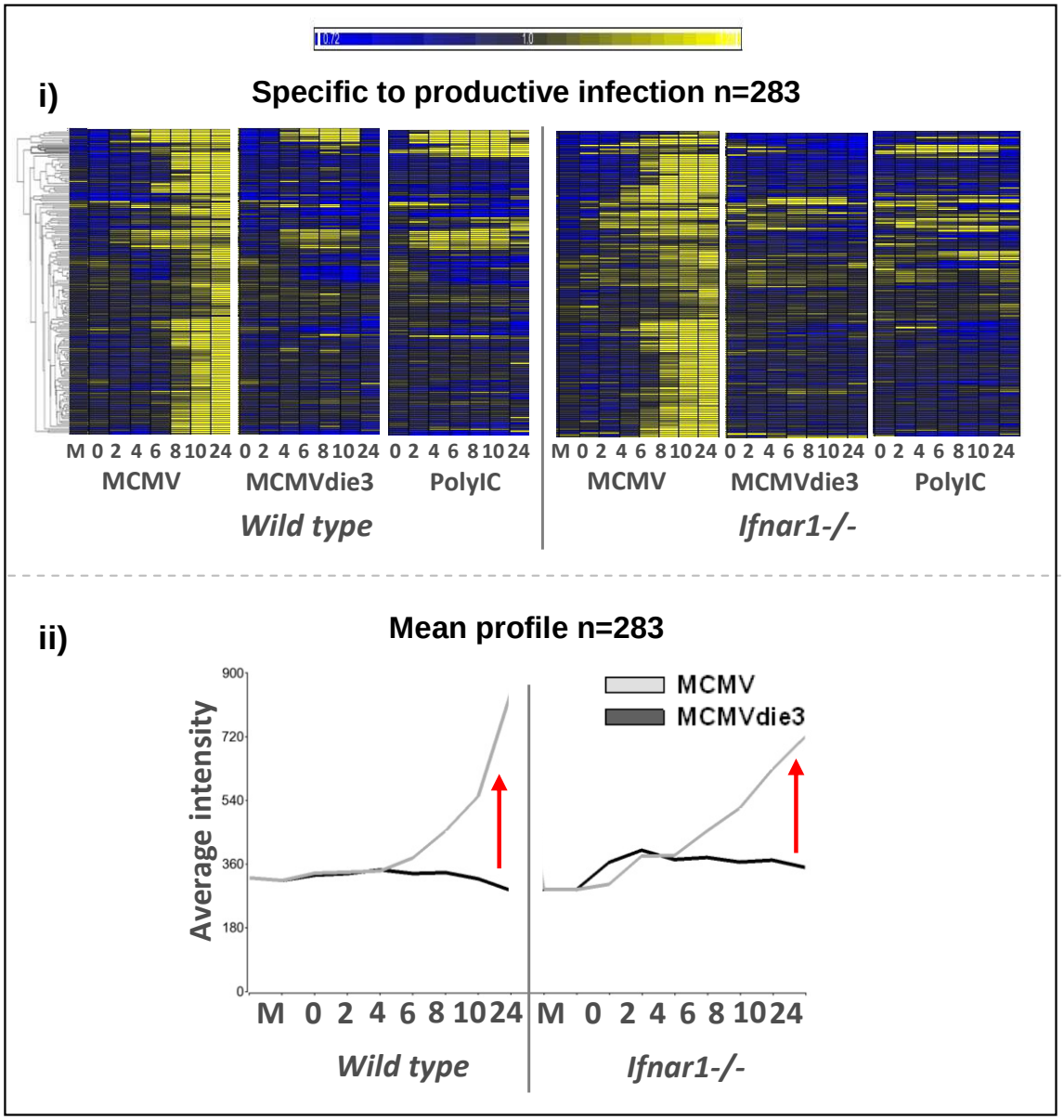

As seen in Figure 6.10, this group of genes was again induced specifically by productive MCMV infection in wild-type BMDMs, and not in response to MCMVdie3 or polyIC. These genes were still inducible in *Ifnar1-/-* BMDMs, suggesting IFN-independent regulation.

Overall, the behaviour of the different macrophage gene expression networks in wild type BMDMs was consistent with observations from previous experiments in Chapter 4 and Chapter 5, providing independent validation for these genes.

6.4 Global exploratory analysis

6.4.1 Unsupervised clustering

After investigating each of the macrophage networks from previous chapters in *Ifnar1-/-* BMDMs, the next step was to investigate global patterns of transcriptional regulation in the macrophage transcriptome. For this purpose, the *Ifnb1-/-* macrophages and the additional polyIC condition were included, and an exploratory, unsupervised clustering approach for the entire data set of 72 samples was undertaken. For this analysis, the BioLayout Express 3D tool (103) was used.

13,244 filtered microarray probes across 72 samples were imported into BioLayout 3D and a network graph was generated using a cut-off level of Pearson=0.9 (for details see Methods). Using this approach, a network graph containing 3,517 highly connected genes was formed. This network contained all the genes most highly correlated *and* changing across the data set. To identify distinct cliques or clusters of co-expressed genes within the data set, the MCL algorithm was applied at a level of MCL=1.5 with minimum cluster number of n=15 (meaning only clusters with 15 or more genes would be included). Clustering with MCL resulted in 2,325 genes arranged into 24 different clusters of co-expression.

An overview of the clusters will now be presented to assess the core relationship between IFN regulation and the macrophage antiviral response to MCMV. Gene lists for all clusters and over-represented functional annotation categories can be found in Supplementary Files 15-26. Clusters will be shown with the expression profiles of each individual gene in the cluster on a single axis with the mean cluster profiled overlaid. Some smaller clusters were excluded from the analysis and are not shown.

6.4.2 IFN-independent genes

6.4.2.1 Genes induced specifically in response to productive MCMV infection

Upon clustering of the data, the largest group of genes to emerge were those up-regulated specifically by productive MCMV infection at 24hpi (Figure 6.11). These genes had similar expression profiles to genes previously identified in Chapter 4 (Figure 4.11, Figure 6.10), and were regulated in an IFN-independent manner. Using the clustering approach, however, identified considerably more genes with this profile (827 genes using the clustering analysis versus 283 genes using the fold change cut-off in Chapter 4). This suggested there were considerably more genes up-regulated specifically in response to productive MCMV infection than previously thought.

Figure 6.11 - Genes induced specifically in response to productive MCMV infection are IFN-independent (n827). The individual expression profiles of every gene in the cluster are shown in grey and the average expression profile of the cluster is shown in solid blue. Normalized log microarray intensity is shown on the Y axis and individual samples are arranged in temporal order on the X axis. .

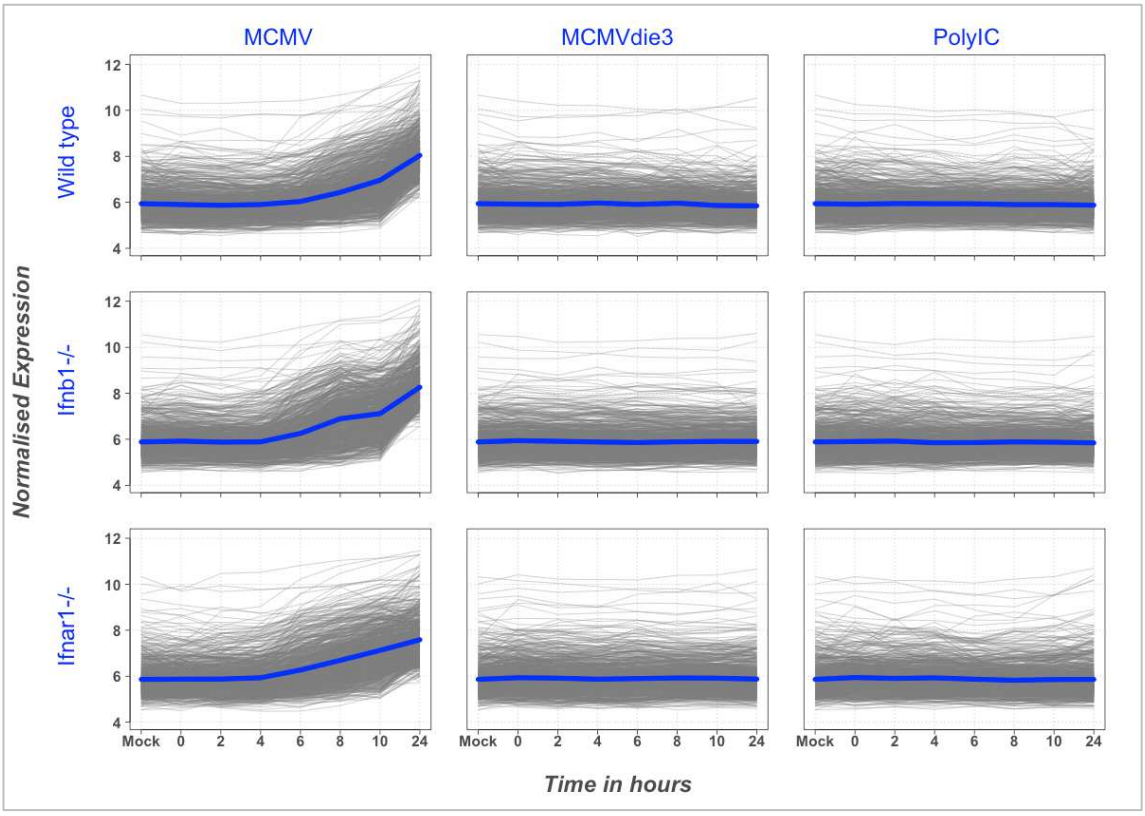

To determine functional annotation for the 827 genes up-regulated specifically in response to productive MCMV infection, the DAVID annotation tool(79) was used. Consistent with the previous analysis in Chapter 4, the genes up-regulated specifically in response to productive MCMV infection at 24hpi had mostly metabolic annotation associated with *glycoprotein* and *membrane* activity, rather than associations with the innate immune response or IFN-signalling (Table 6.3).

Table 6.3 - Functional annotation of genes up-regulated specifically in response to productive MCMV infection (n827). The DAVID annotation tool finds over-represented functional annotation classes within a group of 827 highly correlated genes. The *Category* column indicates annotation database, the *Term* column indicates the functional annotation category of significance and the *count* column indicates the number of genes within the group associated with that term, also represented by a percentage (%). The unadjusted (*PValue*) and adjusted (*Bonferroni*) p-values columns show results from Fishers exact tests generated by DAVID. The top ten annotation classes are shown cut-off with a cut-off of Bonferroni p<0.005.

Category n=827	Annotation Term	Count	%	PValue	Bonferoni
SP_PIR_KEYWORDS	glycoprotein	279	35.05	3.13E-29	1.16E-26
GOTERM_CC_FAT	GO:0005886~plasma membrane	249	31.28	2.33E-28	6.59E-26
SP_PIR_KEYWORDS	membrane	369	46.36	4.43E-28	1.64E-25
SP_PIR_KEYWORDS	signal	229	28.77	9.94E-23	3.69E-20
SP_PIR_KEYWORDS	cell membrane	155	19.47	3.47E-21	1.29E-18
GOTERM_CC_FAT	GO:0044459~plasma membrane part	140	17.59	3.54E-14	1.00E-11
GOTERM_MF_FAT	GO:0004714~transmembrane receptor protein tyrosine kinase activity	21	2.64	3.59E-14	2.51E-11
SP_PIR_KEYWORDS	disulfide bond	177	22.24	8.75E-14	3.25E-11
SP_PIR_KEYWORDS	Immunoglobulin domain	50	6.28	4.07E-10	1.51E-07
SP_PIR_KEYWORDS	cell junction	46	5.78	6.55E-10	2.43E-07

In addition to the large cluster of 827 genes shown above, another smaller cluster induced specifically in response to productive MCMV infection was also found, but with earlier kinetics. This group of 62 genes was also induced independently of the type I IFN pathway, but did not contain any significantly over-represented functional annotation categories.

Figure 6.12 - Genes induced specifically by productive MCMV infection at 8hpi are IFN-independent (n62). The individual expression profiles of every gene in the cluster are shown in grey and the average expression profile of the cluster is shown in solid blue. Normalized log microarray intensity is shown on the Y axis and individual samples are arranged in temporal order on the X axis. .

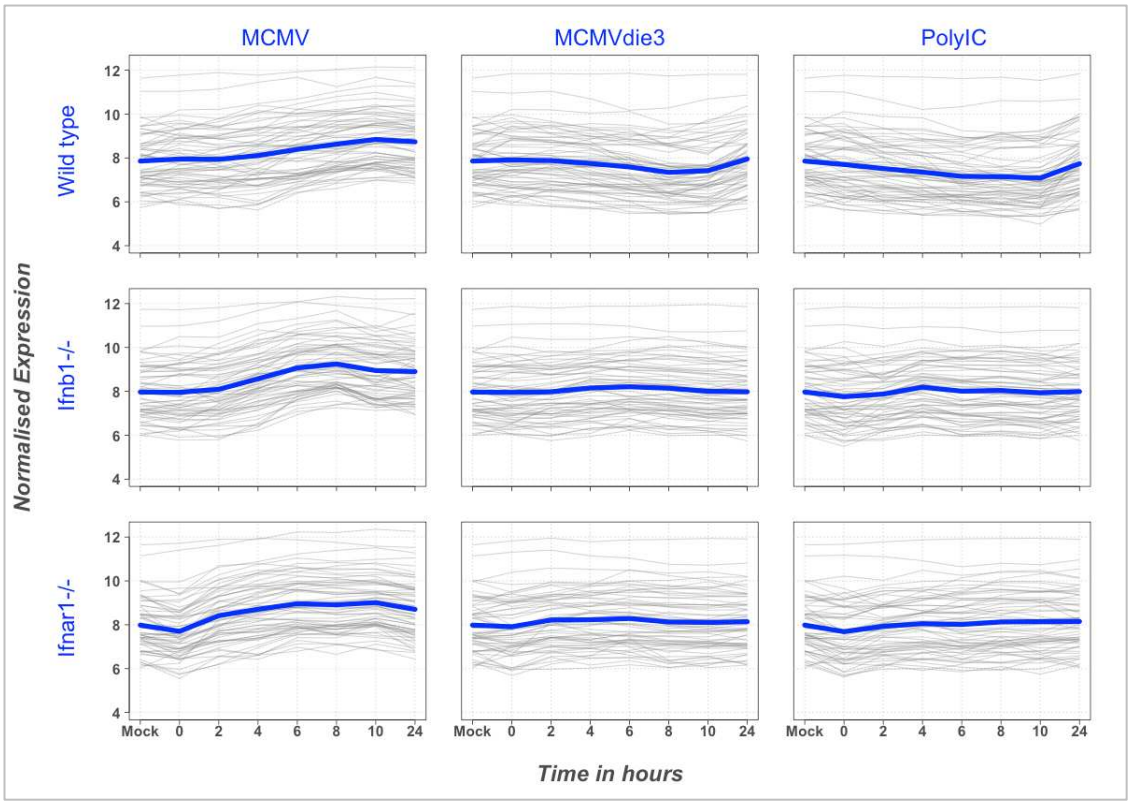

6.4.2.2 Genes induced equivalently by MCMV, MCMVdie3 and polyIC in an IFN-independent manner

In contrast to genes induced specifically by productive MCMV infection, there were also many genes induced by all three stimuli (MCMV, MCMVdie3 and polyIC). Notably, these genes were early-response genes up-regulated in an IFN-independent manner (Figure 6.13).

Figure 6.13 - Pro-inflammatory genes induced in an equivalent manner by MCMV, MCMVdie3 and polyIC are IFN-independent (n48). The individual expression profiles of every gene in the cluster are shown in grey and the average expression profile of the cluster is shown in solid blue. Normalized log microarray intensity is shown on the Y axis and individual samples are arranged in temporal order on the X axis.

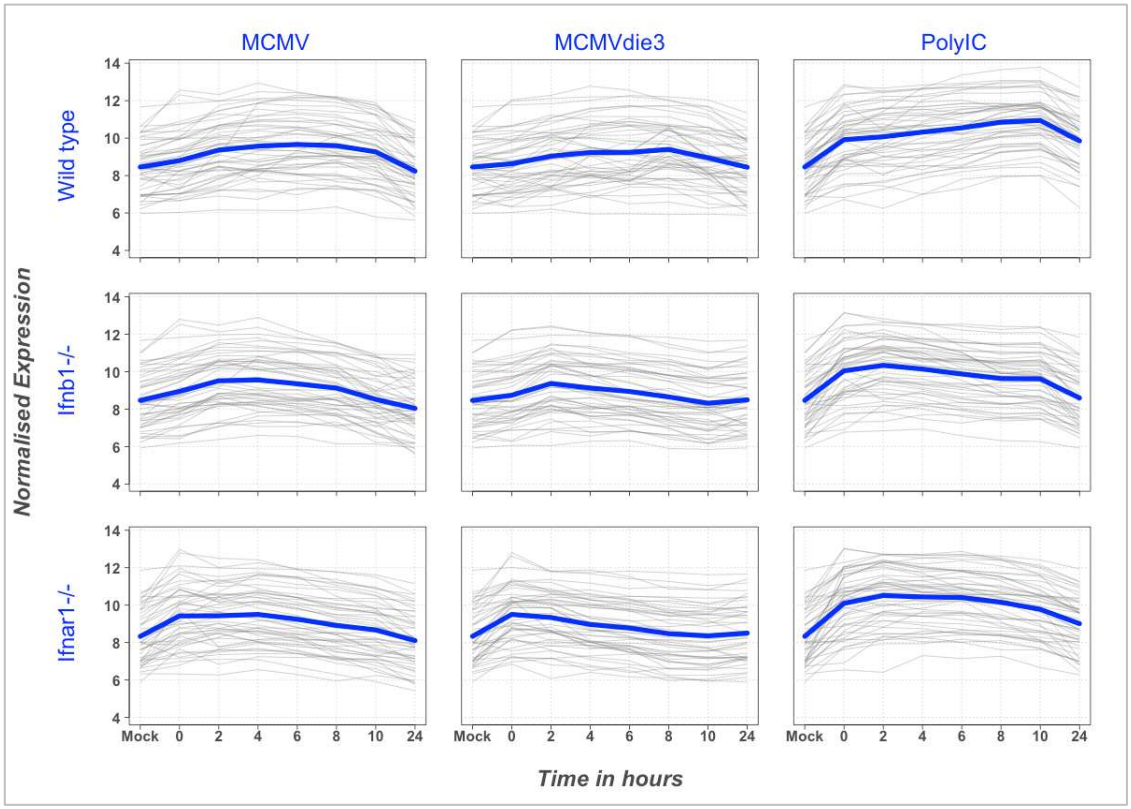

Genes in this group were mostly pro-inflammatory genes including tumor necrosis factor-alpha (*Tnf*), NF-kB subunits (*Nfkb1, Nfkb2, Nfkbia, Nfkbie, Relb*), TNF

associated genes (*Traf2, Fas*), and transcription factors regulating apoptosis (*Bcl2a1a, Bcl2a1b, Bcl2a1c, Bcl2a1d*). These genes were induced rapidly by 0hpi (end of viral adsorption period) but were transient in their expression and returned to basal levels by 10hpi. This group represents IFN-independent early response genes, also described as primary response genes (PRGs)(134).This cluster of 48 genes is enriched with annotation terms associated with *apoptosis* (mmu04210 p1.11E-05, GO:0042981 p0.00323, GO:0043067 p0.003576). This suggested an apoptotic/NFkB response occurring independently of the type I IFN pathway. The rapid induction of this class of inflammatory genes has been shown to occur independently of new protein synthesis and chromatin remodelling after TLR stimulation(100, 247). These genes have also been shown to have unique promoter properties in order to allow rapid transcriptional induction(134).

A similar group of 25 genes was found to be induced rapidly and independently of IFN, but the expression of these genes was shut-off quickly in *Ifnb1-/-* and *Ifnar1-/-* BMDMs (Figure 6.14). The expression of the genes, however, was sustained in wild type BMDMs. The profile suggests type I IFN only partially contributes to the regulation of these genes.

Figure 6.14 - A sub-set of early response genes is induced rapidly by all stimuli but shut-off in the absence of IFN signalling (n25). The individual expression profiles of every gene in the cluster are shown in grey and the average expression profile of the cluster is shown in solid blue. Normalized log microarray intensity is shown on the Y axis and individual samples are arranged in temporal order on the X axis.

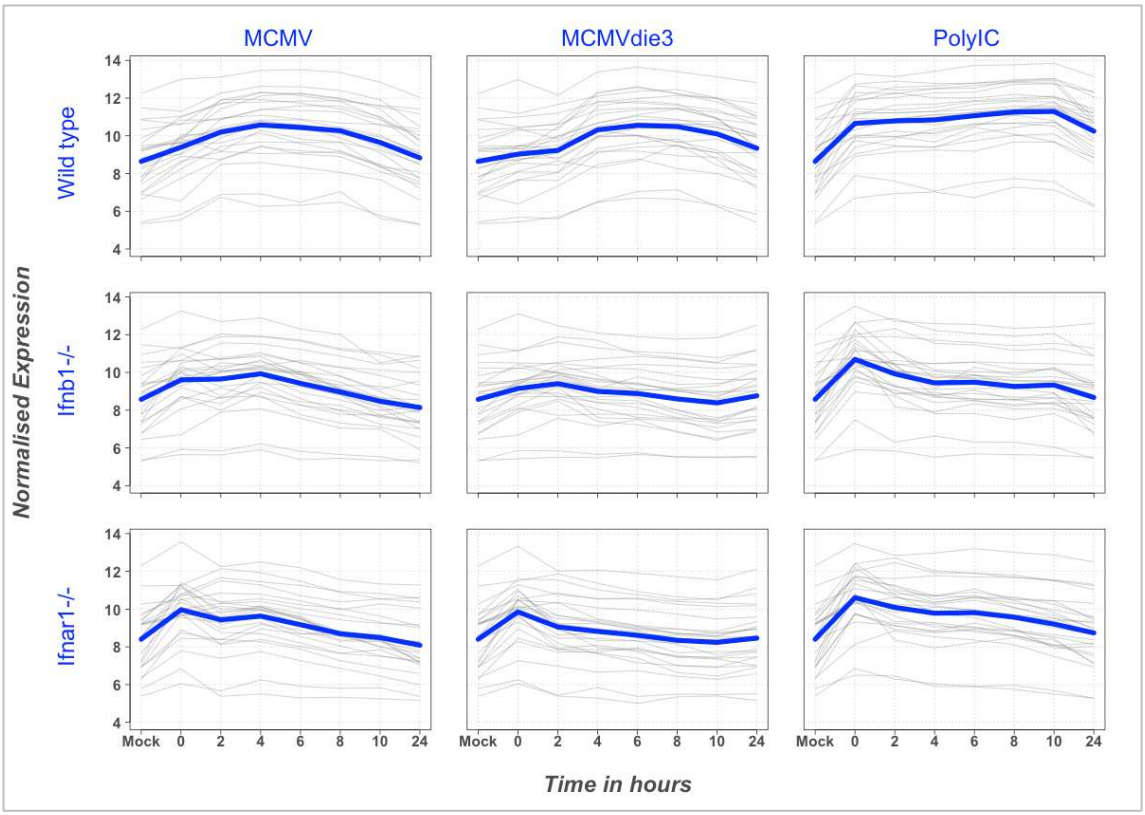

Amongst the group of 25 genes in Figure 6.14, which were induced rapidly but shut-off in the absence of IFN signalling, was *Irf1* (interferon regulatory factor 1) and the negative regulator of IFN signalling *Socs3* (suppressor of cytokine signalling 3). Also in this cluster were macrophage activation markers MIP-1α (*Ccl3*) and MIP-1β (*Ccl4*), immune-stimulated transcription factors (*Junb*, *Nfkbiz*) and signalling components (*Nod2*, *Tank*). The profile of this cluster suggested co-ordinate regulation by both IFN and other mechanisms during the antiviral response, as genes were inducible in *Ifnb1-/-* and *Ifnar1-/-* BMDMs, but could not be sustained in their induction without type I IFN. In addition, genes within this cluster were induced very early by 0hpi (i.e. within the viral adsorption period) suggesting they are rapid-response genes. Three individual examples of genes with this cluster are shown in Figure 6.15 to highlight the profile.

Figure 6.15 – Expression of *Ccl4*, *Irf1* and *Socs3* is sustained in wild-type BMDMs but shut-off rapidly in *Ifnb1-/-* and *Ifnar1-/-* BMDMs. The expression profiles of *Ccl4* (**a**), *Irf1* (**b**) and *Socs3* (**c**) are shown with normalized microarray intensity on the Y axis. Individual samples are arranged in temporal order on the X axis. The 0hpi time point represents the end of the 1.5 hour viral adsorption period.

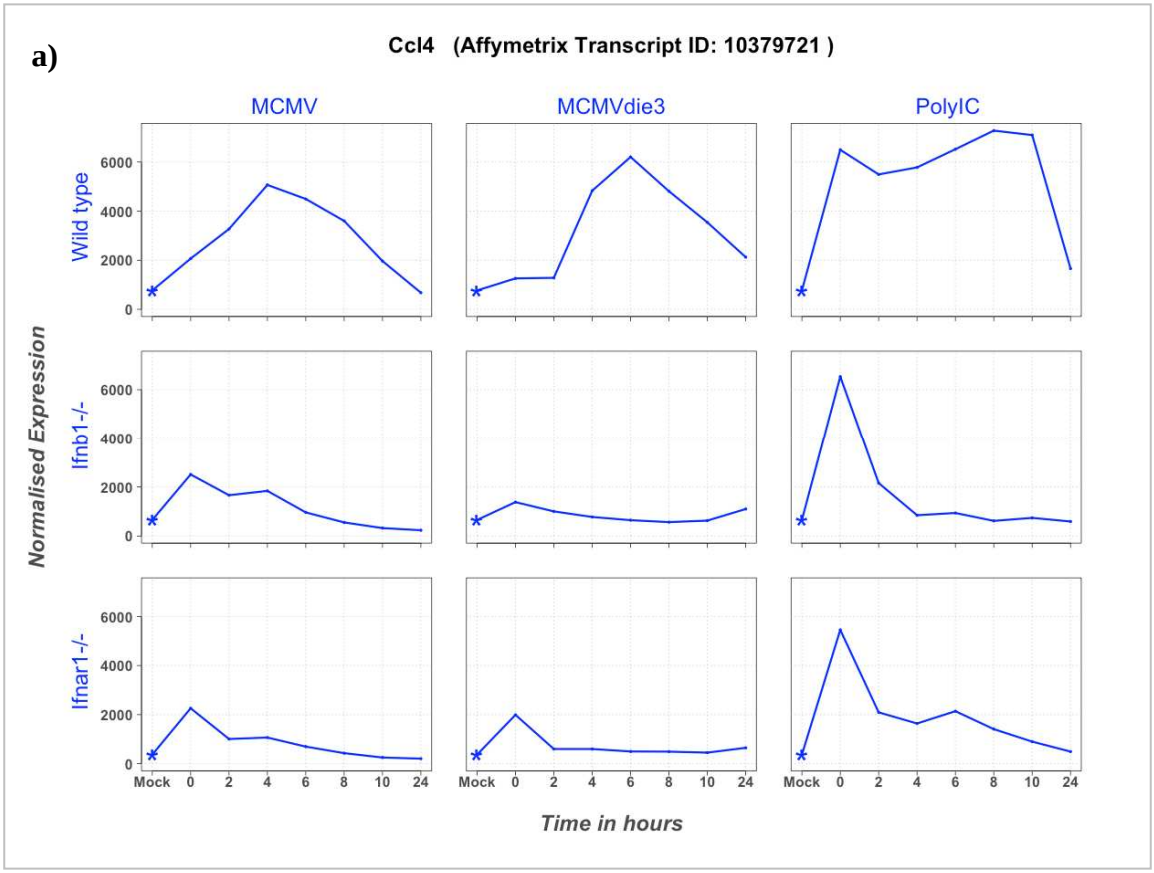

b)

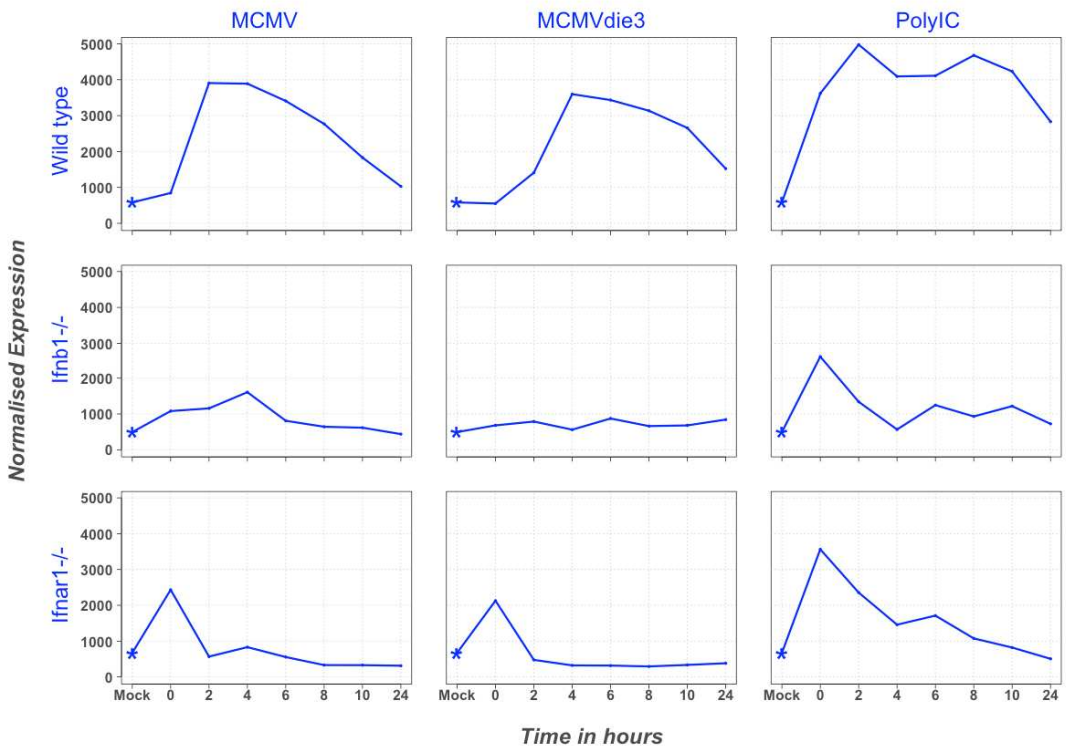
Irf1 (Affymetrix Transcript ID: 10376060)
MCMV
MCMVdie3
PolyIC
Wild type
Ifnb1-/-
Ifnar1-/-
Normalised Expression
0
1000
2000
3000
4000
5000
Mock 0 2 4 6 8 10 24
Time in hours

c)

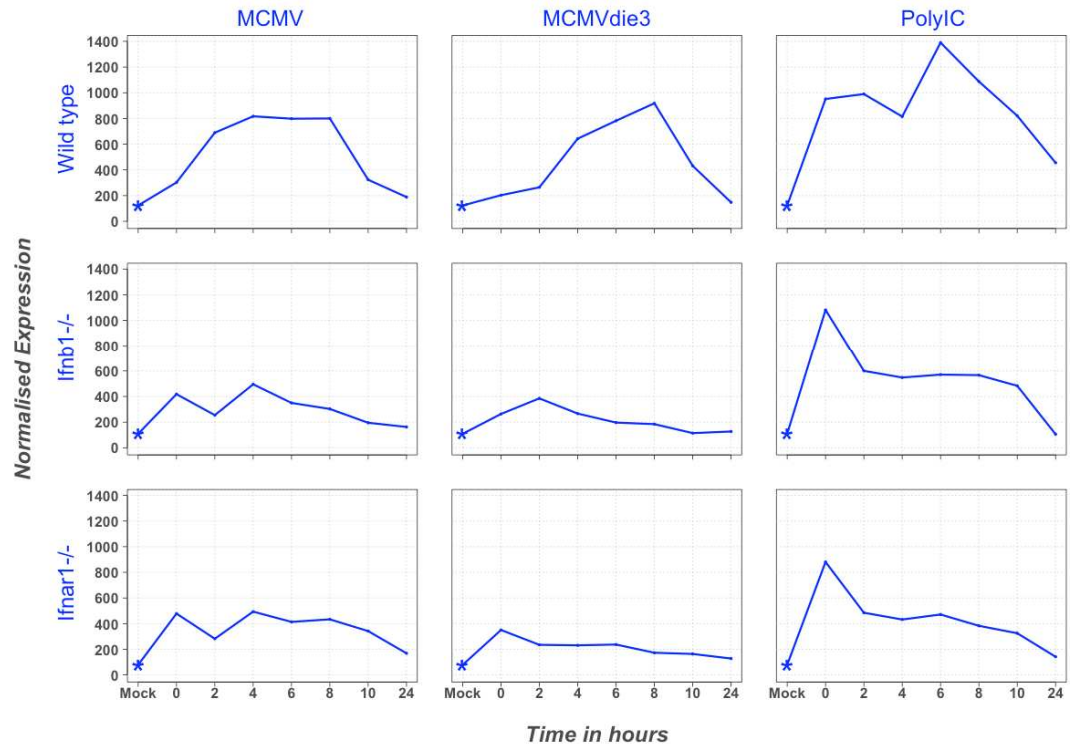
Socs3 (Affymetrix Transcript ID: 10393449)
MCMV
MCMVdie3
PolyIC
Wild type
Ifnb1-/-
Ifnar1-/-
Normalised Expression
0
200
400
600
800
1000
1200
1400
Mock 0 2 4 6 8 10 24
Time in hours

Another important macrophage gene with the same expression profile was colony stimulating factor 1 (*Csf1*) which was induced to high and sustained levels in wild type BMDMs in response to MCMV, MCMVdie3 and polyIC, but induced to lower levels and shut-off in *Ifnb1-/-* and *Ifnar1-/-* BMDMs (Figure 6.16).

Figure 6.16 -Transcriptional induction of *Csf1* is partially dependent on the type I IFN receptor. The expression profile of *Csf1* is shown with normalized microarray intensity on the Y axis. Individual samples are arranged in temporal order on the X axis. The 0hpi time point represents the end of the 1.5 hour viral adsorption period.

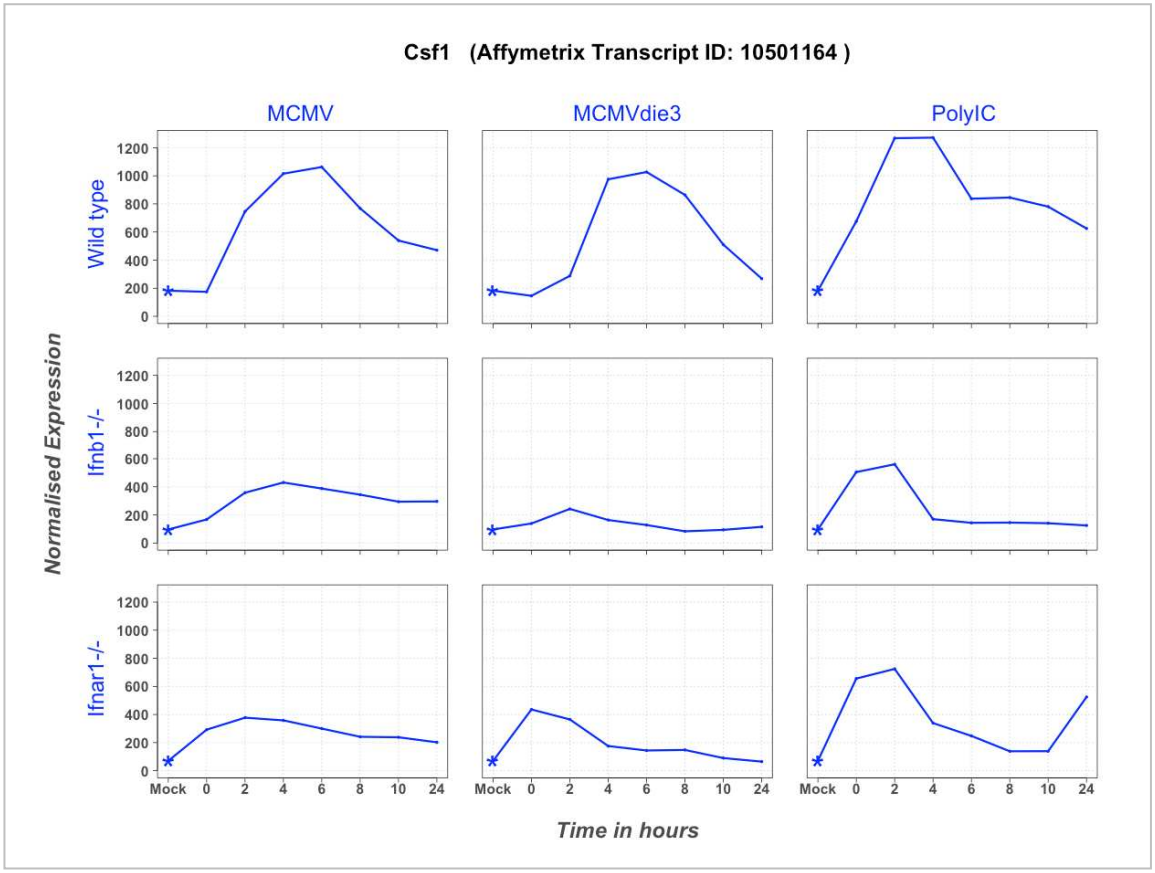

Returning to the clustering analysis, many genes were found to be down-regulated in an equivalent manner by MCMV, MCMVdie3 and polyIC, independently of the type I IFN pathway (Figure 6.17). Genes in this cluster were significantly associated with *phosphoprotein activity* (p=1.14E-04)

Figure 6.17. IFN-independent down-regulation of genes in response to MCMV, MCMVdie3 and polyIC (n141). The individual expression profiles of every gene in the cluster are shown in grey and the average expression profile of the cluster is shown in solid blue. Normalized log microarray intensity is shown on the Y axis and individual samples are arranged in temporal order on the X axis.

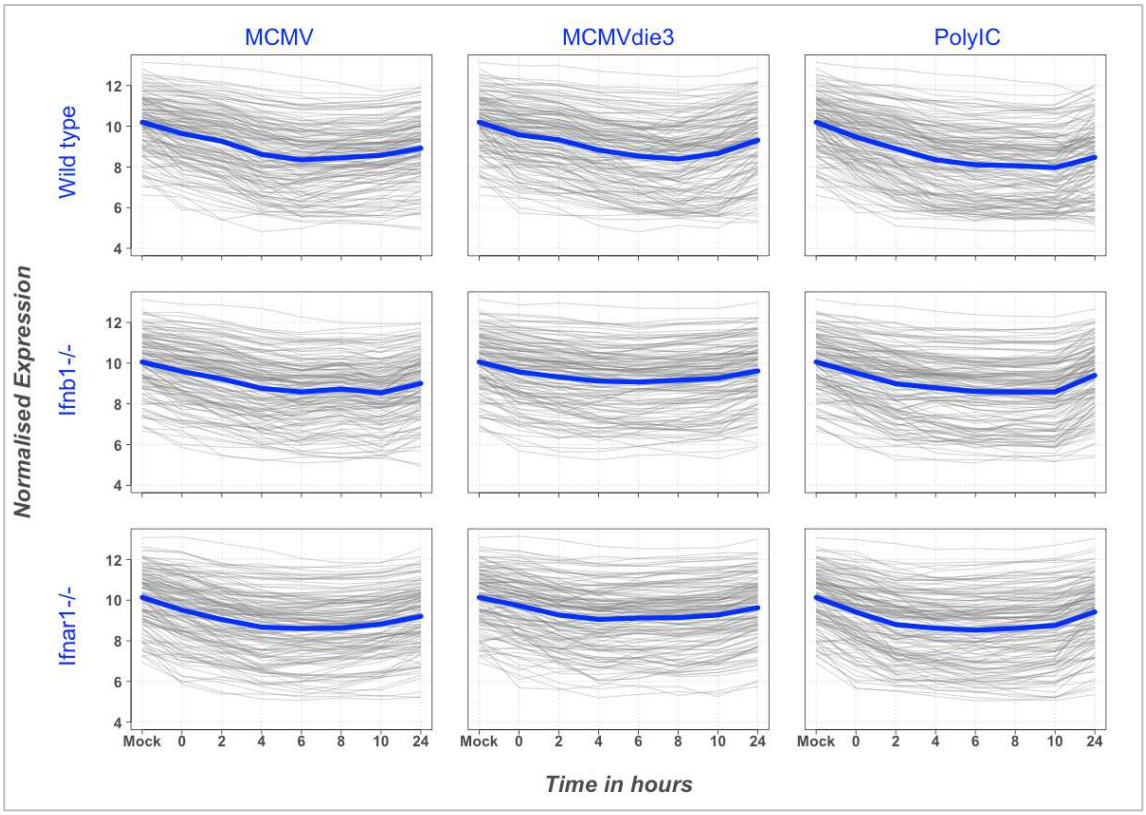

A second cluster of 428 commonly down-regulated genes was also found with a slightly different expression profile (Figure 6.18). Annotation of these genes identified significant over-represented annotation terms associated with *chromosomes, mitosis* and *cell division* (Table 6.4). The down-regulation of these genes was more distinct in the wild-type BMDMs in comparison to the *Ifnb1-/-* and *Ifnar1-/-* cells, suggesting some contribution of type I IFN.

Figure 6.18 - IFN-independent down-regulation of cell cycle genes in response to MCMV, MCMVdie3 and polyIC (n428). The individual expression profiles of every gene in the cluster are shown in grey and the average expression profile of the cluster is shown in solid blue. Normalized log microarray intensity is shown on the Y axis and individual samples are arranged in temporal order on the X axis.

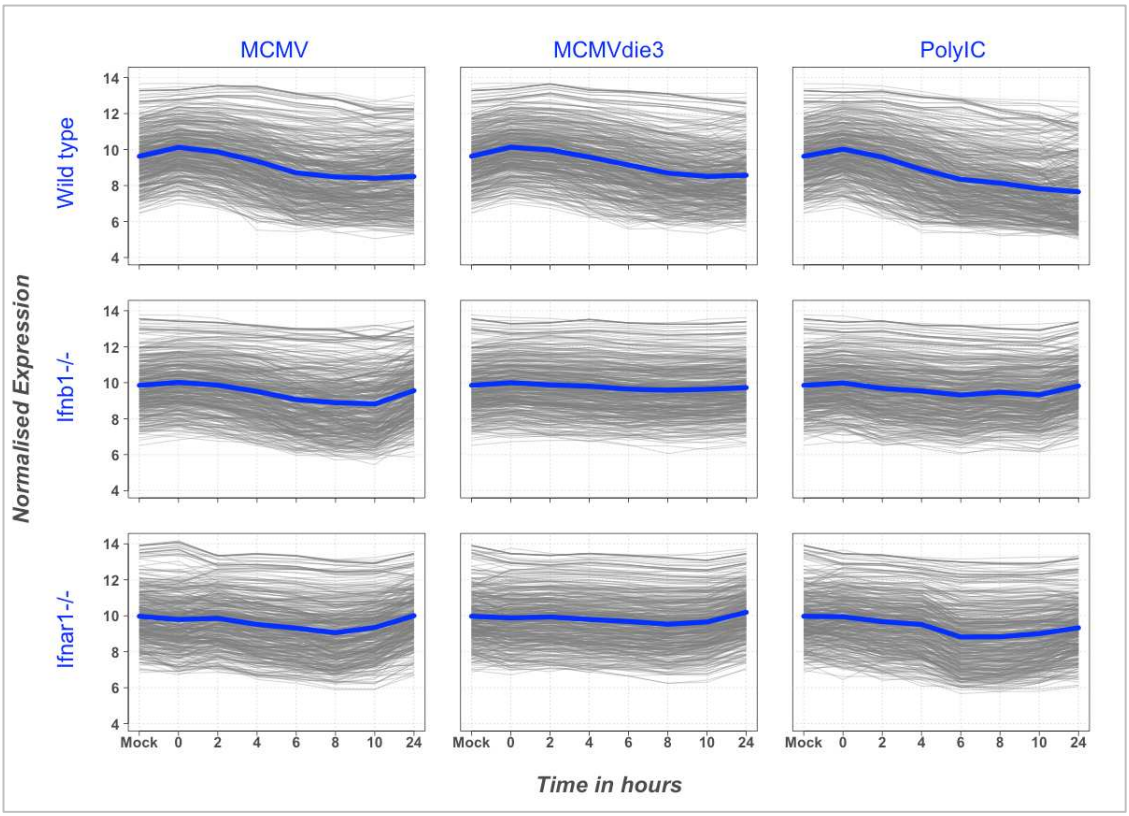

Table 6.4 - Annotation of genes down-regulated in response to MCMV, MCMVdie3 and polyIC in wild-type, *Ifnb1* and *Ifnar1-/-* BMDMs (n428). The DAVID annotation tool finds over-represented functional annotation classes within a group of 428 highly correlated genes. The *Category* column indicates annotation database, the *Term* column indicates the functional annotation category of significance and the *count* column indicates the number of genes within the group associated with that term, also represented by a percentage (%). The unadjusted (*PValue*) and adjusted (*Bonferroni*) p-values columns show results from Fishers exact tests generated by DAVID. The top ten annotation classes are shown cut-off with a cut-off of Bonferroni p<0.005.

Category	Annotation Term	Count	%	PValue	Bonferoni
GOTERM_CC_FAT	GO:0005694~chromosome	98	27.00	1.67E-92	3.47E-90
GOTERM_BP_FAT	GO:0007049~cell cycle	124	34.16	2.26E-92	2.40E-89
SP_PIR_KEYWORDS	cell cycle	109	30.03	3.94E-91	8.47E-89
GOTERM_CC_FAT	GO:0044427~chromosomal part	86	23.69	1.30E-81	2.71E-79
GOTERM_BP_FAT	GO:0022403~cell cycle phase	93	25.62	2.81E-81	2.98E-78
GOTERM_BP_FAT	GO:0000279~M phase	88	24.24	1.72E-80	1.82E-77
GOTERM_BP_FAT	GO:0022402~cell cycle process	98	27.00	4.42E-80	4.68E-77
SP_PIR_KEYWORDS	cell division	80	22.04	7.21E-75	1.55E-72
GOTERM_CC_FAT	GO:0043232~intracellular non-membrane-bounded organelle	150	41.32	3.55E-73	7.38E-71
GOTERM_CC_FAT	GO:0043228~non-membrane-bounded organelle	150	41.32	3.55E-73	7.38E-71
SP_PIR_KEYWORDS	mitosis	70	19.28	5.34E-73	1.15E-70

6.4.3 IFN-dependent genes

6.4.3.1 IFN-dependent up-regulated genes

The second largest cluster emerging from exploratory analysis contained 776 IFN-inducible genes up-regulated by all three stimuli in wild-type BMDMs, with partial dependency on *Ifnb1* and complete dependency on type I IFN receptor (Figure 6.19).

Figure 6.19. Interferon-stimulated genes induced in response to MCMV, MCMVdei3 and polyIC with partial dependency on *Ifnb1* and complete dependency on *Ifnar1* (n776). The individual expression profiles of every gene in the cluster are shown in grey and the average expression profile of the cluster is shown in solid blue. Normalized log microarray intensity is shown on the Y axis and individual samples are arranged in temporal order on the X axis.

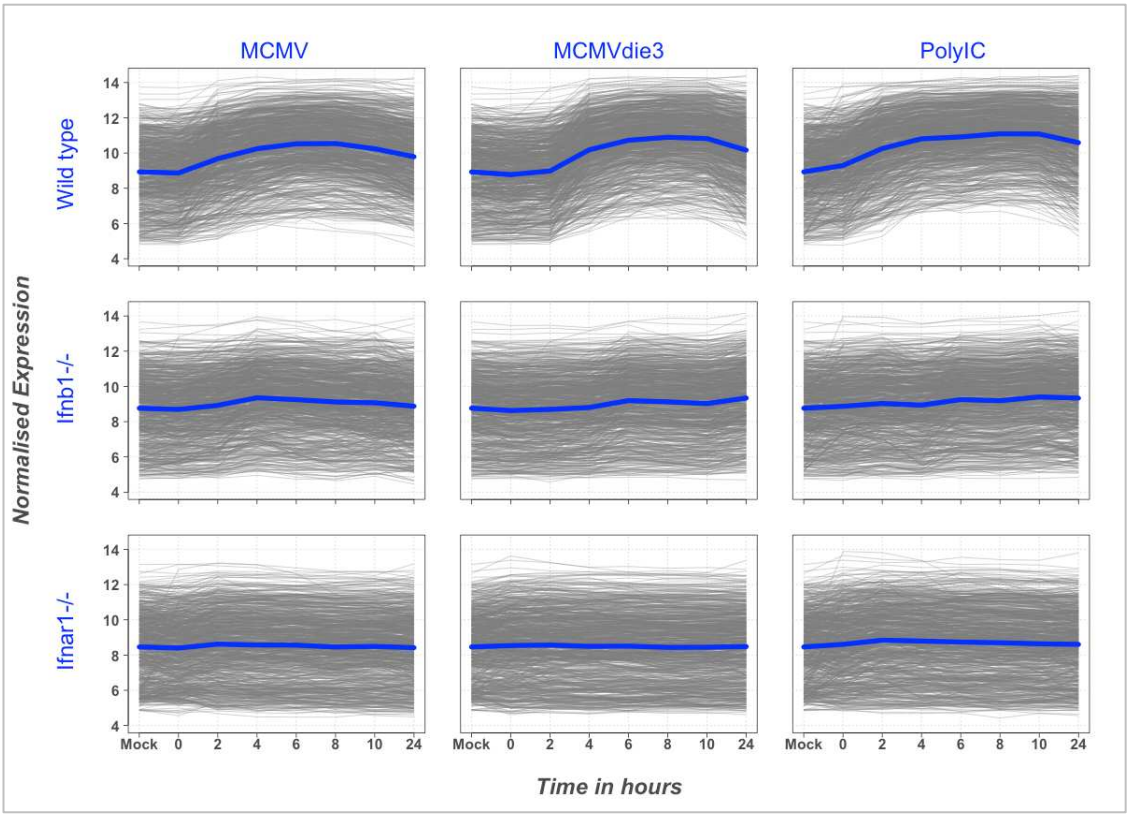

Within this cluster were known, or '*classical*' ISGs including interferon-induced genes (*Ifi203, Ifi204, Ifi205, Ifi35, Ifit1, Ifit2, Ifit3, Isg15, Isg20*), interferon

regulatory factors (*Irf2, Irf7, Irf9*), antimicrobial effectors (*Mx1, Mx2, Oas1a, Oas1b, Oas1c, Oas1g, Oas2, Oas3*), Jak-Stat signalling genes (*Jak2, Stat1, Stat2*), proteosome components (*Psmb8, Psmb9, Tap1, Tap2*), guanylate binding proteins (*Gbp1, Gbp3, Gbp4, Gbp5*), pattern recognition receptors (*Tlr3, Tlr9, Tlr11, Zbp1*) and many MHC class II genes (>10). The cluster also contained interleukins (*Il-6, Il-10, Il-15, Il-18)*. A large number of non-annotated or 'unknown' genes with no previously annotation related to the IFN response were also found within this cluster (for complete list see Supplementary File 21). The moderate up-regulation of these genes in *Ifnb1-/-* BMDMs indicates some contribution of other type I IFNs (i.e. IFN alphas) in regulating ISG expression during the macrophage antiviral response.

The cluster of 776 ISGs represents genes induced in response to both productive and non-productive MCMV infection, and in response to polyIC stimulation. These genes likely reflect the type I IFN-response induced through JAK-STAT signalling. Annotation of these genes, as expected, identified over-representation of classes associated with the innate immune response (GO:0006955 *immune response* p=8.03E-27, GO:009615 *response to virus* p=2.77E-08) and antigen presentation (GO:0019882 p=3.09E-07, GO:0042612 p=6.90E-05). Enriched pathways included *Cytosolic DNA-sensing* (mmu04623 p=0.002) and *Toll-like receptor signalling* (mmu04620 p=0.004)

Although the induction of all ISGs within this cluster was found to be completely dependent on the type I IFN receptor, the induction of some genes also showed a strict dependency on the *Ifnb1* gene which was not expected. The best examples of such genes were *Gbp4*, *Serpina3f* and *Nos2* (Figure 6.20).

Figure 6.20. The induction of some macrophage ISGs is strictly dependent on *Ifnb1*. The expression profiles of *Gbp4* (**a**), *Sepina3f* (**b**) and *Nos2* (**c**) are shown with normalized microarray intensity on the Y axis. Individual samples are arranged in temporal order on the X axis. The 0hpi time point represents the end of the 1.5 hour viral adsorption period.

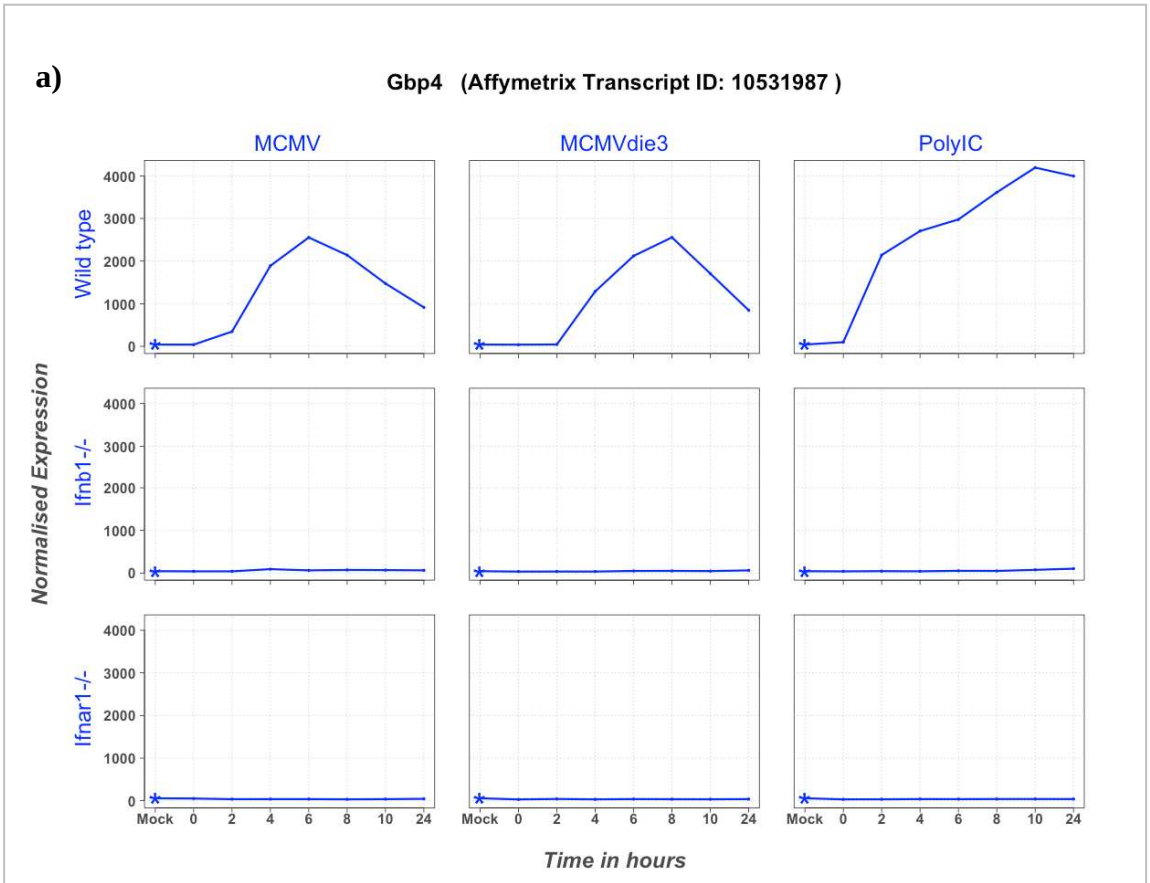
a)
Gbp4 (Affymetrix Transcript ID: 10531987)
MCMV
MCMVdie3
PolyIC
Wild type
Ifnb1-/-
Ifnar1-/-
Normalised Expression
Mock 0 2 4 6 8 10 24
Time in hours

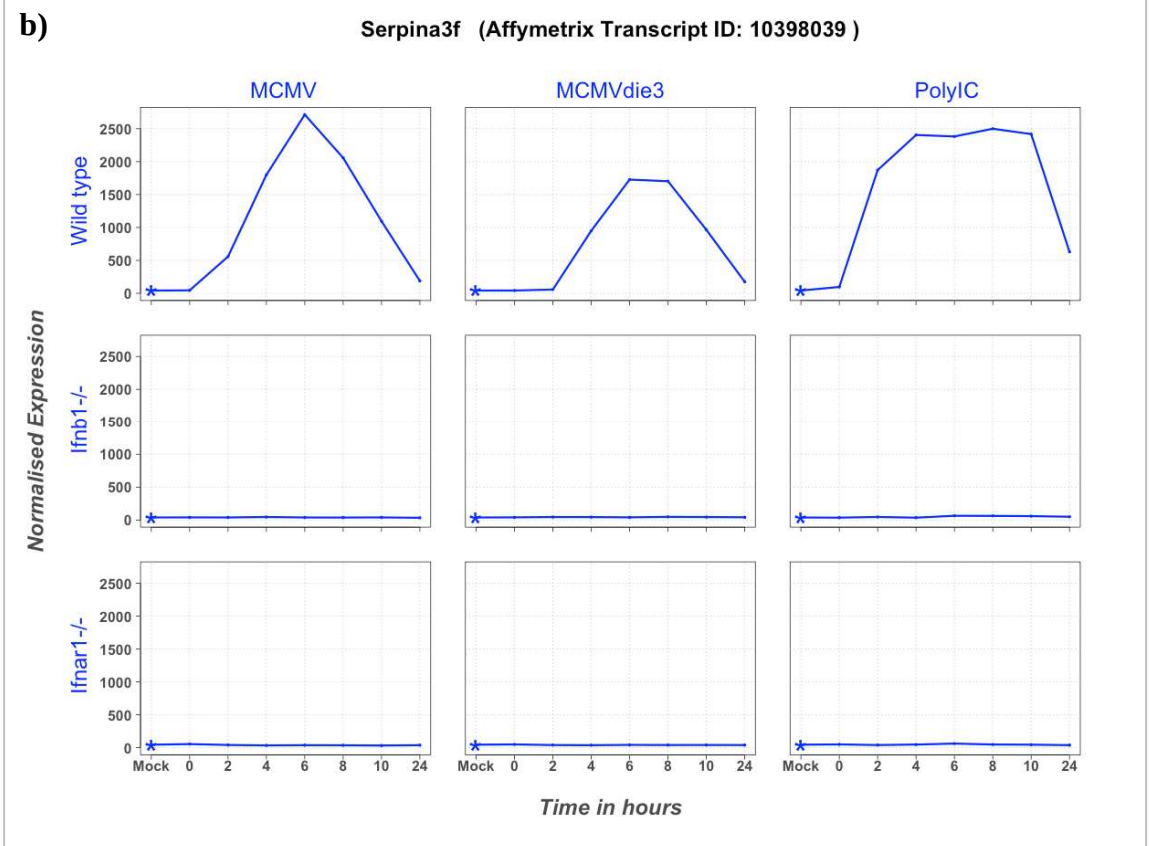
b)
Serpina3f (Affymetrix Transcript ID: 10398039)
MCMV
MCMVdie3
PolyIC
Wild type
Ifnb1-/-
Ifnar1-/-
Normalised Expression
Mock 0 2 4 6 8 10 24
Time in hours

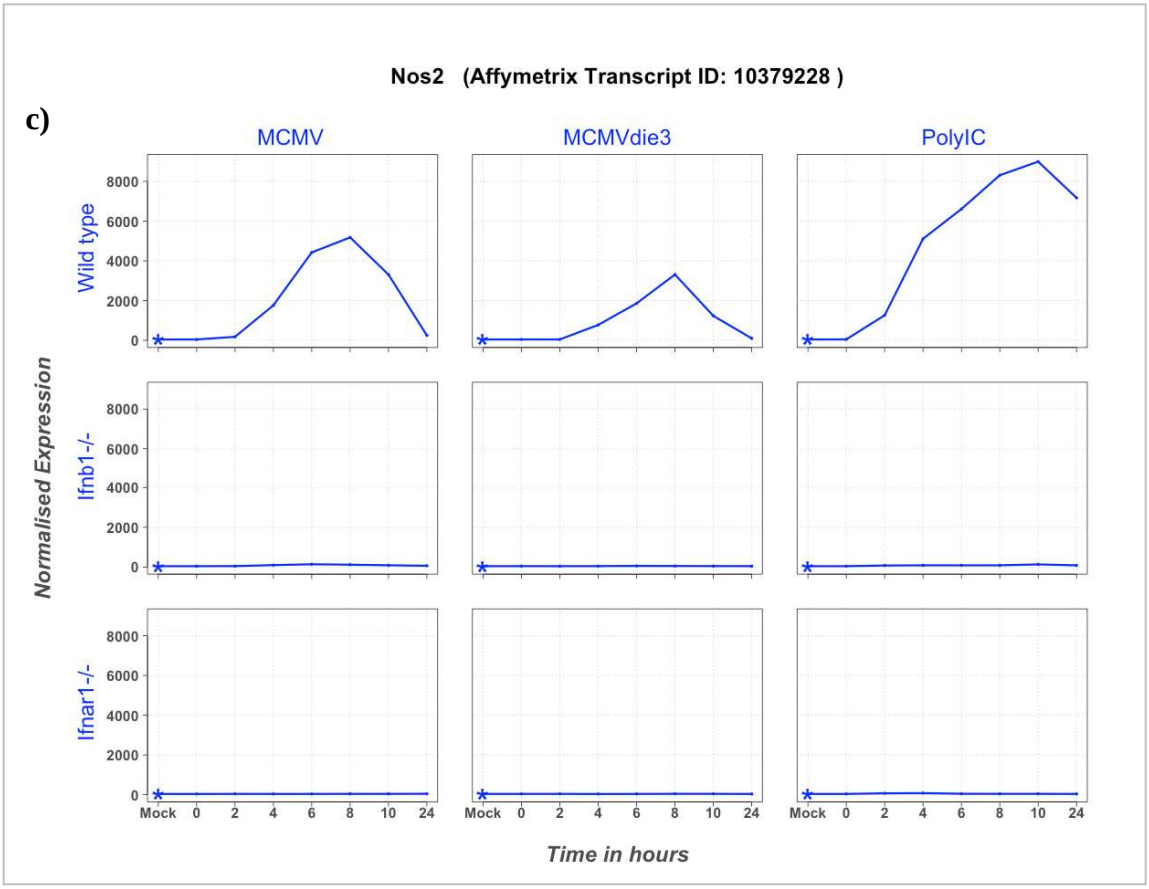

The strict dependency of some, but not all ISGs on *Ifnb1* indicates *Ifnb1* may have some level of specificity in binding the type I IFN receptor and regulating a sub-set of ISGs. It is worth noting however that there were relatively few ISGs with this strict level of *Ifnb1* dependency (i.e. not enough to form their own individual cluster)

Despite small sub-sets of genes regulated with strict *Ifnb1* dependency, most genes within the large cluster of 776 ISGs had only a partial dependency on *Ifnb1* and were still semi-inducible in *Ifnb1-/-* BMDMs (see Figure 6.19). This indicates *Ifnb1-/-* BMDMs have an intermediate phenotype compared to *Ifnar1-/-* cells as inducers of ISGs. Examples of well known ISGs to highlight this intermediate phenotype in *Ifnb1-/-* BMDMs are *Stat1*, and *Mx1* (Figure 6.21).

Figure 6.21 - Induction of *Stat1*, and *Mx1* is partially dependent on *Ifnb1* expression The expression profiles of *Stat1* (**a**) and *Mx1* (**b**) are shown with normalized microarray intensity on the Y axis. Individual samples are arranged in temporal order on the X axis. The 0hpi time point represents the end of the 1.5 hour viral adsorption period.

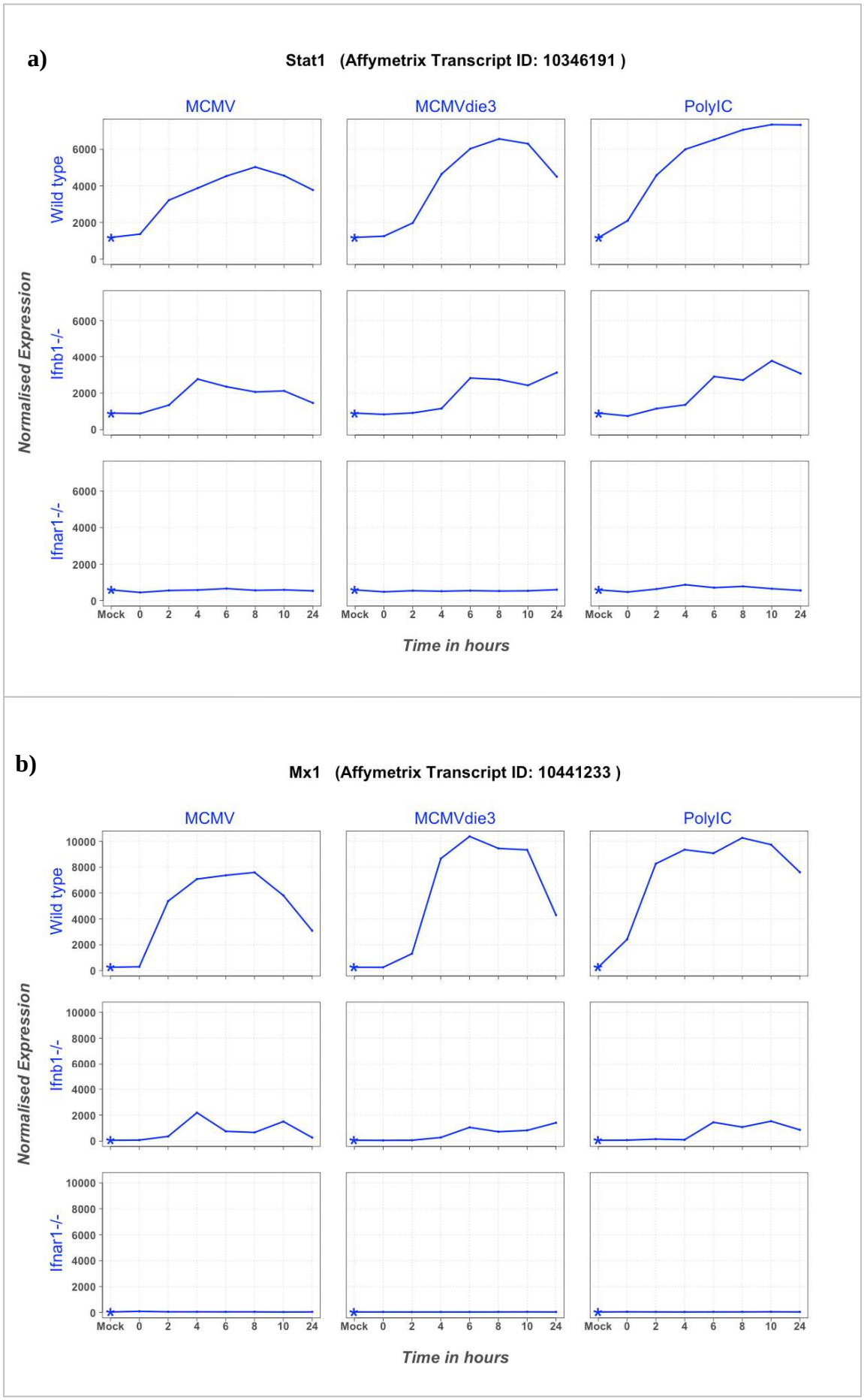
a)
Stat1 (Affymetrix Transcript ID: 10346191)
MCMV
MCMVdie3
PolyIC
Wild type
Ifnb1-/-
Ifnar1-/-
Normalised Expression
0
2000
4000
6000
Mock 0 2 4 6 8 10 24
Time in hours
b)
Mx1 (Affymetrix Transcript ID: 10441233)
MCMV
MCMVdie3
PolyIC
Wild type
Ifnb1-/-
Ifnar1-/-
Normalised Expression
0
2000
4000
6000
8000
10000
Mock 0 2 4 6 8 10 24
Time in hours

The expression profiles of *Irf7*, *Stat1*, and *Mx1* in *Ifnb1-/-* BMDMs indicates other type I IFNs regulate ISGs in the absence of *Ifnb1*. This reflects the functional redundancy amongst type I IFNs during the macrophage antiviral response.

A smaller cluster of genes was also found to be up-regulated in an IFN-dependent manner (Figure 6.22), but with later kinetics than the previous group. These late-induced genes represent a secondary wave of IFN-dependent gene expression peaking between 10-24hpi. These genes were induced to higher levels by polyIC than by MCMV infection, indicating a possible link to dsRNA response.

Figure 6.22 – Genes induced with late kinetics expressed higher in response to polyIC than to MCMV (n86). The individual expression profiles of every gene in the cluster are shown in grey and the average expression profile of the cluster is shown in solid blue. Normalized log microarray intensity is shown on the Y axis and individual samples are arranged in temporal order on the X axis.

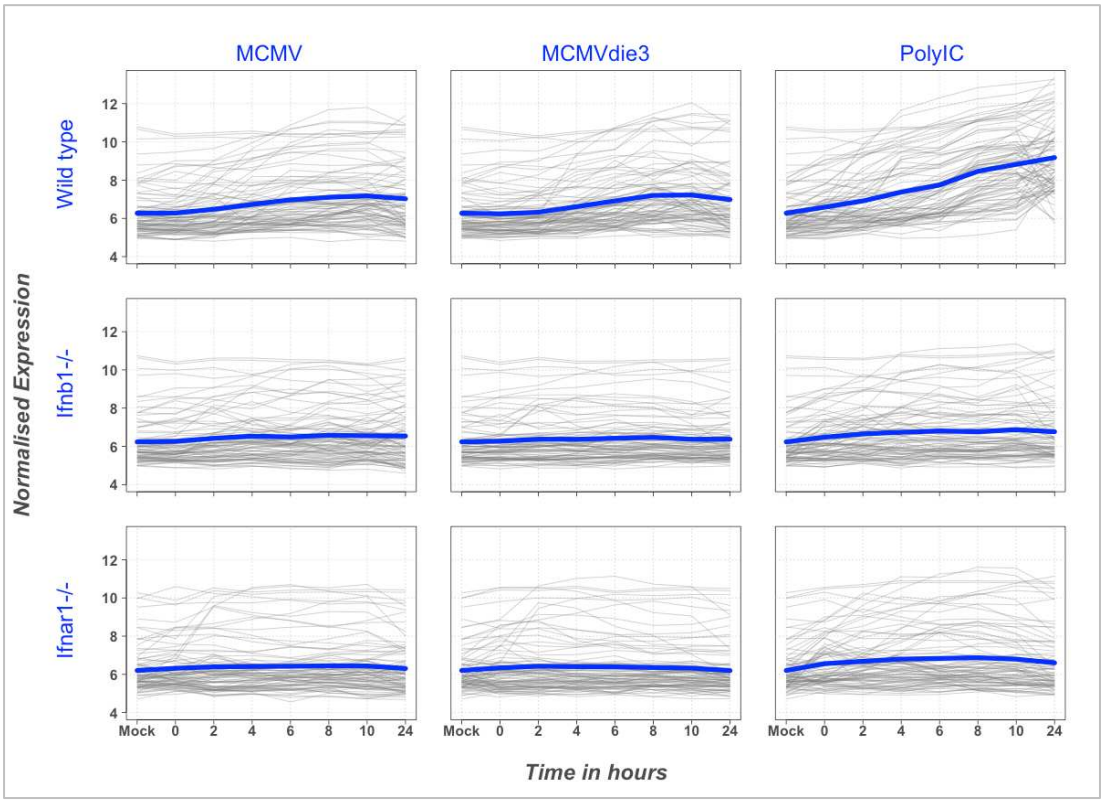

6.4.3.2 IFN-dependent down-regulated genes

An interesting class of genes found in this study were those down-regulated by all three stimuli in an IFN-dependent manner. Figure 6.23 shows the common down-regulation of 66 genes by MCMV, MCMVdie3 and polyIC in an IFN-dependent manner.

Figure 6.23- Genes down-regulated in an IFN-dependent manner by MCMV, MCMVdie3 and polyIC (n66). The individual expression profiles of every gene in the cluster are shown in grey and the average expression profile of the cluster is shown in solid blue. Normalized log microarray intensity is shown on the Y axis and individual samples are arranged in temporal order on the X axis.

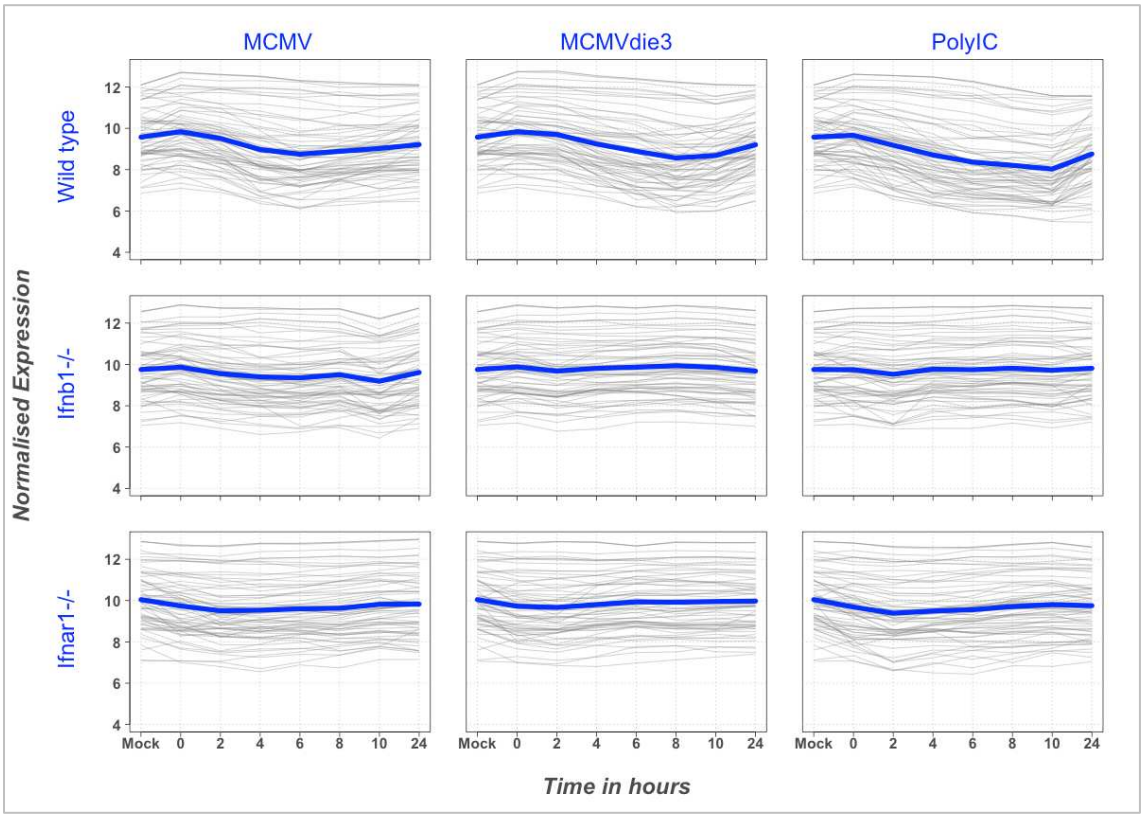

In addition to the cluster shown above, two other IFN-dependent down-regulated clusters were found. Figure 6.24 shows down-regulation of a cluster of 263 genes, whereby down-regulation only occurs in response to MCMVdie3 and polyIC in wild type cells (i.e. inhibited or blocked by productive MCMV infection). In *Ifnb1-/-* and

Ifnar1-/- BMDMs, the ability to down-regulate these genes has been completely lost, and in many cases de-repression or up-regulation of genes occurs in the absence of IFN signalling.

Figure 6.24- IFN-dependent down-regulation inhibited during productive MCMV infection (n263). The individual expression profiles of every gene in the cluster are shown in grey and the average expression profile of the cluster is shown in solid blue. Normalized log microarray intensity is shown on the Y axis and individual samples are arranged in temporal order on the X axis.

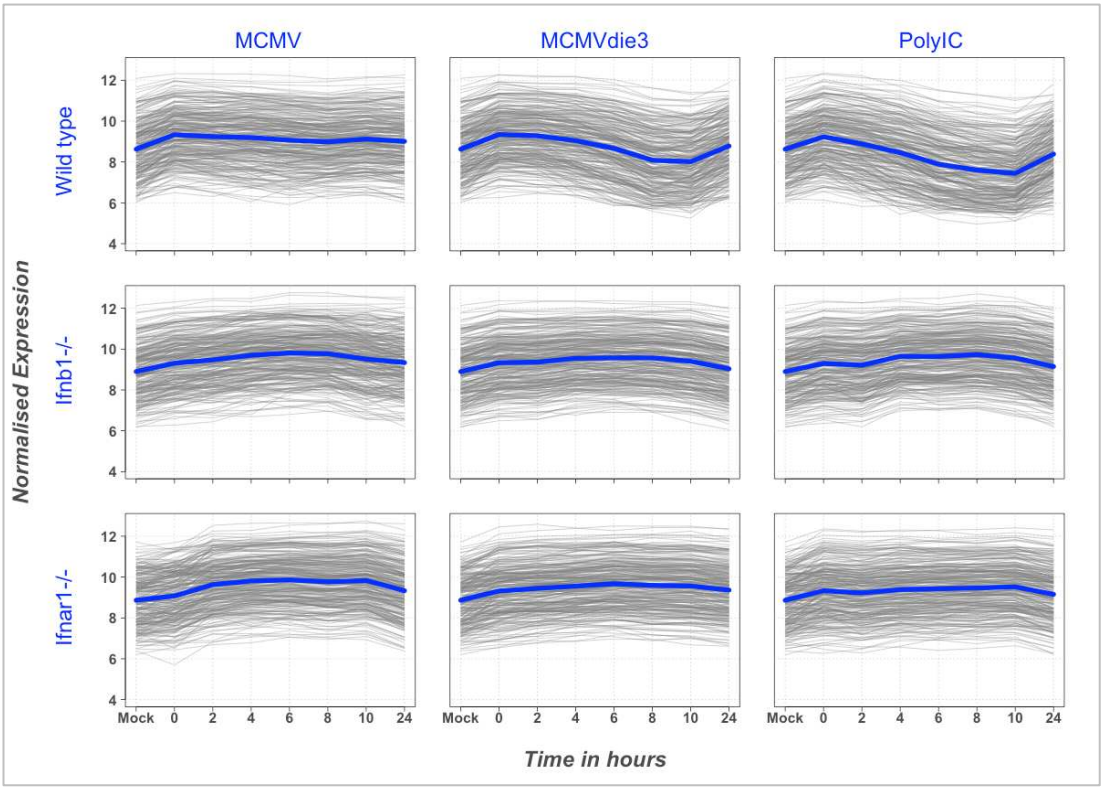

The 263 genes shown above were functionally annotated using DAVID (see Table 6.5), and this indicated highly significant over-representation of genes associated with the *nucleolus* (p=5.4E-70) and *membrane enclosed lumen* (p=2.96E-49), and functions associated with *ribosome biogenesis* (p=2.07E-43) and *ncRNA processing* (p=3.21E-43).

Table 6.5 - Annotation of 263 genes down-regulated in wild-type BMDMs, but de-repressed in *Ifnb1-/-* and *Ifnar1-/-* BMDMs. The DAVID annotation tool was used to find over-represented functional annotation classes within a group of 263 highly correlated genes. The top ten over-represented annotation classes are shown.

Category n=263	Annotation Term	Count	%	PValue	Bonferoni
GOTERM_CC_FAT	GO:0005730~nucleolus	72	28.8	3.65E-72	5.40E-70
GOTERM_CC_FAT	GO:0031974~membrane-enclosed lumen	92	36.8	2.00E-51	2.96E-49
GOTERM_CC_FAT	GO:0070013~intracellular organelle lumen	90	36	1.63E-50	2.41E-48
GOTERM_CC_FAT	GO:0043233~organelle lumen	90	36	2.04E-50	3.02E-48
GOTERM_CC_FAT	GO:0031981~nuclear lumen	79	31.6	7.26E-47	1.07E-44
GOTERM_BP_FAT	GO:0022613~ribonucleoprotein complex biogenesis	42	16.8	2.68E-47	1.67E-44
GOTERM_BP_FAT	GO:0042254~ribosome biogenesis	39	15.6	3.33E-46	2.07E-43
GOTERM_BP_FAT	GO:0034470~ncRNA processing	43	17.2	5.16E-46	3.21E-43
GOTERM_BP_FAT	GO:0034660~ncRNA metabolic process	46	18.4	1.44E-45	8.96E-43

The other cluster to be found down-regulated in an IFN-dependent manner contained 28 genes that were highly associated with the cholesterol and sterol biosynthesis pathway (Figure 6.25 and Table 6.6).

Figure 6.25- IFN-dependent down-regulation of cholesterol biosynthesis genes (n28). The individual expression profiles of every gene in the cluster are shown in grey and the average expression profile of the cluster is shown in solid blue. Normalized log microarray intensity is shown on the Y axis and individual samples are arranged in temporal order on the X axis.

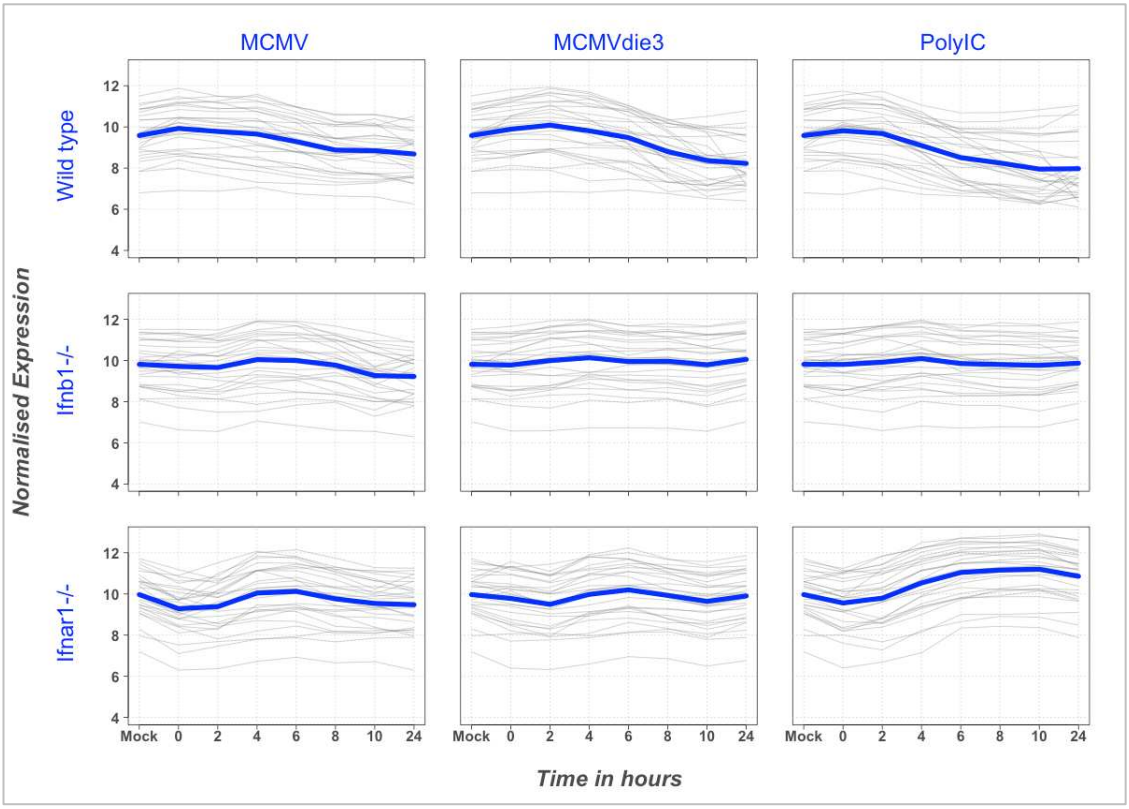

Table 6.6 - Annotation of 28 genes down-regulated in response to MCMV, MCMVdie3 and polyIC in an IFN-dependent manner. The DAVID annotation tool was used to find over-represented functional annotation classes within a group of 28 highly correlated genes. The top ten annotation classes are shown.

Category n=28	Annotation Term	Count	%	PValue	Bonferoni
SP_PIR_KEYWORDS	Steroid biosynthesis	17	68	9.04E-39	6.23E-37
SP_PIR_KEYWORDS	lipid synthesis	19	76	6.26E-37	4.32E-35
SP_PIR_KEYWORDS	sterol biosynthesis	14	56	2.07E-33	1.43E-31
GOTERM_BP_FAT	GO:0016126~sterol biosynthetic process	15	60	1.41E-33	2.29E-31
GOTERM_BP_FAT	GO:0006694~steroid biosynthetic process	16	64	5.75E-30	9.32E-28
GOTERM_BP_FAT	GO:0006695~cholesterol biosynthetic process	13	52	2.20E-29	3.57E-27
GOTERM_BP_FAT	GO:0016125~sterol metabolic process	16	64	2.21E-29	3.58E-27
SP_PIR_KEYWORDS	Cholesterol biosynthesis	12	48	5.39E-29	3.72E-27
GOTERM_BP_FAT	GO:0008610~lipid biosynthetic process	20	80	5.81E-29	9.41E-27
GOTERM_BP_FAT	GO:0008202~steroid metabolic process	17	68	1.60E-26	2.60E-24

Note: In order to improve the visualization and accessibility of microarray data generated in this experiment, an online web-visualization tool was created. This tool allows the user to query the data set based on gene symbol or Affymetrix Transcript ID. Individual expression profiles can be generated for any gene (probe) on the array. The web tool contains a database of expression profile images for every probe. These can be queried and returned as .png image files showing expression across all the conditions of the experiment. This tool is now available for members of the lab and will soon be made available for the wider community.

6.5 Cytokine secretion in response to MCMV and MCMVdie3 in wild-type and *Ifnar1-/-* BMDMs

Although many interesting observations had been made at the transcriptional level via the microarray profiling of IFN-deficient BMDMs, additional validation and assessment of macrophage immunological activity was required at the protein level. This would provide a more functional measure of immune activation in response to MCMV and MCMVdie3 infection in both the absence and presence of type I IFN signalling. For this purpose, a multiplexed bead-based ELISA assay was used to measure cytokine secretion in cell culture supernatants in response to MCMV and MCMVdie3 infection in wild-type and *Ifnar1-/-* BMDMs. Pro-inflammatory (TNFα, IL-6), chemoattractant (RANTES, MIG, MIP-2) and anti-inflammatory (IL-10) cytokines were measured at 2hpi, 6hpi and 10hpi and in mock-infected cells.

As seen in Figure 6.26, the secretion of chemoattractant cytokines RANTES and MIG were found to be completely dependent on the type I IFN receptor. The secretion of MIP-2 however, was found to occur independently of IFN and was secreted in *Ifnar1-/-* (Figure 6.26).

Figure 6.26 – Secretion of RANTES and MIG is dependent on the type I IFN receptor, but secretion of MIP-2 occurs in an IFN-independent manner.
BMDMs from wild-type and *Ifnar1-/-* mice were infected at MOI of 1 PFU/cell with either MCMV or MCMVdie3 and secreted protein levels were measured in cell culture supernatants for RANTES (**a ii**), MIG (**b ii**), and MIP-2 (**c ii**). Error bars indicate standard deviation from three separate cultures. The response to MCMV is shown in light grey and the response to MCMVdie3 is shown in dark grey. mRNA microarray profiles for each gene are also shown on the left (**i**).

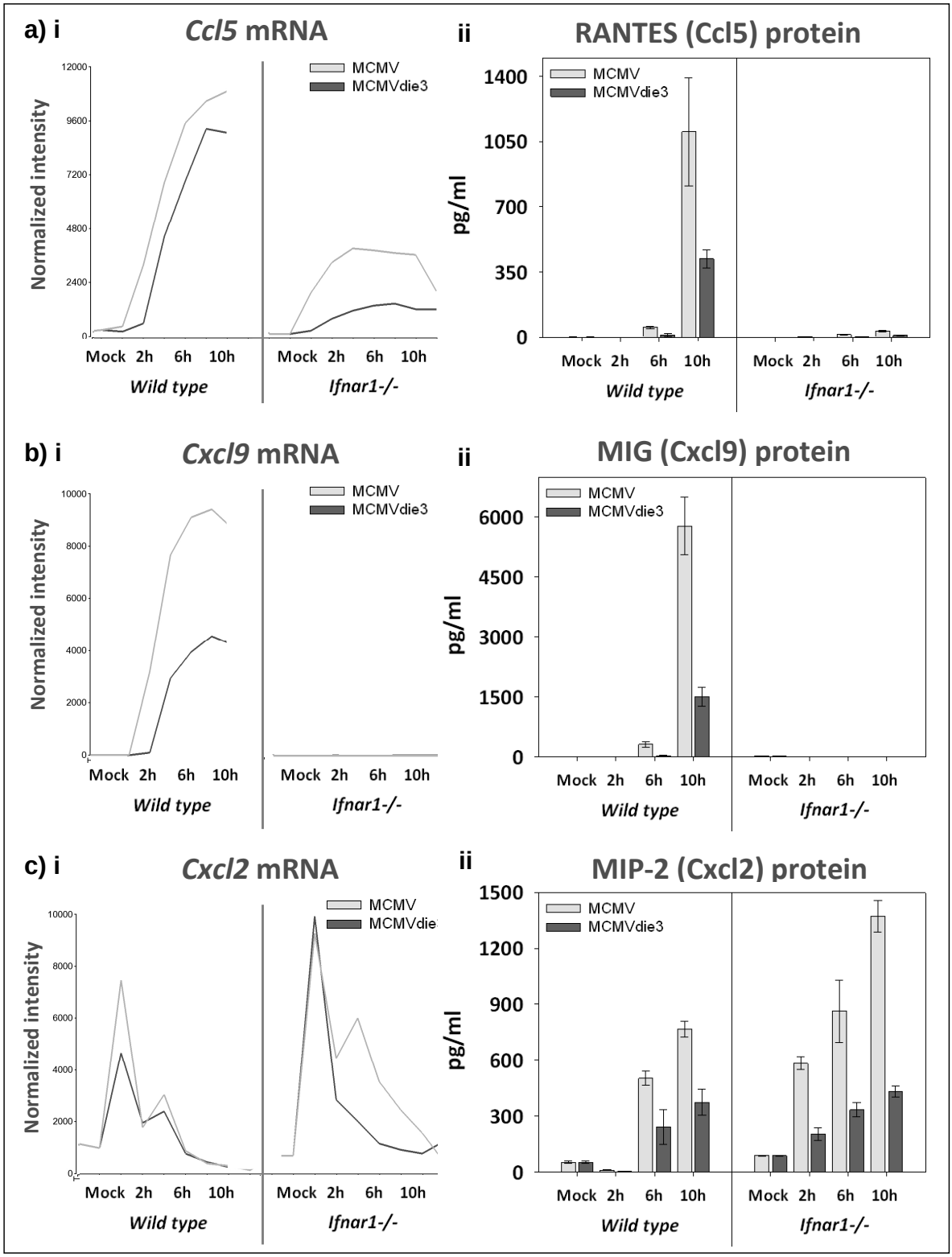
a) i
Ccl5 mRNA
Normalized intensity
MCMV
MCMVdie3
Mock 2h 6h 10h
Wild type
Ifnar1-/-
ii
RANTES (Ccl5) protein
pg/ml
b) i
Cxcl9 mRNA
MIG (Cxcl9) protein
c) i
Cxcl2 mRNA
MIP-2 (Cxcl2) protein

The secretion of pro-inflammatory cytokines TNF and IL-6 were measured in response to MCMV and MCMVdie3 in wild type and *Ifnar1-/-* BMDMs (Figure 6.27). TNF was induced independently of the IFN response in *Ifnar-/-* BMDMs, however levels of secretion for TNF were lower in *Ifnar1-/-* BMDMs compared to wild-type. The induction of IL-6, surprisngly, was found to be completely dependent on type I IFN receptor and no IL-6 was detectable in *Ifnar1-/-* BMDMs, at either the mRNA or secreted protein level.

Figure 6.27 - Secretion of TNF is partially dependent on *Ifnar1* and secretion of IL-6 in completely dependent on *Ifnar1* in BMDMs infected with MCMV. BMDMs from wild-type and *Ifnar1-/-* mice were infected at MOI of 1 PFU/cell with either MCMV or MCMVdie3 and secreted protein levels were measured in cell culture supernatants for TNF (**a ii**) and IL-6 (**b ii**)). Error bars indicate standard deviation from three separate cultures. The response to MCMV is shown in light grey and the response to MCMVdie3 is shown in dark grey. mRNA microarray profiles for each gene are also shown on the left (**i**).

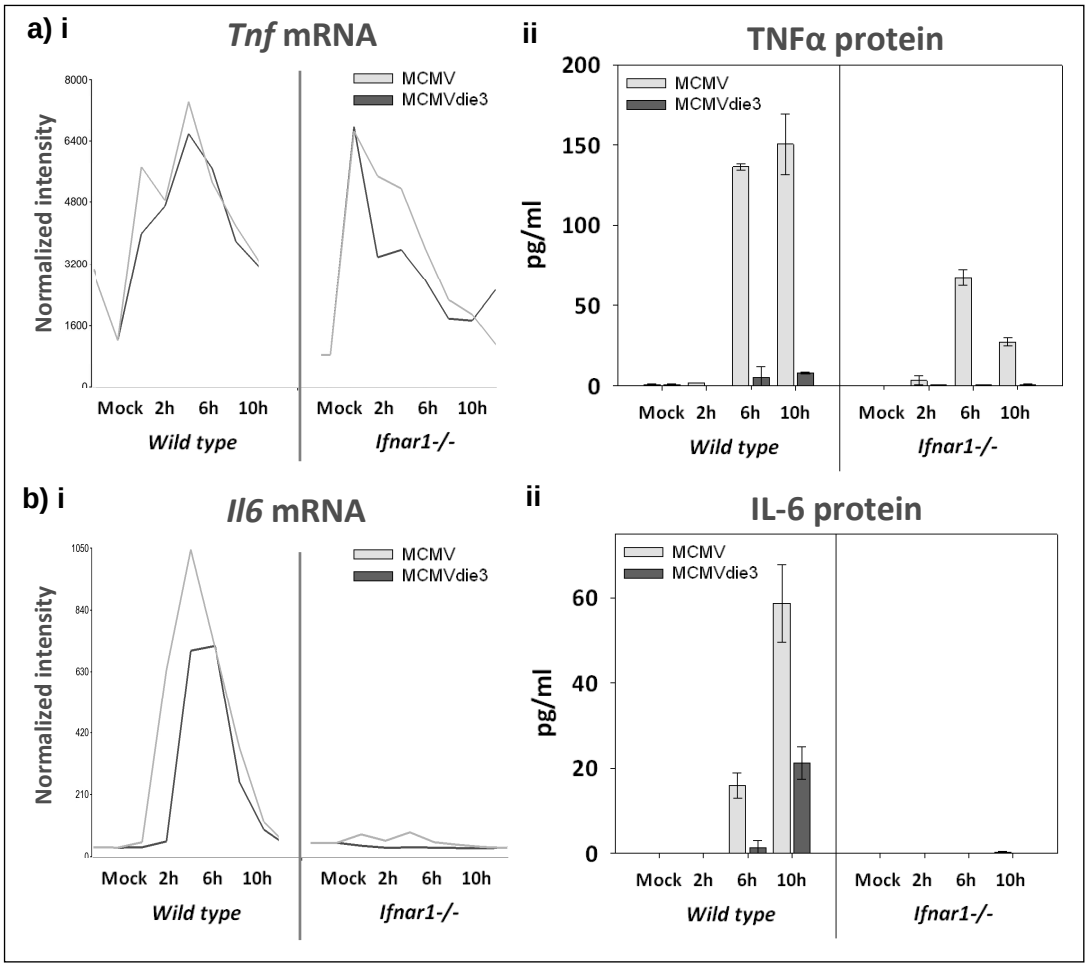

Figure 6.28 shows production of the anti-inflammatory cytokine IL-10 was also completely dependent on the type I IFN receptor. Again, in a similar manner to IL-6, induction of IL-10 at both the mRNA and protein level was undetectable in *Ifnar1-/-* BMDMs.

Figure 6.28 – Secretion of IL-10 is dependent on *Ifnar1* in BMDMs infected with MCMV. BMDMs from wild-type and *Ifnar1-/-* mice were infected at MOI of 1 PFU/cell with either MCMV or MCMVdie3 and secreted protein levels were measured in cell culture supernatants for TNF (**a ii**) and IL-6 (**b ii**)). Error bars indicate standard deviation from three separate cultures. The response to MCMV is shown in light grey and the response to MCMVdie3 is shown in dark grey. mRNA microarray profiles for each gene are also shown on the left (**i**).

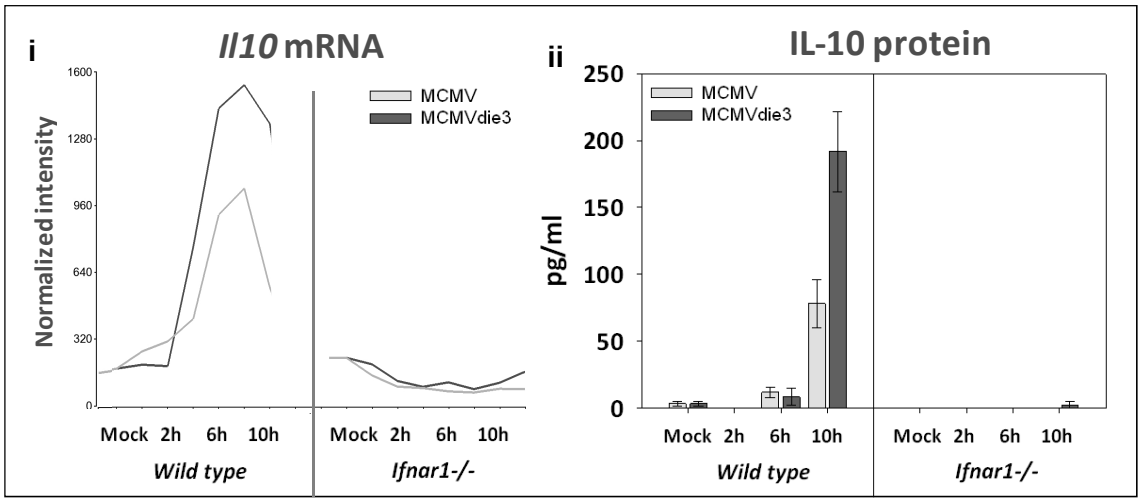

Discussion

The primary objective of this chapter was to determine the role of type I IFN in regulating previously identified gene expression networks during the macrophage response to MCMV infection. This was achieved through dynamic gene-expression profiling of wild type and *Ifnar1-/-* BMDMs infected with MCMV and MCMVdie3. In addition, the relationship between type I IFN and the macrophage transcriptome was investigated in depth using an exploratory clustering approach. This uncovered an extensive body of data providing unique insights into the different classes of genes regulated by type I IFN during the macrophage innate immune response. Finally, in order to integrate transcriptional and protein level data, cytokine secretion was measured in wild type and *Ifnar1-/-* BMDMs in response to MCMV and MCMVdie3 infection. In order to aid the discussion, Table 6.7 provides a summary of the findings in this chapter;

Table 6.7 Summary of Chapter 6 results

Preliminary analysis		
Fig.	**Result**	**Significance**
6.4	*Tnf* and *Icam1* are induced in *Ifnb1-/-* and *Ifnar1-/-* BMDMs	Induction of innate immune response genes still occurs in *Ifnb1-/-*, *Ifnar1-/-* BMDMs
6.5	*Ifnb1* induction is lower in *Ifnar1-/-* BMDMs than wild type	Basal endogenous type I IFN signalling is lower in *Ifnb1-/-* and *Ifnar1-/-* BMDMs
6.6	*Ifna1*, *Ifna2*, *Ifna5* and *Ifna7* are not induced in *Ifnb1-/-* and *Ifnar1-/-* BMDMs	Inducible type I IFN signalling is lower in *Ifnb1-/-* and *Ifnar1-/-* BMDMs
6.7	Induction of PRRs involved in MCMV detection (*Tlr3, Tlr9, Zbp1, Aim2*) is IFN-dependent	Up-regulation of MCMV detection mechanisms in BMDMs is regulated by type I IFN
Focused analysis on previously identified gene networks		
Fig.	**Result**	**Significance**
6.8	Genes up-regulated by MCMV and MCMVdie3 are strictly IFN-dependent	Genes induced by viral entry and/or pre-existing structural components of the virion are IFN-regulated
6.8	Genes down-regulated by MCMV and MCMVdie3 are partially IFN-dependent	Genes suppressed by viral entry and/or pre-existing structural components of the virion are partially IFN-regulated

6.9	Gene networks potentially modulated by productive MCMV infection are IFN-dependent	*De novo* MCMV proteins may modulate IFN-regulated genes during productive infection
6.10 6.11	Genes induced specifically in response to productive MCMV are IFN-independent	Mechanisms other than type I IFN up-regulate genes during the BMDM antiviral response to MCMV
Exploratory clustering analysis		
Fig.	**Result**	**Significance**
6.13	Genes involved in apoptosis are rapidly up-regulated in an IFN-independent manner	The apoptosis/NFkB response to virus infection is not regulated by type I IFN
6.14 6.15	Genes rapidly induced then shut-off in IFN-deficient BMDMs, but sustained in wild type BMDMs	Some genes require coordinate regulation from type I IFN and other mechanisms for sustained induction
6.16	Induction of *Csf1* is partially dependent on the type I IFN receptor	Type I IFN plays a role in *Csf1* regulation during the antiviral response in BMDMs
6.17 6.18	Genes down-regulated in an IFN-independent manner in response to all treatments	Many of the processes suppressed during the macrophage innate immune response are not controlled by type I IFN
6.19	Transcriptional induction of 776 genes with a strict dependence on the type I IFN receptor	776 “ISGs” in the BMDM transcriptome
6.20	Induction of *Gbp4*, *Serpina3f* and *Nos2* is strictly dependent on the *Ifnb1* gene	Some genes have a complete dependency on the *Ifnb1* gene for their induction, and others do not
6.23 6.24	Genes are down-regulated in an IFN-dependent manner in response to MCMV	Some down-regulated processes are controlled by type I IFN and others are not
6.25	Cholesterol biosynthesis genes are down-regulated upon MCMV infection in an IFN-dependent manner	Metabolic pathways in addition to innate immune response pathways are regulated by type I IFN
Cytokine secretion		
Fig.	**Result**	**Significance**
6.26 6.27 6.28	RANTES, MIG, IL-6, and IL-10 secretion occurs in an IFN-dependent manner	Regulation of some cytokines at the protein level is under strict IFN-control in BMDMs
6.26	MIP-2 secretion occurs in an IFN-independent manner	Regulation of some cytokines at the protein level are not under IFN control in BMDMs
6.27	TNF secretion is attenuated in *Ifnar1-/-* BMDMs in response to MCMV infection	Type I IFN may contribute to the regulation of TNF secretion in BMDMs

Preliminary analysis

Before proceeding with in-depth analyses of the microarray data, it was important to first establish whether the data was reliable from a technical and biological perspective. The cross-correlation plot (Figure 6.2) helped achieve this by showing 157 Affymetrix control probes highly correlated in their expression across all samples (Pearson>0.93). This indicated levels of transcription were comparable in the different samples, based on positive and negative controls, and that no outlier samples existed in the data set. In addition, commonly-used housekeeping genes *Gapdh, ActB* and *Ldh* were expressed to equivalent levels across all treatments and cell types.

The basal expression of type I ISGs was found to be considerably higher in wild-type BMDMs that in *Ifnar1-/-* or *Ifnb1-/-* BMDMs (Table 6.1). This is likely to be due to higher levels of STAT1-phosphorylation and higher rates of basal endogenous type I IFN signalling in wild-type BMDM cultures. This would be consistent with data previously shown by Fleetwood *et al*(97). The wild type BMDMs can therefore not be considered equivalent at the initial point of infection in comparison to *Ifnar1-/-* BMDMs. The implication of this result effects the interpretation of all data in this chapter.

As expected, *Ifnb1* and *Ifnar1* transcripts were not detected from the respective deleted loci in the knock-out BMDMs. *Ifnb1* transcripts were detected in *Ifnar1-/-* BMDMs, but notably attenuated (Figure 6.5). This provided more evidence of lower basal endogenous type I IFN signalling in *Ifnar1-/-* BMDMs, and evidence of a lack IFNβ positive feedback (125, 149, 150). The IFNβ feedback loop has been previously described in the literature to amplify the type I IFN response after the initial wave of IFNβ induction. During the primary wave, IFNβ is induced and secreted from the cell, then binds to the type I IFN receptor in an autocrine or paracrine manner to activate signalling through the JAK-STAT pathway. JAK-STAT signalling then leads to IRF7 activation which, in turn, results in a second transcriptional induction of IFNβ(214, 235). The IFNβ secondary feedback loop is

therefore dependent the type I IFN receptor for autocrine/paracrine signaling, and will, therefore, not occur in *Ifnar1-/-* BMDMs. A similar attenuation was also seen for the expression of *Ifna1*, *Ifna2*, *Ifna5* and *Ifna7* genes in *Ifnar1-/-* BMDMs, which is consistent with this interpretation (Figure 6.6).

Expression of *Ifna1, Ifna2, Ifna5* and *Ifna7* genes, however, was also attenuated in *Ifnb1-/-* BMDMs. In fact, these IFNα genes were not induced by any treatment in *Ifnb1-/-* or *Ifnar1-/-* cells, despite being induced to considerable levels in response to MCMV and polyIC in wild-type BMDMs (Figure 6.6). This result suggests that induction of *Ifna1, Ifna2, Ifna5* and *Ifna7* transcripts may also be dependent on the basal endogenous levels of IFN signalling, as well as the type I IFN positive feedback loop. A previous study also suggested IFNβ is required for induction of IFNα in mouse fibroblasts(90).

Another factor worth consideration, is the possibility that a deletion of the *Ifnb1* gene in construction of the *Ifnb1-/-* knockout mouse may have possibly caused a disruption in the expression of other type I IFN genes (*Ifna1, Ifna2, Ifna5* and *Ifna7)* which are all located within ~160-320kb of the *Ifnb1* locus on chromosome 4 of the mouse genome (NCBI37/mm9 July 2007 Assembly). It could be possible that deletion of the *Ifnb1* gene may have affected the other IFNα genes given their close proximity to the *Ifnb1* locus. Deletions in knock-out mice have been known to effect the expression of other genes in close proximity, especially those located on the opposite strand, or within the proximity of a regulatory region(266). Deletion of the *Ifnar1-/-* gene, however, could not have caused such an effect, as *Ifnar1* is located on a different chromosome (chr.16) in comparison to the type I IFNs (chr.4).

After assessing the expression of type I IFNs in wild-type, *Ifnb1-/-* and *Ifnar1-/-* BMDMs, *Tnf* and *Icam1* transcript levels were assessed to determine if the IFN-deficient BMDMs were still capable of mounting an innate immune response against MCMV infection and polyIC. These are IFN-independent genes known to be involved in the innate immune response to infection. *Tnf* and *Icam1* were strongly induced in WT, *Ifnb1-/-* and *Ifnar1-/-* BMDMs in response to MCMV, MCMVdie3

and polyIC (Figure 6.4). This result indicated that *Ifnb1-/-* and *Ifnar1-/-* BMDMs were still capable of mounting an innate immune response to MCMV infection and polyIC stimulation at the gene expression level.

The transcriptional induction of intracellular pattern recognition receptors involved in detection of MCMV was also assessed as a general point of interest. This gave an indication as to the transcriptional profile for some key genes involved in the MCMV response. The expression profiles for *Tlr3*, *Tlr9*, *Zbp1*, and *Aim2* were all regulated in an IFN-dependent manner and with similar kinetics (Figure 6.7).

Focused analysis on previously identified gene networks

The networks identified in previous chapters were overlaid onto the new microarray data and assessed in parallel for their expression in both the presence and absence of type I IFN signalling. This was a fruitful exercise and revealed a number of significant and unexpected results regarding the transcriptional control of these networks by type I IFN.

Firstly, genes up-regulated as part of the initial PRR response to MCMV (i.e. genes. induced in an equivalent manner in response to MCMV *and* MCMVdie3) were strictly dependent on the type I IFN receptor for their regulation (Figure 6.8a). This result suggested the initial PRR response to incoming structural components of the MCMV virion is controlled by type I IFN in BMDMs. This observation is consistent with previous studies reporting IFN-induced transcription in response to both live and UV-inactivated virions early in the response(43, 211, 263, 330, 359). These genes may also be regulated by paracrine type I IFN signalling in BMDM cultures.

Genes down-regulated equivalently by MCMV *and* MCMVdie3 infection were also found to have a strong dependency on the type I IFN receptor (Figure 6.8b). This observation suggests suppression of genes, as well as induction of genes, is under IFN-control during the early stages of the antiviral response (0-6hpi). Furthermore, it indicates incoming structural components of the MCMV virion are sufficient to

induce the down-regulation, as well as up-regulation, of many genes in an IFN-dependent manner. Genes down-regulated in this fashion were mostly involved in cell cycle and DNA replication, suggesting a close link between type I IFN regulation and the cell cycle. This is consistent with the well-documented anti-proliferative properties of type I IFNs(16, 26, 38). Genes in this group are also likely to be regulated, at least in part, by paracrine type I IFN signalling in BMDM cultures.

The four gene networks identified as potentially modulated by productive MCMV infection in Chapter 5 (suppressed or inhibition by wild-type virus only) were also found to have a strong dependency on the type I IFN receptor for their regulation (Figure 6.9). This dependency was seen for up-regulated Cluster 1 and 2 (Figure 6.9a-b), and down-regulated Clusters 3 and 4 (Figure 6.9c-d). This result indicated candidate genes potentially targeted for modulation by *de novo* MCMV proteins are part of the type I IFN response. However not all IFN-regulated genes appear to be affected in this manner. This may suggest that MCMV is capable of targeting certain sub-sets of IFN-regulated genes with specificity during productive infection. The ability of viruses to target the type I IFN response with some level of specificity has been described in detail (44, 185, 282, 295, 306, 307, 376), including for MCMV(237), but the ability of MCMV to target specific transcriptional gene networks has not been described in depth. This effect may be related to the function of MCMV protein M27, which has been shown to modulate *Stat2* activity during infection(392).

If MCMV is capable of targeting macrophage gene expression networks with specificity, it is logical that those networks should be involved in the antiviral response to MCMV infection. This appears to be the case, as the up-regulated MCMV-modulated gene networks are closely associated with immune cell trafficking and leukocyte recruitment (Figure 5.6), and were regulated in an IFN-dependent manner (Figure 6.9a-b). The down-regulated candidate genes are associated with cell cycle control and apoptosis (Figure 5.8), areas which are known to be targeted by MCMV during productive infection(10, 119, 244, 379).

Further evidence of the specificity of MCMV in targeting certain macrophage genes during the antiviral response is the suppression of *Tlr9* (discussed in detail in Chapter 5). From a biological and evolutionary perspective, it is particularly logical for the virus to target the expression of PRRs directly involved in its own detection. *Tlr9* is an example of this, and appears to be targeted with particular specificity by MCMV. The induction of the *Tlr9* gene is also IFN-dependent (Figure 6.7), again suggesting MCMV may be capable of targeting specific IFN-regulated genes during macrophage infection. In the case of *Tlr9*, this effect may be restricted to mouse given that TLR9 is not expressed by human macrophages.

Next, the network of genes induced specifically by productive MCMV infection between 10-24hpi was assessed. These genes were found to be induced in an IFN-independent manner, specifically in response to productive MCMV infection (Figure 6.10). These genes were induced to equivalent levels in wild type and *Ifnar1-/-* BMDMs, but were not induced by MCMVdie3 or polyIC in any cells. The clustering analysis further identified over 800 genes displaying a similar induction profile (induced specifically in response to productive MCMV infection, Pearson>0.9), suggesting this response is more widespread than originally thought. In fact, this class of genes was the most abundant class of any to be found by the clustering analysis (Figure 6.13). This indicates a marked difference in the transcriptomes of productively and non-productively infected BMDMs, even despite low levels of infection at MOI of 1.

The unanswered question regarding these genes is still, however, are they pro- or anti-viral, or merely a metabolic bi-product of lytic infection? Further experimentation is ongoing to answer these questions. Functional annotation of this class of genes identified over-represented terms associated with *glycoprotein* (p1.16E-26) and *plasma membrane* (p6.59E-26). Although these terms are generalized and non-specific, they may indicate some requirement of membrane synthesis and/or glycoprotein production for newly synthesized MCMV virions during productive infection at the end of the replication cycle.

Exploratory clustering analysis

The core relationship between type I IFN and the macrophage transcriptome was made apparent by distinct clustering of co-expressed genes in the exploratory analysis. This identified of both IFN-dependent and IFN-independent gene clusters regulating during the macrophage response to MCMV infection.

The profile of each cluster was presented, along with over-represented functional annotation terms for each cluster. The functional annotation analysis, although informative, was limited in describing the function of each cluster. Some annotation terms (e.g. *glycoprotein, phosphoprotein activity, membrane,* and *signal*) were non-specific and non-informative. Despite this, the functional annotation still provided a reasonable indication of gene activity for most of the different clusters. It also provided an indication of which biological processes were influenced most, or least, by type I IFN signalling.

IFN-independent gene expression

In addition to identifying genes directly regulated by type I IFN, it was also equally important to identify genes regulated in an IFN-independent manner. IFN-independent genes represent alternate signalling pathways activated in parallel to type I IFN during the antiviral response, and may therefore indicate distinct areas of biology not associated with type I IFN regulation.

48 pro-inflammatory genes were induced in an IFN-independent manner in response to all three treatments (Figure 6.13). Genes in this group included *Tnf*, NF-kB subunits (*Nfkb1, Nfkb2, Nfkbia, Nfkbie, Relb*), TNF associated genes (*Traf2, Fas*), and transcription factors regulating apoptosis (*Bcl2a1a, Bcl2a1b, Bcl2a1c, Bcl2a1d*). The up-regulation of these genes represents an alternative arm of the innate immune response induced by MCMV that is Myd88-dependent and regulated independently of type I IFN signalling(100, 134, 247). Over-represented annotation categories for

this group were *apoptosis* and *NF-kB* signalling, suggesting type I IFN does not contribute to the control of these processes at the transcriptional level in BMDMs.

In the literature however, there is evidence of cross-talk between the type I IFN and NF-kB systems (88, 203, 304, 371), and the relationships between type I IFN and apoptosis (153, 179, 371), and type I IFN and the pro-inflammatory response (196). It is possible that the type I IFN and NF-kB responses are regulated independently at the transcriptional level, as seen in this study and elsewhere(120, 264), but interact or overlap at the protein level. Alternatively, some genes may play a role in signalling to both IFN and NF-kB pathways, but are regulated in a different manner to genes in this cluster.

In addition to the up-regulation of IFN-independent genes, there were 25 genes induced rapidly (by 2hpi) in response to all three treatments, but shutoff in *Ifnb1-/-* and *Ifnar1-/-* BMDMs by 6hpi (Figure 6.14 and 6.15). The expression of these genes in wild type BMDMs, however, was sustained until past 10hpi. Genes in this group, therefore, appear to be regulated by both IFN-dependent and IFN-independent mechanisms. It was notable that these genes, although attenuated, were still inducible in *Ifnb1-/-* and *Ifnar1-/-* BMDMs. This suggests their initial induction does not require type I IFN signalling, however, their sustained expression does require IFN. Genes in this group included *Irf1* and *Socs3*, and other important innate immune response genes (*Ccl3, Ccl4, Junb, Nfkbiz, Nod2, Tank*).

Csf1 also displayed a similar profile to this cluster and was strongly induced by MCMV infection (Figure 6.16). This has potentially significant implications, as CSF-1 is required for macrophage proliferation and survival (156). The induction of *Csf1* was higher in wild type BMDMs than *Ifnb1-/-* and *Ifnar1-/-* BMDMs, suggesting a contribution of type I IFN regulation to *Csf1* induction. Evidence exists of regulation at the *Csf1* promoter by NF-kB(147), AP1 and CNBP(195), cAMP and IL1α(183), the SWI/SNF-like BAF Complex(222). There has also been a report of IFNγ-activated STAT1 regulation of *Csf1* via GAS response elements(360). It therefore

appears that *Csf1* may be regulated by both IFN-dependent and IFN-independent factors. This also appears to be the case for *Irf1*(161, 192) and *Socs3*(19, 139, 292).

The exploratory analysis identified clusters of genes down-regulated in an IFN-independent manner in response to all three treatments (Figures 6.17 and 6.18). One of these clusters (Figure 6.18) contained 428 genes which were highly associated with the cell cycle (i.e. *chromosome, cell cycle, cell cycle phase, M phase, cell division, mitosis* etc). The p-values for over-representation of these annotation terms were highly significant (ranging from 3.47E-90 to 1.15E-70). This high level of significance suggests regulation of the cell cycle is under strict control at the gene expression level in BMDMs. These genes, however, were only moderately influenced by type I IFN signalling. The generalized down-regulation of cell cycle genes during the macrophage innate immune response may be associated with a shift away from macrophage differentiation, and towards an activated macrophage M1 phenotype(240).

IFN-dependent gene expression

One of the key novel aspects of conducting the transcriptional profiling analysis of IFN-deficient macrophages was to identify ISGs with a strict dependency on the type I IFN receptor. This would provide a level of mechanistic dependence above and beyond the ISGs described in current ISG databases(8, 72, 318) that have been derived based on exogenous IFN treatment.

For this purpose, a cluster of 776 IFN-dependent inducible genes was identified (Figure 6.19). Genes in this cluster were generally induced strongly by MCMV, MCMVdie3 and polyIC in wild type BMDMs, and not induced in *Ifnar1-/-* BMDMs. This cluster effectively identifies ISGs during the macrophage innate immune response with a strict dependency on the type I IFN receptor for their induction. Interestingly, many genes within this cluster do not have annotation associated with the IFN response (for complete list see Supplementary File 21).

Most genes in the 'ISG' cluster were induced to mild levels in *Ifnb1-/-* BMDMs, indicating either a partial contribution of other type I IFNs (i.e. IFNα genes), or a deficiency in basal type I IFN signalling in *Ifnb1-/-* BMDMs. IFNβ is known to have an increased affinity of binding to the type I IFN receptor in comparison to IFNα(204, 205, 215, 236, 296) which may explain, in part, the profile of this cluster. However, the expression of IFNα genes themselves was very low in *Ifnb1-/-* BMDMs (Figure 6.6), suggesting a lower basal level of endogenous IFN signalling prior to infection/stimulation.

Some ISGs in the data set were completely non-induced in the *Ifnb1-/-* BMDMs, suggesting a complete dependency on the *Ifnb1* gene. The best examples of such genes were *Gbp4, Serpina3f* and *Nos2* (Figure 6.20). The strict dependency of these genes on *Ifnb1* suggests redundancy amongst type I IFNs is not applicable for all ISGs. Examples of genes with this strict dependency, however, were rare and may be attributable to variations in probe efficiencies and/or signal below the limit of detection in *Ifnb1-/-* BMDMs.

Genes down-regulated in an IFN-dependent manner also provided valuable insights into the type I IFN response (Figures 6.23, 6.24 and 6.25). One down-regulated gene cluster was blocked, or inhibited, in its down-regulation by productive MCMV infection (Figure 6.24). This group of genes was down-regulated in response to MCMVdie3 and polyIC, but not in response to the parental strain of MCMV in wild-type BMDMs. Genes in this cluster were highly associated with the *nucleolus*, *membrane enclosed lumen*, and *ribosome biogenesis* (Table 6.5). These genes represent an area of biology possibly targeted by MCMV proteins during productive macrophage infection.

If this is the case, it could be related to MCMV replication occurring in and around the nucleus, or could be related to specific *de novo* MCMV protein function. Viral proteins have been shown to localize to the nucleolus during HSV, IBV and HIV infection (reviewed in (372), and interactions between MCMV(50, 287) and HCMV(14, 383) proteins have been shown to occur with distinct compartments of the nucleus during infection. Therefore, it may be possible that MCMV proteins influence the expression of nucleolus-related genes during infection. A direct functional link between the type I IFN response and this group of genes is difficult to establish. IFN-induced proteins have also been reported to localize in the nucleolus(29, 59, 173, 221, 378), and it may be possible that these genes contribute to the regulation of this particular cluster.

Finally, a group of 28 co-regulated genes were found to be down-regulated by all three treatments in wild type BMDMs, but not down-regulated in *Ifnb1-/-* or *Ifnar1-/-* BMDMs (Figure 6.25). This group indicated another biological process down-regulated in an IFN-dependent manner, as genes in this cluster were highly associated with *cholesterol biosynthesis* and *lipid metabolism* (Table 6.6). This result suggests genes involved in cholesterol biosynthesis are regulated by type I IFN at the gene expression during the response to MCMV infection. This is consistent with the recent findings of Blanc *et al.* at the Division of Pathway Medicine, University of Edinburgh (33)

Overall, the results from the exploratory clustering analysis provided an unique insight into type I IFN regulation of macrophage gene expression during MCMV infection. These insights have not previously been made on this scale, especially in relation to the kinetics of IFN-regulated genes during virus infection. One other study however did investigate temporal gene expression in *Ifnb1-/-* macrophages stimulated with LPS response (355) and found distinct patterns of macrophage gene expression affected by IFNβ. Many of the genes regulated by IFNβ in response to LPS were overlapping with genes regulated by IFNβ in response to MCMV infection. For example, genes such as *Nos2* (iNOS), *Cxcl10* (IP-10) and *Il12 p40* had a strong dependency on IFNβ in both studies, whereas *Tnf* gene expression had little or no dependency on IFNβ in either study. Comparable measurements were also made at the secreted protein level for cytokines IP-10, RANTES and TNF in both studies. IP-10 and RANTES had a strong dependence on type I IFN for secretion in both cases, where as there was only a partial affect of type I IFN on TNF secretion in both studies.

Similar results were also seen in another study investigating the response to Coronavirus infection in *Ifnar1-/-* BMDMs(391). This study showed induction of IFNβ and ISGs (RIG-I, MDA5) was dependent on the type I IFN receptor in response to Coronavirus infection. Secretion of cytokines CXCL10 and IL-10 was also shown to have a strong dependency on the type I receptor, whereas secretion of TNF was only partially reduced in *Ifnar1-/-* BMDMs. These observations were not seen in BMDCs used in the same study.

The response to Listeria monocytogenes(210) has also been investigated in depth using *Ifnar1-/-* macrophages. The response to LPS and bacteria, however, has important differences to the antiviral response at the genome-wide level(174).Tissues from virus-infected IFN knockout mice have also been previously profiled using microarrays(120, 293), however these studies did not encompass any temporal profiling analysis, and were not conducted in controlled experimental setting.

In terms of the overall patterns of transcriptional regulation and genetic dependency observed in this study, it is unclear as to whether these patterns will be equivalent in other cell types, in other experimental settings, or indeed *in vivo*. There will certainly be some major differences in IFN-regulated gene expression in BMDMs and in other contexts, however for many genes, if a true mechanistic dependency on the type I IFN receptor does exists, the dependency should be maintained across other cell types and tissues. If this is the case, the level of information presented here should be of genuine value to the wider community.

Cytokine secretion

After conducting an extensive transcriptional profiling analysis of macrophages at the gene-expression level, it was also important to make measurements at the protein level to provide a more function indication of the response. Having data at both the transcriptional and protein level would provide a more comprehensive systems-level analysis in terms of understanding the response to productive and non-productive MCMV infection, especially in relation to type I IFN signalling. To achieve this, a multiplex bead-based ELISA assay was used to measure secreted cytokine levels BMDM supernatants in response to MCMV and MCMVdie3 infection.

Pro-inflammatory (TNF, IL-6), chemoattractant (RANTES, MIG, MIP-2) and anti-inflammatory (IL-10) cytokines were measured in wild type and *Ifnar1-/-* BMDMs at 2hpi, 6hpi and 10hpi. These cytokines were chosen based on a) their known roles in the innate immune response, b) transcriptional profiles of interest from in the microarray data, and c) availability as part of a multiplexed ELISA platform (see Methods).

Analysis of chemoattractant cytokine secretion indicated secretion of RANTES (*Ccl5*) and MIG (*Cxcl9*) were strictly dependent on the type I IFN receptor at the protein level (Figure 6.26). This result indicated an example IFN-regulated cytokine secretion during the macrophage innate immune response. RANTES (Ccl5) and MIG

(*Cxcl9*) were also not induced at the gene expression level in *Ifnar1-/-* BMDMs, suggesting a mechanistic dependency on type I IFN for their transcriptional regulation.

In contrast, secretion of MIP-2 (*Cxcl2*) occurred independently of the type I IFN receptor (Figure 6.26). Expression of MIP-2 was equivalent or higher in *Ifnar1-/-* BMDMs than in wild type cells, at both the mRNA and protein level. This represents an example of IFN-independent chemoattractant cytokine secretion during the innate immune response in macrophages.

TNF was secreted to high levels specifically in response to productive MCMV infection in wild type BMDMs as per previous experiments (see Chapter 4), however the levels of TNF secretion in *Ifnar1-/-* BMDMs were notably attenuated in comparison to wild type BMDMs (Figure 6.27). This result was unexpected as TNF regulation is controlled primarily by NF-kB and induction has been previously described to occur independent of IFN signalling(92, 281). Some evidence does, however, exist for the contribution of type I IFN signalling in regulation of TNF (355, 384).

IL-6, which has also been shown to regulated primarily by NF-kB at the gene-expression level(216, 327, 368), was induced in a strictly IFN-dependent manner. IL-6 secretion was not detectable in *Ifnar1-/-* BMDMs, and *Il6* transcripts were also below the detection limit of the microarray (Figure 6.27). This result was not expected, and suggested IL-6 may be regulated in an IFN-dependent manner in BMDMs. This is not consistent with the literature, as most published reports focus on the contribution of NF-kB in the transcriptional control of the *Il6* gene(216, 327, 368). Interestingly, however, interferon regulatory factor 1 (*Irf1*) has been shown to play a role in *Il6* regulation(319).

IL-10, the only anti-inflammatory cytokine to be measured, was also found to be induced in a strictly IFN-dependent manner at both the transcriptional and secreted cytokine level (Figure 6.28). Similar to *Tnf* and *Il6*, regulation of the *Il10* gene has

traditionally not been associated with type I IFN signalling(201), and therefore the strict type I IFN dependency observed was not expected. The human *Il10* gene has been shown to be regulated by *Stat3*(363), and mouse *Il10* has also been shown to be regulated by type I IFN in response to LPS stimulation in BMDMs(97).

The results for IL-6 and IL-10, from these experiments, suggest some degree of mechanistic dependence on type I IFN in BMDMs. This result, however, may be related to the attenuated level of basal endogenous type I IFN signalling in *Ifnar1-/-* BMDMs or the level of TNF in the BMDM supernatants. It is also worth noting that protein levels for some of the cytokines, especially Il-6, were quite low (below 200pg/ml). Although this level is still above the detection limit of the assay, higher expression would give more confidence in the data. In addition, the dependency of these factors on type I IFN could potentially be cell-type specific phenomenon, only seen in BMDMs. Again, further experimentation will be required to determine if this is the case.

Overall, the cytokine data provided evidence of a close link between type I IFN regulation and the expression of chemoattractant, pro-inflammatory, and anti-inflammatory cytokines during the macrophage antiviral response to MCMV, observations which are supported by at least one other study(97).

Chapter 7
Final conclusions

The results presented in this thesis represent a number of new findings. Firstly, a genetically modified MCMV strain has been used to represent attenuated (non-productive) viral infection. This approach is an alternative to the UV-inactivation of MCMV which has been used for a number of previous studies(18, 48, 373, 379). The approach of using the MCMVdie3 as an alternative to UV-MCMV has some key advantages, such as the propagation of large quantities of virus on a complementing cells line, and the avoidance of variation between UV-inactivation batches. The approach, however, also has some disadvantages including residual expression of IE genes by the mutant virus, and the potential for secondary site mutations during repeated passage in a complementing cell line.

A major issue in this thesis was the low level of infection achieved in BMDM cultures at MOI of 1 PFU per cell. This meant the phenotypes measured in many of the BMDM experiments were possibly due to paracrine signalling factors, rather than the direct effects of viral infection. To avoid this problem, in hindsight a higher MOI could have been used, or alternatively a more permissive cell-type could have been used. The approach of using a high MOI in a more permissive cell type is consistent with most of the comparable studies in the literature (43, 142, 260, 263, 289, 345). Using BMDMs, however, represents a more physiologically relevant system and a more robust innate immune response to viral infection.

Despite the low levels of infection, important differences were still seen between the response to MCMV and MCMVdie3 at MOI for 1 PFU/cell in BMDMs. This was particularly the case for sub-sets of genes induced specifically by productive infection at 10-24hpi, and the secretion of TNF which occurred only in response to productive infection. These two results represent new findings in light of the literature, and suggest even low levels of productive viral infection in macrophages

are sufficient to induce higher levels of innate immune signalling, either due to host factors or as a result of *de novo* MCMV proteins.

The other novel aspect of the thesis is the time-series gene expression data generated using macrophages from wild-type, *Ifnb1-/-* and *Ifnar1-/-* BMDMs. This data represents a rich and unique resource that does not currently exist in the published literature. Other gene expression profiling studies have been conducted using cells from *Ifnb1-/-* and/or *Ifnar1-/-* mice to investigate the LPS response in macrophages(355), the response to Listeria monocytogenes in macrophages (210), the response to MHV infection in mouse brain tissues (293), and the response to influenza in fibroblasts(120). The response to Coronavirus in *Ifnar1-/-* macrophages has also been measured, but only for a limited number of genes using qRT-PCR(391). None of the abovementioned studies have the depth or resolution of temporal genome-wide profiling compared to the data generated in this thesis. The most similar study, which uses LPS stimulation(355), is comparable in many of the genes identified, but represents a distinct immune stimulus (LPS) compared to virus infection.

The line of experimentation taken in this thesis, like for most studies, has been shaped by the range of techniques available over the period of the investigation. At the beginning of the study, there was a unique opportunity to have access to Affymetrix facilities, including wash, scan and hybridization stations. In addition, there was access to considerable expertise in microarray data analysis and bioinformatics, and an abundance of pre-existing microarray data generated from within the group. The BMDM culture system had also been optimized and was fully operational. For these reasons, a genomics data-driven approach in BMDMs, rather than a hypothesis-driven approach, was taken from the outset.

There are a number of advantages and disadvantages in using a data-driven approach, as opposed to a purely hypothesis-driven approach. One of the key advantages is generating large data sets which are unbiased and can lead to unexpected and unpredicted findings. This often leads to generation of new hypotheses for future

experiments based on data, rather than on preconceptions. The disadvantages of using a data-driven approach, however, are that investigations can often become observational and descriptive, rather than mechanistic in their scope, especially in the case of microarray data. This, I believe, has occurred somewhat with the current body of work, which could be considered by some to be descriptive, rather than mechanistic in its scope. In addition, generalized observations made at the gene expression level can often be misleading, and may not necessarily reflect the most important functional aspects. For these reasons, an attempt to expand the study to the protein level was made through the use of ELISA, and although this was informative, the study could still be further strengthened by the addition of more functional protein-level data.

There are now a number of new techniques available to the group, either directly or through collaborators, that could improve the overall scope of this study. These were not available at the outset and include the use of proteomic and lipidomic profiling techniques to measure the macrophage response to MCMV infection. These techniques are now generating informative data sets to complement gene expression-level observations made in this study. In addition, the transcriptional regulation of macrophage genes can be investigated in more detail using ChIP-seq analysis. Incorporating data from these new techniques, into the observations made in this study, would be undoubtedly beneficial to the overall understanding of the system. In addition, there are a number of other experiments that have been planned to follow up observations from made in this study. These include an investigation of the MCMV M27 ORF, and siRNA screening approach for IFN-dependent and IFN-independent antiviral genes. Although screening will be conducted in fibroblasts, it should still provide valuable insights into the function of macrophage genes in relation to MCMV infection.

Other key findings of this study include the suppression of *Tlr9* by *de novo* MCMV proteins, the differential regulation of IL-10, and the specific up-regulation of genes in response to productive MCMV infection. These findings are being investigated further, and the work is ongoing. In addition to these findings, two key research tools

were also been developed as part of this thesis. These are the qPCR assay to measure MCMV genome copies in infected cells, and the MCMVdie3 mutant virus which can now be used as a valuable control reagent. These tools are useful to other members of the group, and are already being used to aid other studies.

The thesis has filled a niche in the field, and has provided the first investigation of the host response to productive and non-productive MCMV infection in macrophages. As a result, our understanding of the macrophage response to MCMV infection, and to virus infection in general, has been improved. The study has also provided arguably the most detailed account macrophage gene expression in the presence and absence of type I IFN signalling to date. This should be of significant benefit to the wider community.

Appendix 1

Manuscript:

Temporal profiling of the coding and non-coding murine cytomegalovirus transcriptomes

Accepted for publication in *The Journal of Virology*, 30/03/2010

For manuscript see Supplementary Files CD

References

1. 2001. Creating the gene ontology resource: design and implementation. Genome Res **11:**1425-33.
2. **Abenes, G., M. Lee, E. Haghjoo, T. Tong, X. Zhan, and F. Liu.** 2001. Murine cytomegalovirus open reading frame M27 plays an important role in growth and virulence in mice. J Virol **75:**1697-707.
3. **Abraham, A. K., L. Kagan, S. Kumar, and D. E. Mager.** Type I interferon receptor is a primary regulator of target-mediated drug disposition of interferon-beta in mice. J Pharmacol Exp Ther **334:**327-32.
4. **Adam, E., J. L. Melnick, J. L. Probtsfield, B. L. Petrie, J. Burek, K. R. Bailey, C. H. McCollum, and M. E. DeBakey.** 1987. High levels of cytomegalovirus antibody in patients requiring vascular surgery for atherosclerosis. Lancet **2:**291-3.
5. **Adler, B., and C. Sinzger.** 2009. Endothelial cells in human cytomegalovirus infection: one host cell out of many or a crucial target for virus spread? Thromb Haemost **102:**1057-63.
6. **Alcami, A.** 2003. Viral mimicry of cytokines, chemokines and their receptors. Nat Rev Immunol **3:**36-50.
7. **Amit, I., M. Garber, N. Chevrier, A. P. Leite, Y. Donner, T. Eisenhaure, M. Guttman, J. K. Grenier, W. Li, O. Zuk, L. A. Schubert, B. Birditt, T. Shay, A. Goren, X. Zhang, Z. Smith, R. Deering, R. C. McDonald, M. Cabili, B. E. Bernstein, J. L. Rinn, A. Meissner, D. E. Root, N. Hacohen, and A. Regev.** 2009. Unbiased reconstruction of a mammalian transcriptional network mediating pathogen responses. Science **326:**257-63.
8. **Anan'ko, E. A., S. I. Bazhan, O. E. Belova, and A. E. Kel.** 1997. [Mechanisms of transcriptional regulation of interferon-induced genes: description in the IIG-TRRD information system]. Mol Biol (Mosk) **31:**701-13.
9. **Anderson, P., K. Phillips, G. Stoecklin, and N. Kedersha.** 2004. Post-transcriptional regulation of proinflammatory proteins. J Leukoc Biol **76:**42-7.
10. **Andoniou, C. E., and M. A. Degli-Esposti.** 2006. Insights into the mechanisms of CMV-mediated interference with cellular apoptosis. Immunol Cell Biol **84:**99-106.
11. **Andrejeva, J., K. S. Childs, D. F. Young, T. S. Carlos, N. Stock, S. Goodbourn, and R. E. Randall.** 2004. The V proteins of paramyxoviruses bind the IFN-inducible RNA helicase, mda-5, and inhibit its activation of the IFN-beta promoter. Proc Natl Acad Sci U S A **101:**17264-9.
12. **Angulo, A., P. Ghazal, and M. Messerle.** 2000. The major immediate-early gene ie3 of mouse cytomegalovirus is essential for viral growth. J Virol **74:**11129-36.
13. **Ank, N., and S. R. Paludan.** 2009. Type III IFNs: new layers of complexity in innate antiviral immunity. Biofactors **35:**82-7.
14. **Arcangeletti, M. C., F. De Conto, F. Ferraglia, F. Pinardi, R. Gatti, G. Orlandini, A. Calderaro, F. Motta, M. C. Medici, M. Martinelli, P.**

Valcavi, S. V. Razin, C. Chezzi, and G. Dettori. 2003. Human cytomegalovirus proteins PP65 and IEP72 are targeted to distinct compartments in nuclei and nuclear matrices of infected human embryo fibroblasts. J Cell Biochem **90:**1056-67.

15. **Asselin-Paturel, C., A. Boonstra, M. Dalod, I. Durand, N. Yessaad, C. Dezutter-Dambuyant, A. Vicari, A. O'Garra, C. Biron, F. Briere, and G. Trinchieri.** 2001. Mouse type I IFN-producing cells are immature APCs with plasmacytoid morphology. Nat Immunol **2:**1144-50.
16. **Bach, E. A., M. Aguet, and R. D. Schreiber.** 1997. The IFN gamma receptor: a paradigm for cytokine receptor signaling. Annu Rev Immunol **15:**563-91.
17. **Baechler, E. C., F. M. Batliwalla, G. Karypis, P. M. Gaffney, W. A. Ortmann, K. J. Espe, K. B. Shark, W. J. Grande, K. M. Hughes, V. Kapur, P. K. Gregersen, and T. W. Behrens.** 2003. Interferon-inducible gene expression signature in peripheral blood cells of patients with severe lupus. Proc Natl Acad Sci U S A **100:**2610-5.
18. **Bale, J. F., Jr., M. E. O'Neil, and T. Greiner.** 1985. The interaction of murine cytomegalovirus with murine neutrophils: effect on migratory and phagocytic activities. J Leukoc Biol **38:**723-34.
19. **Barclay, J. L., S. T. Anderson, M. J. Waters, and J. D. Curlewis.** 2007. Characterization of the SOCS3 promoter response to prostaglandin E2 in T47D cells. Mol Endocrinol **21:**2516-28.
20. **Barczyk, K., J. Ehrchen, K. Tenbrock, M. Ahlmann, J. Kneidl, D. Viemann, and J. Roth.** Glucocorticoids promote survival of anti-inflammatory macrophages via stimulation of adenosine receptor A3. Blood **116:**446-55.
21. **Barnholt, K. E., R. S. Kota, H. H. Aung, and J. C. Rutledge.** 2009. Adenosine blocks IFN-gamma-induced phosphorylation of STAT1 on serine 727 to reduce macrophage activation. J Immunol **183:**6767-77.
22. **Barral, P. M., J. M. Morrison, J. Drahos, P. Gupta, D. Sarkar, P. B. Fisher, and V. R. Racaniello.** 2007. MDA-5 is cleaved in poliovirus-infected cells. J Virol **81:**3677-84.
23. **Barton, G. M., and J. C. Kagan.** 2009. A cell biological view of Toll-like receptor function: regulation through compartmentalization. Nat Rev Immunol **9:**535-42.
24. **Basta, S., and J. R. Bennink.** 2003. A survival game of hide and seek: cytomegaloviruses and MHC class I antigen presentation pathways. Viral Immunol **16:**231-42.
25. **Bazzoni, F., N. Tamassia, M. Rossato, and M. A. Cassatella.** Understanding the molecular mechanisms of the multifaceted IL-10-mediated anti-inflammatory response: lessons from neutrophils. Eur J Immunol **40:**2360-8.
26. **Beare, D., M. Learmonth, V. Wells, A. Aitken, and L. Mallucci.** 1996. Characterisation and antiproliferative activity of an alpha-type murine interferon from embryonic fibroblasts. Biochim Biophys Acta **1310:**81-5.
27. **Beisser, P. S., C. S. Goh, F. E. Cohen, and S. Michelson.** 2002. Viral chemokine receptors and chemokines in human cytomegalovirus trafficking

and interaction with the immune system. CMV chemokine receptors. Curr Top Microbiol Immunol **269:**203-34.

28. **Bereczky, S., G. Lindegren, H. Karlberg, S. Akerstrom, J. Klingstrom, and A. Mirazimi.** Crimean-Congo hemorrhagic fever virus infection is lethal for adult type I interferon receptor-knockout mice. J Gen Virol **91:**1473-7.
29. **Besse, S., D. Rebouillat, I. Marie, F. Puvion-Dutilleul, and A. G. Hovanessian.** 1998. Ultrastructural localization of interferon-inducible double-stranded RNA-activated enzymes in human cells. Exp Cell Res **239:**379-92.
30. **Beutler, B. A.** 2009. TLRs and innate immunity. Blood **113:**1399-407.
31. **Bilban, M., L. K. Buehler, S. Head, G. Desoye, and V. Quaranta.** 2002. Defining signal thresholds in DNA microarrays: exemplary application for invasive cancer. BMC Genomics **3:**19.
32. **Bisbal, C., T. Salehzada, M. Silhol, C. Martinand, F. Le Roy, and B. Lebleu.** 2001. The 2-5A/RNase L pathway and inhibition by RNase L inhibitor (RLI). Methods Mol Biol **160:**183-98.
33. **Blanc, M., W. Y. Hsieh, K. A. Robertson, S. Watterson, G. Shui, P. Lacaze, M. Khondoker, P. Dickinson, G. Sing, S. Rodriguez-Martin, P. Phelan, T. Forster, B. Strobl, M. Muller, R. Riemersma, T. Osborne, M. R. Wenk, A. Angulo, and P. Ghazal.** Host Defense against Viral Infection Involves Interferon Mediated Down-Regulation of Sterol Biosynthesis. PLoS Biol **9:**e1000598.
34. **Boehme, K. W., M. Guerrero, and T. Compton.** 2006. Human cytomegalovirus envelope glycoproteins B and H are necessary for TLR2 activation in permissive cells. J Immunol **177:**7094-102.
35. **Boehme, K. W., J. Singh, S. T. Perry, and T. Compton.** 2004. Human cytomegalovirus elicits a coordinated cellular antiviral response via envelope glycoprotein B. J Virol **78:**1202-11.
36. **Bogdan, C., and C. Nathan.** 1993. Modulation of macrophage function by transforming growth factor beta, interleukin-4, and interleukin-10. Ann N Y Acad Sci **685:**713-39.
37. **Bogdan, C., Y. Vodovotz, and C. Nathan.** 1991. Macrophage deactivation by interleukin 10. J Exp Med **174:**1549-55.
38. **Borden, E. C., G. C. Sen, G. Uze, R. H. Silverman, R. M. Ransohoff, G. R. Foster, and G. R. Stark.** 2007. Interferons at age 50: past, current and future impact on biomedicine. Nat Rev Drug Discov **6:**975-90.
39. **Borst, E. M., K. Wagner, A. Binz, B. Sodeik, and M. Messerle.** 2008. The essential human cytomegalovirus gene UL52 is required for cleavage-packaging of the viral genome. J Virol **82:**2065-78.
40. **Bourette, R. P., and L. R. Rohrschneider.** 2000. Early events in M-CSF receptor signaling. Growth Factors **17:**155-66.
41. **Bowie, A. G., and L. Unterholzner.** 2008. Viral evasion and subversion of pattern-recognition receptor signalling. Nat Rev Immunol **8:**911-22.
42. **Bozza, S., R. Gaziano, P. Bonifazi, T. Zelante, L. Pitzurra, C. Montagnoli, S. Moretti, R. Castronari, P. Sinibaldi, G. Rasi, E. Garaci, F. Bistoni, and L. Romani.** 2007. Thymosin alpha1 activates the TLR9/MyD88/IRF7-dependent murine cytomegalovirus sensing for induction of anti-viral responses in vivo. Int Immunol **19:**1261-70.

43. **Browne, E. P., B. Wing, D. Coleman, and T. Shenk.** 2001. Altered cellular mRNA levels in human cytomegalovirus-infected fibroblasts: viral block to the accumulation of antiviral mRNAs. J Virol **75:**12319-30.
44. **Brukman, A., and L. W. Enquist.** 2006. Suppression of the interferon-mediated innate immune response by pseudorabies virus. J Virol **80:**6345-56.
45. **Brune, W., C. Menard, J. Heesemann, and U. H. Koszinowski.** 2001. A ribonucleotide reductase homolog of cytomegalovirus and endothelial cell tropism. Science **291:**303-5.
46. **Buck, A. H., J. Perot, M. A. Chisholm, D. S. Kumar, L. Tuddenham, V. Cognat, L. Marcinowski, L. Dolken, and S. Pfeffer.** Post-transcriptional regulation of miR-27 in murine cytomegalovirus infection. RNA **16:**307-15.
47. **Buck, A. H., J. Santoyo-Lopez, K. A. Robertson, D. S. Kumar, M. Reczko, and P. Ghazal.** 2007. Discrete clusters of virus-encoded micrornas are associated with complementary strands of the genome and the 7.2-kilobase stable intron in murine cytomegalovirus. J Virol **81:**13761-70.
48. **Budt, M., L. Niederstadt, R. S. Valchanova, S. Jonjic, and W. Brune.** 2009. Specific inhibition of the PKR-mediated antiviral response by the murine cytomegalovirus proteins m142 and m143. J Virol **83:**1260-70.
49. **Busche, A., A. Angulo, P. Kay-Jackson, P. Ghazal, and M. Messerle.** 2008. Phenotypes of major immediate-early gene mutants of mouse cytomegalovirus. Med Microbiol Immunol **197:**233-40.
50. **Buser, C., F. Fleischer, T. Mertens, D. Michel, V. Schmidt, and P. Walther.** 2007. Quantitative investigation of murine cytomegalovirus nucleocapsid interaction. J Microsc **228:**78-87.
51. **Calvo-Pinilla, E., J. M. Nieto, and J. Ortego.** Experimental oral infection of bluetongue virus serotype 8 in IFNAR(-/-) mice. J Gen Virol.
52. **Cannon, M. J., D. S. Schmid, and T. B. Hyde.** Review of cytomegalovirus seroprevalence and demographic characteristics associated with infection. Rev Med Virol **20:**202-13.
53. **Cardin, R. D., G. B. Abenes, C. A. Stoddart, and E. S. Mocarski.** 1995. Murine cytomegalovirus IE2, an activator of gene expression, is dispensable for growth and latency in mice. Virology **209:**236-41.
54. **Caruso, C., S. Buffa, G. Candore, G. Colonna-Romano, D. Dunn-Walters, D. Kipling, and G. Pawelec.** 2009. Mechanisms of immunosenescence. Immun Ageing **6:**10.
55. **Cecchini, M. G., M. G. Dominguez, S. Mocci, A. Wetterwald, R. Felix, H. Fleisch, O. Chisholm, W. Hofstetter, J. W. Pollard, and E. R. Stanley.** 1994. Role of colony stimulating factor-1 in the establishment and regulation of tissue macrophages during postnatal development of the mouse. Development **120:**1357-72.
56. **Chan, G., E. R. Bivins-Smith, M. S. Smith, P. M. Smith, and A. D. Yurochko.** 2008. Transcriptome analysis reveals human cytomegalovirus reprograms monocyte differentiation toward an M1 macrophage. J Immunol **181:**698-711.
57. **Child, S. J., and A. P. Geballe.** 2009. Binding and relocalization of protein kinase R by murine cytomegalovirus. J Virol **83:**1790-9.

58. **Chiu, Y. H., J. B. Macmillan, and Z. J. Chen.** 2009. RNA polymerase III detects cytosolic DNA and induces type I interferons through the RIG-I pathway. Cell **138:**576-91.
59. **Choubey, D., and P. Lengyel.** 1992. Interferon action: nucleolar and nucleoplasmic localization of the interferon-inducible 72-kD protein that is encoded by the Ifi 204 gene from the gene 200 cluster. J Cell Biol **116:**1333-41.
60. **Cicin-Sain, L., I. Bubic, M. Schnee, Z. Ruzsics, C. Mohr, S. Jonjic, and U. H. Koszinowski.** 2007. Targeted deletion of regions rich in immune-evasive genes from the cytomegalovirus genome as a novel vaccine strategy. J Virol **81:**13825-34.
61. **Cicin-Sain, L., Z. Ruzsics, J. Podlech, I. Bubic, C. Menard, S. Jonjic, M. J. Reddehase, and U. H. Koszinowski.** 2008. Dominant-negative FADD rescues the in vivo fitness of a cytomegalovirus lacking an antiapoptotic viral gene. J Virol **82:**2056-64.
62. **Coelho, L. F., G. Magno de Freitas Almeida, F. J. Mennechet, A. Blangy, and G. Uze.** 2005. Interferon-alpha and -beta differentially regulate osteoclastogenesis: role of differential induction of chemokine CXCL11 expression. Proc Natl Acad Sci U S A **102:**11917-22.
63. **Collins, S. E., R. S. Noyce, and K. L. Mossman.** 2004. Innate cellular response to virus particle entry requires IRF3 but not virus replication. J Virol **78:**1706-17.
64. **Compton, T.** 2004. Receptors and immune sensors: the complex entry path of human cytomegalovirus. Trends Cell Biol **14:**5-8.
65. **Compton, T., E. A. Kurt-Jones, K. W. Boehme, J. Belko, E. Latz, D. T. Golenbock, and R. W. Finberg.** 2003. Human cytomegalovirus activates inflammatory cytokine responses via CD14 and Toll-like receptor 2. J Virol **77:**4588-96.
66. **Compton, T., R. R. Nepomuceno, and D. M. Nowlin.** 1992. Human cytomegalovirus penetrates host cells by pH-independent fusion at the cell surface. Virology **191:**387-95.
67. **Conway, J. G., R. C. Andrews, B. Beaudet, D. M. Bickett, V. Boncek, T. A. Brodie, R. L. Clark, R. C. Crumrine, M. A. Leenitzer, D. L. McDougald, B. Han, K. Hedeen, P. Lin, M. Milla, M. Moss, H. Pink, M. H. Rabinowitz, T. Tippin, P. W. Scates, J. Selph, S. A. Stimpson, J. Warner, and J. D. Becherer.** 2001. Inhibition of tumor necrosis factor-alpha (TNF-alpha) production and arthritis in the rat by GW3333, a dual inhibitor of TNF-alpha-converting enzyme and matrix metalloproteinases. J Pharmacol Exp Ther **298:**900-8.
68. **Dalod, M., T. P. Salazar-Mather, L. Malmgaard, C. Lewis, C. Asselin-Paturel, F. Briere, G. Trinchieri, and C. A. Biron.** 2002. Interferon alpha/beta and interleukin 12 responses to viral infections: pathways regulating dendritic cell cytokine expression in vivo. J Exp Med **195:**517-28.
69. **Davison, A. J.** 2002. Evolution of the herpesviruses. Vet Microbiol **86:**69-88.
70. **De Flora, S., C. Grassi, and L. Carati.** 1997. Attenuation of influenza-like symptomatology and improvement of cell-mediated immunity with long-term N-acetylcysteine treatment. Eur Respir J **10:**1535-41.

71. **de Jong, H. K., T. van der Poll, and W. J. Wiersinga.** The systemic pro-inflammatory response in sepsis. J Innate Immun **2:**422-30.
72. **de Veer, M. J., M. Holko, M. Frevel, E. Walker, S. Der, J. M. Paranjape, R. H. Silverman, and B. R. Williams.** 2001. Functional classification of interferon-stimulated genes identified using microarrays. J Leukoc Biol **69:**912-20.
73. **de Waal Malefyt, R., J. Abrams, B. Bennett, C. G. Figdor, and J. E. de Vries.** 1991. Interleukin 10(IL-10) inhibits cytokine synthesis by human monocytes: an autoregulatory role of IL-10 produced by monocytes. J Exp Med **174:**1209-20.
74. **DeFilippis, V. R.** 2007. Induction and evasion of the type I interferon response by cytomegaloviruses. Adv Exp Med Biol **598:**309-24.
75. **DeFilippis, V. R., D. Alvarado, T. Sali, S. Rothenburg, and K. Fruh.** Human cytomegalovirus induces the interferon response via the DNA sensor ZBP1. J Virol **84:**585-98.
76. **DeFilippis, V. R., T. Sali, D. Alvarado, L. White, W. Bresnahan, and K. J. Fruh.** Activation of the interferon response by human cytomegalovirus occurs via cytoplasmic double-stranded DNA but not glycoprotein B. J Virol **84:**8913-25.
77. **Delaloye, J., T. Roger, Q. G. Steiner-Tardivel, D. Le Roy, M. Knaup Reymond, S. Akira, V. Petrilli, C. E. Gomez, B. Perdiguero, J. Tschopp, G. Pantaleo, M. Esteban, and T. Calandra.** 2009. Innate immune sensing of modified vaccinia virus Ankara (MVA) is mediated by TLR2-TLR6, MDA-5 and the NALP3 inflammasome. PLoS Pathog **5:**e1000480.
78. **Deleault, K. M., S. J. Skinner, and S. A. Brooks.** 2008. Tristetraprolin regulates TNF TNF-alpha mRNA stability via a proteasome dependent mechanism involving the combined action of the ERK and p38 pathways. Mol Immunol **45:**13-24.
79. **Dennis, G., Jr., B. T. Sherman, D. A. Hosack, J. Yang, W. Gao, H. C. Lane, and R. A. Lempicki.** 2003. DAVID: Database for Annotation, Visualization, and Integrated Discovery. Genome Biol **4:**P3.
80. **Deonarain, R., A. Alcami, M. Alexiou, M. J. Dallman, D. R. Gewert, and A. C. Porter.** 2000. Impaired antiviral response and alpha/beta interferon induction in mice lacking beta interferon. J Virol **74:**3404-9.
81. **Deonarain, R., D. Cerullo, K. Fuse, P. P. Liu, and E. N. Fish.** 2004. Protective role for interferon-beta in coxsackievirus B3 infection. Circulation **110:**3540-3.
82. **Dimitriou, I. D., L. Clemenza, A. J. Scotter, G. Chen, F. M. Guerra, and R. Rottapel.** 2008. Putting out the fire: coordinated suppression of the innate and adaptive immune systems by SOCS1 and SOCS3 proteins. Immunol Rev **224:**265-83.
83. **Dokter, W. H., S. B. Koopmans, and E. Vellenga.** 1996. Effects of IL-10 and IL-4 on LPS-induced transcription factors (AP-1, NF-IL6 and NF-kappa B) which are involved in IL-6 regulation. Leukemia **10:**1308-16.
84. **Dolken, L., A. Krmpotic, S. Kothe, L. Tuddenham, M. Tanguy, L. Marcinowski, Z. Ruzsics, N. Elefant, Y. Altuvia, H. Margalit, U. H. Koszinowski, S. Jonjic, and S. Pfeffer.** Cytomegalovirus microRNAs

facilitate persistent virus infection in salivary glands. PLoS Pathog **6:**e1001150.

85. **Dolken, L., J. Perot, V. Cognat, A. Alioua, M. John, J. Soutschek, Z. Ruzsics, U. Koszinowski, O. Voinnet, and S. Pfeffer.** 2007. Mouse cytomegalovirus microRNAs dominate the cellular small RNA profile during lytic infection and show features of posttranscriptional regulation. J Virol **81:**13771-82.
86. **Dorner, B. G., H. R. Smith, A. R. French, S. Kim, J. Poursine-Laurent, D. L. Beckman, J. T. Pingel, R. A. Kroczek, and W. M. Yokoyama.** 2004. Coordinate expression of cytokines and chemokines by NK cells during murine cytomegalovirus infection. J Immunol **172:**3119-31.
87. **Doyle, S. E., R. O'Connell, S. A. Vaidya, E. K. Chow, K. Yee, and G. Cheng.** 2003. Toll-like receptor 3 mediates a more potent antiviral response than Toll-like receptor 4. J Immunol **170:**3565-71.
88. **Du, Z., L. Wei, A. Murti, S. R. Pfeffer, M. Fan, C. H. Yang, and L. M. Pfeffer.** 2007. Non-conventional signal transduction by type 1 interferons: the NF-kappaB pathway. J Cell Biochem **102:**1087-94.
89. **Englen, M. D., Y. E. Valdez, N. M. Lehnert, and B. E. Lehnert.** 1995. Granulocyte/macrophage colony-stimulating factor is expressed and secreted in cultures of murine L929 cells. J Immunol Methods **184:**281-3.
90. **Erlandsson, L., R. Blumenthal, M. L. Eloranta, H. Engel, G. Alm, S. Weiss, and T. Leanderson.** 1998. Interferon-beta is required for interferon-alpha production in mouse fibroblasts. Curr Biol **8:**223-6.
91. **Eskildsen, S., J. Justesen, M. H. Schierup, and R. Hartmann.** 2003. Characterization of the 2'-5'-oligoadenylate synthetase ubiquitin-like family. Nucleic Acids Res **31:**3166-73.
92. **Falvo, J. V., A. V. Tsytsykova, and A. E. Goldfeld.** Transcriptional control of the TNF gene. Curr Dir Autoimmun **11:**27-60.
93. **Fathallah, I., P. Parroche, H. Gruffat, C. Zannetti, H. Johansson, J. Yue, E. Manet, M. Tommasino, B. S. Sylla, and U. A. Hasan.** EBV latent membrane protein 1 is a negative regulator of TLR9. J Immunol **185:**6439-47.
94. **Feire, A. L., H. Koss, and T. Compton.** 2004. Cellular integrins function as entry receptors for human cytomegalovirus via a highly conserved disintegrin-like domain. Proc Natl Acad Sci U S A **101:**15470-5.
95. **Fernandez, J. A., E. G. Rodrigues, and M. Tsuji.** 2000. Multifactorial protective mechanisms to limit viral replication in the lung of mice during primary murine cytomegalovirus infection. Viral Immunol **13:**287-95.
96. **Fiorentino, D. F., A. Zlotnik, T. R. Mosmann, M. Howard, and A. O'Garra.** 1991. IL-10 inhibits cytokine production by activated macrophages. J Immunol **147:**3815-22.
97. **Fleetwood, A. J., H. Dinh, A. D. Cook, P. J. Hertzog, and J. A. Hamilton.** 2009. GM-CSF- and M-CSF-dependent macrophage phenotypes display differential dependence on type I interferon signaling. J Leukoc Biol **86:**411-21.
98. **Fletcher, T. M., 3rd, M. A. Soares, S. McPhearson, H. Hui, M. Wiskerchen, M. A. Muesing, G. M. Shaw, A. D. Leavitt, J. D. Boeke, and**

B. H. Hahn. 1997. Complementation of integrase function in HIV-1 virions. EMBO J **16:**5123-38.

99. **Fossum, E., C. C. Friedel, S. V. Rajagopala, B. Titz, A. Baiker, T. Schmidt, T. Kraus, T. Stellberger, C. Rutenberg, S. Suthram, S. Bandyopadhyay, D. Rose, A. von Brunn, M. Uhlmann, C. Zeretzke, Y. A. Dong, H. Boulet, M. Koegl, S. M. Bailer, U. Koszinowski, T. Ideker, P. Uetz, R. Zimmer, and J. Haas.** 2009. Evolutionarily conserved herpesviral protein interaction networks. PLoS Pathog **5:**e1000570.
100. **Foster, S. L., D. C. Hargreaves, and R. Medzhitov.** 2007. Gene-specific control of inflammation by TLR-induced chromatin modifications. Nature **447:**972-8.
101. **Fraternale, A., M. F. Paoletti, A. Casabianca, L. Nencioni, E. Garaci, A. T. Palamara, and M. Magnani.** 2009. GSH and analogs in antiviral therapy. Mol Aspects Med **30:**99-110.
102. **Fraternale, A., M. F. Paoletti, A. Casabianca, J. Oiry, P. Clayette, J. U. Vogel, J. Cinatl, Jr., A. T. Palamara, R. Sgarbanti, E. Garaci, E. Millo, U. Benatti, and M. Magnani.** 2006. Antiviral and immunomodulatory properties of new pro-glutathione (GSH) molecules. Curr Med Chem **13:**1749-55.
103. **Freeman, T. C., L. Goldovsky, M. Brosch, S. van Dongen, P. Maziere, R. J. Grocock, S. Freilich, J. Thornton, and A. J. Enright.** 2007. Construction, visualisation, and clustering of transcription networks from microarray expression data. PLoS Comput Biol **3:**2032-42.
104. **Friel, H., and H. Lederman.** 2006. A nutritional supplement formula for influenza A (H5N1) infection in humans. Med Hypotheses **67:**578-87.
105. **Galluzzi, L., O. Kepp, E. Morselli, I. Vitale, L. Senovilla, M. Pinti, L. Zitvogel, and G. Kroemer.** Viral strategies for the evasion of immunogenic cell death. J Intern Med **267:**526-42.
106. **Garko-Buczynski, K. A., R. H. Smith, S. K. Kim, and D. J. O'Callaghan.** 1998. Complementation of a replication-defective mutant of equine herpesvirus type 1 by a cell line expressing the immediate-early protein. Virology **248:**83-94.
107. **Gay, N. J., and F. J. Keith.** 1991. Drosophila Toll and IL-1 receptor. Nature **351:**355-6.
108. **Geissmann, F., S. Gordon, D. A. Hume, A. M. Mowat, and G. J. Randolph.** Unravelling mononuclear phagocyte heterogeneity. Nat Rev Immunol **10:**453-60.
109. **Geissmann, F., M. G. Manz, S. Jung, M. H. Sieweke, M. Merad, and K. Ley.** Development of monocytes, macrophages, and dendritic cells. Science **327:**656-61.
110. **Gerrity, D., H. Ryu, J. Crittenden, and M. Abbaszadegan.** 2008. UV inactivation of adenovirus type 4 measured by integrated cell culture qPCR. J Environ Sci Health A Tox Hazard Subst Environ Eng **43:**1628-38.
111. **Ghazal, P., H. Lubon, B. Fleckenstein, and L. Hennighausen.** 1987. Binding of transcription factors and creation of a large nucleoprotein complex on the human cytomegalovirus enhancer. Proc Natl Acad Sci U S A **84:**3658-62.

112. **Ghazal, P., M. Messerle, K. Osborn, and A. Angulo.** 2003. An essential role of the enhancer for murine cytomegalovirus in vivo growth and pathogenesis. J Virol **77:**3217-28.
113. **Ghazal, P., A. E. Visser, M. Gustems, R. Garcia, E. M. Borst, K. Sullivan, M. Messerle, and A. Angulo.** 2005. Elimination of ie1 significantly attenuates murine cytomegalovirus virulence but does not alter replicative capacity in cell culture. J Virol **79:**7182-94.
114. **Gilchrist, M., V. Thorsson, B. Li, A. G. Rust, M. Korb, J. C. Roach, K. Kennedy, T. Hai, H. Bolouri, and A. Aderem.** 2006. Systems biology approaches identify ATF3 as a negative regulator of Toll-like receptor 4. Nature **441:**173-8.
115. **Gilliet, M., W. Cao, and Y. J. Liu.** 2008. Plasmacytoid dendritic cells: sensing nucleic acids in viral infection and autoimmune diseases. Nat Rev Immunol **8:**594-606.
116. **Glaros, T., M. Larsen, and L. Li.** 2009. Macrophages and fibroblasts during inflammation, tissue damage and organ injury. Front Biosci **14:**3988-93.
117. **Glass, M., A. Busche, K. Wagner, M. Messerle, and E. M. Borst.** 2009. Conditional and reversible disruption of essential herpesvirus proteins. Nat Methods **6:**577-9.
118. **Goins, W. F., P. Marconi, D. Krisky, D. Wolfe, J. C. Glorioso, R. Ramakrishnan, and D. J. Fink.** 2002. Construction of replication-defective herpes simplex virus vectors. Curr Protoc Hum Genet **Chapter 12:**Unit 12 11.
119. **Goldmacher, V. S.** 2005. Cell death suppression by cytomegaloviruses. Apoptosis **10:**251-65.
120. **Goodman, A. G., H. Zeng, S. C. Proll, X. Peng, C. Cilloniz, V. S. Carter, M. J. Korth, T. M. Tumpey, and M. G. Katze.** The alpha/beta interferon receptor provides protection against influenza virus replication but is dispensable for inflammatory response signaling. J Virol **84:**2027-37.
121. **Gordon, S.** 2003. Alternative activation of macrophages. Nat Rev Immunol **3:**23-35.
122. **Gough, D. J., N. L. Messina, L. Hii, J. A. Gould, K. Sabapathy, A. P. Robertson, J. A. Trapani, D. E. Levy, P. J. Hertzog, C. J. Clarke, and R. W. Johnstone.** Functional crosstalk between type I and II interferon through the regulated expression of STAT1. PLoS Biol **8:**e1000361.
123. **Gow, D. J., D. P. Sester, and D. A. Hume.** CSF-1, IGF-1, and the control of postnatal growth and development. J Leukoc Biol **88:**475-81.
124. **Grant, K. G., D. M. Krisky, M. M. Ataai, and J. C. Glorioso, 3rd.** 2009. Engineering cell lines for production of replication defective HSV-1 gene therapy vectors. Biotechnol Bioeng **102:**1087-97.
125. **Green, N. M., A. Laws, K. Kiefer, L. Busconi, Y. M. Kim, M. M. Brinkmann, E. H. Trail, K. Yasuda, S. R. Christensen, M. J. Shlomchik, S. Vogel, J. H. Connor, H. Ploegh, D. Eilat, I. R. Rifkin, J. M. van Seventer, and A. Marshak-Rothstein.** 2009. Murine B cell response to TLR7 ligands depends on an IFN-beta feedback loop. J Immunol **183:**1569-76.
126. **Gribaudo, G., S. Ravaglia, L. Guandalini, R. Cavallo, M. Gariglio, and S. Landolfo.** 1996. The murine cytomegalovirus immediate-early 1 protein

stimulates NF-kappa B activity by transactivating the NF-kappa B p105/p50 promoter. Virus Res **45:**15-27.

127. **Guo, Z., S. Garg, K. M. Hill, L. Jayashankar, M. R. Mooney, M. Hoelscher, J. M. Katz, J. M. Boss, and S. Sambhara.** 2005. A distal regulatory region is required for constitutive and IFN-beta-induced expression of murine TLR9 gene. J Immunol **175:**7407-18.
128. **Hale, B. G., R. E. Randall, J. Ortin, and D. Jackson.** 2008. The multifunctional NS1 protein of influenza A viruses. J Gen Virol **89:**2359-76.
129. **Haller, O., G. Kochs, and F. Weber.** 2007. Interferon, Mx, and viral countermeasures. Cytokine Growth Factor Rev **18:**425-33.
130. **Hamilton, J. A.** 1997. CSF-1 signal transduction. J Leukoc Biol **62:**145-55.
131. **Hanson, L. K., J. S. Slater, Z. Karabekian, G. Ciocco-Schmitt, and A. E. Campbell.** 2001. Products of US22 genes M140 and M141 confer efficient replication of murine cytomegalovirus in macrophages and spleen. J Virol **75:**6292-302.
132. **Hanson, L. K., J. S. Slater, Z. Karabekian, H. W. t. Virgin, C. A. Biron, M. C. Ruzek, N. van Rooijen, R. P. Ciavarra, R. M. Stenberg, and A. E. Campbell.** 1999. Replication of murine cytomegalovirus in differentiated macrophages as a determinant of viral pathogenesis. J Virol **73:**5970-80.
133. **Haralambieva, I. H., I. G. Ovsyannikova, N. Dhiman, R. A. Vierkant, R. M. Jacobson, and G. A. Poland.** Differential cellular immune responses to wild-type and attenuated edmonston tag measles virus strains are primarily defined by the viral phosphoprotein gene. J Med Virol **82:**1966-75.
134. **Hargreaves, D. C., T. Horng, and R. Medzhitov.** 2009. Control of inducible gene expression by signal-dependent transcriptional elongation. Cell **138:**129-45.
135. **Harton, J. A., M. W. Linhoff, J. Zhang, and J. P. Ting.** 2002. Cutting edge: CATERPILLER: a large family of mammalian genes containing CARD, pyrin, nucleotide-binding, and leucine-rich repeat domains. J Immunol **169:**4088-93.
136. **Harty, R. N., P. M. Pitha, and A. Okumura.** 2009. Antiviral activity of innate immune protein ISG15. J Innate Immun **1:**397-404.
137. **Hasko, G., P. Pacher, E. A. Deitch, and E. S. Vizi.** 2007. Shaping of monocyte and macrophage function by adenosine receptors. Pharmacol Ther **113:**264-75.
138. **Hayden, M. S., A. P. West, and S. Ghosh.** 2006. NF-kappaB and the immune response. Oncogene **25:**6758-80.
139. **He, B., L. You, K. Uematsu, M. Matsangou, Z. Xu, M. He, F. McCormick, and D. M. Jablons.** 2003. Cloning and characterization of a functional promoter of the human SOCS-3 gene. Biochem Biophys Res Commun **301:**386-91.
140. **Helming, L., J. Bose, J. Ehrchen, S. Schiebe, T. Frahm, R. Geffers, M. Probst-Kepper, R. Balling, and A. Lengeling.** 2005. 1alpha,25-Dihydroxyvitamin D3 is a potent suppressor of interferon gamma-mediated macrophage activation. Blood **106:**4351-8.
141. **Hengel, H., U. H. Koszinowski, and K. K. Conzelmann.** 2005. Viruses know it all: new insights into IFN networks. Trends Immunol **26:**396-401.

142. **Hidmark, A. S., G. M. McInerney, E. K. Nordstrom, I. Douagi, K. M. Werner, P. Liljestrom, and G. B. Karlsson Hedestam.** 2005. Early alpha/beta interferon production by myeloid dendritic cells in response to UV-inactivated virus requires viral entry and interferon regulatory factor 3 but not MyD88. J Virol **79:**10376-85.
143. **Himeda, T., Y. Ohara, K. Asakura, Y. Kontani, M. Murakami, H. Suzuki, and M. Sawada.** 2005. A lentiviral expression system demonstrates that L* protein of Theiler's murine encephalomyelitis virus (TMEV) is essential for virus growth in a murine macrophage-like cell line. Virus Res **108:**23-8.
144. **Himes, S. R., D. P. Sester, T. Ravasi, S. L. Cronau, T. Sasmono, and D. A. Hume.** 2006. The JNK are important for development and survival of macrophages. J Immunol **176:**2219-28.
145. **Hochrein, H., B. Schlatter, M. O'Keeffe, C. Wagner, F. Schmitz, M. Schiemann, S. Bauer, M. Suter, and H. Wagner.** 2004. Herpes simplex virus type-1 induces IFN-alpha production via Toll-like receptor 9-dependent and -independent pathways. Proc Natl Acad Sci U S A **101:**11416-21.
146. **Hofer, M., A. Vacek, M. Pospisil, J. Hola, D. Streitova, and V. Znojil.** 2009. Activation of adenosine A(3) receptors potentiates stimulatory effects of IL-3, SCF, and GM-CSF on mouse granulocyte-macrophage hematopoietic progenitor cells. Physiol Res **58:**247-52.
147. **Hohensinner, P. J., C. Kaun, K. Rychli, A. Niessner, S. Pfaffenberger, G. Rega, R. de Martin, G. Maurer, R. Ullrich, K. Huber, and J. Wojta.** 2007. Macrophage colony stimulating factor expression in human cardiac cells is upregulated by tumor necrosis factor-alpha via an NF-kappaB dependent mechanism. J Thromb Haemost **5:**2520-8.
148. **Hokeness, K. L., W. A. Kuziel, C. A. Biron, and T. P. Salazar-Mather.** 2005. Monocyte chemoattractant protein-1 and CCR2 interactions are required for IFN-alpha/beta-induced inflammatory responses and antiviral defense in liver. J Immunol **174:**1549-56.
149. **Honda, K., A. Takaoka, and T. Taniguchi.** 2006. Type I interferon [corrected] gene induction by the interferon regulatory factor family of transcription factors. Immunity **25:**349-60.
150. **Honda, K., H. Yanai, A. Takaoka, and T. Taniguchi.** 2005. Regulation of the type I IFN induction: a current view. Int Immunol **17:**1367-78.
151. **Hornung, V., and E. Latz.** Intracellular DNA recognition. Nat Rev Immunol **10:**123-30.
152. **Hu, X., K. H. Park-Min, H. H. Ho, and L. B. Ivashkiv.** 2005. IFN-gamma-primed macrophages exhibit increased CCR2-dependent migration and altered IFN-gamma responses mediated by Stat1. J Immunol **175:**3637-47.
153. **Huang, Y., A. Walstrom, L. Zhang, Y. Zhao, M. Cui, L. Ye, and J. C. Zheng.** 2009. Type I interferons and interferon regulatory factors regulate TNF-related apoptosis-inducing ligand (TRAIL) in HIV-1-infected macrophages. PLoS One **4:**e5397.
154. **Hume, D. A.** 2008. Differentiation and heterogeneity in the mononuclear phagocyte system. Mucosal Immunol **1:**432-41.
155. **Hume, D. A.** 2008. Macrophages as APC and the dendritic cell myth. J Immunol **181:**5829-35.

156. **Hume, D. A.** 2006. The mononuclear phagocyte system. Curr Opin Immunol **18:**49-53.
157. **Hume, D. A., W. Allan, B. Fabrus, M. J. Weidemann, A. J. Hapel, and S. Bartelmez.** 1987. Regulation of proliferation of bone marrow-derived macrophages. Lymphokine Res **6:**127-39.
158. **Hummel, M., and M. M. Abecassis.** 2002. A model for reactivation of CMV from latency. J Clin Virol **25 Suppl 2:**S123-36.
159. **Hunter, S., R. Apweiler, T. K. Attwood, A. Bairoch, A. Bateman, D. Binns, P. Bork, U. Das, L. Daugherty, L. Duquenne, R. D. Finn, J. Gough, D. Haft, N. Hulo, D. Kahn, E. Kelly, A. Laugraud, I. Letunic, D. Lonsdale, R. Lopez, M. Madera, J. Maslen, C. McAnulla, J. McDowall, J. Mistry, A. Mitchell, N. Mulder, D. Natale, C. Orengo, A. F. Quinn, J. D. Selengut, C. J. Sigrist, M. Thimma, P. D. Thomas, F. Valentin, D. Wilson, C. H. Wu, and C. Yeats.** 2009. InterPro: the integrative protein signature database. Nucleic Acids Res **37:**D211-5.
160. **Huys, L., F. Van Hauwermeiren, L. Dejager, E. Dejonckheere, S. Lienenklaus, S. Weiss, G. Leclercq, and C. Libert.** 2009. Type I interferon drives tumor necrosis factor-induced lethal shock. J Exp Med **206:**1873-82.
161. **Imanishi, D., K. Yamamoto, H. Tsushima, Y. Miyazaki, K. Kuriyama, M. Tomonaga, and T. Matsuyama.** 2000. Identification of a novel cytokine response element in the human IFN regulatory factor-1 gene promoter. J Immunol **165:**3907-16.
162. **Inohara, N., and G. Nunez.** 2001. The NOD: a signaling module that regulates apoptosis and host defense against pathogens. Oncogene **20:**6473-81.
163. **Isaacson, M. K., and T. Compton.** 2009. Human cytomegalovirus glycoprotein B is required for virus entry and cell-to-cell spread but not for virion attachment, assembly, or egress. J Virol **83:**3891-903.
164. **Isern, E., M. Gustems, M. Messerle, E. Borst, P. Ghazal, and A. Angulo.** The activator protein 1 binding motifs within the human cytomegalovirus major immediate-early enhancer are functionally redundant and act in a cooperative manner with the NF-{kappa}B sites during acute infection. J Virol **85:**1732-46.
165. **Isler, J. A., A. H. Skalet, and J. C. Alwine.** 2005. Human cytomegalovirus infection activates and regulates the unfolded protein response. J Virol **79:**6890-9.
166. **Isomura, H., M. F. Stinski, A. Kudoh, S. Nakayama, S. Iwahori, Y. Sato, and T. Tsurumi.** 2007. The late promoter of the human cytomegalovirus viral DNA polymerase processivity factor has an impact on delayed early and late viral gene products but not on viral DNA synthesis. J Virol **81:**6197-206.
167. **Isomura, H., M. F. Stinski, A. Kudoh, S. Nakayama, T. Murata, Y. Sato, S. Iwahori, and T. Tsurumi.** 2008. A cis element between the TATA Box and the transcription start site of the major immediate-early promoter of human cytomegalovirus determines efficiency of viral replication. J Virol **82:**849-58.
168. **Ito, T., Y. H. Wang, and Y. J. Liu.** 2005. Plasmacytoid dendritic cell precursors/type I interferon-producing cells sense viral infection by Toll-like receptor (TLR) 7 and TLR9. Springer Semin Immunopathol **26:**221-9.

169. **Iversen, A. C., B. Steinkjer, N. Nilsen, J. Bohnhorst, S. H. Moen, R. Vik, P. Stephens, D. W. Thomas, C. A. Benedict, and T. Espevik.** 2009. A proviral role for CpG in cytomegalovirus infection. J Immunol **182:**5672-81.
170. **Jackson, S. E., G. M. Mason, and M. R. Wills.** Human cytomegalovirus immunity and immune evasion. Virus Res.
171. **Janeway, C. A., Jr.** 1989. Approaching the asymptote? Evolution and revolution in immunology. Cold Spring Harb Symp Quant Biol **54 Pt 1:**1-13.
172. **Jarvis, M. A., and J. A. Nelson.** 2002. Human cytomegalovirus persistence and latency in endothelial cells and macrophages. Curr Opin Microbiol **5:**403-7.
173. **Jeffrey, I. W., S. Kadereit, E. F. Meurs, T. Metzger, M. Bachmann, M. Schwemmle, A. G. Hovanessian, and M. J. Clemens.** 1995. Nuclear localization of the interferon-inducible protein kinase PKR in human cells and transfected mouse cells. Exp Cell Res **218:**17-27.
174. **Jenner, R. G., and R. A. Young.** 2005. Insights into host responses against pathogens from transcriptional profiling. Nat Rev Microbiol **3:**281-94.
175. **Jensen, K., R. Talbot, E. Paxton, D. Waddington, and E. J. Glass.** 2006. Development and validation of a bovine macrophage specific cDNA microarray. BMC Genomics **7:**224.
176. **Ji, X., R. Cheung, S. Cooper, Q. Li, H. B. Greenberg, and X. S. He.** 2003. Interferon alfa regulated gene expression in patients initiating interferon treatment for chronic hepatitis C. Hepatology **37:**610-21.
177. **Jonjic, S., A. Krmpotic, J. Arapovic, and U. H. Koszinowski.** 2008. Dissection of the antiviral NK cell response by MCMV mutants. Methods Mol Biol **415:**127-49.
178. **Joo, C. H., Y. C. Shin, M. Gack, L. Wu, D. Levy, and J. U. Jung.** 2007. Inhibition of interferon regulatory factor 7 (IRF7)-mediated interferon signal transduction by the Kaposi's sarcoma-associated herpesvirus viral IRF homolog vIRF3. J Virol **81:**8282-92.
179. **Juang, S. H., S. J. Wei, Y. M. Hung, C. Y. Hsu, D. M. Yang, K. J. Liu, W. S. Chen, and W. K. Yang.** 2004. IFN-beta induces caspase-mediated apoptosis by disrupting mitochondria in human advanced stage colon cancer cell lines. J Interferon Cytokine Res **24:**231-43.
180. **Juckem, L. K., K. W. Boehme, A. L. Feire, and T. Compton.** 2008. Differential initiation of innate immune responses induced by human cytomegalovirus entry into fibroblast cells. J Immunol **180:**4965-77.
181. **Kalejta, R. F.** 2008. Functions of human cytomegalovirus tegument proteins prior to immediate early gene expression. Curr Top Microbiol Immunol **325:**101-15.
182. **Kalejta, R. F.** 2008. Tegument proteins of human cytomegalovirus. Microbiol Mol Biol Rev **72:**249-65, table of contents.
183. **Kamthong, P. J., F. M. Wu, and M. C. Wu.** 2000. cAMP attenuates interleukin-1-stimulated macrophage colony-stimulating factor (M-CSF) expression. Biochem J **350 Pt 1:**115-22.
184. **Kattenhorn, L. M., R. Mills, M. Wagner, A. Lomsadze, V. Makeev, M. Borodovsky, H. L. Ploegh, and B. M. Kessler.** 2004. Identification of proteins associated with murine cytomegalovirus virions. J Virol **78:**11187-97.

185. **Katze, M. G., Y. He, and M. Gale, Jr.** 2002. Viruses and interferon: a fight for supremacy. Nat Rev Immunol **2:**675-87.
186. **Kawai, T., and S. Akira.** The role of pattern-recognition receptors in innate immunity: update on Toll-like receptors. Nat Immunol **11:**373-84.
187. **Kawai, T., and S. Akira.** 2007. Signaling to NF-kappaB by Toll-like receptors. Trends Mol Med **13:**460-9.
188. **Keil, G. M., A. Ebeling-Keil, and U. H. Koszinowski.** 1987. Immediate-early genes of murine cytomegalovirus: location, transcripts, and translation products. J Virol **61:**526-33.
189. **Keil, G. M., A. Ebeling-Keil, and U. H. Koszinowski.** 1987. Sequence and structural organization of murine cytomegalovirus immediate-early gene 1. J Virol **61:**1901-8.
190. **Keil, G. M., A. Ebeling-Keil, and U. H. Koszinowski.** 1984. Temporal regulation of murine cytomegalovirus transcription and mapping of viral RNA synthesized at immediate early times after infection. J Virol **50:**784-95.
191. **Kim, S. K., A. E. Fouts, and J. C. Boothroyd.** 2007. Toxoplasma gondii dysregulates IFN-gamma-inducible gene expression in human fibroblasts: insights from a genome-wide transcriptional profiling. J Immunol **178:**5154-65.
192. **Kirchhoff, S., A. Oumard, M. Nourbakhsh, B. Z. Levi, and H. Hauser.** 2000. Interplay between repressing and activating domains defines the transcriptional activity of IRF-1. Eur J Biochem **267:**6753-61.
193. **Koffron, A. J., M. Hummel, B. K. Patterson, S. Yan, D. B. Kaufman, J. P. Fryer, F. P. Stuart, and M. I. Abecassis.** 1998. Cellular localization of latent murine cytomegalovirus. J Virol **72:**95-103.
194. **Kondo, K., H. Kaneshima, and E. S. Mocarski.** 1994. Human cytomegalovirus latent infection of granulocyte-macrophage progenitors. Proc Natl Acad Sci U S A **91:**11879-83.
195. **Konicek, B. W., X. Xia, T. Rajavashisth, and M. A. Harrington.** 1998. Regulation of mouse colony-stimulating factor-1 gene promoter activity by AP1 and cellular nucleic acid-binding protein. DNA Cell Biol **17:**799-809.
196. **Koyama, S., K. J. Ishii, C. Coban, and S. Akira.** 2008. Innate immune response to viral infection. Cytokine **43:**336-41.
197. **Kraatz, J., L. Clair, J. L. Rodriguez, and M. A. West.** 1999. Macrophage TNF secretion in endotoxin tolerance: role of SAPK, p38, and MAPK. J Surg Res **83:**158-64.
198. **Krmpotic, A., I. Bubic, B. Polic, P. Lucin, and S. Jonjic.** 2003. Pathogenesis of murine cytomegalovirus infection. Microbes Infect **5:**1263-77.
199. **Kropp, K. A., C. O. Simon, A. Fink, A. Renzaho, B. Kuhnapfel, J. Podlech, M. J. Reddehase, and N. K. Grzimek.** 2009. Synergism between the components of the bipartite major immediate-early transcriptional enhancer of murine cytomegalovirus does not accelerate virus replication in cell culture and host tissues. J Gen Virol **90:**2395-401.
200. **Krug, A., A. R. French, W. Barchet, J. A. Fischer, A. Dzionek, J. T. Pingel, M. M. Orihuela, S. Akira, W. M. Yokoyama, and M. Colonna.** 2004. TLR9-dependent recognition of MCMV by IPC and DC generates

coordinated cytokine responses that activate antiviral NK cell function. Immunity **21:**107-19.

201. **Kube, D., H. Rieth, J. Eskdale, P. G. Kremsner, and G. Gallagher.** 2001. Structural characterisation of the distal 5' flanking region of the human interleukin-10 gene. Genes Immun **2:**181-90.
202. **Kumar, V., O. Lockerbie, S. D. Keil, P. H. Ruane, M. S. Platz, C. B. Martin, J. L. Ravanat, J. Cadet, and R. P. Goodrich.** 2004. Riboflavin and UV-light based pathogen reduction: extent and consequence of DNA damage at the molecular level. Photochem Photobiol **80:**15-21.
203. **Lacaze, P., S. Raza, G. Sing, D. Page, T. Forster, P. Storm, M. Craigon, T. Awad, P. Ghazal, and T. C. Freeman.** 2009. Combined genome-wide expression profiling and targeted RNA interference in primary mouse macrophages reveals perturbation of transcriptional networks associated with interferon signalling. BMC Genomics **10:**372.
204. **Lamken, P., S. Lata, M. Gavutis, and J. Piehler.** 2004. Ligand-induced assembling of the type I interferon receptor on supported lipid bilayers. J Mol Biol **341:**303-18.
205. **Langer, J. A., E. C. Cutrone, and S. Kotenko.** 2004. The Class II cytokine receptor (CRF2) family: overview and patterns of receptor-ligand interactions. Cytokine Growth Factor Rev **15:**33-48.
206. **Larrubia, J. R., S. Benito-Martinez, M. Calvino, E. Sanz-de-Villalobos, and T. Parra-Cid.** 2008. Role of chemokines and their receptors in viral persistence and liver damage during chronic hepatitis C virus infection. World J Gastroenterol **14:**7149-59.
207. **Larsson, S., C. Soderberg-Naucler, and E. Moller.** 1998. Productive cytomegalovirus (CMV) infection exclusively in CD13-positive peripheral blood mononuclear cells from CMV-infected individuals: implications for prevention of CMV transmission. Transplantation **65:**411-5.
208. **Le, V. T., M. Trilling, A. Zimmermann, and H. Hengel.** 2008. Mouse cytomegalovirus inhibits beta interferon (IFN-beta) gene expression and controls activation pathways of the IFN-beta enhanceosome. J Gen Virol **89:**1131-41.
209. **Leaman, D. W., M. Chawla-Sarkar, B. Jacobs, K. Vyas, Y. Sun, A. Ozdemir, T. Yi, B. R. Williams, and E. C. Borden.** 2003. Novel growth and death related interferon-stimulated genes (ISGs) in melanoma: greater potency of IFN-beta compared with IFN-alpha2. J Interferon Cytokine Res **23:**745-56.
210. **Leber, J. H., G. T. Crimmins, S. Raghavan, N. P. Meyer-Morse, J. S. Cox, and D. A. Portnoy.** 2008. Distinct TLR- and NLR-mediated transcriptional responses to an intracellular pathogen. PLoS Pathog **4:**e6.
211. **Lee, G. C., H. A. Yi, and C. H. Lee.** 2006. Stimulation of interferon-beta gene expression by human cytomegalovirus via nuclear factor kappa B and phosphatidylinositol 3-kinase pathway. Virus Res **117:**209-14.
212. **Lee, H. R., Y. H. Huh, Y. E. Kim, K. Lee, S. Kim, and J. H. Ahn.** 2007. N-terminal determinants of human cytomegalovirus IE1 protein in nuclear targeting and disrupting PML-associated subnuclear structures. Biochem Biophys Res Commun **356:**499-504.

213. **Leek, J. T., E. Monsen, A. R. Dabney, and J. D. Storey.** 2006. EDGE: extraction and analysis of differential gene expression. Bioinformatics **22:**507-8.
214. **Levy, D. E., I. Marie, E. Smith, and A. Prakash.** 2002. Enhancement and diversification of IFN induction by IRF-7-mediated positive feedback. J Interferon Cytokine Res **22:**87-93.
215. **Lewerenz, M., K. E. Mogensen, and G. Uze.** 1998. Shared receptor components but distinct complexes for alpha and beta interferons. J Mol Biol **282:**585-99.
216. **Libermann, T. A., and D. Baltimore.** 1990. Activation of interleukin-6 gene expression through the NF-kappa B transcription factor. Mol Cell Biol **10:**2327-34.
217. **Liew, F. Y., D. Xu, E. K. Brint, and L. A. O'Neill.** 2005. Negative regulation of toll-like receptor-mediated immune responses. Nat Rev Immunol **5:**446-58.
218. **Lin, R., P. Genin, Y. Mamane, M. Sgarbanti, A. Battistini, W. J. Harrington, Jr., G. N. Barber, and J. Hiscott.** 2001. HHV-8 encoded vIRF-1 represses the interferon antiviral response by blocking IRF-3 recruitment of the CBP/p300 coactivators. Oncogene **20:**800-11.
219. **Lischka, P., and H. Zimmermann.** 2008. Antiviral strategies to combat cytomegalovirus infections in transplant recipients. Curr Opin Pharmacol **8:**541-8.
220. **Liu, B., S. Mink, K. A. Wong, N. Stein, C. Getman, P. W. Dempsey, H. Wu, and K. Shuai.** 2004. PIAS1 selectively inhibits interferon-inducible genes and is important in innate immunity. Nat Immunol **5:**891-8.
221. **Liu, C. J., H. Wang, and P. Lengyel.** 1999. The interferon-inducible nucleolar p204 protein binds the ribosomal RNA-specific UBF1 transcription factor and inhibits ribosomal RNA transcription. EMBO J **18:**2845-54.
222. **Liu, R., H. Liu, X. Chen, M. Kirby, P. O. Brown, and K. Zhao.** 2001. Regulation of CSF1 promoter by the SWI/SNF-like BAF complex. Cell **106:**309-18.
223. **Liu, Z. G.** 2005. Molecular mechanism of TNF signaling and beyond. Cell Res **15:**24-7.
224. **Livak, K. J., and T. D. Schmittgen.** 2001. Analysis of relative gene expression data using real-time quantitative PCR and the 2(-Delta Delta C(T)) Method. Methods **25:**402-8.
225. **Loewendorf, A., and C. A. Benedict.** Modulation of host innate and adaptive immune defenses by cytomegalovirus: timing is everything. J Intern Med **267:**483-501.
226. **Lovinger, G. G., H. P. Ling, R. V. Gilden, and M. Hatanaka.** 1975. Effect of UV Light on RNA-Directed DNA Polymerase Activity of Murine Oncornaviruses. J Virol **15:**1273-5.
227. **Lu, L. L., M. Puri, C. M. Horvath, and G. C. Sen.** 2008. Select paramyxoviral V proteins inhibit IRF3 activation by acting as alternative substrates for inhibitor of kappaB kinase epsilon (IKKe)/TBK1. J Biol Chem **283:**14269-76.

228. **Lund, J., A. Sato, S. Akira, R. Medzhitov, and A. Iwasaki.** 2003. Toll-like receptor 9-mediated recognition of Herpes simplex virus-2 by plasmacytoid dendritic cells. J Exp Med **198:**513-20.
229. **Lynn, D. J., G. L. Winsor, C. Chan, N. Richard, M. R. Laird, A. Barsky, J. L. Gardy, F. M. Roche, T. H. Chan, N. Shah, R. Lo, M. Naseer, J. Que, M. Yau, M. Acab, D. Tulpan, M. D. Whiteside, A. Chikatamarla, B. Mah, T. Munzner, K. Hokamp, R. E. Hancock, and F. S. Brinkman.** 2008. InnateDB: facilitating systems-level analyses of the mammalian innate immune response. Mol Syst Biol **4:**218.
230. **Mack, C., A. Sickmann, D. Lembo, and W. Brune.** 2008. Inhibition of proinflammatory and innate immune signaling pathways by a cytomegalovirus RIP1-interacting protein. Proc Natl Acad Sci U S A **105:**3094-9.
231. **Malmgaard, L., J. Melchjorsen, A. G. Bowie, S. C. Mogensen, and S. R. Paludan.** 2004. Viral activation of macrophages through TLR-dependent and -independent pathways. J Immunol **173:**6890-8.
232. **Manning, W. C., and E. S. Mocarski.** 1988. Insertional mutagenesis of the murine cytomegalovirus genome: one prominent alpha gene (ie2) is dispensable for growth. Virology **167:**477-84.
233. **Mantovani, A., A. Sica, and M. Locati.** 2005. Macrophage polarization comes of age. Immunity **23:**344-6.
234. **Marcello, T., A. Grakoui, G. Barba-Spaeth, E. S. Machlin, S. V. Kotenko, M. R. MacDonald, and C. M. Rice.** 2006. Interferons alpha and lambda inhibit hepatitis C virus replication with distinct signal transduction and gene regulation kinetics. Gastroenterology **131:**1887-98.
235. **Marie, I., J. E. Durbin, and D. E. Levy.** 1998. Differential viral induction of distinct interferon-alpha genes by positive feedback through interferon regulatory factor-7. EMBO J **17:**6660-9.
236. **Marijanovic, Z., J. Ragimbeau, J. van der Heyden, G. Uze, and S. Pellegrini.** 2007. Comparable potency of IFNalpha2 and IFNbeta on immediate JAK/STAT activation but differential down-regulation of IFNAR2. Biochem J **407:**141-51.
237. **Marshall, E. E., and A. P. Geballe.** 2009. Multifaceted evasion of the interferon response by cytomegalovirus. J Interferon Cytokine Res **29:**609-19.
238. **Martin, L., S. C. Pingle, D. M. Hallam, L. P. Rybak, and V. Ramkumar.** 2006. Activation of the adenosine A3 receptor in RAW 264.7 cells inhibits lipopolysaccharide-stimulated tumor necrosis factor-alpha release by reducing calcium-dependent activation of nuclear factor-kappaB and extracellular signal-regulated kinase 1/2. J Pharmacol Exp Ther **316:**71-8.
239. **Martinez, F. O., S. Gordon, M. Locati, and A. Mantovani.** 2006. Transcriptional profiling of the human monocyte-to-macrophage differentiation and polarization: new molecules and patterns of gene expression. J Immunol **177:**7303-11.
240. **Martinez, F. O., A. Sica, A. Mantovani, and M. Locati.** 2008. Macrophage activation and polarization. Front Biosci **13:**453-61.

241. **Martinon, F., K. Burns, and J. Tschopp.** 2002. The inflammasome: a molecular platform triggering activation of inflammatory caspases and processing of proIL-beta. Mol Cell **10:**417-26.
242. **Matsumoto, M., and T. Seya.** 2008. TLR3: interferon induction by double-stranded RNA including poly(I:C). Adv Drug Deliv Rev **60:**805-12.
243. **Maul, G. G., and D. Negorev.** 2008. Differences between mouse and human cytomegalovirus interactions with their respective hosts at immediate early times of the replication cycle. Med Microbiol Immunol **197:**241-9.
244. **McCormick, A. L.** 2008. Control of apoptosis by human cytomegalovirus. Curr Top Microbiol Immunol **325:**281-95.
245. **McGavin, J. K., and K. L. Goa.** 2001. Ganciclovir: an update of its use in the prevention of cytomegalovirus infection and disease in transplant recipients. Drugs **61:**1153-83.
246. **Means, T. K., R. P. Pavlovich, D. Roca, M. W. Vermeulen, and M. J. Fenton.** 2000. Activation of TNF-alpha transcription utilizes distinct MAP kinase pathways in different macrophage populations. J Leukoc Biol **67:**885-93.
247. **Medzhitov, R., and T. Horng.** 2009. Transcriptional control of the inflammatory response. Nat Rev Immunol **9:**692-703.
248. **Menard, C., M. Wagner, Z. Ruzsics, K. Holak, W. Brune, A. E. Campbell, and U. H. Koszinowski.** 2003. Role of murine cytomegalovirus US22 gene family members in replication in macrophages. J Virol **77:**5557-70.
249. **Messerle, M., B. Buhler, G. M. Keil, and U. H. Koszinowski.** 1992. Structural organization, expression, and functional characterization of the murine cytomegalovirus immediate-early gene 3. J Virol **66:**27-36.
250. **Messerle, M., I. Crnkovic, W. Hammerschmidt, H. Ziegler, and U. H. Koszinowski.** 1997. Cloning and mutagenesis of a herpesvirus genome as an infectious bacterial artificial chromosome. Proc Natl Acad Sci U S A **94:**14759-63.
251. **Messerle, M., G. M. Keil, and U. H. Koszinowski.** 1991. Structure and expression of murine cytomegalovirus immediate-early gene 2. J Virol **65:**1638-43.
252. **Mettenleiter, T. C.** 2004. Budding events in herpesvirus morphogenesis. Virus Res **106:**167-80.
253. **Mezger, M., M. Steffens, C. Semmler, E. M. Arlt, M. Zimmer, G. I. Kristjanson, T. F. Wienker, M. R. Toliat, T. Kessler, H. Einsele, and J. Loeffler.** 2008. Investigation of promoter variations in dendritic cell-specific ICAM3-grabbing non-integrin (DC-SIGN) (CD209) and their relevance for human cytomegalovirus reactivation and disease after allogeneic stem-cell transplantation. Clin Microbiol Infect **14:**228-34.
254. **Mibayashi, M., L. Martinez-Sobrido, Y. M. Loo, W. B. Cardenas, M. Gale, Jr., and A. Garcia-Sastre.** 2007. Inhibition of retinoic acid-inducible gene I-mediated induction of beta interferon by the NS1 protein of influenza A virus. J Virol **81:**514-24.
255. **Miller, M. D., and M. S. Krangel.** 1992. Biology and biochemistry of the chemokines: a family of chemotactic and inflammatory cytokines. Crit Rev Immunol **12:**17-46.

256. **Mitchell, B. M., A. Leung, and J. G. Stevens.** 1996. Murine cytomegalovirus DNA in peripheral blood of latently infected mice is detectable only in monocytes and polymorphonuclear leukocytes. Virology **223:**198-207.
257. **Mocarski, E. S., Jr.** 2002. Immunomodulation by cytomegaloviruses: manipulative strategies beyond evasion. Trends Microbiol **10:**332-9.
258. **Mocarski, E. S., Jr., and G. W. Kemble.** 1996. Recombinant cytomegaloviruses for study of replication and pathogenesis. Intervirology **39:**320-30.
259. **Mocarski, E. S., G. W. Kemble, J. M. Lyle, and R. F. Greaves.** 1996. A deletion mutant in the human cytomegalovirus gene encoding IE1(491aa) is replication defective due to a failure in autoregulation. Proc Natl Acad Sci U S A **93:**11321-6.
260. **Mogensen, T. H., J. Melchjorsen, L. Malmgaard, A. Casola, and S. R. Paludan.** 2004. Suppression of proinflammatory cytokine expression by herpes simplex virus type 1. J Virol **78:**5883-90.
261. **Mosser, D. M., and J. P. Edwards.** 2008. Exploring the full spectrum of macrophage activation. Nat Rev Immunol **8:**958-69.
262. **Mossman, K. L.** 2002. Activation and inhibition of virus and interferon: the herpesvirus story. Viral Immunol **15:**3-15.
263. **Mossman, K. L., P. F. Macgregor, J. J. Rozmus, A. B. Goryachev, A. M. Edwards, and J. R. Smiley.** 2001. Herpes simplex virus triggers and then disarms a host antiviral response. J Virol **75:**750-8.
264. **Mukhopadhyay, A., S. Shishodia, X. Y. Fu, and B. B. Aggarwal.** 2002. Lack of requirement of STAT1 for activation of nuclear factor-kappaB, c-Jun NH2-terminal protein kinase, and apoptosis by tumor necrosis factor-alpha. J Cell Biochem **84:**803-15.
265. **Mulhern, O., B. Harrington, and A. G. Bowie.** 2009. Modulation of innate immune signalling pathways by viral proteins. Adv Exp Med Biol **666:**49-63.
266. **Muller, U.** 1999. Ten years of gene targeting: targeted mouse mutants, from vector design to phenotype analysis. Mech Dev **82:**3-21.
267. **Munch, K., M. Messerle, B. Plachter, and U. H. Koszinowski.** 1992. An acidic region of the 89K murine cytomegalovirus immediate early protein interacts with DNA. J Gen Virol **73 (Pt 3):**499-506.
268. **Natarajan, M., K. M. Lin, R. C. Hsueh, P. C. Sternweis, and R. Ranganathan.** 2006. A global analysis of cross-talk in a mammalian cellular signalling network. Nat Cell Biol **8:**571-80.
269. **Nhu, Q. M., N. Cuesta, and S. N. Vogel.** 2006. Transcriptional regulation of lipopolysaccharide (LPS)-induced Toll-like receptor (TLR) expression in murine macrophages: role of interferon regulatory factors 1 (IRF-1) and 2 (IRF-2). J Endotoxin Res **12:**285-95.
270. **Nilsson, R., V. B. Bajic, H. Suzuki, D. di Bernardo, J. Bjorkegren, S. Katayama, J. F. Reid, M. J. Sweet, M. Gariboldi, P. Carninci, Y. Hayashizaki, D. A. Hume, J. Tegner, and T. Ravasi.** 2006. Transcriptional network dynamics in macrophage activation. Genomics **88:**133-42.
271. **Noda, S., S. A. Aguirre, A. Bitmansour, J. M. Brown, T. E. Sparer, J. Huang, and E. S. Mocarski.** 2006. Cytomegalovirus MCK-2 controls

mobilization and recruitment of myeloid progenitor cells to facilitate dissemination. Blood **107:**30-8.

272. **Noyce, R. S., S. E. Collins, and K. L. Mossman.** 2009. Differential modification of interferon regulatory factor 3 following virus particle entry. J Virol **83:**4013-22.
273. **Noyce, R. S., S. E. Collins, and K. L. Mossman.** 2006. Identification of a novel pathway essential for the immediate-early, interferon-independent antiviral response to enveloped virions. J Virol **80:**226-35.
274. **Oualikene, W., L. Lamoureux, J. M. Weber, and B. Massie.** 2000. Protease-deleted adenovirus vectors and complementing cell lines: potential applications of single-round replication mutants for vaccination and gene therapy. Hum Gene Ther **11:**1341-53.
275. **Paladino, P., D. T. Cummings, R. S. Noyce, and K. L. Mossman.** 2006. The IFN-independent response to virus particle entry provides a first line of antiviral defense that is independent of TLRs and retinoic acid-inducible gene I. J Immunol **177:**8008-16.
276. **Palamara, A. T., C. F. Perno, S. Aquaro, M. C. Bue, L. Dini, and E. Garaci.** 1996. Glutathione inhibits HIV replication by acting at late stages of the virus life cycle. AIDS Res Hum Retroviruses **12:**1537-41.
277. **Palamara, A. T., C. F. Perno, M. R. Ciriolo, L. Dini, E. Balestra, C. D'Agostini, P. Di Francesco, C. Favalli, G. Rotilio, and E. Garaci.** 1995. Evidence for antiviral activity of glutathione: in vitro inhibition of herpes simplex virus type 1 replication. Antiviral Res **27:**237-53.
278. **Panne, D., T. Maniatis, and S. C. Harrison.** 2007. An atomic model of the interferon-beta enhanceosome. Cell **129:**1111-23.
279. **Park, G. W., K. G. Linden, and M. D. Sobsey.** Inactivation of murine norovirus, feline calicivirus and echovirus 12 as surrogates for human norovirus (NoV) and coliphage (F+) MS2 by ultraviolet light (254 nm) and the effect of cell association on UV inactivation. Lett Appl Microbiol **52:**162-7.
280. **Patel, D., Y. Nan, M. Shen, K. Ritthipichai, X. Zhu, and Y. J. Zhang.** Porcine reproductive and respiratory syndrome virus inhibits type I interferon signaling by blocking STAT1/STAT2 nuclear translocation. J Virol **84:**11045-55.
281. **Pelletier, C., N. Varin-Blank, J. Rivera, B. Iannascoli, F. Marchand, B. David, A. Weyer, and U. Blank.** 1998. Fc epsilonRI-mediated induction of TNF-alpha gene expression in the RBL-2H3 mast cell line: regulation by a novel NF-kappaB-like nuclear binding complex. J Immunol **161:**4768-76.
282. **Perdiguero, B., and M. Esteban.** 2009. The interferon system and vaccinia virus evasion mechanisms. J Interferon Cytokine Res **29:**581-98.
283. **Pfeffer, L. M., J. G. Kim, S. R. Pfeffer, D. J. Carrigan, D. P. Baker, L. Wei, and R. Homayouni.** 2004. Role of nuclear factor-kappaB in the antiviral action of interferon and interferon-regulated gene expression. J Biol Chem **279:**31304-11.
284. **Pitkaranta, A., K. Linnavuori, M. Roivainen, and T. Hovi.** 1988. Induction of interferon-alpha in human leukocytes by polioviruses: wild-type strains are better inducers than attenuated strains. Virology **165:**476-81.

285. **Pixley, F. J., and E. R. Stanley.** 2004. CSF-1 regulation of the wandering macrophage: complexity in action. Trends Cell Biol **14:**628-38.
286. **Pollock, J. L., R. M. Presti, S. Paetzold, and H. W. t. Virgin.** 1997. Latent murine cytomegalovirus infection in macrophages. Virology **227:**168-79.
287. **Popa, M., Z. Ruzsics, M. Lotzerich, L. Dolken, C. Buser, P. Walther, and U. H. Koszinowski.** Dominant negative mutants of the murine cytomegalovirus M53 gene block nuclear egress and inhibit capsid maturation. J Virol **84:**9035-46.
288. **Powers, C., V. DeFilippis, D. Malouli, and K. Fruh.** 2008. Cytomegalovirus immune evasion. Curr Top Microbiol Immunol **325:**333-59.
289. **Prescott, J., C. Ye, G. Sen, and B. Hjelle.** 2005. Induction of innate immune response genes by Sin Nombre hantavirus does not require viral replication. J Virol **79:**15007-15.
290. **Prescott, J. B., P. R. Hall, V. S. Bondu-Hawkins, C. Ye, and B. Hjelle.** 2007. Early innate immune responses to Sin Nombre hantavirus occur independently of IFN regulatory factor 3, characterized pattern recognition receptors, and viral entry. J Immunol **179:**1796-802.
291. **Prichard, M. N., N. Gao, S. Jairath, G. Mulamba, P. Krosky, D. M. Coen, B. O. Parker, and G. S. Pari.** 1999. A recombinant human cytomegalovirus with a large deletion in UL97 has a severe replication deficiency. J Virol **73:**5663-70.
292. **Qin, H., K. L. Roberts, S. A. Niyongere, Y. Cong, C. O. Elson, and E. N. Benveniste.** 2007. Molecular mechanism of lipopolysaccharide-induced SOCS-3 gene expression in macrophages and microglia. J Immunol **179:**5966-76.
293. **Raaben, M., M. J. Groot Koerkamp, P. J. Rottier, and C. A. de Haan.** 2009. Type I interferon receptor-independent and -dependent host transcriptional responses to mouse hepatitis coronavirus infection in vivo. BMC Genomics **10:**350.
294. **Ramsey, S. A., S. L. Klemm, D. E. Zak, K. A. Kennedy, V. Thorsson, B. Li, M. Gilchrist, E. S. Gold, C. D. Johnson, V. Litvak, G. Navarro, J. C. Roach, C. M. Rosenberger, A. G. Rust, N. Yudkovsky, A. Aderem, and I. Shmulevich.** 2008. Uncovering a macrophage transcriptional program by integrating evidence from motif scanning and expression dynamics. PLoS Comput Biol **4:**e1000021.
295. **Randall, R. E., and S. Goodbourn.** 2008. Interferons and viruses: an interplay between induction, signalling, antiviral responses and virus countermeasures. J Gen Virol **89:**1-47.
296. **Rani, M. R., and R. M. Ransohoff.** 2005. Alternative and accessory pathways in the regulation of IFN-beta-mediated gene expression. J Interferon Cytokine Res **25:**788-98.
297. **Rapp, M., P. Lucin, M. Messerle, L. C. Loh, and U. H. Koszinowski.** 1994. Expression of the murine cytomegalovirus glycoprotein H by recombinant vaccinia virus. J Gen Virol **75 (Pt 1):**183-8.
298. **Rathinam, V. A., Z. Jiang, S. N. Waggoner, S. Sharma, L. E. Cole, L. Waggoner, S. K. Vanaja, B. G. Monks, S. Ganesan, E. Latz, V. Hornung, S. N. Vogel, E. Szomolanyi-Tsuda, and K. A. Fitzgerald.** The AIM2

inflammasome is essential for host defense against cytosolic bacteria and DNA viruses. Nat Immunol **11:**395-402.
299. **Rawlinson, W. D., H. E. Farrell, and B. G. Barrell.** 1996. Analysis of the complete DNA sequence of murine cytomegalovirus. J Virol **70:**8833-49.
300. **Raza, S., K. A. Robertson, P. A. Lacaze, D. Page, A. J. Enright, P. Ghazal, and T. C. Freeman.** 2008. A logic-based diagram of signalling pathways central to macrophage activation. BMC Syst Biol **2:**36.
301. **Rebhun, J. F., A. F. Castro, and L. A. Quilliam.** 2000. Identification of guanine nucleotide exchange factors (GEFs) for the Rap1 GTPase. Regulation of MR-GEF by M-Ras-GTP interaction. J Biol Chem **275:**34901-8.
302. **Reddehase, M. J., J. Podlech, and N. K. Grzimek.** 2002. Mouse models of cytomegalovirus latency: overview. J Clin Virol **25 Suppl 2:**S23-36.
303. **Redpath, S., A. Angulo, N. R. Gascoigne, and P. Ghazal.** 1999. Murine cytomegalovirus infection down-regulates MHC class II expression on macrophages by induction of IL-10. J Immunol **162:**6701-7.
304. **Reimer, T., M. Brcic, M. Schweizer, and T. W. Jungi.** 2008. poly(I:C) and LPS induce distinct IRF3 and NF-kappaB signaling during type-I IFN and TNF responses in human macrophages. J Leukoc Biol **83:**1249-57.
305. **Rock, R. B., S. Hu, A. Deshpande, S. Munir, B. J. May, C. A. Baker, P. K. Peterson, and V. Kapur.** 2005. Transcriptional response of human microglial cells to interferon-gamma. Genes Immun **6:**712-9.
306. **Rose, K. M., R. Elliott, L. Martinez-Sobrido, A. Garcia-Sastre, and S. R. Weiss.** Murine coronavirus delays expression of a subset of interferon-stimulated genes. J Virol **84:**5656-69.
307. **Roth-Cross, J. K., L. Martinez-Sobrido, E. P. Scott, A. Garcia-Sastre, and S. R. Weiss.** 2007. Inhibition of the alpha/beta interferon response by mouse hepatitis virus at multiple levels. J Virol **81:**7189-99.
308. **Roy, C. R., and E. S. Mocarski.** 2007. Pathogen subversion of cell-intrinsic innate immunity. Nat Immunol **8:**1179-87.
309. **Sabat, R., G. Grutz, K. Warszawska, S. Kirsch, E. Witte, K. Wolk, and J. Geginat.** Biology of interleukin-10. Cytokine Growth Factor Rev **21:**331-44.
310. **Sabbah, A., T. H. Chang, R. Harnack, V. Frohlich, K. Tominaga, P. H. Dube, Y. Xiang, and S. Bose.** 2009. Activation of innate immune antiviral responses by Nod2. Nat Immunol **10:**1073-80.
311. **Sadler, A. J., and B. R. Williams.** 2008. Interferon-inducible antiviral effectors. Nat Rev Immunol **8:**559-68.
312. **Saederup, N., S. A. Aguirre, T. E. Sparer, D. M. Bouley, and E. S. Mocarski.** 2001. Murine cytomegalovirus CC chemokine homolog MCK-2 (m131-129) is a determinant of dissemination that increases inflammation at initial sites of infection. J Virol **75:**9966-76.
313. **Saederup, N., Y. C. Lin, D. J. Dairaghi, T. J. Schall, and E. S. Mocarski.** 1999. Cytomegalovirus-encoded beta chemokine promotes monocyte-associated viremia in the host. Proc Natl Acad Sci U S A **96:**10881-6.
314. **Saklatvala, J., J. Dean, and A. Clark.** 2003. Control of the expression of inflammatory response genes. Biochem Soc Symp**:**95-106.

315. **Salazar-Mather, T. P., and K. L. Hokeness.** 2003. Calling in the troops: regulation of inflammatory cell trafficking through innate cytokine/chemokine networks. Viral Immunol **16:**291-306.
316. **Salazar-Mather, T. P., and K. L. Hokeness.** 2006. Cytokine and chemokine networks: pathways to antiviral defense. Curr Top Microbiol Immunol **303:**29-46.
317. **Salazar-Mather, T. P., C. A. Lewis, and C. A. Biron.** 2002. Type I interferons regulate inflammatory cell trafficking and macrophage inflammatory protein 1alpha delivery to the liver. J Clin Invest **110:**321-30.
318. **Samarajiwa, S. A., S. Forster, K. Auchettl, and P. J. Hertzog.** 2009. INTERFEROME: the database of interferon regulated genes. Nucleic Acids Res **37:**D852-7.
319. **Sanceau, J., T. Kaisho, T. Hirano, and J. Wietzerbin.** 1995. Triggering of the human interleukin-6 gene by interferon-gamma and tumor necrosis factor-alpha in monocytic cells involves cooperation between interferon regulatory factor-1, NF kappa B, and Sp1 transcription factors. J Biol Chem **270:**27920-31.
320. **Sanders, R. L., C. L. Clark, C. S. Morello, and D. H. Spector.** 2008. Development of cell lines that provide tightly controlled temporal translation of the human cytomegalovirus IE2 proteins for complementation and functional analyses of growth-impaired and nonviable IE2 mutant viruses. J Virol **82:**7059-77.
321. **Santhakumar, D., T. Forster, N. N. Laqtom, R. Fragkoudis, P. Dickinson, C. Abreu-Goodger, S. A. Manakov, N. R. Choudhury, S. J. Griffiths, A. Vermeulen, A. J. Enright, B. Dutia, A. Kohl, P. Ghazal, and A. H. Buck.** Combined agonist-antagonist genome-wide functional screening identifies broadly active antiviral microRNAs. Proc Natl Acad Sci U S A **107:**13830-5.
322. **Saraiva, M., and A. O'Garra.** The regulation of IL-10 production by immune cells. Nat Rev Immunol **10:**170-81.
323. **Scalzo, A. A., A. J. Corbett, W. D. Rawlinson, G. M. Scott, and M. A. Degli-Esposti.** 2007. The interplay between host and viral factors in shaping the outcome of cytomegalovirus infection. Immunol Cell Biol **85:**46-54.
324. **Schleiss, M. R.** 2008. Cytomegalovirus vaccine development. Curr Top Microbiol Immunol **325:**361-82.
325. **Schroder, K., M. Lichtinger, K. M. Irvine, K. Brion, A. Trieu, I. L. Ross, T. Ravasi, K. J. Stacey, M. Rehli, D. A. Hume, and M. J. Sweet.** 2007. PU.1 and ICSBP control constitutive and IFN-gamma-regulated Tlr9 gene expression in mouse macrophages. J Leukoc Biol **81:**1577-90.
326. **Scrivano, L., J. Esterlechner, H. Muhlbach, N. Ettischer, C. Hagen, K. Grunewald, C. A. Mohr, Z. Ruzsics, U. Koszinowski, and B. Adler.** The m74 gene product of murine cytomegalovirus (MCMV) is a functional homolog of human CMV gO and determines the entry pathway of MCMV. J Virol **84:**4469-80.
327. **Shimizu, H., K. Mitomo, T. Watanabe, S. Okamoto, and K. Yamamoto.** 1990. Involvement of a NF-kappa B-like transcription factor in the activation of the interleukin-6 gene by inflammatory lymphokines. Mol Cell Biol **10:**561-8.

328. **Shirota, H., K. J. Ishii, H. Takakuwa, and D. M. Klinman.** 2006. Contribution of interferon-beta to the immune activation induced by double-stranded DNA. Immunology **118:**302-10.
329. **Siegal, F. P., N. Kadowaki, M. Shodell, P. A. Fitzgerald-Bocarsly, K. Shah, S. Ho, S. Antonenko, and Y. J. Liu.** 1999. The nature of the principal type 1 interferon-producing cells in human blood. Science **284:**1835-7.
330. **Simmen, K. A., J. Singh, B. G. Luukkonen, M. Lopper, A. Bittner, N. E. Miller, M. R. Jackson, T. Compton, and K. Fruh.** 2001. Global modulation of cellular transcription by human cytomegalovirus is initiated by viral glycoprotein B. Proc Natl Acad Sci U S A **98:**7140-5.
331. **Simon, C. O., C. K. Seckert, D. Dreis, M. J. Reddehase, and N. K. Grzimek.** 2005. Role for tumor necrosis factor alpha in murine cytomegalovirus transcriptional reactivation in latently infected lungs. J Virol **79:**326-40.
332. **Sindre, H., G. Haraldsen, S. Beck, K. Hestdal, D. Kvale, P. Brandtzaeg, M. Degre, and H. Rollag.** 2000. Human intestinal endothelium shows high susceptibility to cytomegalovirus and altered expression of adhesion molecules after infection. Scand J Immunol **51:**354-60.
333. **Sindre, H., G. E. Tjoonnfjord, H. Rollag, T. Ranneberg-Nilsen, O. P. Veiby, S. Beck, M. Degre, and K. Hestdal.** 1996. Human cytomegalovirus suppression of and latency in early hematopoietic progenitor cells. Blood **88:**4526-33.
334. **Smith, M. S., G. L. Bentz, J. S. Alexander, and A. D. Yurochko.** 2004. Human cytomegalovirus induces monocyte differentiation and migration as a strategy for dissemination and persistence. J Virol **78:**4444-53.
335. **Smith, M. S., G. L. Bentz, P. M. Smith, E. R. Bivins, and A. D. Yurochko.** 2004. HCMV activates PI(3)K in monocytes and promotes monocyte motility and transendothelial migration in a PI(3)K-dependent manner. J Leukoc Biol **76:**65-76.
336. **Smyth, G. K.** 2004. Linear models and empirical bayes methods for assessing differential expression in microarray experiments. Stat Appl Genet Mol Biol **3:**Article3.
337. **Spencer, J. V., K. M. Lockridge, P. A. Barry, G. Lin, M. Tsang, M. E. Penfold, and T. J. Schall.** 2002. Potent immunosuppressive activities of cytomegalovirus-encoded interleukin-10. J Virol **76:**1285-92.
338. **Stanier, P., A. D. Kitchen, D. L. Taylor, and A. S. Tyms.** 1992. Detection of human cytomegalovirus in peripheral mononuclear cells and urine samples using PCR. Mol Cell Probes **6:**51-8.
339. **Steinberg, C., K. Eisenacher, O. Gross, W. Reindl, F. Schmitz, J. Ruland, and A. Krug.** 2009. The IFN regulatory factor 7-dependent type I IFN response is not essential for early resistance against murine cytomegalovirus infection. Eur J Immunol **39:**1007-18.
340. **Stenberg, R. M., D. R. Thomsen, and M. F. Stinski.** 1984. Structural analysis of the major immediate early gene of human cytomegalovirus. J Virol **49:**190-9.
341. **Stockinger, S., B. Reutterer, B. Schaljo, C. Schellack, S. Brunner, T. Materna, M. Yamamoto, S. Akira, T. Taniguchi, P. J. Murray, M. Muller, and T. Decker.** 2004. IFN regulatory factor 3-dependent induction

of type I IFNs by intracellular bacteria is mediated by a TLR- and Nod2-independent mechanism. J Immunol **173:**7416-25.

342. **Sweet, M. J., C. C. Campbell, D. P. Sester, D. Xu, R. C. McDonald, K. J. Stacey, D. A. Hume, and F. Y. Liew.** 2002. Colony-stimulating factor-1 suppresses responses to CpG DNA and expression of toll-like receptor 9 but enhances responses to lipopolysaccharide in murine macrophages. J Immunol **168:**392-9.
343. **Sweet, M. J., and D. A. Hume.** 2003. CSF-1 as a regulator of macrophage activation and immune responses. Arch Immunol Ther Exp (Warsz) **51:**169-77.
344. **Tabeta, K., P. Georgel, E. Janssen, X. Du, K. Hoebe, K. Crozat, S. Mudd, L. Shamel, S. Sovath, J. Goode, L. Alexopoulou, R. A. Flavell, and B. Beutler.** 2004. Toll-like receptors 9 and 3 as essential components of innate immune defense against mouse cytomegalovirus infection. Proc Natl Acad Sci U S A **101:**3516-21.
345. **Taddeo, B., A. Esclatine, and B. Roizman.** 2002. The patterns of accumulation of cellular RNAs in cells infected with a wild-type and a mutant herpes simplex virus 1 lacking the virion host shutoff gene. Proc Natl Acad Sci U S A **99:**17031-6.
346. **Takahama, H., T. Kinoshita, and F. Sasaki.** 1992. Structural and endocytotic differences of fibroblasts and macrophages in the tail fin of amphibian larvae during metamorphosis. Arch Histol Cytol **55:**437-48.
347. **Takeshita, S., J. R. Gage, T. Kishimoto, D. L. Vredevoe, and O. Martinez-Maza.** 1996. Differential regulation of IL-6 gene transcription and expression by IL-4 and IL-10 in human monocytic cell lines. J Immunol **156:**2591-8.
348. **Tang-Feldman, Y. J., G. R. Lochhead, S. R. Lochhead, C. Yu, and C. Pomeroy.** Interleukin-10 repletion suppresses pro-inflammatory cytokines and decreases liver pathology without altering viral replication in murine cytomegalovirus (MCMV)-infected IL-10 knockout mice. Inflamm Res.
349. **Tang, F., Q. Du, and Y. J. Liu.** Plasmacytoid dendritic cells in antiviral immunity and autoimmunity. Sci China Life Sci **53:**172-82.
350. **Tang, Q., L. Li, and G. G. Maul.** 2005. Mouse cytomegalovirus early M112/113 proteins control the repressive effect of IE3 on the major immediate-early promoter. J Virol **79:**257-63.
351. **Tang, Q., and G. G. Maul.** 2003. Mouse cytomegalovirus immediate-early protein 1 binds with host cell repressors to relieve suppressive effects on viral transcription and replication during lytic infection. J Virol **77:**1357-67.
352. **Tassiulas, I., X. Hu, H. Ho, Y. Kashyap, P. Paik, Y. Hu, C. A. Lowell, and L. B. Ivashkiv.** 2004. Amplification of IFN-alpha-induced STAT1 activation and inflammatory function by Syk and ITAM-containing adaptors. Nat Immunol **5:**1181-9.
353. **Taylor, R. T., and W. A. Bresnahan.** 2005. Human cytomegalovirus immediate-early 2 gene expression blocks virus-induced beta interferon production. J Virol **79:**3873-7.
354. **Taylor, R. T., and W. A. Bresnahan.** 2006. Human cytomegalovirus immediate-early 2 protein IE86 blocks virus-induced chemokine expression. J Virol **80:**920-8.

355. **Thomas, K. E., C. L. Galligan, R. D. Newman, E. N. Fish, and S. N. Vogel.** 2006. Contribution of interferon-beta to the murine macrophage response to the toll-like receptor 4 agonist, lipopolysaccharide. J Biol Chem **281:**31119-30.
356. **Travassos, L. H., L. A. Carneiro, M. Ramjeet, S. Hussey, Y. G. Kim, J. G. Magalhaes, L. Yuan, F. Soares, E. Chea, L. Le Bourhis, I. G. Boneca, A. Allaoui, N. L. Jones, G. Nunez, S. E. Girardin, and D. J. Philpott.** Nod1 and Nod2 direct autophagy by recruiting ATG16L1 to the plasma membrane at the site of bacterial entry. Nat Immunol **11:**55-62.
357. **Trevani, A. S., A. Chorny, G. Salamone, M. Vermeulen, R. Gamberale, J. Schettini, S. Raiden, and J. Geffner.** 2003. Bacterial DNA activates human neutrophils by a CpG-independent pathway. Eur J Immunol **33:**3164-74.
358. **Tross, D., L. Petrenko, S. Klaschik, Q. Zhu, and D. M. Klinman.** 2009. Global changes in gene expression and synergistic interactions induced by TLR9 and TLR3. Mol Immunol **46:**2557-64.
359. **Tsitoura, E., J. Thomas, D. Cuchet, K. Thoinet, P. Mavromara, and A. L. Epstein.** 2009. Infection with herpes simplex type 1-based amplicon vectors results in an IRF3/7-dependent, TLR-independent activation of the innate antiviral response in primary human fibroblasts. J Gen Virol **90:**2209-20.
360. **Tsuchimoto, D., A. Tojo, and S. Asano.** 2004. A mechanism of transcriptional regulation of the CSF-1 gene by interferon-gamma. Immunol Invest **33:**397-405.
361. **Tsutsui, Y., I. Kosugi, and H. Kawasaki.** 2005. Neuropathogenesis in cytomegalovirus infection: indication of the mechanisms using mouse models. Rev Med Virol **15:**327-45.
362. **Uematsu, S., and S. Akira.** 2008. Toll-Like receptors (TLRs) and their ligands. Handb Exp Pharmacol**:**1-20.
363. **Unterberger, C., K. J. Staples, T. Smallie, L. Williams, B. Foxwell, A. Schaefer, B. Kempkes, T. P. Hofer, M. Koeppel, M. Lohrum, H. Stunnenberg, M. Frankenberger, and L. Ziegler-Heitbrock.** 2008. Role of STAT3 in glucocorticoid-induced expression of the human IL-10 gene. Mol Immunol **45:**3230-7.
364. **Upton, J. W., W. J. Kaiser, and E. S. Mocarski.** 2008. Cytomegalovirus M45 cell death suppression requires receptor-interacting protein (RIP) homotypic interaction motif (RHIM)-dependent interaction with RIP1. J Biol Chem **283:**16966-70.
365. **Valchanova, R. S., M. Picard-Maureau, M. Budt, and W. Brune.** 2006. Murine cytomegalovirus m142 and m143 are both required to block protein kinase R-mediated shutdown of protein synthesis. J Virol **80:**10181-90.
366. **Valentine, R., and G. L. Smith.** Inhibition of the RNA polymerase III-mediated dsDNA-sensing pathway of innate immunity by vaccinia virus protein E3. J Gen Virol **91:**2221-9.
367. **Valledor, A. F., M. Comalada, L. F. Santamaria-Babi, J. Lloberas, and A. Celada.** Macrophage proinflammatory activation and deactivation: a question of balance. Adv Immunol **108:**1-20.
368. **Vanden Berghe, W., K. De Bosscher, E. Boone, S. Plaisance, and G. Haegeman.** 1999. The nuclear factor-kappaB engages CBP/p300 and histone

acetyltransferase activity for transcriptional activation of the interleukin-6 gene promoter. J Biol Chem **274:**32091-8.

369. **Varnum, S. M., D. N. Streblow, M. E. Monroe, P. Smith, K. J. Auberry, L. Pasa-Tolic, D. Wang, D. G. Camp, 2nd, K. Rodland, S. Wiley, W. Britt, T. Shenk, R. D. Smith, and J. A. Nelson.** 2004. Identification of proteins in human cytomegalovirus (HCMV) particles: the HCMV proteome. J Virol **78:**10960-6.
370. **Wagner, M., S. Jonjic, U. H. Koszinowski, and M. Messerle.** 1999. Systematic excision of vector sequences from the BAC-cloned herpesvirus genome during virus reconstitution. J Virol **73:**7056-60.
371. **Wang, K., D. Scheel-Toellner, S. H. Wong, R. Craddock, J. Caamano, A. N. Akbar, M. Salmon, and J. M. Lord.** 2003. Inhibition of neutrophil apoptosis by type 1 IFN depends on cross-talk between phosphoinositol 3-kinase, protein kinase C-delta, and NF-kappa B signaling pathways. J Immunol **171:**1035-41.
372. **Wang, L., X. M. Ren, J. J. Xing, and A. C. Zheng.** The nucleolus and viral infection. Virol Sin **25:**151-7.
373. **Wang, X., and D. G. Chen.** 2009. Recombinant murine cytomegalovirus vector activates human monocyte-derived dendritic cells in a NF-kappaB dependent pathway. Mol Immunol **46:**3462-5.
374. **Wang, Z., M. K. Choi, T. Ban, H. Yanai, H. Negishi, Y. Lu, T. Tamura, A. Takaoka, K. Nishikura, and T. Taniguchi.** 2008. Regulation of innate immune responses by DAI (DLM-1/ZBP1) and other DNA-sensing molecules. Proc Natl Acad Sci U S A **105:**5477-82.
375. **Weber, B., and H. W. Doerr.** 1994. Diagnosis and epidemiology of transfusion-associated human cytomegalovirus infection: recent developments. Infusionsther Transfusionsmed **21 Suppl 1:**32-9.
376. **Weber, F., G. Kochs, and O. Haller.** 2004. Inverse interference: how viruses fight the interferon system. Viral Immunol **17:**498-515.
377. **Weinstock-Guttman, B., D. Badgett, K. Patrick, L. Hartrich, R. Santos, D. Hall, M. Baier, J. Feichter, and M. Ramanathan.** 2003. Genomic effects of IFN-beta in multiple sclerosis patients. J Immunol **171:**2694-702.
378. **Welsh, G. I., S. Kadereit, E. M. Coccia, A. G. Hovanessian, and E. F. Meurs.** 1999. Colocalization within the nucleolus of two highly related IFN-induced human nuclear phosphoproteins with nucleolin. Exp Cell Res **250:**62-74.
379. **Wiebusch, L., A. Neuwirth, L. Grabenhenrich, S. Voigt, and C. Hagemeier.** 2008. Cell cycle-independent expression of immediate-early gene 3 results in G1 and G2 arrest in murine cytomegalovirus-infected cells. J Virol **82:**10188-98.
380. **Wilkins, C., and M. Gale, Jr.** Recognition of viruses by cytoplasmic sensors. Curr Opin Immunol **22:**41-7.
381. **Wu, C. H., H. Huang, L. Arminski, J. Castro-Alvear, Y. Chen, Z. Z. Hu, R. S. Ledley, K. C. Lewis, H. W. Mewes, B. C. Orcutt, B. E. Suzek, A. Tsugita, C. R. Vinayaka, L. S. Yeh, J. Zhang, and W. C. Barker.** 2002. The Protein Information Resource: an integrated public resource of functional annotation of proteins. Nucleic Acids Res **30:**35-7.

382. **Wu, G., Y. Z. Fang, S. Yang, J. R. Lupton, and N. D. Turner.** 2004. Glutathione metabolism and its implications for health. J Nutr **134:**489-92.
383. **Xu, Y., K. S. Colletti, and G. S. Pari.** 2002. Human cytomegalovirus UL84 localizes to the cell nucleus via a nuclear localization signal and is a component of viral replication compartments. J Virol **76:**8931-8.
384. **Yarilina, A., and L. B. Ivashkiv.** Type I interferon: a new player in TNF signaling. Curr Dir Autoimmun **11:**94-104.
385. **Yoneyama, M., M. Kikuchi, T. Natsukawa, N. Shinobu, T. Imaizumi, M. Miyagishi, K. Taira, S. Akira, and T. Fujita.** 2004. The RNA helicase RIG-I has an essential function in double-stranded RNA-induced innate antiviral responses. Nat Immunol **5:**730-7.
386. **Yurochko, A. D., E. S. Hwang, L. Rasmussen, S. Keay, L. Pereira, and E. S. Huang.** 1997. The human cytomegalovirus UL55 (gB) and UL75 (gH) glycoprotein ligands initiate the rapid activation of Sp1 and NF-kappaB during infection. J Virol **71:**5051-9.
387. **Zabel, B. A., L. Zuniga, T. Ohyama, S. J. Allen, J. Cichy, T. M. Handel, and E. C. Butcher.** 2006. Chemoattractants, extracellular proteases, and the integrated host defense response. Exp Hematol **34:**1021-32.
388. **Zeremski, M., L. M. Petrovic, and A. H. Talal.** 2007. The role of chemokines as inflammatory mediators in chronic hepatitis C virus infection. J Viral Hepat **14:**675-87.
389. **Zhang, T., V. Kruys, G. Huez, and C. Gueydan.** 2002. AU-rich element-mediated translational control: complexity and multiple activities of trans-activating factors. Biochem Soc Trans **30:**952-8.
390. **Zhao, W., M. Liu, and K. L. Kirkwood.** 2008. p38alpha stabilizes interleukin-6 mRNA via multiple AU-rich elements. J Biol Chem **283:**1778-85.
391. **Zhou, H., J. Zhao, and S. Perlman.** Autocrine interferon priming in macrophages but not dendritic cells results in enhanced cytokine and chemokine production after coronavirus infection. MBio **1**.
392. **Zimmermann, A., M. Trilling, M. Wagner, M. Wilborn, I. Bubic, S. Jonjic, U. Koszinowski, and H. Hengel.** 2005. A cytomegaloviral protein reveals a dual role for STAT2 in IFN-{gamma} signaling and antiviral responses. J Exp Med **201:**1543-53.
393. **Zornetzer, G. A., M. B. Frieman, E. Rosenzweig, M. J. Korth, C. Page, R. S. Baric, and M. G. Katze.** Transcriptomic analysis reveals a mechanism for a prefibrotic phenotype in STAT1 knockout mice during severe acute respiratory syndrome coronavirus infection. J Virol **84:**11297-309.
394. **Zucchini, N., G. Bessou, S. Traub, S. H. Robbins, S. Uematsu, S. Akira, L. Alexopoulou, and M. Dalod.** 2008. Cutting edge: Overlapping functions of TLR7 and TLR9 for innate defense against a herpesvirus infection. J Immunol **180:**5799-803.
395. **Zucchini, N., K. Crozat, T. Baranek, S. H. Robbins, M. Altfeld, and M. Dalod.** 2008. Natural killer cells in immunodefense against infective agents. Expert Rev Anti Infect Ther **6:**867-85.
396. **Zurcher, T., J. Pavlovic, and P. Staeheli.** 1992. Mouse Mx2 protein inhibits vesicular stomatitis virus but not influenza virus. Virology **187:**796-800.